

# Final Report

## AE3200 Design Synthesis Exercise

*Faculty of Aerospace Engineering; TU Delft, Tuesday 25<sup>th</sup> June, 2024*

### Group 25: A First Look at Planet 9

|                      |         |                         |         |
|----------------------|---------|-------------------------|---------|
| Anton Smit           | 5079217 | Dhafin Praditya Rizaldi | 5494532 |
| Flavio Claudio Padua | 5448492 | Isha Moharir            | 5230721 |
| Iván Pedrero Crespo  | 5493463 | Milan Ludlage           | 4662725 |
| Pepijn Jeukens       | 5497671 | Ruth Euniki Vraka       | 5487404 |
| Jim Vissers          | 4659678 | Thijmen Duran           | 5571855 |

*This page is intentionally left blank.*

# Nomenclature

|                |  |               |   |
|----------------|--|---------------|---|
| <b>ADCS</b>    | Attitude Determination and Control Subsystem                 | <b>AHP</b>    | Analytical Hierarchy Process                            |
| <b>AU</b>      | Astronomical Unit  | <b>AWGN</b>   | Additive White Gaussian Noise                           |
| <b>BoL</b>     | Begin of Life  | <b>BWM</b>    | Best-Worst Method                                       |
| <b>CAD</b>     | Computer Aided Design  | <b>CHU</b>    | Command Handling Unit                                   |
| <b>CMG</b>     | Control Moment Gyroscope                                     | <b>CNC</b>    | Computer Numerical Control                              |
| <b>COTS</b>    | Commercially Of The Shelf                                    | <b>DHAU</b>   | Data Handling and Acquisition Unit                      |
| <b>DISN</b>    | Deep Space Network   | <b>DOD</b>    | Depth of Discharge                                      |
| <b>DOT</b>     | Design Option Tree   | <b>DSM</b>    | Deep Space Maneuvers                                    |
| <b>ECSS</b>    | European Cooperation for Space Standardization               | <b>EEPROM</b> | Electronically Erasable Programmable Read Only Memory   |
| <b>EIRP</b>    | Equivalent Isotropic Radiated Power                          | <b>EM</b>     | Engineering Model                                       |
| <b>eMMRTG</b>  | Enhanced Multi-Mission Radioisotope Thermoelectric Generator | <b>ENKI</b>   | Energetic NIBIRU Kick Interstage                        |
| <b>ENLIL</b>   | Efficient NIBIRU Long-range Interstage Launcher              | <b>EoL</b>    | End of Life   |
| <b>EPS</b>     | Electrical Power System                                      | <b>ESA</b>    | European State Agency                                   |
| <b>FBS</b>     | Functional Breakdown Structure                               | <b>FDIR</b>   | Fault Detection Isolation and Recovery                  |
| <b>FFD</b>     | Functional Flow Diagram                                      | <b>FIT</b>    | Failure in Time   |
| <b>FoS</b>     | Factor of Safety   | <b>FPGA</b>   | Field Programmable Gate Array                           |
| <b>GPS</b>     | Global Positioning System                                    | <b>GPHS</b>   | General Purpose Heat Source                             |
| <b>HGA</b>     | High Gain Antenna  | <b>IEM</b>    | Integrated Electronics Module                           |
| <b>IMU</b>     | Inertial Measurement Unit                                    | <b>IST</b>    | End-to-End Information System Testing                   |
| <b>JUICE</b>   | Jupiter Icy Moons Explorer                                   | <b>JWST</b>   | James Webb Space Telescope                              |
| <b>KBO</b>     | Kuiper Belt Object   | <b>MBSE</b>   | Model-based System Engineering                          |
| <b>MGA</b>     | Multiple Gravity Assist                                      | <b>MLI</b>    | Multi-layered Insulation                                |
| <b>MMH</b>     | Monomethyl hydrazine   | <b>MOO</b>    | Modes of Operation                                      |
| <b>MOT</b>     | Mission Operation Team                                       | <b>MPD</b>    | Magnetoplasmadynamic                                    |
| <b>MS</b>      | Margin of Safety   | <b>MST</b>    | Mission Scenario Test                                   |
| <b>MTBF</b>    | Mean Time Between Failures                                   | <b>N2O4</b>   | Nitrogen Tetroxide                                      |
| <b>NASA</b>    | National Aeronautics and Space Administration                | <b>NIBIRU</b> | Novel, Intelligent, Beyond Interplanetary Research Unit |
| <b>OBC</b>     | On-board Computer  | <b>OBDH</b>   | On-board Data Handling                                  |
| <b>ORT</b>     | Operational Readiness Test                                   | <b>PAF</b>    | Payload Adapter Fitting                                 |
| <b>PCDU</b>    | Power Conditioning and Distribution Unit                     | <b>PMD</b>    | Power Management and Distribution system                |
| <b>PyGMO</b>   | Python Parallel Global Multiobjective Optimizer              | <b>RAMS</b>   | Reliability, Availability, Maintainability & Safety     |
| <b>R&amp;D</b> | Research & Development                                       | <b>RF</b>     | Radio Frequency   |
| <b>RTG</b>     | Radioisotope Thermoelectric Generator                        | <b>RTPV</b>   | Radioisotope Thermophotovoltaics                        |

|                 |                                 |              |   |
|-----------------|---------------------------------|--------------|---|
| <b>SC</b>       | Spacecraft                      | <b>SF</b>    | Safety Factor                                     |
| <b>SLOC</b>     | Source Lines of Code            | <b>SMAD</b>  | Space Mission Analysis and Design                 |
| <b>SNR</b>      | Signal to Noise Ratio           | <b>SRAM</b>  | Static Random Access Memory                       |
| <b>SSR</b>      | Solid State Recorder            | <b>STEM</b>  | Segmented Thermoelectric Modular                  |
| <b>STS</b>      | Stress-Testing and Simulation   | <b>SWOT</b>  | Strengths, Weaknesses, Opportunities, and Threats |
| <b>S&amp;M</b>  | Structures and Materials        | <b>TBD</b>   | To Be Determined                                  |
| <b>TCS</b>      | Thermal Control System          | <b>TFDIR</b> | Fault Detection Isolation and Recovery            |
| <b>TIG</b>      | Tungsten Inert Gas              | <b>TNO</b>   | Trans-Neptunian Objects                           |
| <b>TOF</b>      | Time-Of-Flight                  | <b>TRL</b>   | Technology Readiness Level                        |
| <b>TUDAT</b>    | TUDeft Astrodynamics Toolbox    | <b>TVAC</b>  | Thermal Vacuum                                    |
| <b>TT&amp;C</b> | Telemetry, Tracking and Command | <b>USD</b>   | United States Dollar                              |
| <b>WBS</b>      | Work Breakdown Structure        | <b>WFD</b>   | Work Flow Diagram                                 |

## Executive Overview

*Contributors: Iván, Isha, Milan, Jim*

At 30 AU, Neptune is the farthest known planet in the Solar System. Beyond it lies the Kuiper Belt, extending to 50 AU, with clustered Trans-Neptunian Objects (TNOs) possibly indicating an unidentified mass, potentially a planet called Planet 9. The NIBIRU mission, launching in 2038, aims to image and characterise Planet 9. The report details the design of this mission, emphasising the challenge of reaching Planet 9 within 50 years. This mission will travel farther than any human-made object and make a close approach to the Sun. Careful design of all subsystems and their integration is imperative, and this is the report's focus.

### Mission Objectives

The mission objectives are divided into primary and secondary aims. The primary objectives focus on measurements taken when observing Planet 9, advancing our understanding of its characteristics. These objectives include confirming the existence and location of Planet 9, estimating its mass and radius, capturing an iconic image for press release, identifying surface and atmospheric features, detecting moons or rings, determining atmospheric composition, analysing oxygen isotope ratios, and identifying potential biosignatures. Confirming Planet 9's location will involve indirect measurements through gravitational perturbations observed in Kuiper Belt Objects (KBOs), refining the trajectory and increasing mission success chances.

The secondary objectives are pursued during the trajectory, post-commissioning phase, or if Planet 9's location is inaccurately predicted. These objectives include characterising solar system planets used for gravity assists, studying targets of opportunity in the Kuiper Belt, and analysing the termination shock, heliopause, and heliosphere bow shock. By collecting data during gravitational assists and throughout its journey, NIBIRU will contribute valuable scientific information about these regions and the interstellar medium.

### Summary of Concept Trade-off

Before the detailed design phase, an extensive trade-off was performed to select the mission concept for the team to proceed with. Four mission concepts were considered: Concept C1 involves a spacecraft that will physically reach Planet 9 and perform in-situ measurements, communicating directly with Earth. This concept can fulfill all main mission objectives. Concept C2 is similar to C1 but communicates with Earth through relay satellites, allowing for stronger signal and more data transmission. Concept C3 features a single space telescope orbiting close to Earth, observing Planet 9 from afar and performing imaging

and spectroscopy in the infrared spectrum. Concept C4 involves a constellation of four space telescopes orbiting close to Earth, working together as an interferometric array for higher resolving capability.

Six criteria were used for the trade-off: Science Objectives, Risk, Cost, Communications, Flexibility, and Sustainability. Science Objectives assess the spacecraft's ability to fulfill mission objectives, including mass and radius estimation, atmospheric and surface composition, presence of moons and rings, and spatial resolution. Risk evaluates the concept's exposure to complexity and profile risks. Complexity risks include design, trajectory, operational complexity, and technology readiness level (TRL). Profile risks include the number of spacecraft, cruise phase survivability, and mission duration feasibility. Cost assesses the financial performance, distinguishing between development, production, manufacturing, and operational costs. Communications evaluates the ability to communicate with Earth, considering the ability to close the link budget and the signal-to-noise ratio. Flexibility assesses the concept's ability to deviate from its main objectives, considering required  $\Delta V$ , power needs, and secondary objectives. Sustainability evaluates the environmental impact, including the scale of ground operations and the type and amount of propellant used.

The trade-off matrix revealed that Concept C1 was the best-performing mission concept, scoring highest in Science Objectives, Risk, and overall feasibility. Sensitivity analysis showed C1 remained the winning concept in over 95% of scenarios, further validating the trade-off. Therefore, Concept C1, a spacecraft performing in-situ measurements and communicating directly with Earth, was chosen for the detailed design phase of this mission.

## Design Process

To facilitate a smooth design process for concept C1, a specific approach was adopted which included making a Functional Breakdown Structure (FBS), a Functional Flow Diagram (FFD), using several design tools and adopting an iteration process. To begin the design, mission requirements were reviewed, ensuring the spacecraft meets these throughout the design phase. Key requirements include the incorporation of an imaging system, high-resolution imaging capabilities, a stable communication link at 550 Astronomical Units (AU), instruments for mass and radius determination of Planet 9, subsystems with at least a 50-year lifespan, resistance to radiation and vibrational loads, communication and orientation capabilities, and adherence to cost and timeline constraints.

A model-based systems engineering (MBSE) tool was used to centralise all engineering information, facilitating tracking subsystem components, requirements, and iterations, ensuring organized and accessible information. Subsystem design required constant monitoring of inter-subsystem influences. Changes in one subsystem could affect others, necessitating clear communication among team members. Models were designed to ensure matching inputs and outputs, facilitating accurate subsystem sizing and integration.

## Subsystem Detailed Design

### Payload

The payload subsystem is responsible for fulfilling the missions science objectives. A small market analysis was performed to find similar missions and their instruments. With science instruments always being purpose- designed and built representative instruments were found to find mass, power and thermal properties to aid other subsystems in design.

Four instruments were selected: the N'LORRI imager capable of taking an iconic image from 50 million km away, the ISHTAR imaging spectrometer to characterise the planet's atmospheric and surface composition, the NCREX cosmic ray telescope to characterise the cosmic ray environment en-route to Planet 9, and the PSP particle science package to characterise lower energy radiation and particles encountered during the trajectory. Additionally the large telecommunications antenna will allow estimation of Planet 9's mass through Doppler tracking.

### EPS

The Electrical Power Subsystem (EPS) for the mission involves power generation, storage, and distribution to ensure the spacecraft operates effectively throughout the mission. Initially, a market analysis was

conducted to evaluate the available options for these components. NASA's eMMRTG was chosen for power generation due to its advanced development stage and expected readiness by 2038. Despite more advanced radioisotope thermoelectric generators (RTGs) being proposed, their lower technology readiness levels made the eMMRTG the most viable option.

Power generation will rely on two eMMRTGs, each providing an initial power of 145 W with a degradation rate of 2.5% per year, resulting in an estimated 39.866 W after 51 years en-route to Planet 9. Since this output is insufficient alone, the subsystem incorporates four VES16 8s4p batteries from Saft, each with a 512 Wh capacity. These batteries provide additional power during peak demands and recharge during low-power modes.

The final EPS design comprises two eMMRTGs, one Power Conditioning and Distributing Unit (PCDU), and four VES16 8s4p batteries, totaling 157.989 kg. The eMMRTGs are mounted externally, while the PCDU and batteries are housed inside the spacecraft. Operational modes were established to manage power effectively: SAFE, OPERATIONS, COMMUNICATIONS, and CHARGE. Each mode dictates the status of subsystems to optimise power usage, ensuring mission objectives can be achieved even with limited power availability.

## **TT&C**

The Telecommunications (TT&C) subsystem is designed to ensure reliable communication between the spacecraft and the ground stations, which is crucial for mission success. It comprises a complex arrangement of components, including antennas, transceivers and other communication hardware.

First, a market analysis was conducted to identify the most effective communication technologies used in previous deep space missions. This analysis highlighted the need for a large, deployable antenna capable of maintaining long-distance communications with Earth. The subsystem includes a main foldable antenna with a diameter of 7.81 [m], offering a high gain of 54 [dB] and a narrow beamwidth of 0.33 [degrees] to optimise signal strength and integrity over vast distances. The main antenna's specifications, including its power output of 568 [W] and a bit rate of 264 [bps], were carefully calculated to meet the mission's requirements while ensuring efficient power consumption and data handling capabilities.

Additionally, the hardware setup includes robust cables, sophisticated transceivers capable of both sending and receiving data, frequency converters and modulators/demodulators to process signals effectively. A series of filters (low-pass, high-pass and notch) were also integrated to minimise noise and prevent interference, ensuring clear and reliable communication channels.

The TT&C subsystem's deployment strategy incorporates a dual-antenna configuration to enhance reliability and continuous connectivity, particularly through challenging conditions such as those expected at the Kuiper Belt. The secondary smaller antenna acts as a backup, maintaining communication during the deployment phase of the main antenna or in the event of failure.

## **ADCS**

The Attitude Determination and Control System (ADCS) plays a role in managing the spacecraft's orientation and position for mission-critical tasks such as communication, navigation and scientific observations. The ADCS design began with an extensive market analysis, focusing on selecting the most efficient sensors and actuators suitable for long-duration deep space operations.

The control method during cruise phases involves spin stabilization, chosen for its low power consumption and simplicity. During critical operations such as scientific observations or close flybys, three-axis stabilization is employed, utilizing thrusters for precise control. This dual-method approach optimizes power use during less critical phases and enhances control during key mission events.

Due to the mission's power constraints and the need for efficient maneuvering, hydrazine thrusters were chosen, specifically, Aerojet Rocketdyne's MR-401 0.08N and MR-111G 4N. The chosen sensors, the HORUS star trackers and the Honeywell HG9900 Inertial Measurement Units (IMUs), were evaluated against mission requirements such as power consumption, mass, and pointing accuracy. The final design of the ADCS has a mass of about 260 kg, a power usage of 41 W and an estimated cost of 3.4 million Euros.

## Astrodynamics

In planning the mission to Planet 9, selecting the optimal trajectory is essential for minimising mission duration, fuel consumption, and ensuring overall success. This involves determining the most efficient path for the spacecraft, considering various trajectory requirements and simulation setups. Key requirements include achieving scientific objectives within 50 years and avoiding close proximity to the Sun.

The trajectory optimisation process utilised gravity assist and Oberth maneuvers to enhance spacecraft velocity. Gravity assists leverage the orbital motion of planets to alter the spacecraft's direction and speed, while Oberth maneuvers exploit higher velocities at periapsis to maximise velocity change. Simulations were conducted using the TUDelft Astrodynamics Toolbox (TUDAT), incorporating gravity assists from Jupiter and a solar Oberth maneuver. The trajectory was optimised to minimise the total  $\Delta V$ , crucial for efficient fuel use.

The optimised trajectory, departing Earth on January 22, 2038, involves a 7.47-year journey to Jupiter, a 2.10-year leg to the Sun, and a final 39.97-year leg to Planet 9. This results in a total mission duration of 49.5 years, successfully meeting the 50-year requirement. Further improvements could be explored by testing different optimization algorithms and transfer body orders.

## Propulsion

The propulsion system designed for the mission to Planet 9 is a highly optimised, pressure-fed liquid bipropellant system, specifically tailored to meet stringent mission requirements while maintaining cost-effectiveness and reliability. The selected propulsion type utilises nitrogen tetroxide (N<sub>2</sub>O<sub>4</sub>) and monomethylhydrazine (MMH) as the propellant combination, chosen for their high density and hypergolic properties, ensuring spontaneous ignition upon contact.

The propulsion system's design is required to deliver a total  $\Delta V$  of 4.84 [km/s], conform to a mass limit of 97,586 [kg], and fit within physical dimensions of 18 [m] in height and 7.6 [m] in width. To meet these specifications, the system incorporates several stages, which allows for the sequential use and discarding of propulsion components, thereby reducing mass and optimising the payload capacity throughout different mission phases. The first Energetic NIBIRU Kick Interstage (ENKI) and second Efficient NIBIRU Long-range Interstage Launcher (ENLIL) kick-stages carry 13,963 [kg] and 14,880 [kg] of propellant respectively, ensuring sufficient thrust for critical mission maneuvers.

Thrust generation is optimised to minimise burn time and maximise efficiency, with an emphasis on reducing gravity losses. The selected thrusters are capable of achieving these operational requirements while supporting a rapid burn cycle to conserve fuel and reduce the mission's overall duration.

## Thermal Control

The Thermal Control System (TCS) for the NIBIRU mission uses off-the-shelf components, drawing from missions like New Horizons and Parker Solar Probe. New Horizons employed Multi-Layered Insulation (MLI) and radiators to maintain its temperature, while Parker Solar Probe utilised a thermal protection system to shield against intense solar radiation. The NIBIRU mission will combine these approaches to handle both cold and hot environments, using components such as Kapton ITO for MLI and ceramic carbon tiles for heat protection.

The thermal control requirements include continuous temperature monitoring and maintaining the spacecraft's temperature between 270 and 290 K. The design process begins with simplifying assumptions and defining the thermal environment for both the Beginning-of-Life (BoL) and End-of-Life (EoL) stages.

Thermal control for the kickstages, ENKI and ENLIL, was designed to maintain a temperature between 270 and 290 K as well. For proximity to the Sun, a heat shield similar to that of Parker Solar Probe was proposed, scaled to the NIBIRU mission's requirements. The kickstages used ceramic carbon tiles for thermal protection, iteratively designed to balance heat input and dissipation.

The TCS uses components such as radiators, thermal sensors, and MLI, with detailed specifications ensuring the system meets all requirements. The final mass of the TCS is 441.62 kg, with a power usage of 12 mW and a cost of €545,304.89, ensuring a reliable thermal control system for the NIBIRU mission.

## Structures and Materials

A trade-off analysis was conducted to select the material for the main structure, considering common space application materials like aluminum, magnesium, titanium, beryllium alloys, steel, and composites. The chosen material was Aluminium 2024-T36, followed by CFRP-epoxy and 6061-T6.

The central tube structure was chosen for its efficient load transfer, crucial for handling NIBIRU's heavy launch loads. This cylindrical structure will be surrounded by panels arranged cubically for increased strength and protection. The main load-carrying cylinder was sized to prevent structural failure from vibrations and quasi-static loads during launch and ascent. NIBIRU and its kickstages will be designed as two cantilevered beams, assuming efficient load transfer between stages. The spacecraft bus and kickstages have heights of 1.5 m and 14.05 m, respectively. The cylinder's diameter for the spacecraft bus is 0.9 m, fitting all components, while the kickstage matches the Payload Adapter Fitting (PAF) at 2.624 m for efficient load transfer. Final cylinder masses are 27.02 kg (spacecraft bus) and 3709.64 kg (kickstages), with thicknesses of 2.083 mm and 11.52 mm, respectively.

For micrometeoroid protection, a 40PPI core Open Foam Aluminum Panel sandwich structure with a 25.4 mm core and 0.254 mm face and rear thicknesses was chosen, being capable of stopping debris up to 3 mm in diameter at 7 km/s. The panels weigh 82.865 kg in total and are connected by vertical and horizontal stringers.

Regarding radiation protection, aluminum is an excellent shielding material, about 100 times more resistant than other common spacecraft materials. MLI adds extra protection against solar and infrared radiation. Additionally, NIBIRU will endure extreme solar radiation, protected by a specialised shield inspired by the Solar Parker Probe. The ENLIL kickstage will also have ceramic tile protection on the side facing the Sun. However, further research is needed to confirm the efficacy of these protections for the mission.

## OBDH

The final design of the On-Board Data Handling (OBDH) system features architecture tailored for deep space exploration. Central to the system is the OBC, which manages all spacecraft operations, data handling, fault detection, and recovery. The OBC utilises a Mongoose V processor, supported by an EEPROM for non-volatile memory and SRAM for temporary data storage. An FPGA accelerates AI and machine learning tasks.

The system employs a network architecture for high data rates and fault tolerance, with a DHAU for subsystem telemetry and a CHU for subsystem commands. Scientific and critical telemetry data are stored in an SSR with an 8 GByte capacity, ensuring ample storage for long missions. The clock, a deep space crystal oscillator, provides precise timekeeping essential for navigation and operations. Redundant hardware, housed in an IEM made of aluminum for radiation protection, ensures mission continuity. The design meets stringent requirements for reliability, autonomy, and data handling, making it suitable for the mission's extended duration and harsh conditions in the outer solar system.

## System Integration

System integration for NIBIRU involved designing and assembling the final CAD model in 3DEXperience, a Computer Aided Design (CAD) tool. The compliance matrix was created to ensure that all mission requirements are met.

The total mass of the NIBIRU spacecraft is 40,648 kg with the spacecraft itself weighing 2,400 kg, the kickstage ENKI 18,575 kg, and the kickstage ENLIL 19,673 kg. Power distribution is optimised to maintain stable communications while keeping all subsystems functional. The final design ensures all components are compliant with mission requirements, verified through rigorous testing and inspection, and supported by detailed technical diagrams and budget calculations.

## Sensitivity Analysis

Sensitivity analysis was conducted on the spacecraft mass,  $\Delta V$ , power and cost. For the mass, the focus was on the propulsion subsystem due to its significant mass contribution. Key parameters assessed included the spacecraft dry bus mass, required  $\Delta V$  for each stage, number of stages, and propellant

properties. The required  $\Delta V$  exhibited the most uncertainty, significantly impacting total spacecraft mass, especially propellant mass.

The spacecraft’s mass is highly sensitive to the required V, especially during the closest approach to the Sun due to the Oberth maneuver’s effectiveness. Sensitivity analysis shows that increasing the Solar Oberth Maneuver distance significantly raises the required V, with a permissible offset of 1.496 million km given the propulsion system’s capability.

Spacecraft power, crucial for subsystem operation and communication, was analysed, focusing on OBDH and ADCS subsystems. OBDH power consumption, driven by computer and SSR components, showed moderate sensitivity. ADCS, the most power-intensive subsystem, was highly sensitive to changes in sensor power consumption, affecting overall mission feasibility. These analyses highlighted the importance of accurate  $\Delta V$  and power estimations for successful mission design and execution.

Mission costs are highly sensitive to unexpected design and development expenses, as seen with the James Webb Telescope’s cost overruns. The design and development phase can see fluctuating yearly costs between €25M and €200M. Component production costs, mostly for off-the-shelf components, are expected to remain stable. Ground segment costs depend on contact hours with the Deep Space Network, scaling with the amount of data sent. Mission operations costs vary significantly, influenced by the level of spacecraft autonomy, with yearly costs ranging from €10M to €30M, impacting the total mission cost substantially. Thus, precise budgeting and cost management are critical to the mission’s success.

### Technical Risk Assessment

Technical risks were split by space segment, as well as schedule and cost risks. In total 114 risks were identified, and out of these 43 risks needed to be accepted with a contingency action in place. The highest level risks included those to do with the launcher, OBDH failure, and TT&C complications. Mitigation actions were devised for each risk and the risk maps before and after undertaking mitigation actions are shown in table 7.5 and table 7.6.

Table 1: Pre-Mitigation and Post-Mitigation Risk Maps

Table 2: Pre-Mitigation Risk Map

|        |              |   |  |   |  |                                    |
|--------|--------------|---|--|---|--|------------------------------------|
| Impact | Catastrophic | RSK-STR-06, RSK-STR-07, RSK-STR-13, RSK-COM-01, RSK-COM-06, RSK-EPS-07, RSK-ADC-09, RSK-AST-03, RSK-OBDH-01, RSK-OBDH-04, RSK-OBDH-06, RSK-OBDH-08, RSK-OBDH-12, RSK-OBDH-17, RSK-OBDH-24 | RSK-STR-01, RSK-STR-08, RSK-STR-10, RSK-STR-12, RSK-COM-04, RSK-EPS-01, RSK-EPS-06, RSK-TCS-02, RSK-TCS-04, RSK-TCS-08, RSK-TCS-10, RSK-ADC-10, RSK-ADC-11, RSK-PRO-02, RSK-PRO-03, RSK-AST-06, RSK-OBDH-22      | RSK-STR-02, RSK-STR-09  | RSK-AST-01   |                                    |
|        | Critical     | RSK-COM-08, RSK-ADC-08, RSK-PRO-04, RSK-OBDH-05, RSK-OBDH-10, RSK-OBDH-13, RSK-OBDH-16, RSK-OBDH-18, RSK-OBDH-23  | RSK-STR-03, RSK-STR-11, RSK-COM-07, RSK-EPS-02, RSK-PLD-03, RSK-PLD-04, RSK-TCS-01, RSK-TCS-05, RSK-ADC-01, RSK-ADC-03, RSK-OBDH-07, RSK-OBDH-11, RSK-OBDH-15, RSK-OBDH-21, RSK-OBDH-25, RSK-OBDH-27, RSK-SCH-11 | RSK-STR-05, RSK-COM-02, RSK-EPS-04, RSK-PLD-05, RSK-TCS-03, RSK-TCS-06, RSK-TCS-09, RSK-ADC-02, RSK-ADC-04, RSK-PRO-01, RSK-AST-04, RSK-AST-07, RSK-OBDH-02, RSK-OBDH-03, RSK-OBDH-14, RSK-OBDH-26, RSK-OBDH-28, RSK-SCH-04, RSK-SCH-07, RSK-SCH-08 | RSK-PLD-02, RSK-AST-02, RSK-SCH-01, RSK-SCH-02, RSK-SCH-03, RSK-SCH-05, RSK-SCH-10 | RSK-CST-03                         |
|        | Marginal     | RSK-COM-05, RSK-ADC-07  | RSK-EPS-05, RSK-PLD-01, RSK-TCS-07, RSK-ADC-06, RSK-OBDH-09  | RSK-TCS-11, RSK-CST-02  | RSK-AST-05, RSK-SCH-06, RSK-SCH-09, RSK-CST-01, RSK-CST-04                         | RSK-STR-04, RSK-PRO-06, RSK-CST-01 |
|        | Negligible   |   | RSK-EPS-03   | RSK-OBDH-19, RSK-OBDH-20  |  | RSK-COM-03                         |
|        |              | Improbable  | Remote   | Occasional  | Probable   | Frequent                           |
|        |              |   |  | Likelihood  |  |                                    |

Table 3: Post-Mitigation Risk Map

|        |              |   |  |   |                                    |          |
|--------|--------------|---|--|---|------------------------------------|----------|
| Impact | Catastrophic | RSK-STR-06, RSK-STR-13, RSK-COM-01, RSK-EPS-07, RSK-AST-03, RSK-OBDH-01   | RSK-STR-02, RSK-STR-10, RSK-STR-12, RSK-COM-04, RSK-EPS-01, RSK-EPS-06, RSK-TCS-02, RSK-TCS-08, RSK-TCS-10, RSK-PRO-02, RSK-PRO-03, RSK-AST-06   |   |                                    |          |
|        | Critical     | RSK-STR-07, RSK-COM-06, RSK-COM-08, RSK-ADC-09, RSK-PRO-04, RSK-OBDH-06, RSK-OBDH-08, RSK-OBDH-10, RSK-OBDH-12, RSK-OBDH-16, RSK-OBDH-17, RSK-OBDH-18 | RSK-STR-01, RSK-STR-03, RSK-STR-05, RSK-STR-08, RSK-STR-09, RSK-STR-11, RSK-COM-07, RSK-EPS-02, RSK-PLD-03, RSK-TCS-04, RSK-TCS-05, RSK-TCS-06, RSK-TCS-09, RSK-ADC-01, RSK-ADC-02, RSK-ADC-03, RSK-ADC-04, RSK-ADC-05, RSK-PRO-01, RSK-PRO-05, RSK-AST-04, RSK-AST-07, RSK-OBDH-03, RSK-OBDH-07, RSK-OBDH-27, RSK-OBDH-28, RSK-SCH-04, RSK-SCH-08, RSK-SCH-11 | RSK-COM-02, RSK-PLD-02, RSK-AST-02, RSK-OBDH-02, RSK-SCH-01, RSK-SCH-02, RSK-SCH-03, RSK-SCH-07, RSK-SCH-10, RSK-CST-03 |                                    |          |
|        | Marginal     | RSK-COM-05, RSK-OBDH-04, RSK-OBDH-09, RSK-OBDH-13, RSK-OBDH-15, RSK-OBDH-23, RSK-OBDH-24  | RSK-PLD-05, RSK-TCS-03, RSK-TCS-05, RSK-TCS-07, RSK-TCS-11, RSK-ADC-06, RSK-ADC-10, RSK-OBDH-11, RSK-OBDH-14, RSK-OBDH-21, RSK-OBDH-22, RSK-OBDH-25, RSK-ADC-07, RSK-OBDH-05   | RSK-PRO-06, RSK-AST-01, RSK-SCH-05, RSK-SCH-06, RSK-SCH-09, RSK-CST-04  | RSK-STR-04, RSK-AST-05, RSK-CST-01 |          |
|        | Negligible   |   | RSK-EPS-03   |   | RSK-COM-03                         |          |
|        |              | Improbable  | Remote   | Occasional  | Probable                           | Frequent |
|        |              |   |  | Likelihood  |                                    |          |

### Market Analysis

A comprehensive market analysis was crucial for the NIBIRU spacecraft design, highlighting opportunities and strategic utilisation. The analysis provided insight into various subsystems, revealing opportunities and strategic utilisation.

The cost breakdown shows the total subsystem cost at €367.3 million. Including design, development, operations, and safety budgets, the total mission cost is €3441.6 million. A significant portion of the budget is allocated for ground operations and the Deep Space Network, with an annual operational cost of €26.56 million over 50 years, totalling €1328 million. The launch, not included in the budget, is estimated at €2 million.

The ROI is promising, considering the growing spacecraft market, expected to reach \$10.4 billion by 2032, and the increasing number of deep space missions. NIBIRU's unique mission to Planet 9 will provide unprecedented data on the outer solar system, potentially increasing public interest and funding for future missions. The societal impact includes advancements in science, technology, education, and culture. Exploring Planet 9 will refine planetary formation models and inspire future generations in STEM fields. The mission will also drive technological innovation in propulsion, communication, and materials science, with potential spin-offs benefiting other industries.

## **Sustainable Development Strategy**

Sustainability can be defined as "The ability to meet the needs of the present at a global scale without compromising the ability of future generations to meet their own needs" [2]. Hence, the design of NIBIRU involves the integration of sustainability principles that maintain environmental, social and economic health over time without depleting resources or harming ecosystems. For this, the launcher, propulsion and power generation, material selection, and trajectory performance were adequately weighed against sustainability, to ensure the most sustainable mission possible without harming mission feasibility.

A mission to Planet 9 can enhance sustainability through technological advancements, scientific research, and inspiring policies focused on sustainable development. Successful space missions foster global cooperation, which can improve global resource management and prioritize sustainable development.

## **Project Design and Development**

The Project Design & Development (PDD) phase for NIBIRU focuses on post-DSE activities, involving detailed design, manufacturing, testing, and integration, ensuring the spacecraft's readiness for a 2038 launch. The project timeline, visualised in a Gantt chart, spans 10 years and involves extensive collaboration among thousands of individuals.

The detailed design phase, lasting four years, will refine the mission's components, influenced by updates on Planet 9's location. Key partners such as Thales Alenia Space and Airbus will lead the manufacturing process, ensuring the assembly of complex components across various specialised facilities.

Testing will occur concurrently with manufacturing, focusing on rigorous structural and thermal evaluations. ESA's ESTEC facility will be pivotal, providing vibration, acoustic, shock, thermal vacuum, and electromagnetic compatibility testing. Integration and launch preparation involve assembling the Proto-Flight Model (PFM), Flight Model (FM), and a spare, readying them for launch from Kennedy Space Center. The spacecraft will undergo final checks, RTG installation, and fueling before integration with SpaceX's Starship.

The Reliability, Availability, Maintainability, and Safety (RAMS) analysis ensures the design meets high standards for mission longevity. This involves extensive testing of Commercial-of-the-shelf (COTS) components and adherence to safety protocols during manufacturing and assembly. The operational phases, from launch to end-of-life, include commissioning, secondary objectives like studying Jupiter and the Kuiper Belt, and primary objectives focused on Planet 9. The spacecraft will use its advanced communication systems and autonomous operations to achieve its scientific goals, ensuring a significant return on investment through valuable data acquisition and long-term mission success.

## **Recommendations**

Several recommendations are made to further improve the design presented in this report. Firstly, further research should be conducted to develop a more detailed thermal control solution to protect the spacecraft during the solar Oberth maneuver at 10 solar radii. Additionally, a close Sun maneuver would not be necessary if more RTGs could be used. Since RTGs degrade over time, having additional units would ensure that the required power for NIBIRU at end-of-life could be maintained for over 50 years. This would allow for a longer journey to Planet 9 with less reliance on flyby bodies for  $\Delta V$  assistance. Finally, the N'LORRI camera on NIBIRU can resolve Planet 9 from about 21 AU. If Planet 9 is not exactly at the hypothesised location but somewhere in the vicinity, a trajectory adjustment would require only a minimal amount of thrust, which could be managed using the on-board ADCS propellant.

## TABLE OF CONTENTS

|  |           |  |            |
|--|-----------|--|------------|
| Nomenclature                                 | i         | 5.2 Compliance Matrix . . . . .                      | 88         |
| Executive Overview                           | ii        | 5.3 Technical Diagrams . . . . .                     | 90         |
| Introduction                                 | 1         | 5.4 Budget Breakdowns . . . . .                      | 90         |
| <b>1 Mission Objectives</b>                  | <b>1</b>  | <b>6 Sensitivity Analysis</b>                        | <b>91</b>  |
| 1.1 Primary Objectives . . . . .             | 2         | 6.1 Spacecraft Mass . . . . .                        | 91         |
| 1.2 Secondary Objectives . . . . .           | 2         | 6.2 $\Delta V$ . . . . .                             | 92         |
| <b>2 Summary of Concept Trade-off</b>        | <b>3</b>  | 6.3 Spacecraft Power . . . . .                       | 92         |
| 2.1 Mission Concepts . . . . .               | 3         | 6.4 Cost . . . . .                                   | 95         |
| 2.2 Trade-off Criteria . . . . .             | 3         | 6.5 Planet 9 Location . . . . .                      | 97         |
| 2.3 Trade-off Weights . . . . .              | 4         | <b>7 Technical Risk Assessment</b>                   | <b>98</b>  |
| 2.4 Trade-off Results . . . . .              | 4         | 7.1 Risk Identification & Assessment . . . . .       | 98         |
| <b>3 Design Process</b>                      | <b>4</b>  | 7.2 Risk Mitigation . . . . .                        | 107        |
| 3.1 Requirements . . . . .                   | 4         | 7.3 Contingency Plan . . . . .                       | 111        |
| 3.2 Functional Diagrams . . . . .            | 5         | 7.4 Risk Maps . . . . .                              | 113        |
| 3.3 Model Based System Engineering . . . . . | 5         | <b>8 Market Analysis</b>                             | <b>115</b> |
| 3.4 Iteration Process . . . . .              | 5         | 8.1 Cost Breakdown . . . . .                         | 115        |
| <b>4 Subsystem Detailed Design</b>           | <b>5</b>  | 8.2 Return on Investment . . . . .                   | 116        |
| 4.1 Payload . . . . .                        | 5         | 8.3 Societal Impact . . . . .                        | 117        |
| 4.2 EPS . . . . .                            | 12        | 8.4 Market Gap . . . . .                             | 118        |
| 4.3 Telecommunications . . . . .             | 16        | <b>9 Sustainable Development Strategy</b>            | <b>119</b> |
| 4.4 ADCS . . . . .                           | 23        | 9.1 Sustainability in Design . . . . .               | 119        |
| 4.5 Astrodynamics . . . . .                  | 34        | 9.2 Product Contribution to Sustainability . . . . . | 120        |
| 4.6 Propulsion . . . . .                     | 42        | <b>10 Project Design &amp; Development</b>           | <b>121</b> |
| 4.7 Thermal Control System . . . . .         | 52        | 10.1 Activities after DSE . . . . .                  | 121        |
| 4.8 Structures and Materials . . . . .       | 60        | 10.2 RAMS Analysis . . . . .                         | 124        |
| 4.9 On-Board Data Handling . . . . .         | 73        | 10.3 Operations and Logistics . . . . .              | 126        |
| <b>5 System Integration</b>                  | <b>87</b> | <b>Conclusion</b>                                    | <b>128</b> |
| 5.1 Final CAD Model . . . . .                | 87        |  |            |

# Introduction

*Contributors: Pepijn, Jim, Isha*

At a distance of 30 Astronomical Units (AU), Neptune is currently the farthest known planet in the Solar System. Beyond Neptune lies the Kuiper Belt, extending to approximately 50 AU, which contains the Solar System's most distant known objects [3]. According to Batygin and Brown [4], a number of these Trans-Neptunian Objects (TNOs) typically cluster close to one another, which could indicate the presence of an unidentified mass farther from the Sun. This mass could be large enough to be a super-Earth or a mini-Neptune. However, the possibility of this mass being a cluster of KBOs, a primordial black hole, or a grouping of dark matter has not been completely discarded [5]. Therefore, due to the substantial evidence supporting the existence of this new planet, which has been named Planet 9, astronomers are currently conducting thorough searches. Characterising Planet 9 would be extremely valuable in understanding the origins and development of planetary formation. The prospect of it being a super-Earth is particularly intriguing, given that numerous extrasolar star systems contain super-Earths. This is where the NIBIRU (Novel, Intelligent, Beyond Interplanetary Research Unit) mission comes in. If NIBIRU confirms that Planet 9 is a super-Earth, it could imply that our Solar system shares more similarities with other star systems than what is currently believed [6].

Observations from Earth are challenging due to the minimal reflection of Solar rays by a planet located at 550 AU [5, 7]. Therefore, observations will need to be done from space, and this is where NIBIRU comes in. NIBIRU aims to launch in 2038, travel to Planet 9, and image and characterise the physical properties of the planet. One of the toughest requirements is reaching Planet 9 within 50 years, which means designing a mission that will travel farther than any human-made object and make one of the closest approaches to the Sun. This necessitates careful design and integration of all subsystems, which is the focus of this report.

In previous reports, the conceptual design was laid out, as well as a trade-off between possible mission configurations. This report serves to detail the final design of the NIBIRU mission. According to a study done in February 2024 [7], researchers investigated the potential locations of Planet 9, determining that approximately 78% of the sky does not contain this elusive celestial body. This finding suggests that if Planet 9 exists, it is likely confined to the remaining 22% of the sky. For the purposes of our mission design, it is assumed that Planet 9 is located centrally within this 22% range and has a semi-major axis of 550 AU [7]. It is recognised that as new data becomes available, the assumed location may need adjustment, impacting the mission design. However, this approach allows us to use the mission as a demonstrator for advanced space exploration techniques. Additionally, our mission design also has secondary objectives that will be pursued along the spacecraft's trajectory. These objectives ensure that the mission remains valuable and yields scientific returns, even if Planet 9 is not found in the anticipated location.

The report is structured as follows. Chapter 1 outlines the objectives of the NIBIRU mission. Next, chapter 2 provides a summary of the trade-off performed in the previous design phase as a recap. Following this, chapter 3 explains the plan of action for this detailed design phase. Chapter 4 delves into the detailed design of each subsystem, including the trajectory design. The integration of subsystem designs at the system level is presented in chapter 5, which includes a 3D render of the spacecraft. After finalizing the design, it is crucial to define its sensitivity to parameters that could lead to infeasibility, which is addressed in chapter 6. Additionally, the technical risks associated with the mission are outlined in chapter 7, and a market analysis is conducted in chapter 8. To ensure the mission's development is sustainable, chapter 9 describes the strategy to achieve this. Finally, chapter 10 delves into the project design and development of the NIBIRU mission.

# 1 Mission Objectives

In this chapter, the objectives of the mission will be outlined, including both primary and secondary aims. The primary objectives in section 1.1 will detail the purposes for which NIBIRU is designed, while the secondary objectives in section 1.2 are posed to increase the scientific value of the mission. These secondary goals can be pursued during the trajectory to Planet 9, after the commissioning phase, or in the event that Planet 9 is at a different location than anticipated.

## 1.1 Primary Objectives

*Contributors: Isha*

The primary objectives of NIBIRU's mission focus on the measurements that can be taken when it is directly looking at Planet 9. These objectives are crucial for advancing our understanding of this celestial body and its characteristics. The primary objectives of this mission can be seen below in table 1.1:

**Table 1.1:** Primary Objectives

|  |   |   |  |
|--|---|---|--|
| <b>PL9-SCO-08:</b> Confirm the location of Planet 9  | <b>PL9-SCO-01:</b> Estimate mass and radius of Planet 9 | <b>PL9-SCO-02:</b> Take an iconic picture of Planet 9 for press release | <b>PL9-SCO-03:</b> Identify surface/atmospheric features |
| <b>PL9-SCO-04:</b> Determine presence of moons/rings | <b>PL9-SCO-05:</b> Determine atmospheric composition    | <b>PL9-SCO-06:</b> Determine oxygen isotope ratios                      | <b>PL9-SCO-07:</b> Identify potential biosignatures      |

One of the primary objectives, which involves confirming the existence of Planet 9, will be approached differently. By travelling to Planet 9, NIBIRU will conduct measurements on KBOs and transmit the collected data back to Earth. This data will be used to monitor newly discovered KBOs in the region. By continuously observing these KBOs from Earth, we aim to detect gravitational perturbations that they may experience. These perturbations can provide indirect evidence of Planet 9's existence, location, and other orbital parameters. Furthermore, the data gathered and the improved estimates of its parameters will be useful in refining the trajectory. The continuous monitoring and analysis of KBO trajectories will help us make necessary corrections, thereby increasing the chances of a completely successful mission.

## 1.2 Secondary Objectives

*Contributors: Isha*

In addition to the primary objectives, the mission includes several secondary objectives that can be pursued during the trajectory, after the commissioning phase, or in the event that Planet 9's location is inaccurately predicted. These secondary goals ensure that the mission remains valuable and productive, thereby reducing the risk of mission failure. Most of these objectives can be carried out during the trajectory phase itself, maximising the scientific return of the mission. The secondary objectives below in table 1.2.

**Table 1.2:** Secondary Objectives

|  |  |  |   |  |
|--|--|--|---|--|
| <b>PL9-SCO-09:</b><br>Characterise solar system planets used for gravity assists | <b>PL9-SCO-10:</b><br>Characterise targets of opportunity in the Kuiper belt | <b>PL9-SCO-11:</b><br>Characterise termination shock | <b>PL9-SCO-12:</b><br>Characterise heliopause | <b>PL9-SCO-13:</b><br>Characterise heliosphere bow shock |
|--|--|--|---|--|

As the spacecraft will perform gravitational assist maneuvers around solar system planets, it will collect data to characterise these systems. This could include studying the planets' atmospheres, magnetic fields, and anything else of interest to the scientific community at the time. During the transit through the Kuiper Belt, NIBIRU will identify and study various KBOs. These observations will provide valuable information about the composition, structure, and dynamics of these distant solar system bodies, and aid in understanding how Planet 9 might affect gravity perturbations. Furthermore, the spacecraft will

measure and analyse the termination shock, which is the boundary where the solar wind slows down abruptly as it meets the interstellar medium [8]. The heliopause is the boundary between the heliosphere and interstellar space [8]. The spacecraft will gather data to characterise this region, providing insights into the interactions between solar and interstellar winds. Finally, the mission will study the heliosphere bow shock, the area where the interstellar medium is deflected around the moving heliosphere [8]. This information will improve our understanding of how our solar system interacts with the interstellar environment.

Even in the event that Planet 9 becomes an unreachable target during the trajectory, the NIBIRU mission will serve as a valuable technology demonstrator. The spacecraft's ability to travel to a distance of 550 AU, an effort never accomplished before, will showcase advancements in space travel technology and long-duration deep space missions. This capability ensures that the mission can continue making observations and collecting data in deep space, contributing to our overall knowledge of the solar system and beyond.

## 2 Summary of Concept Trade-off

Before this detailed design phase, an extensive trade-off was performed to select the mission concept the team would go forward with for detailed design. In this chapter, this trade-off will be summarised. First, in section 2.1, the four main mission concepts that were deemed feasible enough for the trade-off will be explained. Then, in section 2.2, the trade-off criteria and sub criteria will be addressed. Next, section 2.3 will talk about the weights of these criteria. Section 2.4 will show the trade-off table and final choice of mission concept that was chosen to go into the detailed design.

### 2.1 Mission Concepts

*Contributors: Anton, Flavio, Pepijn*

Four mission concepts were considered in performing the trade-off. These are summarised below.

- **Concept C1:** a spacecraft that will physically reach Planet 9 and perform in-situ measurements. This has the advantage of being capable of fulfilling all of the main mission objectives set by the project guide [9]. The spacecraft communicates directly with Earth.
- **Concept C2:** a spacecraft that will physically reach Planet 9 and perform in-situ measurements. The spacecraft will communicate with Earth through relay satellites, which allow for a stronger signal. This design allows more data to be transmitted back to Earth in same time span.
- **Concept C3:** a single space telescope orbiting close to Earth that observes Planet 9 from afar. The spacecraft will consist of a single collecting surface and will be capable of performing imaging and spectroscopy tasks in the infrared part of the spectrum.
- **Concept C4:** a constellation of four space telescopes orbiting close to Earth that observes Planet 9 from afar. The telescopes work together as an interferometric array, and perform imaging and spectroscopy tasks in the infrared part of the spectrum. Due to the higher baseline, the constellation will have a higher resolving capability than a single telescope.

### 2.2 Trade-off Criteria

*Contributors: Flavio*

The process of selecting appropriate criteria is a decisive step of the trade-off, as it directly affects the outcome of the latter. For this reason, a key requirements analysis was performed, also taking into account the important of each stakeholder. The stakeholders and their requirements were ranked by relevance to the mission. Out of the 12 criteria that were initially defined, the ones that were considerably less relevant have been immediately discarded. Merging the remaining criteria that had points in common, left the team with only six trade-off criteria in the end. For each criterion, some sub-criteria were specified to facilitate the scoring process for each mission concept.

Six criteria were used for the trade-off: Science Objectives, Risk, Cost, Communications, Flexibility, and Sustainability. Science Objectives assess the spacecraft's ability to fulfill mission objectives, including mass and radius estimation, atmospheric and surface composition, presence of moons and rings, and

spatial resolution. Risk evaluates the concept’s exposure to complexity and profile risks. Complexity risks include design, trajectory, operational complexity, and Technology Readiness Level (TRL). Profile risks include the number of spacecraft, cruise phase survivability, and mission duration feasibility. Cost assesses the financial performance, distinguishing between development, production, manufacturing, and operational costs. Communications evaluates the ability to communicate with Earth, considering the ability to close the link budget and the signal-to-noise ratio. Flexibility assesses the concept’s ability to deviate from its main objectives, considering required  $\Delta V$ , power needs, and secondary objectives. Sustainability evaluates the environmental impact, including the scale of ground operations and the type and amount of propellant used.

### 2.3 Trade-off Weights

*Contributors: Flavio*

Once the criteria have been defined, the last step before performing the trade-off is the assignment of weights to each of these criteria. The aforementioned key requirements analysis was particularly useful for this as it allowed the team to compile a ranking for the criteria based on importance. This in turn facilitated the implementation of the Best-Worst Method (BWM) [10], as each team member was able to compile their own relative criteria scores. The BWM outputted a weight for each of the criteria, which are shown below. Weights were later defined also for the sub-criteria to facilitate the ranking of mission concepts. It is important to note that these sub-criteria weights were not obtained using the BWM once more, rather they were defined based on critical thinking.

- |                             |                         |
|-----------------------------|-------------------------|
| 1. Science Objectives - 28% | 4. Communications - 15% |
| 2. Risk - 23%               | 5. Flexibility - 11%    |
| 3. Cost - 17%               | 6. Sustainability - 6%  |

### 2.4 Trade-off Results

*Contributors: Flavio*

Once all trade-off weights were determined, it was possible to score the mission concepts for each criterion. The scoring system used is: 4 (green): excellent, exceeds requirements, 3 (blue): good, meets requirements, 2 (yellow): correctable deficiencies, 1 (red): unacceptable. Once all mission concepts were scored, it was possible to compile a trade-off matrix, from which the best design was determined.

**Table 2.1:** Trade-Off Matrix, Showing C1 as the Winning Mission Concept

| Mission Concept | Science Objectives (28%) | Risk (23%) | Cost (17%) | Comms. (15%) | Flex. (11%) | Sus. (6%) | Weighted Average |
|-----------------|--------------------------|------------|------------|--------------|-------------|-----------|------------------|
| C1              | 4                        | 3          | 3          | 3            | 2           | 2         | 3.11             |
| C2              | 4                        | 1          | 2          | 2            | 2           | 1         | 2.27             |
| C3              | 1                        | 3          | 3          | 4            | 4           | 4         | 2.76             |
| C4              | 2                        | 2          | 2          | 4            | 4           | 3         | 2.58             |

As can be seen in table 2.1, it was concluded that C1 is the best performing mission concept for the criteria considered. It is also important to note that the second-best concept, C3, scored considerably lower than C1, which is desired, as it indicates that the trade-off had a sufficient confidence level. In the subsequent sensitivity analysis, when manipulating the criteria weights, C1 remained the winning concept for over 95% of the scenarios analysed, which further proved the validity of the trade-off. This means that the single spacecraft that will go to Planet 9 will be investigated further in this report, entering the detailed design.

## 3 Design Process

In this section, the design process for concept C1 will be explained. The technical diagrams that were used to start the detailed design, the used tools and the iteration process are shown.

### 3.1 Requirements

*Contributors: Thijmen*

The mission requirements have been further processed to get subsystem requirements from them. The

design has been made in compliance with these subsystem requirements, which are explained in chapter 4. To assure that the final design is in compliance with the mission requirements which are the basis for the subsystem requirements a compliance matrix has been made which will be further discussed in section 5.2.

### 3.2 Functional Diagrams

*Contributors: Thijmen*

Before starting the detailed design of the subsystems, a functional breakdown structure and a functional flow diagram were created. The functional breakdown structure in figure 10.3 at the end of the document describes all functions that the system needs to be able to perform. These functions are then broken down in subsystem functions. The functional breakdown structure will be used to define the subsystem requirements. With these requirements, subsequently, the detailed design of the subsystems can be performed. The functional flow diagram in figure 10.4 will help to see the inter-dependencies between the subsystems. In the functional flow diagram, the functions of the subsystems are connected by arrows, indicating the flow of the functions. This will help when setting up the models, to see what design parameters have an influence on each other.

### 3.3 Model Based System Engineering

*Contributors: Thijmen*

To aid the design and iteration process, an MBSE tool was used. This tool acts as central hub for all engineering information, to help in the overview of the systems engineering process. A component tree was created where all relevant information on the subsystem components can be stored and accessed by all members of the team. This helps everyone keep track of the changes in iterations, without information being lost in engineering meetings and discussions.

In the tool, the team also could keep track of the requirements. This makes sure there is one central space, where everyone can review the requirements. Then, the requirements can also be validated and verified systematically. The MBSE tool ensures that all engineering information is centralised. The use of this tool is not further shown in the report, but it has been used by the team to keep everything organised and central.

### 3.4 Iteration Process

*Contributors: Thijmen*

During the detailed design phase, the influence of each subsystem's design on the others must be constantly monitored. For instance, if the TT&C subsystem needs a better pointing accuracy for a new iteration, the ADCS will need to be more accurate, potentially changing the type of sensors or actuators used. This change in the ADCS will then have an influence on other subsystems. This chain reaction of modifications needs to be monitored by the team to make sure there are no faults in the design. This was done by using the established dependencies and making sure that the people involved in those chain reactions communicate well.

Lastly, the models to design the subsystems were built so that the inputs and outputs of the different models match. For example, the pointing accuracy posed by the telecommunications system is an output of the TT&C system model and is then used as an input for the ADCS system sizing.

## 4 Subsystem Detailed Design

This chapter entails the detailed design of each subsystem. The order of these is as follows: Payload, EPS, TT&C, ADCS, Astrodynamics, Propulsion, Thermal control, Structures and Materials, and finally OBDH. Each subsystem design (excluding astrodynamics) includes a market analysis, the subsystem requirements, the design process, verification and validation and a summary of the final design including a compliance matrix.

### 4.1 Payload

*Contributors: Jim*

The payload subsystem is responsible for ensuring the mission's primary science objectives, shown in section 1.1, are met. Additionally it aims to satisfy as many of the secondary objectives, shown in section 1.2, as possible. It was determined that a camera and imaging spectrometer will allow the spacecraft to satisfy

all primary science objectives. In this section a small market analysis of science instruments is performed, followed by the payload requirements. Then the observation environment near Planet 9 is investigated and instrument options are investigated and selected. Finally the Planet 9 science operations are discussed.

#### 4.1.1. Market analysis

Science instruments used in deep-space exploration missions are always purpose-built to complete the science goals of their respective missions [11]. Due to their complexity the instruments are most often developed by several universities and research institutes working together. The funding for these instruments comes mainly from the space agencies developing the mission. As an example, JUICE's MAJIS spectrometer was developed chiefly by France's Institut d'Astrophysique Spatiale and the Italian Istituto Nazionale di Astrofisica. Funding was provided by the respective countries space agencies (CNES and ASI) [12]. Interested outside parties and industry also contribute to an instruments development and funding. All of this makes putting a number on the cost of an instrument very difficult, but the costs can run into the tens of millions of euros.

#### 4.1.2. Payload requirements

Requirements for the payload subsystem are generated to ensure its design complies with the overall goal of the mission. The payload requirements flow directly from the stakeholder requirements pertaining to the mission's science objectives. The requirements can be seen in table 4.1.

Table 4.1: Payload Subsystem Requirements

| ID             | Requirement  |
|----------------|--|
| PL9-SUB-PLD-03 | The payload subsystem shall carry an imaging system  |
| PL9-SUB-PLD-04 | The payload subsystem shall operate in the temperature range 238-308 [K]                           |
| PL9-SUB-PLD-07 | The payload subsystem shall carry an imaging spectrometer  |
| PL9-SUB-PLD-08 | The payload subsystem camera shall have a per pixel angular resolution better than 9.25 [microrad] |
| PL9-SUB-PLD-09 | The payload subsystem camera shall operate in the wavelength range 0.38-0.7 [micron]               |
| PL9-SUB-PLD-10 | The payload subsystem shall carry instruments capable of characterising the Kuiper Belt            |
| PL9-SUB-PLD-11 | The payload subsystem shall carry instruments capable of characterising the Heliopause             |
| PL9-SUB-PLD-12 | The payload subsystem shall carry instruments capable of characterising the interstellar medium    |

#### 4.1.3. Planet 9 observation environment

The observation environment for the main instruments (imager and imaging spectrometer) will be determined by the radiation being reflected or emitted by Planet 9. If an insufficient amount of photons reach the detectors, integration times will become too high leading to smeared images. As such, a photon budget is constructed to estimate the number of photons being emitted or reflected by Planet 9's surface.

Planet 9 is estimated to be located about 550 AU away from the Sun. Current estimates put the mass of the planet at about 6  $M_{\oplus}$  [4]. The most interesting possibilities for a planet in this mass range would be a mini-Neptune or a super-Earth. The amount of photons coming from these planets is determined mainly by their effective radiating temperature and their albedo.

Because of the large uncertainties regarding the size and composition of Planet 9, a worst-case scenario for the observation environment will be considered. This would be a relatively small and cold super-Earth, since a mini-Neptune is expected to be larger and hotter (due to its atmosphere and gravitational contraction). This planet would have a radius of 1.2  $R_{\oplus}$ , as this is commonly defined as the lowest size limit for a super-Earth. The planet's temperature is determined via the equation for thermal equilibrium

equation (4.1).

$$T_{\text{eq}} = \left( \frac{L_{\text{th}} + L_{\text{rad}}}{4\pi R_{\text{pl}}^2 \sigma \epsilon} \right)^{\frac{1}{4}} \text{ [K]} \quad \text{with } L_{\text{th}} = (1 - A_v) F_{\odot} \pi R_{\text{pl}}^2 \text{ [W]} \quad (4.1)$$

Here  $L_{\text{th}}$  is the power radiating from the planet due to reflected Sunlight, and  $L_{\text{rad}}$  the power due to radiogenic heating. The latter is the heat generated due to radioactive decay within the planet's interior [13]. A value similar to that of Earth is assumed at 20 terrawatts [14]. For the Bond albedo  $A_v$  a low value of 0.1 ( $\approx$  that of the Moon) is assumed. The planet is also assumed to be a blackbody radiator ( $\epsilon = 1$ ). With the solar flux  $F_{\odot}$  at 550 AU being  $4\text{mWm}^{-2}$  this amounts to an effective radiating temperature of 26.6 K.

To find out whether acceptable integration times can be reached a simple SNR model accounting only for photon noise can be used, seen in equation (4.2). Other sources such as dark current noise and read noise are neglected as these are mainly related to the detector cooling and the specifics of detector design.<sup>1</sup>

$$\Delta t = \frac{\text{SNR}^2}{I_{\text{pix}} \eta_q} \text{ [s]} \quad (4.2)$$

Here  $\eta_q$  is the detector's quantum efficiency with a value of 0.2 assumed. It accounts for the detector not registering a signal for every photon that hits it.  $I_{\text{pix}}$  is the photon flux  $\frac{\text{photons}}{\text{s pixel}}$  or the number of photons incident on a pixel per second. To arrive at the photon flux incident on a pixel, first the photon flux coming from the planet has to be determined. For the planet's thermal radiation this is given by Planck's law for spectral radiant emittance and the equation for photon energy:

$$B_{\lambda} = \frac{2\pi hc}{\lambda^5} \frac{1}{\exp\left(\frac{hc}{\lambda k_B T}\right) - 1} \text{ [Wm}^{-2}\text{m}^{-1}] \quad (4.3)$$

$$E_{\text{photon}} = \frac{hc}{\lambda} \text{ [J]} \quad (4.4)$$

Here  $h$ ,  $k_B$  and  $c$  are Planck's constant, Boltzmann's constant and the speed of light in vacuum respectively. By dividing equation (4.3) with equation (4.4) the number of photons emitted per second, per square meter can be calculated for a given wavelength bin. By summing these bins over a wavelength range the total amount of photons  $\text{s}^{-1}\text{m}^{-2}$  is determined. Finally multiplying by the planet's surface area  $A_{\text{pl}}$  the planet's photon flux  $I_{\text{pl}}$  is calculated.

To determine the photon flux per pixel a scaling factor of  $\frac{A_{\text{pl}}}{A_{\text{pix}}}$  has to be applied. Here  $A_{\text{pl}}$  is the planet's area and  $A_{\text{pix}}$  the area of a pixel projected onto the planet through the instrument's optical system. Assuming a square pixel this area will be the spatial resolution squared. This makes it a function of the pixel's angular resolution and the instrument's distance to the planet.

In addition to the planet's thermal emissions a certain amount of sunlight is reflected by the planet. Equation (4.3) and equation (4.4) are again used but now with the Sun's effective temperature of 5777 K. This intensity is then scaled by  $\left(\frac{\text{radius Sun}}{\text{distance planet}}\right)^2$  and the albedo  $A_v$  to get the intensity of radiation reflected by Planet 9. The same process as for the thermal emission is then performed to obtain  $I_{\text{pix}}$  for the reflected sunlight.

From figure 4.1 it can be seen that the radiation from the Sun reflected by planet 9 is dominant up to a wavelength of about 23 micron. By looking at the reflection spectra we are limited to viewing the portion of the planet illuminated by sunlight. The spacecraft will approach Planet 9 from the Sun-facing side such that the reflection spectrum can be characterised.

<sup>1</sup>URL [https://www.stsci.edu/instruments/wfpc2/Wfpc2\\_hand\\_current/ch6\\_exposuretime6.html](https://www.stsci.edu/instruments/wfpc2/Wfpc2_hand_current/ch6_exposuretime6.html) [cited 18 June 2024]

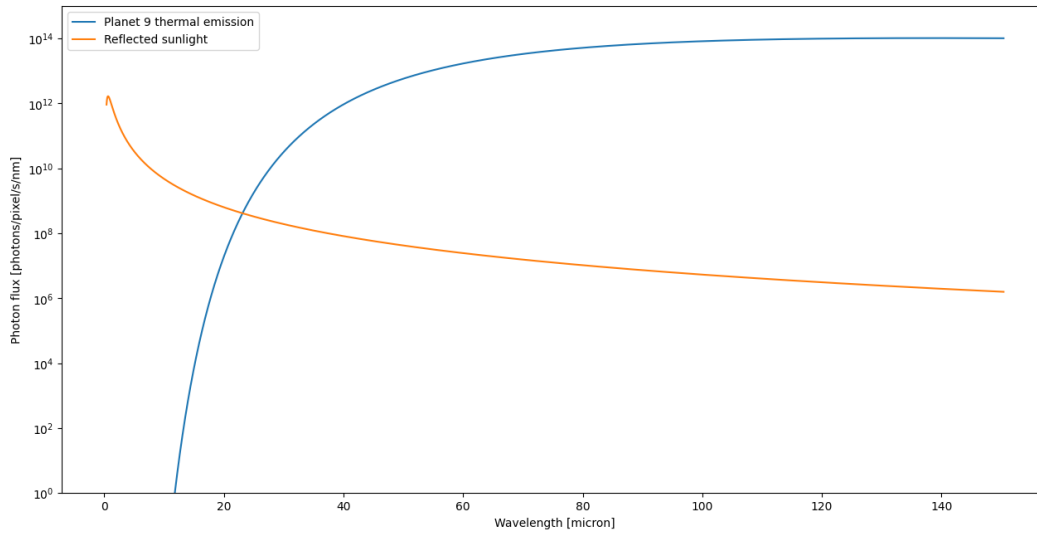


**Figure 4.1:** Number of Photons Incident on a Pixel for Thermal and Reflected Radiation Coming from Planet 9

While higher infrared wavelengths in the thermal spectrum (17-1000 micron) show interesting features for gaseous hydrogen and other trace molecules [15], shorter infrared wavelengths (0.17-17 micron) contain all the features needed to characterise the molecules related to our science objectives [16, 17]. With this in mind, in combination with higher wavelength spectrometers having worse spatial resolution for the same telescope aperture size, the choice is made to look at Planet 9's reflection spectra below 23 micron.

#### 4.1.4. Verification and validation

A check will be performed for the chosen main instruments and their respective spatial resolutions to determine whether the photon flux for given wavelength and spectral resolution (wavelength bin) results in acceptable integration times. To verify the calculations, unit tests were written for the different functions and checked against hand calculations. Additionally a generated blackbody spectrum was checked against one with known values (the Sun).

#### 4.1.5. Instrument options

In this section the scientific instruments that will help fulfil the mission primary and secondary objectives are outlined. Due to the highly specialised nature of scientific instruments it is not always possible to choose an "off-the-shelf" component, but a similar instrument will help gauge the mass, power and thermal attributes that influence other parts of the design. First the main instruments will be treated, after which the secondary objective-related instruments are covered.

#### Imager

For the imager a number of existing camera's used on deep space/planetary exploration missions were investigated. From the camera's investigated only New Horizon's LORRI and Cassini's ISS narrow angle camera satisfy the angular resolution requirement PL9-SUB-PLD-08, shown in table 4.1. The LORRI camera satisfies the resolution requirement on a much lower mass and power budget compared to the ISS camera and is thus selected [18, 19]. In section 4.1.6 the chosen instrument will be expanded upon. LORRI's specifications can be seen in table 4.2. LORRI has been proven to be reliable and is currently flying on the LUCY mission as well.<sup>2</sup>

<sup>2</sup>URL <https://lucy.swri.edu/instruments/LORRI.html> [cited 18 June 2024]

**Table 4.2:** LORRI Imager Specifications [18]

| <b>LORRI Imager Specifications</b> |           |            |
|------------------------------------|-----------|------------|
| Telescope aperture diameter        | 208       | [mm]       |
| Passband (panchromatic)            | 0.35-0.85 | [micron]   |
| Field-of-view                      | 0.29x0.29 | [deg]      |
| Pixel resolution                   | 4.95      | [microrad] |
| Image format                       | 1024x1028 | [pixel]    |
| Bits per pixel                     | 12        | [bits]     |
| Mass                               | 8.6       | [kg]       |
| Power required                     | 5         | [W]        |

### Imaging Spectrometer

For the imaging spectrometer there are many instruments that have flown, covering a wide array of spectral ranges. The ranges most often covered during missions characterising gas planets and their moons has been the near-to mid-infrared (0.7-5 micron) range. As outlined in section 4.1.3 however, higher infrared wavelengths are also interesting. Currently no spectrometer has flown that combines these in a single instrument, but an instrument like Cassini's CIRS that combines different wavelength ranges using multiple focal planes could be developed [15].

Due to the more specialised nature of spectrometers a representative instrument is chosen in Galileo's NIMS spectrometer that operates in the 0.7-5.2 micron band. It must be noted that this specific instrument has rather poor spatial resolution compared to the chosen imager. A simplified version of the MAJIS flown in JUICE (as investigated in this Ice Giants CDF report [20]) could prove a better option, but it has not yet been developed.

### Additional Instruments

The secondary objectives are centered on characterising the bodies and environments encountered during the trajectory. As outlined in section 4.5 these are Jupiter, the Sun, the Kuiper Belt, the Heliopause and the interstellar medium (ISM). The latter two are especially ill-explored, with only 2 spacecraft having reach them, and instruments capable of characterising them will add great value to the mission. A number of similar mission were investigated and a list of additional instruments are outlined.

- **Mass Spectrometer:** This instrument measures the mass-to-charge ratio of ions. It also determines the isotopic composition of elements to provide insights into their age and origin. The number of particles in free space is of course limited, but it is widely used in space missions to analyse the composition of (tenuous) planetary atmospheres. Notable missions that used a similar instrument are the Cassini-Huygens with the Ion and Neutral Mass Spectrometer (INMS) [11] and the planned Europa Clipper with the MASPEX instrument.<sup>3</sup> This instrument could aid in analysing chance particles encountered during transit of the Kuiper Belt and beyond.
- **Magnetometer:** This instruments measures the magnetic field around a planet to investigate its magnetosphere and interaction with solar wind. It can also be used to characterise the Heliopause. Magnetometers were used in multiple past space missions, including the Magnetic Field Experiment (MAG) instrument on the Juno mission and the magnetometer aboard the Voyager spacecraft [11].
- **Plasma Spectrometer:** This instrument analyses the properties and composition of plasma (ions and electrons) in the spacecraft's environment to understand its composition, density, temperature, and velocity, by measuring the particle's kinetic energy. The Cassini spacecraft had a plasma spectrometer, called Cassini Plasma Spectrometer (CAPS) [11]. With this instrument the plasma environment encountered in the Kuiper Belt and Heliopause can be investigated.
- **Energetic Particle Detector:** This measures high-energy particles to understand the radiation environment and particle interaction. It could also aid in determining the size, shape, and dynamics of Planet 9's magnetosphere. It was used in the Galileo and Juno missions to Jupiter

<sup>3</sup>URL <https://europa.nasa.gov/spacecraft/instruments/maspex/> [cited 30 May 2024]

[11]. Understanding the radiation environment in the Kuiper Belt, Heliopause and ISM will prove valuable.

- **Cosmic Ray Detector:** This scientific instrument detects and characterises cosmic rays to understand very high-energy particle environments. These particles typically include electrons, protons and alpha particles. The Voyager missions included a Cosmic Ray Subsystem (CRS) in the payload and looked for particles from our solar system but also from other stars [11]. Such an instrument could shed new light on the influence the Sun has on the Solar System's radiation environment.
- **Atmospheric Probe:** Similar to the atmospheric probe carried by Galileo that characterised Jupiter's atmosphere[11]. Due to amount of unknowns related to the presence/composition of Planet 9's atmosphere it is hard to justify taking such a heavy payload item along. With an atmospheric probe weighing in excess of 300kg it is deemed infeasible for this mission [11].

#### 4.1.6. Final design

The final design of the payload is presented in this section. The instruments were chosen taking into account the requirements related to payload and in conjunction with mainly the EPS, OBDH, Telecommunications and Astrodynamics subsystems. Changes in these subsystems influence the payload (and each other) greatly. For example, if the trajectory would not be able to take us close to Planet 9 it would require a far larger telescope assembly for the imager. The four chosen instruments can be seen in table 4.3, and will be treated in sequence.

**Table 4.3:** List of Instruments Chosen to Fly on the NIBIRU Mission

| Instrument | Type                                 | Mass [kg] | Power (max) [W] | Reference               |
|------------|--------------------------------------|-----------|-----------------|-------------------------|
| N'LORRI    | Camera                               | 8.6       | 5               | New Horizons LORRI [18] |
| ISHTAR     | Imaging Spectrometer                 | 18        | 12              | Galileo NIMS [16]       |
| NCREX      | Cosmic Ray Telescope                 | 5.5       | 6.7             | LRO CRaTER [21]         |
| PSP        | Low- to high energy particle science | 50.6      | 72              | JUICE PEP [22]          |

#### N'LORRI Imager

For the imager **N'LORRI** (NIBIRU LOng Range Reconnaissance Imager) is chosen with New Horizon's LORRI as a reference. Here the requirement for an iconic image was driving, as a clear image allows for fulfilling science objectives **PL9-SCO-01 to 04** [23, 24]. A minimum distance to Planet 9 was determined in conjunction with the astrodynamics team at 50 million km ( $\approx \frac{1}{3}$  AU). This distance is derived from Voyager 2's approach to Neptune, where its imager was able to generate an acceptable image.<sup>4</sup> At this distance LORRI is able to capture an image about 70 pixels across in the case that Planet 9 is a small super-Earth.

In conjunction with the OBDH team a change is made to reduce the image size. Instead of LORRI's 12bits per pixel, 10 will be used. While it will reduce the possible light level values from 4096 to 1024, it helps reduce the amount of data per image. In addition to this lossless compression will be applied by the instrument computer to reduce the data size by a factor of 7 [20].

N'LORRI is mounted inside the spacecraft, with its aperture facing out of the spacecraft's front panel. When not in operation at Jupiter, a door mechanism protects the instrument from contamination and Solar radiation during the first leg of the mission. The instrument's can remain operational for a temperature range between 148 and 313 K [18]. The CCD detector must stay below 203 K to ensure an acceptable SNR, for which a titanium cold finger is attached to a small radiator outside the spacecraft [18].

#### ISHTAR Imaging Spectrometer

The **ISHTAR** (Infrared Scanner for Hyperspectral Target Analysis and Reconnaissance) imaging spectrometer will characterise Planet 9's surface and atmosphere, fulfilling science objectives **PL9-SCO-05 to 07**. Based on Galileo's NIMS instrument, it operates in the wavelength range 0.7-5.2 [micron], and has a high enough spectral resolution to distinguish gaseous constituents present in atmospheres [16]. With an angular resolution similar to JUICE's MAJIS a small super-Earth Planet 9 can be resolved at a distance of 50 million

<sup>4</sup>URL <https://voyager.jpl.nasa.gov/mission/science/neptune/> [cited 18 June 2024]

km, allowing for characterisation to start at the same time as N'LORRI [12]. At this distance an average of the planetary spectrum is observed, with better detail the closer NIBIRU gets the Planet 9.

ISHTAR is also housed within the spacecraft shell, with its aperture facing out of the front panel. When not in operation at Jupiter, a door mechanism protects the instrument from contamination and Solar radiation during the first leg of the mission. The instrument remains operational for a temperature range of 100-313 K [12]. The detector has to be kept at a temperature of 65 K during operation, which is again achieved by a cold finger attached to a radiator outside the spacecraft [16].

### **NCREX Cosmic Ray Telescope**

The **NCREX** (NIBIRU Cosmic Ray EXperiment) cosmic ray telescope is chosen to characterise the very high-energy particles (cosmic rays) encountered during the mission. This allows the mission to fulfil science objectives **PL9-SCO-09 to 13**. NCREX is not a telescope in the traditional sense, but instead 'focuses' high-energy particles by only allowing entry on one side. The particles then pass through several layers of material surrounded by detectors. Very high energy particles will only be slowed down, while lower energy particles can be stopped completely. The detectors are able to detect the energy lost by the particles and through this characterise the particles and the rate at which these pass through the instrument [25].

The instrument is mounted on the front face of the spacecraft, with the telescope facing towards free space. Due to the isotropic nature of cosmic rays its orientation does not matter so long as its view is not obstructed. The instrument has an operational temperature range of 243-308 K [21].

### **PSP Particle Science Package**

The **PSP** (Particle Science Package) is based on JUICE's particle science package (PEP). It consists of 6 instruments capable of detecting and characterising high energy particles such as electrons and hot plasma, as well as lower energy particles found in exospheres and free space [22]. It is capable of performing mass spectroscopy to identify ions as well as neutral elements. Magnetospheres can also be characterised by analysing charged particles. PSP allows the mission to fulfil science objectives **PL9-SCO-09 to 13** [26]. The instruments can also aid in characterising Planet 9's iono/atmosphere (**PL9-SCO-05**). The instrument is mounted on the front panel with the detectors facing free space. The instrument operates between 243-308 K [27].

### **Radio Science Experiment**

While not a science instrument in and of itself the large antenna of the TT&C subsystem will be used to estimate the gravity constant  $\mu = GM$  (satisfying **PL9-SCO-01**) of Planet 9, like New Horizon's REX did for Pluto and Charon [28]. It does this by measuring the change in Doppler shift over time, which occurs due to changes in velocity of the spacecraft. REX was able to determine  $\mu$  extremely accurately, but it is a bold assumption that this method will work accurately 14 times further from Earth. Solar wind over this long distance has an effect on the radio signal propagation and the accuracy at which changes in velocity can be determined [28].

### **Golden Record**

If all goes well, the NIBIRU spacecraft will at some point become the furthest object sent out by humanity. Even after the onset of the EoL phase it will serve as an envoy of our Solar System. As such a golden record similar to that of the Voyager missions will be carried. It will be updated to current standards but still serve as a snapshot of humanity, Earth and the Solar System for anything that would chance upon the spacecraft in the future.

#### **4.1.7. Planet 9 science operations**

In this section NIBIRU's Planet 9 science operations are covered. The secondary objective segment of the mission's science operations is covered in section 10.3.

N'LORRI is able to resolve Planet 9 from a distance of about 21 AU in the case that it is a small super-Earth. From this point on science operations related to Planet 9 can begin. Aided by large ground-based telescope and spacecraft tracking N'LORRI can search for Planet 9 and keep it in sight. Small adjustments to the trajectory can be made if necessary in the run-up to the Planet 9 flyby. NIBIRU will need to perform this

flyby manoeuvre in a completely autonomous manner (like JUICE's upcoming Callisto flyby) as the light delay results in a five day communication lag, making real-time intervention impossible.<sup>5</sup>

NIBIRU will enter Planet 9's sphere of influence at a distance of  $\approx 14.4$  AU (assuming a mass of  $6 M_{\oplus}$ ). From then on the spacecraft's trajectory can be tracked to estimate how much it is perturbed by Planet 9 and its potential satellites. Once at a distance of 50 million km, N'LORRI is capable of obtaining high resolution images of Planet 9 to accomplish the related science objectives. A large number of images will be taken at different distances and exposure times to ensure the planet, potential moons and rings can be detected. Use will be made of dynamic targeting such that N'LORRI can identify potential targets for ISHTAR, ensuring interesting features can be sampled with the spectrometer.

As NIBIRU gets closer to Planet 9 more detail will become available, with the planet filling N'LORRI's FoV at a distance of 3 million km. During the period of closest approach, over several hours the spacecraft will send radio signals to Earth such that DSN ground stations can accurately characterise the accelerations that the spacecraft is subjected to by Planet 9. As NIBIRU moves behind the planet, N'LORRI and ISHTAR can no longer observe the reflectance spectra making it an ideal moment to use the PSP to shed light on the particle and radiation environment near Planet 9. Depending on the precise trajectory and available propellant, NIBIRU will aim N'LORRI and ISHTAR at the planet's limb illuminated by the Sun from behind the planet to characterise its atmosphere in more detail.

While NIBIRU is able to take many images and spectrometer acquisitions, only a small part can be sent to Earth due to the very limited available data rate. In conjunction with EPS and Telecommunications, 170 N'LORRI images and 170 spectrometer acquisitions can be sent back in the year after the Planet 9 flyby. After which power degradation starts severely limiting the data rate. Some kind of data curation will thus be necessary, to be run on the FPGA computer covered in section 4.9. This process is made very difficult due to the many unknowns surrounding Planet 9. Detailed models or ground-based observations could help predict what an image could look like to identify obvious failures but there remains a risk of good science getting lost. Nonetheless there is bound to be good data within the 340 high resolution images and spectrometer acquisitions that are sent back. This final design is in compliance with the requirements as shown in section 4.1.2.

## 4.2 EPS

*Contributors: Pepijn*

The EPS is the subsystem responsible for ensuring there is enough power available for all other subsystems. To do this, first a market analysis has been performed in section 4.2.1, after which the requirements for the design were stated again in section 4.2.2. The power generation is discussed in section 4.2.3, power storage in section 4.2.4 and finally the distribution of the power is described in section 4.2.5. To ensure that the limited power available is able to fulfil the requirements different modes are introduced in section 4.2.6. Lastly, the design procedure has been verified and validated in section 4.2.7 and the final design is summarised in section 4.2.8.

### 4.2.1. Market analysis

Before going into the design of the EPS, it is wise to look at available options for power generation, storage and distribution. NASA has manufactured many RTGs in the past for both Mars and deep space missions. Currently, they are working on the latest design of RTG called the eMMRTG [29]. This is an improvement on the MMRTG which was flown on the Mars Science Laboratory. More efficient concepts like the 3-GPHS Advanced Small RTG, GPHS is a General Purpose Heat Source, or the 16-GPHS STEM-RTG, where STEM stands for Segmented Thermoelectric & Modular, are proposed however their TRL is still very low while the eMMRTG is further in development and it is thought that it should be available for launch in 2034 [29–31].

The EPS will also need batteries to store power to achieve the peak power requirements. For this, secondary batteries should be used as they can be recharged [32, 33]. These batteries will have to be able to have numerous charge and discharge cycles as the spacecraft will not have a lot of available power when Planet 9 is reached so it will need to use the batteries to achieve the peak power.

<sup>5</sup>URL [https://www.esa.int/Enabling\\_Support/Operations/Juice\\_aces\\_Callisto\\_flyby\\_test](https://www.esa.int/Enabling_Support/Operations/Juice_aces_Callisto_flyby_test) [cited 18 June 2024]

Lastly, a power distribution system will need to be used to ensure that the power reaches all of the components that need it. This can either be done by a combination of a PCU (power conditioning unit) and a PDU (power distribution unit) or a singular PCDU [33]. These subsystems regulate the power that is outputted by the power source, discharging of the batteries and ensure that the power is distributed from the EPS to the other components [33].

#### 4.2.2. Requirements

Before the design of the EPS begins a look must be taken to the requirements according to which the EPS must be designed. These requirements can be found below in Table 4.4.

Table 4.4: EPS Requirements

| ID             | Requirement  |
|----------------|--|
| PL9-SUB-EPS-01 | The EPS shall continuously monitor power consumption levels of all subsystems      |
| PL9-SUB-EPS-03 | The EPS shall be able to provide the required power to all subsystems              |
| PL9-SUB-EPS-05 | The EPS subsystem shall remain in the operational temperature range of 250-305 [K] |

From PL9-SUB-EPS-03 it follows that the power must be available during mission operations so all subsystems shared their power required which is then used to design the power modes which will be further discussed in Subsection 4.2.6. PL9-SUB-EPS-05 was designed in collaboration with the thermal control system to ensure that the temperature would stay within the margins for all subsystems while having enough power to control the temperature.

#### 4.2.3. Power generation

NASA is developing newer generation RTGs to power its and ESA's future space missions. NASA is currently using MMRTG and is upgrading the system to the eMMRTG to have a more efficient system which will decrease the degradation rate per year by 2.3%/year [29]. There are also ideas for even more advanced RTGs like the 16-GPHS STEM-RTG which will have a higher BoL power output and a lower degradation rate. However due to the low TRL of 2 and NASA first finalising the design of the eMMRTG it is deemed that the eMMRTG will be the only available next-generation RTG by 2034 [29–31].

The eMMRTGs have a BoL power of 145  $W_{el}$  and a degradation rate of 2.5% per year [20, 29]. The dimensions are, 0.65 m in diameter fin tip to fin tip, and it has a height of 0.69 m. The mass is 45 kg of which 3.5 kg is the Plutonium-238 which is the fuel of the eMMRTG [20, 29]. Lastly, the eMMRTG emits 1854  $W_{th}$  at BoL with a degradation rate of 0.6889% per year, which will be important for the design of the TC system [20].

Due to regulations, the satellite will have to wait between 1 and 3 years before it can launch, for NIBIRU it will be assumed this takes 1 year [20]. Furthermore, with a 50-year trajectory to arrive at Planet 9, it will mean that the eMMRTG has been decaying for 51 years, so only 27.49% of BoL power is remaining, leading to an output of only 39.866  $W_{el}$  for the RTG. CDF study: CDF-187(C) shows limited availability of the Plutonium-238 fuel [20]. It states that there are 5 RTGs that can be fueled for all missions in the year 2019, for the mission to Planet 9 we will assume that 2 of the RTGs are available and that the others are used for other missions like missions to Uranus, Neptune or another rover to Mars [20]. This means that there is 79.732  $W_{el}$  available for the spacecraft when it reaches Planet 9. As this will not be enough to power the entire spacecraft, usage of batteries is required and a plan must be made for which subsystems are powered on at which times. This will be discussed in the following sections.

#### 4.2.4. Power storage

To ensure that other subsystems have more available power at certain times the power needs to be stored. The sizing of the batteries is with the following formula [32].

$$P = \frac{E_{bat} \cdot DOD \cdot N \cdot n}{t} \quad (4.5)$$

Here  $P$  is the power [W],  $E_{bat}$  is the capacity in [Wh],  $t$  the time the power is used [h], DOD is the depth of discharge in [%],  $N$  is the number of batteries [-] and  $n$  is the efficiency of the transmission between the battery and the power load in [%] which from literature is 90% [32, 33].

The VES16 8s4p battery of Saft<sup>6</sup> will be used on board of the satellite, it has a capacity of 512 Wh, voltage range of 25-32.8 V, dimensions of 308x180x90 (LxWxH in mm), and a mass of 5.80 kg [34]. Four of these batteries will be on board the spacecraft to increase the available power. The batteries will make use of a 30% DOD to ensure that the batteries will last for a longer time and they will be used for 1 hour per cycle. This results in 552.96 W of additional power in peak conditions.

The batteries will have to be charged again after their hour of supplying the spacecraft with more power. This will be done by a charging mode where the spacecraft will only operate the necessary components and charge the batteries with the remaining power. As the eMMRTGs output 79.732 W of which 56.528 W is available for charging the batteries, it will take 10 hours and 52 minutes to charge the batteries again.

#### 4.2.5. Power distribution

As the power is now generated and stored it still needs to be distributed to all of the subsystems. Luckily this can be done by the PCDU. This system will regulate all the power and handle the charge of the batteries [33]. Furthermore, it allocates the required power to all of the other subsystems via the cabling making sure that all subsystems are served on their required voltage level. The mass of the entire power management distribution system (PMD) so the PCDU and the cables can be estimated with the following formula [33].

$$M_{PMD} = 0.071 \cdot P_{EPS,EOL} + 0.15 \quad (4.6)$$

$M_{PMD}$  is the mass of the PMD in kg, and  $P_{EPS,EOL}$  is the end of life power in W. It should be noted that it deals with the EoL power and not BoL, for NIBIRU the EoL power comprises of the 79.732 W that is still generated by the RTGs and the 552.96 W that is stored in the batteries. This gives the total mass of the PMD to be 44.79 kg. The mass and volume of the PCDU can be estimated by the following formula [33].

$$M_{PCDU} = \frac{P_{PCDU}}{P_{sp_{PCDU}}} \quad (4.7) \quad V_{PCDU} = \frac{P_{PCDU}}{P_{\rho_{PCDU}}} \quad (4.8)$$

Here  $P_{PCDU}$  is the maximum controlled power by the PCDU in W, this is the total power at the start of the mission. For NIBIRU that is 290 W from the RTG and 552.96 W from the batteries, even though the batteries will not be used at BoL they should be included here for a safety margin in case the batteries have to be used at the start of the mission as well.  $P_{sp_{PCDU}}$  is the specific power and for PCDU it is 145 W/kg,  $P_{\rho_{PCDU}}$  is the power density and is 92 W/dm<sup>3</sup> for PCDU [33]. This leads to a mass of 5.714 kg and a volume of 9.005 dm<sup>3</sup> for the PCDU. Lastly, no power system can exist without any power losses, therefore it will be assumed that the power losses of the EPS will be 5% of the generated power [33][32].

#### 4.2.6. Power modes

As less than 80 W is being generated by the RTGs once the spacecraft arrives at Planet 9 and the batteries can only provide 552.96 W for an hour before having to recharge for 10.87 hours a plan must be made to distribute the power so that all of the objectives can be completed. For that, the mission will make use of four different Modes of Operations (MOO): SAFE, OPERATIONS, COMMUNICATIONS, and CHARGE. These four modes will be described in more detail below. In all of the modes different systems are turned on/off as can be seen below in table 4.5.

<sup>6</sup>URL <https://saft.com/products-solutions/products/saft-solution-leo-and-small-geo-applications> [cited 11 June 2024]

**Table 4.5:** Status of Subsystems per Mode

|         | SAFE | OPERATIONS | COMMUNICATIONS | CHARGE |
|---------|------|------------|----------------|--------|
| COMMS   | ON   | OFF        | ON             | OFF    |
| PAYLOAD | OFF  | ON         | OFF            | OFF    |
| ADCS    | ON   | ON         | ON             | OFF    |
| TC      | ON   | ON         | ON             | ON     |
| OBDH    | ON   | ON         | ON             | ON     |
| S&M     | OFF  | OFF        | OFF            | OFF    |
| EPS     | ON   | ON         | ON             | ON     |
| PROP    | OFF  | OFF        | OFF            | OFF    |

### SAFE

The SAFE mode is the mode the satellite will hopefully spend the least amount of time in. It will only be activated in case of an emergency on the satellite, for example, certain subsystems are overheating, the payload is not working, etc. During the SAFE mode, only the most important subsystems will still be turned on. The OBDH, EPS and TC will have to be on all the time but the ADCS and COMMS systems are also on to correctly orient the spacecraft for communications with Earth. It will take a long time due to the sheer distance however, with the help from the ground station it is assumed that the problem can be resolved and the satellite can move into one of its three operational modes.

### OPERATIONS

The first operational mode is the OPERATIONS mode. Here the payload is turned on, the ADCS points the spacecraft correctly and then the payload will perform its observations. As pointing and doing the operations will take a lot of power this is a separate mode. It does use 12% of a single battery to ensure all systems have enough power, so the operations mode can be active for 33.33 consecutive hours at Planet 9 before needing to recharge. Once this mode is successfully completed the satellite will move on to the COMMUNICATIONS mode.

### COMMUNICATIONS

This mode is all about transmitting all of the gathered data back to Earth. This is done with the help of the batteries which will allow more power for the antenna to transmit more bits per second. This means that the RTG is responsible for supplying the power to the remaining systems at this time and the antenna will use the battery power for one hour.

### CHARGE

Because the previous mode has drained the batteries they need to be recharged. This will be done by shutting down all subsystems except for the EPS and the OBDH as they need to be on at all times. The next 10.87 hours the batteries will charge and after they have reached the maximum capacity the spacecraft will go into the COMMUNICATIONS mode again to continue transmitting all of the data.

#### 4.2.7. Verification and validation

To ensure that the EPS is designed correctly the design has to be verified and validated. For the verification part unit tests have been performed where the computer model is checked against analytical calculations for every formula. This showed that the model is fully accurate compared to the analytical calculations and hence the model used is verified. The model has been validated with the help of the analysis method, making use of literature to prove that the used formulas are correctly integrated into the design [32, 33, 35].

#### 4.2.8. Final design

The final design of the EPS includes 2 eMMRTGs, 1 PCDU, and 4 VES16 8s4p batteries [20, 29, 32–34]. The eMMRTG has the size of 0.65 m in diameter fin tip to fin tip, a height of 0.69 m, a fuel mass of 3.5 kg and a total mass of 45 kg. The PCDU will have dimensions of 100x100x900.5 (LxWxH in mm) and a mass of 5.714 kg, and the cables have a mass of 39.075 kg. The battery has a mass of 5.80 kg and dimensions of 308x180x90 (LxWxH in mm) which will be spread out throughout the spacecraft. The eMMRTGs

are located on the outside of the spacecraft while the PCDU and the batteries are on the inside of the spacecraft. The final total mass of the EPS will be 157.989 kg. This design is in compliance with the requirements as set out in section 4.2.2.

To ensure that the mission objectives can be met, the power has been divided over all subsystems based on which systems needs to be on in which mode as shown in table 4.5. This finally led to the power allocation shown in table 4.6, this power allocation is only for the moment at which we arrive at Planet 9 there is a different power allocation for when performing the secondary objectives. All additional available power will then go towards the communication system to increase the possible bit rate. The required power is based on what all subsystems need to operate their components and then the communications subsystem is allocated all remaining power to achieve the highest possible bit rate.

**Table 4.6:** Power Allocated per Subsystem per MOO for Primary Objectives at Planet 9, All Power is in Watts

| Mode   | Available | EPS    | OBDH   | COMMS    | PAYLOAD | ADCS  | TC     | Total    |
|--------|-----------|--------|--------|----------|---------|-------|--------|----------|
| SAFE   | 79.7321   | 3.9866 | 19.216 | 15.2783  | 0.0     | 41.25 | 0.0012 | 79.7321  |
| OPS    | 96.3209   | 3.9866 | 33.799 | 0.0000   | 17.0    | 41.25 | 0.0012 | 96.0368  |
| COMMS  | 632.6921  | 3.9866 | 19.216 | 568.2383 | 0.0     | 41.25 | 0.0012 | 632.6921 |
| CHARGE | 79.7321   | 3.9866 | 19.216 | 0.0000   | 0.0     | 0.00  | 0.0012 | 23.2038  |

## 4.3 Telecommunications

*Contributors: Anton*

Telecommunications is the subsystem that is responsible for all communications to external parties outside of the spacecraft itself. It makes sure the spacecraft can communicate with either a designated ground station, or any other spacecraft. Traditionally, the telecommunications subsystem is also called the Tracking, Telemetry & Command (TT&C), which will be used as abbreviation from now on.

### 4.3.1. Market analysis

Before designing a specific antenna and telecommunication system, it can be useful to gather information from relevant other missions, specifically other deep space missions; like Voyager and New Horizons, since these spacecraft have to communicate over a large distance as well. The New Horizons spacecraft has an antenna diameter of 2.1 [m] [36], and according to calculations for the link budget which can be seen in table 4.8, that will not close the budget. Another way must be found to close this budget and safely communicate to Earth.

There have been missions to space with significantly bigger antennae than the ones from Voyager and New Horizons. Some of the missions are for example SkyTerra<sup>7</sup> and the KRT-10 space telescope [37], who were supposed to use a diameter of 22 and 10 [m] antenna respectively. The former launched in 2010 and carried the biggest space-antenna ever, however at first the whole antenna did not deploy correctly.<sup>8</sup> After some attempts it luckily fully deployed. These mission designs can be used to see how bigger antennae are carried into space by a size limited payload bay.

Here the foldable antennae come into play. Foldable antennae are antennae that are folded into a more compact shape, such that they fit into the payload bay of the used launcher. This way the antenna can be bigger than the launcher payload bay. Later in the mission, when the spacecraft is in space, the antenna can fold out to its intended size. It is however very complicated to unfold these antennae in space. There are multiple ways to fold antennae in a compact way, two will be covered here: the umbrella technique and the screw technique.

#### Umbrella technique

For the umbrella technique [38], the spars of the antenna dish are expanded outwards, creating a dish structure, like in figure 4.2. This is a complex way, since the rods that are essentially the spars for the dish structure have to be shaped in such a way that they have the desired radius of the dish. This is important since the waves have to be deflected off of the dish, falling on the detector in the focal point. The filament between the spars has to be made from a flexible material with a low heat expansion coefficient, like

<sup>7</sup>URL [https://space.skyrocket.de/doc\\_sdat/skyterra-1.htm](https://space.skyrocket.de/doc_sdat/skyterra-1.htm) [cited 10 June 2024]

<sup>8</sup>URL [https://space.skyrocket.de/doc\\_sdat/skyterra-1.htm](https://space.skyrocket.de/doc_sdat/skyterra-1.htm) [cited 10 June 2024]

carbon fibre reinforced silicone [38]. This ensures that the filament in between the spars does not break, yet that it forms correctly when folded out.

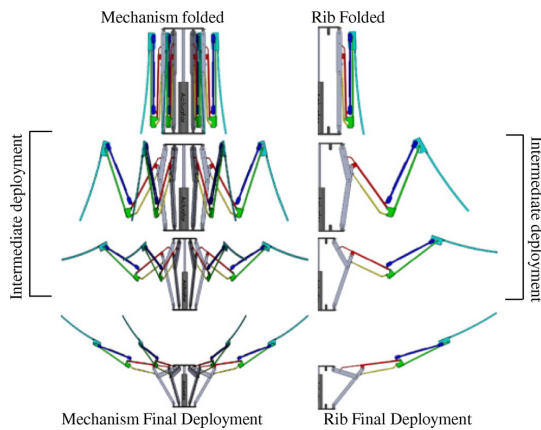


Figure 4.2: Umbrella Design for Expanding Antenna [38]

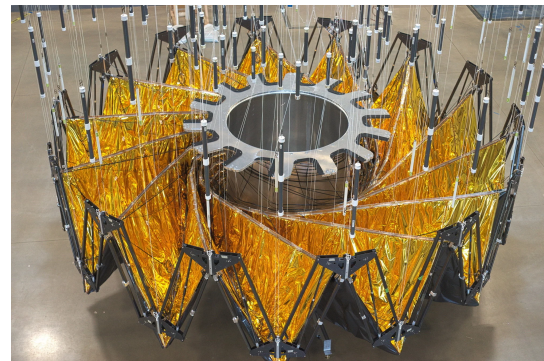


Figure 4.3: Screw-Design from Origami Inspired Unfolding Mechanism

### Screw technique

The other way to unfold an antenna is to use the screw technique, used for example on Starshade.<sup>9</sup> The principle of this technique is rotating the antenna inwards, creating a cylinder that is very compact, using origami techniques. Origami originates from Japan and it includes the art of decorative or functional paper-folding [39]. Figure 4.3 shows the origami folding mechanism behind the screw technique. This is also a viable way to fold the antenna, except for the way to put a parabolic 3D structure to the antenna dish. This is quite hard and may be too difficult to implement.

### Lay-out antenna

It is necessary to have a parabolic antenna dish, since this is the best way to have an antenna with the highest gain possible [40]. The radius of the dish, the diameter, the height of the dish, and the focal point. There are for a parabolic antenna dish a few options for designing as well, for now a Cassegrain design will be utilized, as shown in figure 4.4, since this also gives the best gain out of all known options[40].

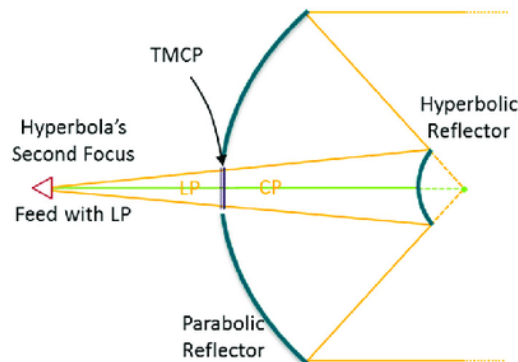


Figure 4.4: Schematic View of a Cassegrain Antenna Design [41]

### Self-pointing antenna

One way to potentially save fuel on board for other ADCS manoeuvres is to have an antenna that is self-pointing. This means that the On-board computer (OBC) can send a message to the antenna and order it to point in a certain direction. However, for an antenna that is likely to be relatively big compared to the spacecraft as a whole, it is not useful to have this. Since action gives an equal opposite reaction, the spacecraft itself will have a spin as well, when the antenna is pointed. This would then have to be corrected as well. A fixed antenna can thus be a good option.

### Ground station

Finally, it is important to make use of an appropriate ground station. There are two big deep space ground stations, from NASA and from ESA. NASA's Deep Space Network (DSN) has three 70 [m] antenna

<sup>9</sup>URL <https://science.nasa.gov/resource/10m-starshade-inner-disk-deployment/> [Cited 10 June 2024]

dishes scattered around Earth.[42] ESA's Estrack has three 35 [m] dishes scattered around Earth.<sup>10</sup> Since communication will be a significant challenge for reaching Planet 9, it has been chosen to make use of the DSN from NASA. with 70 [m] antenna dishes, more gain can be produced, allowing for better communications.

### 4.3.2. Telecommunications requirements

The TT&C subsystem can only be designed after the requirements are set up, since this is the base of the functioning of the subsystem. The requirements can be seen in table 4.7.

Table 4.7: Telecommunications Subsystem Requirements

| ID             | Requirement   |
|----------------|---|
| PL9-SUB-TEL-01 | The TT&C subsystem shall communicate to the ADCS subsystem the required antenna position                                    |
| PL9-SUB-TEL-03 | The TT&C subsystem shall encode outgoing data into the AWGN Channel format for transmission                                 |
| PL9-SUB-TEL-04 | The TT&C subsystem shall transmit encoded messages to Earth-based stations via 8.15 [GHz] frequencies                       |
| PL9-SUB-TEL-05 | The TT&C subsystem shall monitor 7.5 [GHz] communication channels for receiving incoming messages from Earth-based stations |
| PL9-SUB-TEL-06 | The TT&C subsystem shall decode received messages into a format readable by onboard systems                                 |
| PL9-SUB-TEL-07 | The downlink rate shall be more than 137 [bps]  |
| PL9-SUB-TEL-08 | The downlink signal-to-noise ratio shall be at least 3 [dB]   |
| PL9-SUB-TEL-09 | The uplink rate shall be more than 34 [kbps]  |
| PL9-SUB-TEL-10 | The uplink signal-to-noise ratio shall be at least 3 [dB]   |
| PL9-SUB-TEL-11 | The TT&C subsystem shall remain in the temperature range of 50 - 295 [K]  |

### 4.3.3. Link budget

One of the most important parts of the telecommunication is the Link Budget. This is a tool to make sure that your communication is actually feasible. Table 4.8 shows the link budget for the NIBIRU mission.

Table 4.8: Link Budget for the NIBIRU Mission

| Item                             | Symbol     | Units | Source            | Downlink | Uplink   |
|----------------------------------|------------|-------|-------------------|----------|----------|
| Frequency                        | $f$        | GHz   | Input Parameter   | 8.15     | 7.5      |
| Transmitting Power               | $P$        | Watts | Input Parameter   | 568      | 400000   |
| Transmitting Power               | $P$        | dBW   | $10\log(P)$       | 27.5     | 56.02    |
| Transmitter Line Loss            | $L_l$      | dB    | Input Parameter   | -1       | -1       |
| Transmit Antenna Beamwidth       | $\theta_t$ | deg   | Input Parameter   | 0.33     | 0.04     |
| Peak Transmit Antenna Gain       | $G_{pt}$   | dB    | SMAD eq           | 53.94    | 72.27    |
| Transmit Antenna Diameter        | $D_t$      | m     | SMAD eq           | 7.81     | 70.00    |
| Transmit Antenna Pointing Offset | $e_t$      | deg   | Input Parameter   | 0.003    | 0.005    |
| Transmit Antenna Pointing Loss   | $L_{pt}$   | dB    | SMAD eq           | -0.001   | -0.188   |
| Transmit Antenna Gain            | $G_t$      | dB    | $G_{pt} + L_{pt}$ | 53.94    | 72.09    |
| Equiv. Isotropic Radiated Power  | $EIRP$     | dBW   | $P + L_l + G_t$   | 80.49    | 127.11   |
| Propagation Path Length          | $S$        | km    | Input Parameter   | 8.23E+10 | 8.23E+10 |
| Space Loss                       | $L_s$      | dB    | SMAD eq           | -328.98  | -328.26  |
| Propagation & Polarization Loss  | $L_a$      | dB    | SMAD figure       | -0.3     | -0.3     |
| Receive Antenna Diameter         | $D_r$      | m     | Input Parameter   | 70       | 7.81     |
| Peak Receive Antenna Gain        | $G_{rp}$   | dB    | SMAD eq           | 71.10    | 51.33    |
| Receive Antenna Beamwidth        | $\theta_r$ | deg   | SMAD eq           | 0.037    | 0.359    |
| Receive Antenna Pointing Error   | $e_r$      | deg   | Input Parameter   | 0.005    | 0.003    |
| Receive Antenna Pointing Loss    | $L_{pr}$   | dB    | SMAD eq           | -0.22    | -0.001   |

*Continued on the next page*

<sup>10</sup>URL [https://www.esa.int/Enabling\\_Support/Operations/ESA\\_Ground\\_Stations/Estrack\\_ground\\_stations](https://www.esa.int/Enabling_Support/Operations/ESA_Ground_Stations/Estrack_ground_stations) [cited 10 June 2024]

| <i>Continued from previous page</i> |                |       |                   |           |           |
|-------------------------------------|----------------|-------|-------------------|-----------|-----------|
| Item                                | Symbol         | Units | Source            | Downlink  | Uplink    |
| Receive Antenna Gain                | $G_r$          | dB    | $G_{rp} + L_{pr}$ | 70.88     | 51.32     |
| System Noise Temperature            | $T_s$          | K     | SMAD table        | 135       | 614       |
| Data Rate                           | $R$            | bps   | Input Parameter   | 264       | 34972     |
| $E_b/N_0$ (1)                       | $E_b/N_0$      | dB    | SMAD eq           | 5.17      | 5.15      |
| Carrier-to-Noise Density Ratio      | $C/N$          | dB-Hz | SMAD eq           | 29.38     | 50.59     |
| Bit Error Rate                      | $BER$          | -     | Input Parameter   | $10^{-5}$ | $10^{-7}$ |
| Required $E_b/N_0$ (2)              | Req. $E_b/N_0$ | dB-Hz | SMAD figure       | 0.154     | 0.154     |
| Implementation Loss (3)             | -              | dB    | Estimate          | -2        | -2        |
| Margin                              | -              | dB    | (1) - (2) + (3)   | 3.01      | 3.00      |

A few things can be distinguished within this table. The first column is the specific item that is contributing to either the direct dB for the link margin, or a calculation that needs to be made for later purposes. The symbols and units are shown next, and then the source where the item comes from, either from calculations, being an input parameter, or values directly gotten from SMAD [40]. It should also be noted that, some cells are coloured grey. These cells indicate that they come from either calculations or they can not be changed directly.

This link budget was set up by first determining a frequency at which the downlink data had to be sent. Usually, X-band communication is used for deep space missions [43]. A value of 8.15 GHz was chosen, which lies in the X-band. Next the power is determined. This comes from the EPS, and how much can be distributed to the TT&C subsystem, this is then converted into dB by equation (4.9) [44].

$$X[dB] = 10 \cdot \log \left( \frac{X}{X_{ref}} \right) \quad (4.9)$$

Transmitter line loss is the loss from wires within the transmitting body. The antenna beamwidth is an input parameter that can be chosen to vary the transmitting antenna diameter. The beamwidth of an antenna is the angle at which the antenna gain is send, for simplicity it is assumed that in this whole angle has a constant gain, and that no signal is send beyond this angle. From the peak transmitting antenna gain, shown in empirical equation equation (4.10), and the beamwidth, the diameter follows, using empirical equation equation (4.11) [40].

$$G_{pt} = 10 \cdot \log \left( \frac{27000}{\theta_t^2} \right) \quad (4.10) \quad D_t = \frac{21}{f \cdot \theta_t} \quad (4.11)$$

A pointing offset is chosen in combination with the ADCS subsystem. Finally the equivalent isotropic radiated power ( $EIRP$ ) is calculated, as shown in equation (4.12) [40].

$$EIRP = P + L_l + G_t \quad (4.12)$$

The next section of the link budget is the path loss that follows from the amount of distance that the electromagnetic (EM) waves have to travel. This influences the power of the generated waves. This is easily calculated with equation (4.13) [40], where  $d$  is the distance in meter,  $f$  is the frequency used, and  $c$  is the speed of light.

$$L_s = 20 \cdot \log \left( \frac{4 \cdot \pi \cdot d \cdot f}{c} \right) \quad (4.13)$$

Next is the section of the link budget that covers the receiving part of part of the signal, also knows as the  $\frac{G}{T}$ . This starts by setting the receiving antenna diameter as the 70 [m], as stated earlier, this is the diameter of the DSN. From this the peak antenna gain is calculated, as well as the beamwidth, using a rewritten form of equation (4.10) and equation (4.11). Once again, the pointing error is 4 [mdeg] [45]. For now however, a 25% margin is taken, and 0.005 [deg] is taken. The pointing loss is calculated and the system noise temperature comes from SMAD as well. Finally the  $\frac{G}{T}$  is shown in equation (4.14) [40].

$$\frac{G}{T} = G - 10 \cdot \log(T) \quad (4.14)$$

Finally for the link budget, there is the signal to noise ratio (SNR) and the margin implemented with this

SNR. The data rate is first determined, in consult with the payload and OBDH subsystems. Since the payload system is generating the data, and the OBDH is capable of storing data. From all of the above mentioned, a signal to noise ratio  $\frac{E_b}{N_0}$  is calculated. Next the Carrier-to-Noise density ratio is calculated and the bit error rate is determined. Combining the bit error rate and a certain coding scheme, the required  $\frac{E_b}{N_0}$  is determined, using SMAD again. The AWGN channel capacity coding was used [40]. The implementation loss covers the atmospheric losses and rain attenuation. Finally, a margin can be set up. This margin should preferably be bigger than 3 [dB], to ensure a stable connection [44].

The uplink budget is constructed the other way around, starting with the ground station antenna dish diameter, power, frequency, and pointing offset as inputs, calculating the *EIRP*. The space loss is calculated again with equation (4.13). The  $\frac{C}{T}$  is constructed by the receiving (spacecraft) antenna diameter and pointing offset. The data rate and a bit error rate are defined, and from all this a link budget margin follows as well for the uplink.

#### 4.3.4. Design iterations

It can be seen that the link budget, as discussed in section 4.3.3, is a major driving factor within the iteration process. Next to this, it is important to know which subsystems are depended on TT&C and on which subsystems TT&C relies itself. The TT&C relies on the following subsystems:

- EPS: The amount of power that can be given to the TT&C
- ADCS: The accuracy with which can be pointed
- Structures: Where the antenna can be placed
- Payload: How much data is generated
- OBDH: How much data can be stored within the OBC

With these dependencies, the input values in the link budget in table 4.8 can be adapted. A first problem that came to light was that the antenna would have to be very big, probably bigger than the payload bay. This means that one of the folding mechanism, explained in section 4.3.1, has to be used. Since the umbrella technique has had more research, this technique was chosen. The screw technique has not been applied to antennae yet in practise, so it is not yet known if it functions with the curvature of an antenna. A first link budget was created, where the power was relatively low, the bit rate relatively high, the ADCS provided a first estimate on pointing accuracy, and a transmitting spacecraft antenna diameter of 18 [m] was used.

In the mean time, EPS further refined its strategy for distributing power, and more power could be given to the TT&C subsystem. This lowered the antenna size with a significant amount, to 10 [m]. The bit rate had to be decreased as well, which meant that the data produced by the payload would take longer to transmit back to Earth. Therefore, the OBDH would have to store more data. The pointing accuracy stayed constant during these iterations.

Finally, the EPS defined the exact amount of power that would be distributed to the TT&C subsystem. The pointing accuracy was also finalized and the payload data generation was defined, this could then conclude the link budget as well. In final combination with the power subsystem, the amount of time it would take to transmit the generated data was calculated in communications mode, including recharging the batteries. The final size of the antenna was concluded at 7.81 [m], making it 231 [kg].

#### 4.3.5. TT&C hardware

It is important, that when the signal is received by the antenna or when a signal is transmitted, that this signal can be interpreted in the correct way. For this, a few components are needed. The components that are mostly needed are: cables, transceivers, frequency converters, (de)modulators, and filters.

##### Cables

Cables in a spacecraft's telecommunications subsystem connect the antenna to transceivers and the OBDH system. Coaxial cables and waveguides transmit Radio-Frequency (RF) signals, while fiber optics handle

high-speed data transfer.<sup>11</sup> Shielded twisted pair (STP) cables reduce electromagnetic interference for low-speed data links.<sup>12</sup> Power cables supply electrical power to the TT&C components. Proper cabling ensures robust signal integrity and efficient data communication throughout the spacecraft's systems, enabling reliable operations and communication with ground control.

### Transceivers

Transceivers in the telecommunications subsystem of a spacecraft play a crucial role in ensuring effective communication between the spacecraft and ground stations. A transceiver combines the functions of a transmitter and a receiver, allowing the spacecraft to send and receive data. It typically consists of a radio, an amplifier, and an antenna. The radio generates and modulates an electromagnetic wave to create a signal for transmission and demodulates incoming signals for reception. Amplifiers boost the signal power before transmission, ensuring it can travel long distances, while low noise amplifiers enhance received signals, making them easier to process despite potential weak signal strength and noise.<sup>13</sup>

Transceivers used in deep space missions often operate in various frequency bands such as S-band, X-band, and Ka-band [43]. These bands are chosen based on the mission requirements and the need to avoid interference.

### Frequency converters

In a deep space mission, a frequency modulator is essential in the telecommunications subsystem for encoding data onto a carrier wave for transmission. This process, known as modulation, allows digital data to be superimposed onto high-frequency electromagnetic waves, typically in the RF range, to ensure it can travel vast distances through space [43].

The modulator takes the digital data from the spacecraft's systems, such as scientific instruments or control commands, and modulates it onto a carrier wave. This modulated signal is then amplified by a power amplifier before being transmitted via the spacecraft's antenna. At the receiving end, a demodulator extracts the original data from the received signal, ensuring accurate communication with ground stations or other spacecraft.

### Filters

Filters are employed to eliminate unwanted frequencies, reduce noise, and prevent interference, ensuring that the communication signals are clean and clear. There are 3 main filters:

- **Low-pass filter:** allow signals below a specific frequency to pass and block higher frequencies, which is useful for removing high-frequency noise.<sup>14</sup>
- **High-pass filter:** allow high-frequency signals to pass while blocking lower frequencies, useful for removing low-frequency noise and interference.<sup>14</sup>
- **Notch filter:** are used to block a narrow band of frequencies and are particularly useful in eliminating specific unwanted signals or interference at known frequencies.<sup>15</sup>

### Communication flow diagram

In figure 4.5 the communication flow diagram can be viewed. This is a diagram that shows how data moves through the system and between the system and its environment.

---

<sup>11</sup>URL <https://www.phoenix-fiber.com/posts/fiber-optic-cables-revolutionizing-high-speed-data-transmission> [cited 13 June 2024]

<sup>12</sup>URL <https://www.techtarget.com/searchnetworking/definition/shielded-twisted-pair> [cited 13 June 2024]

<sup>13</sup>URL <https://www.quora.com/What-are-the-main-differences-between-a-low-frequency-amplifier-and-high-frequency-amplifier-circuits> [cited 11 June 2024]

<sup>14</sup>URL <https://www.mixinglessons.com/pass-filter/> [cited 11 June 2024]

<sup>15</sup>URL <https://www.analog.com/en/resources/glossary/notch-filter.html> [cited 11 June 2024]

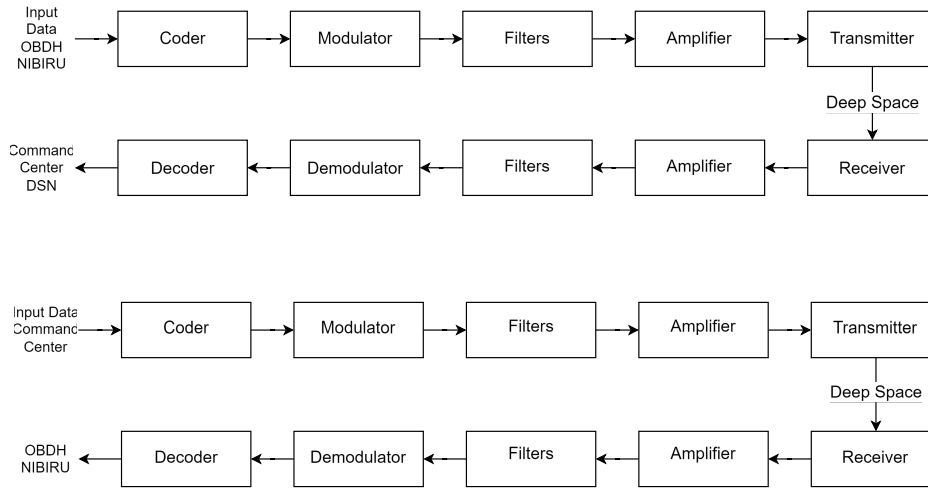


Figure 4.5: Communication Flow Diagram of NIBIRU

#### 4.3.6. Verification and validation

To ensure that all values obtained for the TT&C subsystems are correct, verification and validation has to be performed. This was done by checking all numbers from the link budget analytically, and running the link budget by experts. The radiation plot was obtained by a python program, for which unit tests were performed to make sure this was verified as well. In comparison to other missions, the antenna is very big, and the bitrate is very low. However, there has never been a mission that has gone this far away, so it is normal that the values are extreme.

#### 4.3.7. Final design

The final communications design will consist of one foldable 7.81-meter diameter antenna, and one 1-meter diameter antenna, both mounted on different sides of the NIBIRU spacecraft. This is done to ensure proper connection with Earth during the time that the big antenna is still folded in. The 1 m diameter antenna is used up until 50 AU, the edge of the Kuiper Belt. After this, the big antenna is folded out. This minimizes the risk of the big antenna being hit by debris of the Kuiper Belt. A transceiver will be present as well as coaxial cables to transfer data from the antenna to the OBDH and from the OBDH to the antenna.

The final values of the link budget can be viewed in table 4.8, however the most important values will be stated here again:

- Diameter big antenna: 7.81 [m]
- Gain: 54 [dB]
- Beamwidth: 0.33 [degrees]
- Power output: 568 [W]
- Bit rate: 264 [bps]

The bit rate of 264 [bps] means, considering the amount of data generated at Planet 9 is 0.467 [Gigabit], that it takes a total of 1 full year to transmit all data. This results in a total of around 750 cycles of batteries charging and discharging. This is a long time, however it is the most optimal that it can be made. The amount of contact hours needed to send back the data for only the primary objectives is 780 hours. Including the secondary objectives, 40 day cycles will be considered to acquire data and send back data during the trajectory from the outer Kuiper Belt to Planet 9, which will take a total of 36 years, so 329 cycles can be made. Since with distance the bitrate that can be send changes, an average of 15 days sending time has been taken as sending time. For 329 cycles, 15 days of sending 24 hours constantly, 119000 hours of sending time is needed. This drastically increases the operational costs.

#### Radiation Plot

A radiation plot is a polar plot that shows the amount of gain that is radiated for certain angles. Since the beamwidth is very small, as well as the pointing offset, it is assumed that for NIBIRU that it is a straight

line, and not a bubble. This means that all information is sent only in the 0.33 [degrees] angle, and no information is sent outside of this angle. This results in the radiation plot depicted in figure 4.6.

Next, a CAD design has to be made of the big antenna and its unfolding mechanism. The unfolding mechanism is inspired by a design from Vasisht Hasanzade [38]. It can be seen in figure 4.7.

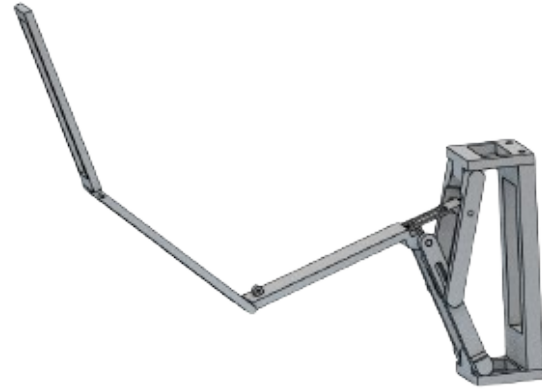
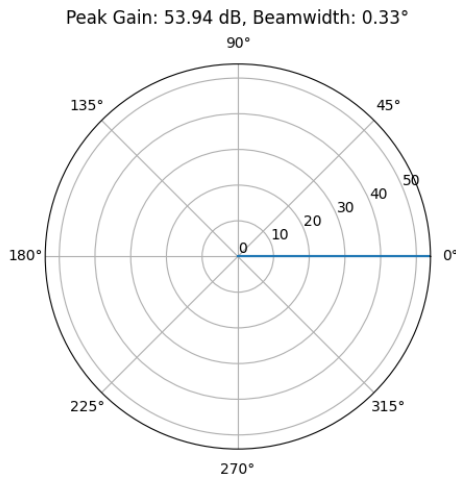


**Figure 4.6:** Radiation Plot for the 7.81-Meter Antenna of NIBIRU

**Figure 4.7:** CAD Design for the Extended Umbrella Antenna

To finalise the design, a cost estimation also needs to be made. For this, a paper was used that calculated cost based on weight percentages of the spacecraft [46]. From this, it turned out that the telecommunication subsystem is roughly 13%. This would turn out to be 38.7 million euros. For the mass, the antenna is 231 [kg], and 6 umbrella actuators are used, with a total of 1369 [kg]. With all these values, the requirements from section 4.3.2 have been met in the design.

## 4.4 ADCS

*Contributors: Milan*

The ADCS is a critical component of spacecraft systems, responsible for managing the orientation and positioning of the spacecraft in space. The primary objectives of the ADCS are to accurately determine the spacecraft's orientation and position, and control it to achieve desired orientations and positions. This subsystem ensures that the spacecraft maintains the correct attitude for tasks such as communication, propulsion, scientific observations and keeping the correct trajectory. The attitude determination will be done by sensors and attitude control will be performed by a number of actuators.

The design of the ADCS will be as follows. First, a market analysis will be performed in section 4.4.1 to determine the available sensors and actuators that are on the market. On top of that, the sensors and actuators of comparable missions will be analysed. Then, section 4.4.2 will outline the different control modes and states the ADCS requirements. Furthermore, in section 4.4.3 the spacecraft control type will be selected; either passive control, spin control, three-axis control or a combination of these. Next, the disturbance environment for the different mission phases will be analysed and the total impulse from disturbances calculated. Then, in section 4.4.5 the minimal thrust force for stability and accuracy are calculated. This determines the type of thrusters selected in section 4.4.6. The pointing accuracy and knowledge will influence the sensor choice in section 4.4.7. Moreover, the propellant and pressuriser tanks are sized in section 4.4.8. Then the verification and validation process is explained in section 4.4.9. Lastly, the final ADCS design will be summarised in section 4.4.10.

### 4.4.1. Market analysis

To make a decision on the types of sensors and actuators for the design, all the options available on the market should be considered. The most common sensors are earth sensors, horizon sensors, star trackers, GPS receivers, magnetometers, gyroscopes and inertial measurement units [47, 48]. The performance of these depends highly on the mission profile. For example, the earth sensors, horizon sensors and GPS receivers are efficient in earth orbit satellites. However, for the mission to planet 9 at 550 AU, these sensors

are not useful. Sun sensors are only effective in attitude determination to a distance of about 3 AU from the Sun, and hence will also not be useful for the greater part of the mission. Magnetometers measure the magnetic field around the spacecraft. They are not suitable as a primary reference for orientation in deep space in the absence of a magnetosphere. These sensor options will be eliminated and the remaining sensor options are star trackers, inertial measurement units and gyroscopes. To have a redundancy and very accurate position determination, clocks and ground based radio signals can also be used.

For the control actuators, the main options are reaction wheels, control moment gyros, magnetic torquers and thrusters [47]. Magnetic torquers interact with the magnetic field of a planetary body to generate torques. These are only feasible in environments with a strong magnetic field and hence will not be useful for the entire mission duration to planet 9. Some reaction wheels have peak power usage of 100 W or more.<sup>16</sup> Control moment gyros are similar to reaction wheels and provide more overall control but use even more power than reaction wheels. Due to the limited amount of power available explained in section 4.2.1, the only viable option for attitude control is a combination of small thrusters used for both larger maneuvers and to counteract disturbances.

The NIBIRU mission can be compared to similar space missions. This will give a better understanding of the necessary actuators and sensors of far planetary exploration and deep space missions. The first comparable mission is the New Horizons. It was launched in 2006 to conduct a flyby of Jupiter and continued to research the Kuiper Belt, going to a distance from the Sun of more than 50 AU. It used sun sensors during the initial near Earth phase, star trackers for precise attitude determination and IMU's and gyroscopes to provide data on the spacecraft's velocities and accelerations. For attitude control it used hydrazine thrusters for trajectory corrections and spin stabilization during most of the cruise phase [49]. Another mission that can be compared to NIBIRU is the Cassini mission, launched in 1997 to study Saturn and its characteristics, at around 9.5 AU. It used star trackers, IMUs, sun sensors and magnetometers for attitude determination and reaction wheels and hydrazine thrusters for control [50]. The last comparable missions that are considered are the Voyager missions, launched in 1977. They are the farthest human-made objects from Earth, with Voyager 1 at around 163 AU in interstellar space. They made use of star trackers, IMUs and sun sensors for precise attitude determination and hydrazine thrusters and spin stabilization for control [51][52].

These mission are comparable to the NIBIRU mission due to their large distance to the Sun. None of these spacecraft relied on solar panels but used RTGs for power generation. This resulted in a limited amount of available power for the ADCS and hence sensors and actuators that need significant amounts of power were mostly avoided. This will help in the sensor and actuator selection of the ADCS in section 4.4.7 and section 4.4.6.

#### 4.4.2. ADCS requirements and control modes

There are a number of mission and subsystem requirements that the ADCS must abide by. The requirements, together with the constraints of other subsystems will determine the final design of the ADCS. All the ADCS requirements are shown in section 4.4.2.

Table 4.9: ADCS Requirements

| ID              | Requirement   |
|-----------------|---|
| PL9-SUB-ADCS-01 | The ADCS shall determine the attitude of NIBIRU.  |
| PL9-SUB-ADCS-02 | The ADCS shall receive the desired attitude of NIBIRU from Earth-based stations.              |
| PL9-SUB-ADCS-03 | The ADCS shall be able to adjust the NIBIRU's orientation.                                    |
| PL9-SUB-ADCS-04 | The ADCS shall be able to provide 3-axis control.   |
| PL9-SUB-ADCS-06 | The ADCS shall be able to counteract all expected disturbances.                               |
| PL9-SUB-ADCS-07 | The ADCS shall be able to maintain a pointing accuracy of smaller than 0.01 degrees per axis. |
| PL9-SUB-ADCS-16 | The ADCS shall be able to provide pointing knowledge of smaller than 0.01 degrees per axis.   |
| PL9-SUB-ADCS-18 | The ADCS shall have an operational lifetime of at least 50 years.                             |
| PL9-SUB-ADCS-19 | The ADCS shall have a reliability of at least 85% for its operational period.                 |
| PL9-SUB-ADCS-20 | The ADCS shall be operational in a temperature range of 263 - 323 K.                          |
| PL9-SUB-ADCS-21 | The ADCS shall have a slew rate of more than $9.89 \cdot 10^{-7}$ radians per second.         |

<sup>16</sup>URL <https://aerospace.honeywell.com/us/en/products-and-services/product/hardware-and-systems/space/small-satellite-specific-bus-products/hr04-hc7-hc9-reaction-wheel-assemblies> [cited 12 June 2024]

| ID              | Requirement  |
|-----------------|--|
| PL9-SUB-ADCS-22 | The ADCS shall have a pointing stability of smaller than 0.005 degrees per second. |

Now the different control modes will be discussed. Typical control modes include, orbit insertion, acquisition, normal/on-station, slew, safe and special [40]. However, each space mission is different and hence deviations can be made according to the mission requirements and mission profile. The control modes for the NIBIRU ADCS are:

1. Orbit/Flyby Insertion mode: The trajectory subsystem has decided that the space vehicle will not be in orbit around Planet 9 but instead will perform a flyby. During the cruise there are three options for spacecraft control. These are spin stabilization and 3-axis control. Attitude determination and control systems will not be on the entire trajectory and will be turned on at time intervals to check if trajectory is okay.
2. Acquisition: This control mode happens after the trajectory phase is done and the spacecraft needs to prepare for using the payload instruments to do measurements of Planet 9. Attitude determination will need to be done and the spacecraft needs to be controlled to have the payload pointing in the right direction.
3. Normal/On-Station: This mode is used for the most important part of the mission, the flyby. The subsystem requirements for this mode should drive the design. The pointing stability and slew rate necessary for the measurements during the flyby are the most important parameters.
4. Slew: This mode is used when the spacecraft needs to change orientation from the antenna pointing to Earth to the kick-stage thrusters pointing correctly and vice versa. The slew rate determined by the flyby will also be used during other slew operations.
5. Contingency/Safe: This mode will be activated when an error occurs. When this happens, the redundant attitude determination (sensors) and control (actuators) will be activated. Another option would be that if for some reason the telecommunication subsystem requires some more power, part of the ADCS subsystem needs to be turned off for that power to be available.
6. Special: This mode refers to any secondary objectives performed before or after the main flyby. This could refer to looking at Jupiter and the Sun during the gravity assists or inspecting the heliosphere and heliopause.

#### 4.4.3. Selection of spacecraft control type

Now the method for spacecraft control needs to be chosen. A distinction can be made between the control method during the cruise phase when fine accuracy is not required and the control method during communication and payload measurements.

The first option is a passive control technique called gravity-gradient control, which uses the inertial properties of a spacecraft to keep it pointed towards the Earth. This option is usually used on small spacecraft in low-Earth orbits and hence is not a viable options for the NIBIRU mission.

The next option is also a passive control technique called spin stabilization. It employs gyroscopic stability to resist disturbance torques. There is a distinction to be made between pure spin stabilisation and dual spin stabilisation. The dual spin stabilisation has two sections spinning at different rates about the same axis, providing more stability than the pure spin stabilization, and also the ability to keep one axis stable. If a sensor was placed on this axis it could still be used for attitude determination. The dual spin consists of spinning motors and thrusters, which needs a lot of power (>30 W) to be operated. In pure spin stabilisation, the entire spacecraft rotates around one axis the provide gyroscopic stability. Advantages of this method compared to dual spin is its lower power consumption and simplicity. A disadvantage is that it needs propellant for spinning the spacecraft up and down when communication or payload operations need to be performed.

The last control type is called three axis control. There are multiple different control techniques. Most of these use either momentum wheels, reaction wheels or control moment gyros, or a combination of these. As stated earlier, due to power unavailability, this is not an option and the only remaining option for three

axis control is to use a thruster system. This method has high accuracy, depending on the thruster forces and no constraints on maneuverability [40].

### Cruise

For the cruise phase when Earth communication is not required, pure spin stabilization is chosen. The main reason for this is the reduced power usage. When it is necessary to communicate with Earth the spin stabilization is 'turned off'. This means the thrusters are used to spin down the spacecraft. Once the spacecraft's spin rate is reduced to zero, the thrusters can be used to stabilize and control the spacecraft's orientation with the antenna pointing to earth. This does mean that the sensors must also be turned on for attitude determination. The thrusters will need to have a high pointing accuracy and stability and the sensors a high pointing knowledge. After completing the communication with Earth, the spacecraft can be spun up again to resume spin-stabilized mode. This involves spinning up the spacecraft to achieve the required rotational speed for gyroscopic stability.

During the flyby, high pointing accuracy, pointing knowledge and pointing stability is required to point the payload instruments towards Planet 9. This can only be done with three-axis stabilisation control.

#### 4.4.4. Disturbance and slew force and impulse

To size the thrusters that are necessary to spin a despin the spacecraft, as well as slewing the spacecraft for antenna pointing, the disturbance and slew forces need to be calculated. The disturbance and slew impulses are necessary to calculate the propellant mass which is outlined in section 4.4.8. As the disturbances change depending on what phase of the trajectory the spacecraft is in, the trajectory is divided into 7 different phases. The reason for the number of phases stems from the different disturbance environments in the vicinity of the Earth, Jupiter and the Sun, and the fact that the mass moments of inertia change after each kick-stage.

1. Phase 1: The moment the spacecraft is released from the launch vehicle until it is 0.2 AU away from Jupiter.
2. Phase 2: 0.2 AU from Jupiter until the moment the first stage of the kick-stage burns, at a distance of 600.000 [km] from Jupiter.
3. Phase 3: The moment after the burn of the first stage, at a distance of 600.000 [km] from Jupiter until a distance of 0.2 AU away from Jupiter.
4. Phase 4: From 0.2 AU away from Jupiter until 1 AU away from the Sun.
5. Phase 5: From 1 AU away from the Sun until the moment the second stage of the kick-stage burns, at a distance of 10 solar radii from the Sun.
6. Phase 6: The moment after the burn of the second stage, at a distance of 10 solar radii from the Sun, until 1 AU away from the Sun.
7. Phase 7: From 1 AU away from the Sun until 550 AU away from the Sun.

Before the disturbance environment calculations are performed, the required slew rate for accurate payload instrument measurements must be calculated. This can be done by assuming that the slew rate needs to be largest when it is the closest to Planet 9. It is assumed that this needs to happen 2 degrees before the spacecraft is at its closest distance to the planet. The slew rate calculation is shown in equation (4.15) and equation (4.16).

$$D_{2^\circ} = D_9 \cdot \tan \theta \quad (4.15) \quad \dot{\theta} = \theta \cdot \frac{V_9}{D_{2^\circ}} = 9.89 \times 10^{-7} [\text{rad/s}] \quad (4.16)$$

In these equations,  $D_{2^\circ}$  is the absolute distance travelled by the spacecraft during the 2 degree slew,  $D_9 = 0.44$  AU is the closest distance to Planet 9 (from astrodynamics subsystem),  $\theta = 0.0349$  rad is the 2 degree angle in radians, and  $V_9 = 65.12$  km/s is the spacecraft's velocity at Planet 9. Notice that this value for the required slew rate is extremely low. Although the velocity would indicate a large required slew rate, the distance to planet 9 during the flyby results in a very low slew rate. This is the slew rate that will be used for all slew calculations, including slewing the spacecraft for antenna pointing, as no requirement is set on that.

To calculate the required angular acceleration for this slew rate, equation (4.17) and equation (4.18) can be used.

$$t_\alpha = 0.05 \cdot \Delta t \quad [40] \quad (4.17) \quad \alpha = \frac{\dot{\theta}}{t_\alpha} = 1.98 \cdot 10^{-5} \text{ [rad/s}^2\text{]} \quad [40] \quad (4.18)$$

In these equations,  $\Delta t = 1$  s is the time it takes to get the required slew rate, 0.05 is the fraction of the time during which acceleration and deceleration occurs, assumed to be 5% each.

The slew rate  $\dot{\theta}$  and the angular acceleration  $\alpha$  will be helpful during the force and impulse calculations for the different mission phases.

### Phase 1: Launch till 0.2 AU from Jupiter

During the first phase of the mission, there are several different disturbances acting on the spacecraft. These are the gravity disturbances of Earth and Jupiter, the solar radiation disturbance calculated at Earth and the magnetic disturbances of Earth and Jupiter. All of these will be calculated to find the largest disturbance torque. First the gravity disturbances are calculated in equation (4.19) and equation (4.20).

$$T_{G,Earth} = \frac{3\mu_{Earth}}{2D_{Earth}^3} |I_{z,1} - I_{y,1}| \sin(2\phi) \quad [40] \quad (4.19) \quad T_{G,J} = \frac{3\mu_J}{2D_J^3} |I_{z,1} - I_{y,1}| \sin(2\phi) \quad [40] \quad (4.20)$$

In these equations,  $\mu_{Earth}$  and  $\mu_J$  are the gravitational constants of Earth and Jupiter, respectively.  $D_{Earth}$  and  $D_J$  are the closest distance to Earth and the closest distance to Jupiter during this phase, including their radii.  $|I_{z,1} - I_{y,1}|$  is the absolute difference in mass moment of inertia between the z- and y-axis, before the first stage separation. These values stem from the CAD model inertia calculations.  $\phi$  is the maximum deviation of the z-axis, assumed to be 30 degrees.

Next up is the solar radiation disturbance. This value will be the highest closest to Earth and hence only this disturbance torque will be analysed in equation (4.22).

$$F_{Earth} = \frac{F_s}{c} A_s (1 + q) \cos(I_{Sun}) \quad [40] \quad (4.21) \quad T_{sp,Earth} = F_{Earth} \cdot c_{diff} \quad [40] \quad (4.22)$$

In these equations,  $F_{Earth}$  is the solar radiation force at Earth,  $F_s = 1367 \text{ W/m}^2$  is the solar constant at Earth,  $c = 3.0 \cdot 10^8 \text{ m/s}$  is the speed of light,  $A_s$  is the spacecraft surface area to the Sun (from CAD model).  $q = 1$  is the reflective factor from 0 to 1 where the worst case scenario of  $q = 1$  is chosen. The same reasoning was applied to the angle of incidence of the Sun  $I_{Sun}$ , for which a value of 0 [rad] was chosen. Lastly,  $c_{diff} = 0.4 \text{ [m]}$  is the difference between the center of solar pressure and the center of gravity, for which a safe and sensible number was picked [40].

Lastly, the magnetic disturbances closest to Earth (at beginning of phase 1) and 0.2 AU from Jupiter (at end of phase 1) were analysed. For this, equation (4.23), equation (4.24), equation (4.25) and equation (4.26) are used.

$$B_{Earth} = \frac{2M_{Earth}}{D_{Earth}^3} \quad [40] \quad (4.23) \quad T_{m,Earth} = d \cdot B_{Earth} \quad [40] \quad (4.24)$$

$$B_J = \frac{2M_J}{D_J^3} \quad [40] \quad (4.25) \quad T_{m,J} = d \cdot B_J \quad [40] \quad (4.26)$$

In the above equations,  $B_{Earth}$  and  $B_J$  are the magnetic field strengths at the closest distance to Earth and Jupiter,  $M_{Earth} = 7.96 \cdot 10^{15} \text{ [Tm}^3\text{]}$  and  $M_J = 2.83 \cdot 10^{20} \text{ [Tm}^3\text{]}$  are the magnetic moments of the Earth and Jupiter.  $d = 80 \text{ [Am}^2\text{]}$  is the residual magnetic dipole of the space vehicle, which is caused by unintentional magnetisation of its materials and onboard equipment. For space vehicles with very large masses, like the NIBIRU including the kick-stages, a value of 80  $\text{[Am}^2\text{]}$  is a reasonable and safe estimate [40].

From these values for  $T_{G,Earth}$ ,  $T_{G,J}$ ,  $T_{sp,Earth}$ ,  $T_{m,Earth}$  and  $T_{m,J}$ , the highest disturbance torque was taken to calculate the largest disturbance force. This disturbance force is then taken to be equal to the force required to spin and de-spin the spacecraft to the desired spin rate  $\omega$ . Eventually this results in the total disturbance impulse of phase 1 of the mission. The calculation steps are shown in the equations below

and will be explained afterwards.

$$F_{dist1} = \frac{T1_{max}}{L} \quad (4.27)$$

In equation (4.27), the disturbance force  $F_{dist1}$  necessary to spin the spacecraft is calculated by dividing the maximum disturbance torque  $T1_{max}$  by the moment arm  $L = 0.75$  [m], which is half of the length of the sides of the spacecraft cube.

$$\omega_1 \geq \sqrt{\frac{3T1_{max}}{I_{z,1}}} \quad (4.28)$$

Equation (4.28) uses a rule of thumb to estimate the angular velocity required to have gyroscopic stability. The angular velocity  $\omega_1$  should be equal to or higher than the expression on the right. It is assumed that the two expressions are equal [53].

$$\alpha_1 = \frac{T1_{max}}{I_{z,1}} \quad (4.29)$$

In equation (4.29), the angular acceleration can be calculated by dividing the maximum disturbance torque by the mass moment of inertia of the z-axis.

$$t_{spin1} = \frac{\omega_1}{\alpha_1} \quad (4.30)$$

Once the angular acceleration  $\alpha_1$  and the angular velocity  $\omega$  are known, the time to spin to reach the required angular velocity can be calculated with equation (4.30). This is the time the thrusters will be firing per spin up/spin down.

$$t_{totaldist1} = (1 + 1) \cdot 7 \cdot 52 \cdot t_{phase1} \cdot t_{spin1} \quad (4.31)$$

Equation (4.31) calculates the total time the thrusters will be firing to spin the spacecraft in phase 1 of the mission. It assumes that the spacecraft will communicate with Earth once a day. Hence the thrusters will be used to first spin down the spacecraft, and after communication spin up again  $(1 + 1)$ . The spacecraft will have its antenna pointing to Earth during the trajectory and hence many large slews to rotate the z-axis of the spacecraft are not required. These spin up/spin down manoeuvres will thus be done 7 times a week and  $7 \cdot 52$  times a year. It is then multiplied by  $t_{phase1}$ , which is the total duration of phase 1 and lastly multiplied by the time to spin to reach the angular velocity  $t_{spin1}$ .

$$I_{dist1} = F_{dist1} \cdot t_{total1} \quad (4.32)$$

Now, the total thruster impulse caused by disturbances can easily be calculated with equation (4.32).

As mentioned earlier, there will be a moment where slewing the spacecraft is necessary. During phase 1, the only slewing required is to point the spacecraft from having the kick-stage pointing to Earth (directly after being released from the launch vehicle), to the antenna pointing to Earth. To calculate the force necessary to do this manoeuvre,  $\dot{\theta}$  and  $\alpha$  from the aforementioned equation (4.16) and equation (4.18) need to be used. This will ultimately be used to calculate the slew impulse of phase 1 of the mission. The process for this is outlined below.

$$F_{slew1} = \frac{I_{z,1}\alpha}{L} \quad (4.33)$$

In equation (4.33), the slew force necessary to slew the spacecraft the required amount is calculated. It uses the mass moment of inertia of the z-axis and the moment arm, as well as the angular acceleration required for the slew.

$$t_{slew1} = \dot{\theta} \alpha \quad (4.34)$$

equation (4.34) calculates the time it takes to accelerate the spacecraft to the required slew rate.

$$t_{totalslew1} = 1 \cdot t_{slew1} \quad (4.35)$$

Equation (4.35) shows the total time the thrusters will be firing to slew the spacecraft. As can be seen, the slewing manoeuvre will only be performed once during this mission phase.

$$I_{slew1} = F_{slew1} \cdot t_{totalslew1} \quad (4.36)$$

Finally, the total thrust impulse necessary to slew is calculated with equation (4.36).

### Remaining Phases

The procedure to calculate the disturbance and slew forces and impulses for the remaining 6 phases follows a similar procedure. The disturbance and slew impulses from the mission phases are outlined in table 4.10.

**Table 4.10:** Disturbance, Slew and Impulses

| Phase | Disturbance Impulse [Ns] | Slew Impulse [Ns]    |
|-------|--------------------------|----------------------|
| 1     | $2.29 \cdot 10^5$        | $1.39 \cdot 10^{-3}$ |
| 2     | $2.82 \cdot 10^2$        | $1.39 \cdot 10^{-3}$ |
| 3     | $6.32 \cdot 10^1$        | $1.39 \cdot 10^{-3}$ |
| 4     | $2.98 \cdot 10^2$        | 0                    |
| 5     | $1.23 \cdot 10^3$        | $1.35 \cdot 10^{-3}$ |
| 6     | $7.72 \cdot 10^2$        | $6.41 \cdot 10^{-4}$ |
| 7     | $1.21 \cdot 10^4$        | 0                    |

The disturbance and slew impulses will be added to calculate the the total impulse and this will be used to estimate the propellant mass. The total impulse is shown in equation (4.37)

$$I_{total} = 244,024 \text{ [Ns]} \quad (4.37)$$

### 4.4.5. Thrust force for pointing stability and accuracy

To calculate the minimum thrust force necessary for pointing stability and to minimise the effects of jitter, the following procedure is performed.

$$p_{stabrad} = p_{stabdeg} \cdot \frac{\pi}{180} \quad (4.38)$$

Equation (4.38) converts the pointing stability requirement of  $0.005 \text{ [deg/s]}$  to  $\text{[rad/s]}$ .

$$\alpha_{stab} = p_{stabrad} / t_{control} \quad (4.39)$$

In equation (4.39), the required angular acceleration for stability is calculated by dividing the pointing stability by the time to control the spacecraft, assumed to be 2 s.

$$T_{z,stab} = I_{z,1} \cdot \alpha_{stab} \quad (4.40)$$

Equation (4.40) calculates the minimal torque required for stability. This entails multiplying the smallest mass moment of inertia during the mission, in this case  $I_{z,1}$ , by the angular acceleration  $\alpha_{stab}$ .

$$F_{z,stab} = \frac{T_{z,stab}}{L} = 0.028 \text{ [N]} \quad (4.41)$$

Finally, the minimum thrust force for stability can be calculated with equation (4.41). It divides the torque by the moment arm  $L$ .

Now the minimal thrust for pointing accuracy needs to be calculated. The pointing accuracy requirement is to have a pointing accuracy of 0.01 deg or better. The process to calculate this minimal thrust force is shown below.

$$p_{accrad} = p_{accdeg} \cdot \frac{\pi}{180} \quad (4.42)$$

Again, first the pointing accuracy needs to be converted to radians, this is done in equation (4.42).

$$\dot{\theta}_{acc} = \frac{p_{accrad}}{t_{slew}} \quad (4.43)$$

Equation (4.43) calculates the required slew rate for the accuracy requirement by dividing the pointing accuracy by the time to slew, assumed to be 1 s.

$$\alpha_{acc} = \frac{\dot{\theta}_{acc}}{t_{burn} \cdot 2} \quad (4.44)$$

In equation (4.44), the minimum angular acceleration is found. In this equation,  $t_{burn} = 0.02$  s is the minimum burn time for a thruster. For hydrazine thrusters, which is the propellant type chosen in section 4.4.8, this is typically around 1 to 20 ms. To get a safe estimate, this is set equal to 20 ms. This is multiplied by 2 to account for both acceleration and deceleration.

$$F_{z,acc} = \frac{I_{z,1} \cdot \alpha_{acc}}{L} = 2.83 \text{ [N]} \quad (4.45)$$

Finally, equation (4.45) calculates the minimum required thrust force for accuracy. It multiplies the smallest value of mass moment of inertia with the angular acceleration and divides that by the moment arm, which is equal to 0.75 [m].

Hence, this means we need two different types of thrusters. One should be able to abide by the stability requirement and the other will take care of the accuracy requirement. These thrusters will be chosen in section 4.4.6.

#### 4.4.6. Thruster selection

In this subsection the type of thrusters will be selected. As mentioned, 2 different types of thrusters are necessary. The most common propellant type for ADCS thrusters is hydrazine. This will also be used in the NIBIRU mission. Although hydrazine is a highly toxic carcinogenic, the benefits outweigh this attribute. Important advantages of using hydrazine compared to for example cold gas thrusters are its higher specific impulse and thrust-to-weight ratio. Moreover, it is a monopropellant and hence does not need an oxidizer to ignite. Lastly, hydrazine thrusters have a history of successful use in space missions and they have been used in similar missions such as the Voyager missions, Cassini and New Horizons.

It is chosen to use off-the-shelf thruster components to reduce the overall cost of the space mission. There are numerous different thrusters sold by various companies with different thrust levels. Companies that were analysed include MOOG, ArianeGroup and Aerojet RocketDyne. In the end, it is decided to use two kinds of hydrazine thrusters from Aerojet RocketDyne. These thrusters are outlined below in table 4.11.

**Table 4.11:** Characteristics of Two Aerojet RocketDyne Rocket Engine Assemblies with Monopropellant [54]

| Characteristic                   | MR-401      | MR-111G    |
|----------------------------------|-------------|------------|
| Steady state thrust [N]          | 0.08        | 4          |
| Thrust range [N]                 | 0.07-0.09   | 1.8-4.9    |
| Feed pressure [bar]              | 14.8-18.6   | 6.7-24.1   |
| Valve power [W]                  | 8.25        | 8.25       |
| Mass [kg]                        | 0.6         | 0.37       |
| Engine length/exit diameter [cm] | 23.3 x 5.58 | 19.5 x 1.9 |
| Specific impulse [s]             | 180-184     | 219-229    |
| Single burn life [s]             | 0-900       | 10000      |
| Operational temperature [° C]    | -10 to +50  | -10 to +50 |

The 4N thruster will be used for the accuracy requirement, as mentioned earlier. By placing these thrusters in a configuration with 3 thrusters in 4 corners (so 12 thrusters in total), each on a different side of the spacecraft, 3-axis stability with redundancy is achieved. This configuration is shown in figure 4.8, where the larger thrusters are highlighted with blue circles. The bigger 4N thrusters are the thrusters closest to each corner. The thrusters on the top and bottom surface are positioned at an angle such that the exhaust does not affect the antenna or the kick-stages. Despite this angle, this still means the spacecraft is 3-axis stable due to the fact that the thruster on the opposite side is also placed at this same angle.

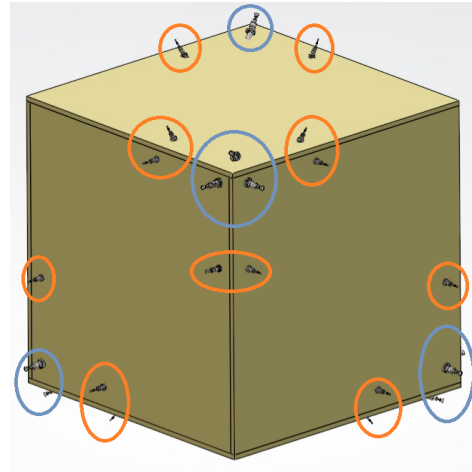


Figure 4.8: Thruster Configuration

The minimum thruster force for stability was calculated with equation (4.41) and is equal to 0.028 N. However, the thrusters chosen have a thrust range of 0.07 to 0.09 N. These thrusters can still comply to have a thrust force of 0.028 N. This can be accomplished by decreasing the moment arm of these small thrusters. The moment arm is changed from 0.75 m to 0.20 m. Another problem arises from this however. It is not desired to place thrusters on each side of the spacecraft close to the middle of the surfaces. The main reason for this is the location of the radiators, which are placed on two sides of the spacecraft with a radius of 0.45 m. The solution to this is to place two thrusters on the sides, both with a moment arm of 0.20 m, instead of one thruster. Hence, for 3-axis stability complying with the stability requirement, a total of 24 small thrusters is used. The configuration of the small thrusters is also shown in figure 4.8. The small thrusters are the thrusters positioned more to the middle of the spacecraft sides; the ones highlighted with orange circles. The ones on the top and bottom surface are placed at an angle as well, for the same reason as the bigger thrusters.

#### 4.4.7. Sensor selection

As mentioned, there are multiple sensor options that are unfeasible for the NIBIRU mission. The options that are not useful for this mission are Earth sensors, horizon sensors, GPS receivers and magnetometers. The remaining options are star trackers, IMU's, gyroscopes and an onboard autonomous clocks. The onboard clock is part of the OBDH subsystem and will be elaborated on in section 4.9. For the NIBIRU mission it is chosen to use a combination of star trackers and IMU's.

Star trackers capture images of stars and compare them to an onboard star catalog to accurately determine the spacecraft's attitude. There are two types of star trackers; one type has one axis accuracy and needs two star trackers with a 90 degree direction difference to have full 3-axis accuracy, the other type has build-in 3-axis accuracy and only one will be required to determine the attitude.

Inertia measurement units (IMU's) combine gyroscopes and accelerometers in a single unit to determine the spacecraft's angular velocity and acceleration, respectively. They are useful for short-term stability but require calibration with other sensors to avoid drift. Hence, one IMU will be used alongside the two different star trackers for complete 3-axis attitude determination.

There are numerous star trackers and IMU's on the market and hence some of these off-the-shelf components are chosen. To determine which type of star tracker and IMU is best for the NIBIRU mission, the requirements in terms of power, mass and pointing knowledge have to be taken into consideration. The characteristics of several star trackers and IMU's by different companies (such as Ball Aerospace, Jena Optronik, Rocket Lab, Honeywell, Northrop Grumman and Sodern Ariane Group) are analysed and compared. Finally, it is decided to use the HORUS star tracker made by Sodern Ariane Group and the Honeywell HG9900 IMU. These attitude determination sensors have the following characteristics, as shown in table 4.12.

**Table 4.12:** Attitude Determination Sensor Characteristics

| Characteristic               | HORUS Star Tracker [55] | HG9900 IMU [56] |
|------------------------------|-------------------------|-----------------|
| Manufacturer                 | Sodern Ariane Group     | Honeywell       |
| Pointing performance/bias    | 0.00306 degrees         | 0.0035 deg/hr   |
| Dimensions (LxHxW) [cm]      | 14.1x14.1x25.0          | 14.0x16.3x13.6  |
| Mass [kg]                    | 1.6                     | 2.72            |
| Nominal power [W]            | 9.5                     | 8               |
| Peak power [W]               | 11.5                    | 10              |
| Operational lifetime [years] | >18                     | >15             |
| Reliability [FIT]            | 172                     | N/A             |
| Operational temperature [K]  | 243-323                 | 233-344         |

The characteristics of these sensors align with the ADCS requirements. It should be taken into consideration that the operational lifetime of these sensors is lower than the mission lifetime of 50 years. Hence, redundant components need to be taken. In terms of star trackers, 8 will be taken onboard the spacecraft. 2 star trackers will need to be turned on at all times. This means that a minimum of  $50/18 = 2.78 \approx 3$  pairs of star trackers are necessary, assuming an operational lifetime of at least 18 years. To have some redundancy in terms of unexpected failures, an additional 2 star trackers are taken. For the IMU's, the operational lifetime is at least 15 years. Since only one is necessary to be turned on, a minimum of  $50/15 = 3.33 \approx 3$  IMU's are needed. 2 additional IMU's are also taken for redundancy purposes, and so in total 5 IMU's.

The IMU's will be inside the spacecraft to measure angular velocities and accelerations. The star trackers are positioned such that two star trackers will be used at all times, along different axes.

#### 4.4.8. Propellant mass and tank sizing

Now the propellant tanks for the ADCS can be sized. First, the propellant mass can be calculated with equation (4.46).

$$M_{prop} = \frac{I_{total}}{I_{sp} \cdot g} = 132.7 \text{ [kg]} \quad (4.46)$$

In this equation,  $I_{total}$  is the total impulse calculated in section 4.4.4,  $I_{sp} = 187.5 \text{ [s]}$  is the average specific impulse of the hydrazine thrusters selected in section 4.4.6 and  $g = 9.81 \text{ [m/s}^2\text{]}$  is the gravitational acceleration at Earth.

To account for the simplifications and assumptions made during the disturbance impulse calculations, a safety factor of 1.5 is applied to add a safe margin to the propellant mass estimation. This is shown in equation (4.47).

$$M_{prop,SF} = M_{prop} \cdot SF = 199.0 \text{ [kg]} \quad (4.47)$$

Then the volume and radius of the propellant tanks can simply be calculated with equation (4.48) and equation (4.49).

$$V_{prop} = 1.1 \cdot \frac{M_{prop,SF}}{\rho_{prop}} = 0.212 \text{ [m}^3\text{]} \quad (4.48) \quad R_{prop} = \left( \frac{V_{prop}}{\frac{4}{3}\pi} \right)^{1/3} = 0.370 \text{ [m]} \quad (4.49)$$

In these equations,  $1.1 = 1 + k_{ullage}$ , where  $k_{ullage} = 0.1$  is the ullage volume fraction and  $\rho_{prop}$  is the density of hydrazine. The ullage volume factor will be further explained in the propulsion subsystem section 4.6.6. Furthermore, the sizing of the tank of the pressurizer tanks for ADCS follows the same procedure as the tank sizing of the main tanks, outlined in section 4.6.6. Table 4.13 shows the important values related to propellant and pressuriser tank sizing. The pressuriser that is used is Helium gas and the material of the tanks is Titanium Ti-10V-2Fe, the same as for the main tanks.

**Table 4.13:** Propellant and Pressuriser Tank Values

| Parameter                  | Value    | Units |
|----------------------------|----------|-------|
| Mass Propellant            | 132.7    | kg    |
| Mass Propellant SF         | 199.0    | kg    |
| Volume Propellant Tank     | 0.2121   | $m^3$ |
| Radius Propellant Tank     | 0.3700   | m     |
| Pressuriser Mass           | 14.14    | kg    |
| Volume Pressuriser Tank    | 0.06638  | $m^3$ |
| Radius Pressuriser Tank    | 0.2512   | m     |
| Thickness Propellant Tank  | 0.01000  | m     |
| Thickness Pressuriser Tank | 0.01000  | m     |
| Mass Propellant Tank       | 0.01720  | kg    |
| Mass Pressuriser Tank      | 0.007929 | kg    |

The price per kg for the propellant and pressuriser are €183 and €652, respectively.<sup>17</sup> The price of the material of the tanks can also be estimated. Assuming the Titanium Ti-10V-2Fe alloy will be used, the price per [kg] is €23.80 [57]. As less than a kilo of material per tank is probably necessary, these costs will be neglected.

#### 4.4.9. Verification and validation

The design of the ADCS made extensive use of Python to calculate the important values such as the total impulse, the minimum required force and the size of the propellant tanks. Hence, the code had to be verified. The verification process includes removing any syntax and logic errors from the code. Next, to make sure that the equation and calculation process was done correctly in Python, each line of code was calculated by hand. Moreover, some extreme and critical value tests were performed to test the model's response to a number of conditions.

The model was validated to determine the accuracy of the results. The main parameter used for this model validation is the propellant mass of 132.7 kg. This mass was calculated with the total impulse of all disturbances and slews. As mentioned earlier, the NIBIRU mission can be compared to several other deep space/planetary exploration missions. The New Horizons mission was loaded with approximately 77 kg of hydrazine propellant at launch [49]. The Voyager missions each carried about 100 [kg] of hydrazine monopropellant [58]. These were launched in 1973 and are still expected to have enough propellant until 2030. Hence, the calculated value of 132.7 kg for the NIBIRU mission seems like a feasible value. However, a lot of assumptions were made to do the ADCS calculations. To make sure that the amount of propellant is not too low, the worst case was usually chosen as an assumption. Moreover, a safety factor of 1.5 was taken, leading to a total propellant mass taken aboard the NIBIRU spacecraft of 199.0 kg. The requirement verification is performed in section 4.4.10.

#### 4.4.10. Final design

The requirements from section 4.4.2 have all been complied with in the design. Table 4.14 shows the final design values for the ADCS. The total ADCS mass is 258.38 N and the estimated cost is around €M3.4. The power for the Aerojet RocketDyne MR-111G 4N thrusters is left blank, as these use the same valve as the smaller thruster. Hence, no additional power is required. A total of 2 out of the 8 star trackers will be on at all times, leading to a total power required of 23 W for the star trackers. Only one IMU needs to be turned on and so this requires 10 W of power. The propellant and pressuriser of course do not require any power either. This results in a total required power for the ADCS of 41.25 W.

<sup>17</sup>URL [https://www.dla.mil/Portals/104/Documents/Energy/Standard%20Prices/Aerospace%20Prices/E\\_2019Oct1AerospaceStandardPrices\\_190920.pdf?ver=2019-09-26-081849-240](https://www.dla.mil/Portals/104/Documents/Energy/Standard%20Prices/Aerospace%20Prices/E_2019Oct1AerospaceStandardPrices_190920.pdf?ver=2019-09-26-081849-240) [cited 18 June 2024]

**Table 4.14:** Final ADCS Values

| Component  | Mass [kg]     | Max Power [W] | Estimated Cost [€M] |
|--|---------------|---------------|---------------------|
| HORUS Star Trackers<br>(8 components)            | 12.8          | 23            | 2.40                |
| HG 9900 IMU's<br>(5 components)                  | 13.6          | 10            | 0.25                |
| Aerojet RocketDyne MR-401<br>(24 components)     | 14.4          | 8.25          | 0.48                |
| Aerojet RocketDyne MR-111G 4N<br>(12 components) | 4.44          | -             | 0.24                |
| Hydrazine Propellant                             | 199.0         | -             | 0.0364              |
| Pressuriser Helium                               | 14.14         | -             | 0.00922             |
| <b>Total</b>                                     | <b>258.38</b> | <b>41.25</b>  | <b>3.4156</b>       |

These values were obtained after numerous iterations, discussions and compromises with other subsystems that had a significant influence on the design of the ADCS. These subsystem were mainly structures (placement of the thrusters), telecommunications (pointing accuracy and stability requirements) and astrodynamics (location and time of spacecraft for disturbance calculations). The heat shield was not taken into consideration for the ADCS. As the top and bottom surface of the spacecraft could not support a simple 3-axis stability attitude control system due to the kick-stages and the antenna, a creative 3-axis control system was applied. When it was clear that a heat shield was a necessity because of the distance to the Sun, this became a problem for attitude control. The heat shield would be on one side of the spacecraft, but this side is crucial for the functioning of the ADCS. Hence, further design and research will have to determine a thruster configuration that could have 3-axis control with the heat shield on one side of the spacecraft.

In the design process for ADCS, it is assumed that the spacecraft will communicate with Earth once a day. However, it could be that it will be decided to communicate with Earth less often. This would increase the reliability of spacecraft components. This means the required propellant mass will decrease. The design is hence extra safe and the additional propellant could be used for any trajectory corrections if necessary.

## 4.5 Astrodynamics

*Contributors: Dhafin, Flavio*

In planning a mission to Planet 9, an essential aspect is the selection of an optimal trajectory. Trajectory selection refers to the process of determining the most efficient path for a spacecraft to follow in order to reach its destination. This process is crucial for several reasons, primarily because it directly impacts the mission duration, fuel consumption, and overall success. In this section, the trajectory requirements, the simulation setup, the optimisation process and the results will be discussed.

### 4.5.1. Trajectory requirements

Prior to designing the trajectory for the spacecraft, it is important to identify the requirements that are related to the trajectory. These requirements are listed below:

**Table 4.15:** Astrodynamics Subsystem Requirements

| ID             | Requirement  |
|----------------|--|
| PL9-MIS-TP-3.4 | NIBIRU shall be in range to take a picture of Planet 9                   |
| PL9-MIS-TP-4.5 | NIBIRU shall not fly closer than 0.04 AU from the Sun                    |
| PL9-MIS-CN-2.1 | A launcher that is completely operational by 2034 shall be used          |
| PL9-STK-ESA-02 | NIBIRU shall complete its science objectives within 50 years from launch |

One challenge that threatens the feasibility of the mission is the requirement to complete science objectives within 50 years from launch, which implies that the spacecraft needs to reach Planet 9 in less than 50 years as well. As of today, the furthest man-made object ever created is the Voyager 1, with a current

distance of 136 AU from the Sun. However, Voyager 1 was launched nearly 50 years ago which suggests that NIBIRU's mission profile has to be novel and innovative [51].

In the study of potential trajectories to Planet 9, a notable paper titled "*Can We Fly to Planet 9?*" proposes several intriguing paths that utilise solar Oberth maneuvers [5]. This technique involves a powered flyby around the Sun, harnessing its gravitational pull to significantly increase the spacecraft's velocity therefore reducing the mission's time of flight. Thus, a solar Oberth maneuver offers a massive degree of feasibility to the mission especially with regards to reaching Planet 9 within 50 years. To further provide a justification why a solar Oberth maneuver is critical to the mission, the same paper mentioned that an optimised Jupiter flyby will lead to a time of flight of approximately 94 years, while trajectories that include solar Oberth maneuvers lead to time of flights of 40-60 years [5]. However, although such a maneuver has never been attempted due to the extreme thermal challenges posed by the Sun's proximity, the success of the Parker Solar Probe demonstrates that a spacecraft can be engineered to withstand distances as close as 10 solar radii from the Sun. Consequently, trajectories incorporating solar Oberth maneuvers will be included in the trajectory selection. In this section, the process of selecting an optimum trajectory to Planet 9 will be discussed in detail.

The question of what an optimum trajectory entails is a valid one. To address this problem, it is useful to determine several astrodynamics parameters that are influential to the trajectory determination. A prevalent parameter in describing spacecraft trajectories is the  $\Delta V$ , which is a measure of the increase in velocity that the propulsion subsystem is capable of providing. Higher  $\Delta V$ 's are achievable by carrying more propellant on board and/or utilising a more efficient propulsion system. Additionally, the time of flight (TOF) of the trajectory is also a crucial parameter in the mission profile, as it determines whether NIBIRU will reach Planet 9 under the specified 50 years requirement. Therefore, the aim of optimising the trajectory is to design a sufficiently low  $\Delta V$  to reach Planet 9 under 50 years.

#### 4.5.2. Gravity assist and oberth maneuver

As the 50 year requirement poses a challenge for the feasibility of the mission, it is crucial to identify some techniques that space missions have inherited that helps in reducing its flight duration. With this in mind, two techniques are considered: gravity assist and Oberth maneuver, both of which are briefly explained below.

The benefit of gravity assists is the change in the spacecraft's velocity due to the orbits of other planetary bodies. This can be explained in the context of conservation of momentum. When a spacecraft is approaching a planet at a certain velocity, the gravitational force of the planet will attract the spacecraft. With the orbital motion of the planet around the Sun, the spacecraft can alter its direction as well as its velocity after performing the flyby. In theory, the conservation of momentum ensures that if the spacecraft gains velocity, then the flyby planet would have lost velocity, and vice versa. However, the flyby planet has a significantly higher mass which suggests that this change in velocity is negligible. On the other hand, this is not the case for the spacecraft as it is relatively much lighter than the planet thus amplifying its change in velocity. The most common usage of gravity assists is to gain velocity, however there are several missions that have used planetary flybys to slow down the spacecraft in order to ease orbit insertion or land on the planet's surface [59].

Another technique to reduce flight duration is Oberth maneuver, which occurs when a spacecraft performs an engine burn under the influence of a planet's gravitational force, such as during a planetary flyby. The main advantage of such maneuvers is that the spacecraft will gain more velocity if it fires its engines when the spacecraft is initially at a higher velocity before the burn. To further justify this claim, consider a spacecraft performing an Oberth maneuver at the periapsis of a parabolic orbit around a planet. The velocity at the periapsis of a parabolic orbit is formally known as the escape velocity,  $V_{esc}$ . The change in the specific kinetic energy of the spacecraft before and after the burn can be expressed as the following,

where  $\Delta V$  is the change in the spacecraft velocity provided by the burn [59]:

$$\Delta e_k = \frac{1}{2}(V_{esc} + \Delta V)^2 - \frac{1}{2}V_{esc}^2 \quad (4.50)$$

$$= V_{esc}\Delta V + \frac{1}{2}\Delta V^2 \quad (4.51)$$

By examining Equation (4.50), it is clear that for a fixed  $\Delta V$ , a larger change in the specific kinetic energy will be obtained by the spacecraft if the velocity at which the burn is applied is higher. Exploiting these two trajectory techniques will aid in increasing the spacecraft's velocity which leads to the improvement of the feasibility of the mission, especially when the 50 year requirement is considered.

### 4.5.3. Trajectory simulation setup

The computer model that will be used to simulate the spacecraft's trajectory is provided by the TUDAT, which is an open-source astrodynamics library with a wide range of tools for trajectory design.<sup>18</sup> As mentioned previously, it is essential to make use of gravity assists and Oberth maneuvers to minimize the flight time of the spacecraft. Fortunately, TUDAT offers a useful tool in the library for this application, which is the transfer trajectory module that supports the determination of multiple gravity assist (MGA) trajectories.<sup>19</sup>

Prior to discussing the programming flow of the simulation, it is relevant to discuss a few terminologies that are used in describing the spacecraft's trajectory within TUDAT. Firstly, a *node* specifies the bodies that the spacecraft will encounter. In the case of the NIBIRU mission the *departure node* is Earth, where as the *arrival node* is Planet 9. Any planetary bodies that the spacecraft will visit to perform gravity assists are called *swingby nodes*. Secondly, a *leg* is the path between nodes, which leads to the relation of the number of legs being one less than the number of nodes.

#### Setup and Evaluation

Having defined the terminologies, the programming flow is described within the following steps, note that the inputs to the functions will be discussed further:

1. Use `mga_settings_unpowered_unperturbed_legs` to initialise the transfer leg and transfer node settings. This will take as input the transfer body order, the departure and arrival orbit, as well as the minimum pericenters for which the spacecraft can reach when performing flybys.
2. Initialise the transfer trajectory object using `create_transfer_trajectory`. It takes as inputs the bodies, the transfer body order, the previously initialised transfer leg and transfer node settings, and lastly the central body of the simulation (commonly taken as the Sun)
3. Input the necessary parameters to evaluate the trajectory. Three sets of parameters need to be specified: *node times*, *leg free parameters* and *node free parameters*. The specifics of what these parameters imply are the following:
  - Node times: This set of parameters include the node times of each planetary encounter which starts at the departure at Earth, all the desired times to reach the planetary flybys and the time to reach Planet 9. The node time is expressed in seconds after J2000, which starts at January 1, 2000 at noon. For example, consider the following transfer body order: Earth, Jupiter, Planet 9. The node times of each body needs to be specified. For instance, say that the spacecraft needs to launch at a certain date. Simply convert that date to seconds after J2000 using a function called `convert_date_string_to_ephemeris_time`. This can then be done for all the other bodies. The result will then be an array consisting of the node times of the planetary encounters of size  $N \times 1$ , where  $N$  is the number of nodes.
  - Leg free parameters: This set of parameters only need to be defined if the spacecraft plans on performing deep space maneuvers (DSM) during the transfer legs. This means that somewhere

<sup>18</sup>URL: <https://docs.tudat.space/en/latest/index.html> [cited 19 June 2024]

<sup>19</sup>URL: [https://docs.tudat.space/en/latest/\\_src\\_user\\_guide/prelim\\_mission\\_design/mga\\_transfer.html](https://docs.tudat.space/en/latest/_src_user_guide/prelim_mission_design/mga_transfer.html) [cited 19 June 2024]

in between the transfer legs, the engine will burn and provide some additional  $\Delta V$ . For the application of this mission, this was not desired as the propulsion system will only be active at the planetary flybys. Therefore, this set of parameters are left as an array full of zeros of size  $N \times 1$ , where  $N$  is the number of nodes.

- Node free parameters: In the case that an orbit at the arrival node is desired, this set of parameters is left as an array full of zeros of size  $N \times 3$ , where  $N$  is the number of nodes. However, if a flyby at the arrival node is desired, the last row of this array needs to be specified as: the periapsis altitude of the planet's (closest) approach, the orbital plane angle (with respect to the incoming velocity and node velocity) at the arrival node and the  $\Delta V$  at the arrival node. Note that this specific order of parameters need to be followed.

4. Evaluate the transfer trajectory object to retrieve the required  $\Delta V$  at each node, using the evaluate function of the transfer trajectory object, which takes as inputs the node times, leg free parameters and node free parameters.

### Propagating the orbit of Planet 9

Another task that needs to be performed is the orbit propagation of Planet 9, which is not included in the default set of bodies provided in TUDAT. Fortunately, TUDAT offers functionalities that allow for custom creation of bodies, given the following parameters:

- The gravitational parameter of the new body
- Initial states of the new body, expressed in either Cartesian or Keplerian states both of which contains six elements. Keplerian states will be selected as available ephemeris data regarding Planet 9's potential location and orbital parameters are expressed as such. The order of these states are as follows: semi-major axis, eccentricity, orbit inclination, argument of periapsis, longitude of ascending node and true anomaly.
- The epoch at which the initial states are defined, expressed in seconds after J2000.
- The frame orientation at which the initial states are defined in.
- The frame origin of the frame orientation.

The most recent paper at the time of performing the necessary research estimates that the mass of Planet 9 is approximately 6.6 Earth masses, which suggests that the gravitational parameter is also 6.6 times that of Earth, which amounts to  $2.6307629 \times 10^{15} [m^3 s^{-2}]$  [60].

In order to specify these parameters, it is useful to refer to sources that specify the potential locations of Planet 9. A combination of sources are used to obtain values regarding the potential orbital parameters of Planet 9. As for the current location of Planet 9, the most recent paper that was published at the time of researching this topic will be used. The paper mentions that there exists a remaining 22% of the sky that has not yet been observed in searching for Planet 9 [60]. The middle of this region is taken as the estimated current location of Planet 9. Note that these parameters are expressed in ecliptic coordinates centered around the Sun.

**Table 4.16:** Assumed Orbital Parameters and Location of Planet 9 [60–62]

| Orbital Parameters                | Value |
|-----------------------------------|-------|
| Semi-major Axis [AU]              | 500   |
| Aphelion Distance [AU]            | 630   |
| Longitude of Ascending Node [deg] | 45    |
| Orbit Inclination [deg]           | 20    |
| Argument of Periapsis [deg]       | 150   |
| Location                          | Value |
| Current Distance [AU]             | 550   |
| Right Ascension [deg]             | 75    |
| Declination [deg]                 | 20    |

From this set of data, the initial states of Planet 9 can be defined. Out of the six initial Keplerian states that need to be defined, four of them are specified: the semi-major axis, longitude of ascending node, longitude of ascension node and orbit inclination are specified. As for the eccentricity and true anomaly, further calculations need to be performed.

#### *Eccentricity*

The following formula calculates the aphelion distance, where  $a$  is the semi-major axis and  $e$  is the eccentricity [59]:

$$r_a = a(1 + e), e = \frac{r_a}{a} - 1 \quad (4.52)$$

By substituting the relevant values, the eccentricity of Planet 9 is found to be 0.23.

#### *True Anomaly*

A very useful equation in astrodynamics is the orbit equation, which is displayed below where  $r$  is the distance between the focal point and the orbiting body,  $e$  is the eccentricity and  $\theta$  is the true anomaly of the orbiting body [59]:

$$r = \frac{a(1 - e^2)}{1 + e \cos(\theta)}, \theta = \arccos\left(\frac{1}{e} \left(\frac{a}{r}(1 - e^2) - 1\right)\right) \quad (4.53)$$

Given the current distance of 550 AU, a semi-major axis of 500 AU and the previously calculated eccentricity of 0.23, the true anomaly is found to be 127.18°.

Having defined all six necessary Keplerian states to propagate its orbit, the last task is to define the epoch at which the previously calculated initial states are defined at. Since the location of Planet 9 was published in a paper that was released in 7 March 2024, this will be taken as the epoch of the initial state. Note that in the program itself, this date needs to be transformed to seconds after J2000.

### 4.5.4. Trajectory optimiser setup

As the possibilities of input parameters to the evaluation of the transfer trajectory are endless, it is essential to select the set of parameters that will optimise the transfer trajectory. As mentioned previously in the introduction of this section, an optimum trajectory is one that minimises the total  $\Delta V$  that the spacecraft needs to provide through out its journey to Planet 9. Therefore, the aim of this subsection is to provide an overview of the optimisation process for the trajectory selection.

The first step in constructing the optimiser is to define the set of parameters that will be used to optimise the total  $\Delta V$ . It is useful to return to the previous subsection to identify such parameters. As discussed in Step 3 in Section 4.5.3, the set of parameters the need to be specified to evaluate the trajectory are the node times of each planetary encounter. In addition to the node times, the node free parameters at the arrival node need to be defined in the case that a flyby is desired at the arrival node. However, these node free parameters do not need to be specified for orbits at the arrival node. Note that the leg free parameters will not be altered as they are not required for trajectories with unpowered legs, which is the case for this mission.

Having defined the set of parameters that will be used to optimise the trajectory, the next step is to set up the optimisation procedure. The optimisation procedure is inspired by an example of trajectory optimisation provided in the TUDAT documentation. In this example, a module called Python Parallel Global Multiobjective Optimizer (PyGMO) library is used.<sup>20</sup> Two aspects are important in this process: the optimisation problem and the optimiser itself.

#### Optimisation Problem

The optimisation problem needs to be specified as a class in Python. Within this class, two functions are

<sup>20</sup>URL: [https://docs.tudat.space/en/latest/\\_src\\_getting\\_started/\\_src\\_examples/notebooks/pygmo/asteroid\\_orbit\\_optimization/aoo\\_custom\\_environment.html](https://docs.tudat.space/en/latest/_src_getting_started/_src_examples/notebooks/pygmo/asteroid_orbit_optimization/aoo_custom_environment.html) [cited 19 June 2024]

necessary to be constructed: `get_bounds` and `fitness`. The `get_bounds` functions returns two lists, where the first list consists of the lower bounds of the input parameters and the second list consists of the upper bounds. The `fitness` takes as input a list of length  $N$  where  $N$  is the number of input parameters that will be used to optimise the problem, this list is also known as the *design parameter vector*. This function returns the value that needs to be optimised, which in this case is the total  $\Delta V$  of the transfer trajectory.

### Optimiser

The optimiser itself is relatively simple to setup. The optimisation problem needs to first be initialised, with all the parameter bounds that will be tested for in the optimiser. Then the optimisation problem can be passed to the `problem` function, such that it becomes an optimisation problem that PyGMO can work with. Then, an optimisation algorithm needs to be selected using the `problem` function. In the example shown in TUDAT, an optimiser called *Simple Genetic Algorithm* is used which is also the one used for this mission's trajectory optimisation. From here, simply specify the population size, the number of generations and the seed number. A brief explanation of what these variables imply is as follows:

- *Population Size*: This determines the number of randomly chosen sets of parameters in each generation. The higher the population size, the more diverse this selection of randomised parameters will be.
- *Number of Generations*: This determines the number of iterations that the optimiser will perform.
- *Seed Number*: As the optimiser will randomly select the parameters based on the given bounds, it is important to maintain reproducible results. Therefore, a seed number should be specified.

#### 4.5.5. Optimisation results

As mentioned previously, performing the optimisation requires the initialisation of the problem class. This involves setting the bounds of the parameters that will be tested. Prior to setting these bounds however, the transfer trajectory object needs to be initialised. The following input parameters are used to initialise the transfer trajectory object; note that these parameters will not be altered over the duration of the optimisation:

- Departure Orbit = 300 km altitude, circular orbit (eccentricity = 0)
- Arrival Orbit = None, this is specified as NaN values for flyby at the arrival node.
- Transfer body order = Earth-Jupiter-Sun-Planet 9
- Minimum Pericenters = Default values, except for the Sun where a minimum distance of 0.04 AU is given, such that the requirement PL9-MIS-TP-4.5 is met.

Additionally, the optimisation problem can be initialised by defining the bounds for which the parameters will be modified under. This is displayed in the following table:

**Table 4.17:** Input Parameters of the Transfer Trajectory Object

| Parameter                                 | Lower Bound       | Upper Bound       |
|---|-------------------|-------------------|
| <i>Departure Date [years]</i>             | January 1st, 2034 | January 1st, 2040 |
| <i>Leg 1 TOF (Earth-Jupiter) [years]</i>  | 1                 | 8                 |
| <i>Leg 2 TOF (Jupiter-Sun) [years]</i>    | 1                 | 8                 |
| <i>Leg 3 TOF (Sun-Planet9) [years]</i>    | 30                | 40                |
| <i>Planet 9 Periapsis Altitude [AU]</i>   | 0.1               | 0.3               |
| <i>Planet 9 Arrival Orbital Angle [°]</i> | 0                 | 360               |
| <i><math>\Delta V</math> at Planet 9</i>  | 0                 | 0                 |

After the optimiser is executed, the program randomly selects a departure date between 2034 and 2040. The lower bound of 2034 is selected such that the requirement PL9-MIS-CN-2.1 is complied with. Once a random departure date is selected, a Time-Of-Flight (TOF) is then randomly selected for each of the trajectory legs between the bounds listed above. The TOF lower bounds are present to provide sufficient time for the spacecraft to reach the destination planet of each leg without the need for an unrealistic

$\Delta V$ . In other words, if a lower bound of zero years is set and the program randomly selects a TOF of 1 day between Jupiter and the Sun, the results will be useless as the output will be an incredibly large required  $\Delta V$  at Jupiter. Additionally, the upper bounds ensure that the 50 years requirement, as stated in PL9-STK-ESA-02, is complied with. The Planet 9 periapsis altitude upper bound was set at 0.3 AU, since the maximum distance at which useful measurements of the planet can be performed is 0.5 AU, meaning that the aforementioned periapsis value would give a window during which performing measurements is possible. This also ensures that the PL9-MIS-TP-3.4 requirement is met. It is also important to note that the  $\Delta V$  at Planet 9 was set to 0, as the plan is to perform a flyby and therefore no  $\Delta V$  will be required to slow down and insert the spacecraft in orbit.

It is also possible to set three additional parameters to calibrate the randomisation of the optimizer:

- **seed**: this is particularly useful to be able to reproduce results. For the final results a seed of 21 was used.
- **num\_gen**: this establishes the number of times results will be generated. After the generation is finished, the program selects the result with the smallest  $\Delta V$ . A value of 40 was used for the final results.
- **pop\_size**: this refers to the number of random initialisations made per each trajectory parameter during each generation. A value of 100 was used for the final results.

Once the optimiser is executed for the aforementioned parameters, the total TOF is just over 49.5 years which leads to an arrival at Planet 9's where the  $\Delta V$  required at each of the bodies along the trajectory are as follows:

- at Earth (provided by launcher after in-orbit refueling): 7080 m/s
- at Jupiter: 1420 m/s
- at Sun: 3416 m/s
- at Planet 9: 0 m/s

Once more, the null value of  $\Delta V$  at Planet 9 follows from the fact that no orbit insertion maneuvers will be performed. As for the optimum design parameters, the following results are obtained:

**Table 4.18:** Parameters for Optimum Trajectory

| Parameter                                 | Value              |
|---|--------------------|
| <i>Departure Date [years]</i>             | January 22nd, 2038 |
| <i>Leg 1 TOF (Earth-Jupiter) [years]</i>  | 7.47               |
| <i>Leg 2 TOF (Jupiter-Sun) [years]</i>    | 2.10               |
| <i>Leg 3 TOF (Sun-Planet9) [years]</i>    | 39.97              |
| <i>Planet 9 Periapsis Altitude [AU]</i>   | 0.24               |
| <i>Planet 9 Arrival Orbital Angle [°]</i> | 115.72             |
| <i><math>\Delta V</math> at Planet 9</i>  | 0                  |

As mentioned previously, the total TOF of the mission is slightly over 49.5 years, however the simulation was able to yield a precise arrival date at Planet 9 of July 26th, 2087. Lastly, keeping track of the states of the spacecraft leads to a visual representation of the trajectory, as displayed in Figure 4.9.

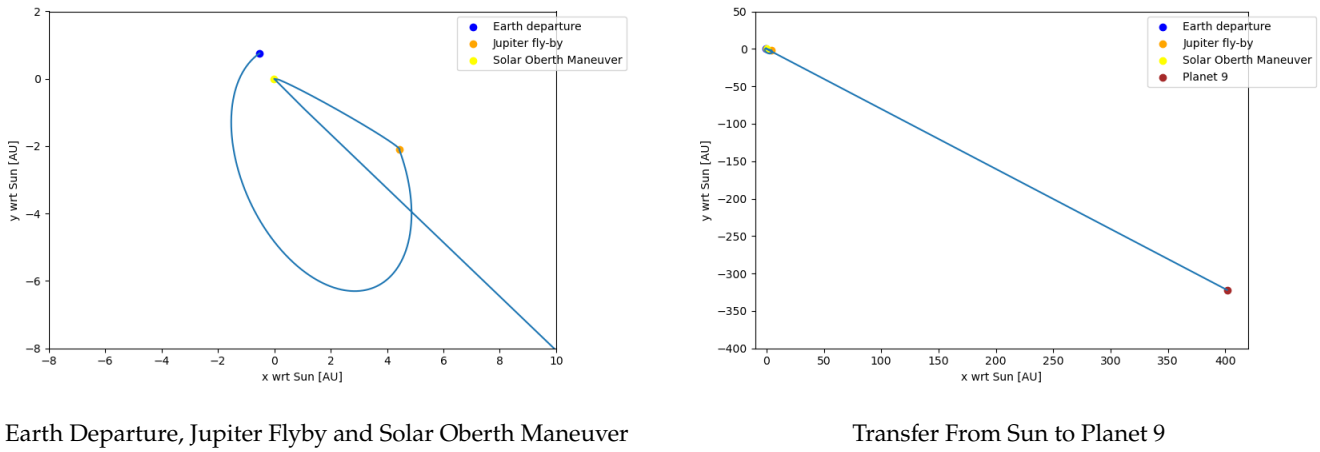


**Figure 4.9:** Visual Representation of the Trajectory of NIBIRU from Earth Departure to Planet 9 Arrival

#### 4.5.6. Verification and Validation

As the trajectory selection process involves the use of computer tools, it is crucial to perform verification and validation on them. Verification ensures that the program was free of computer and calculation errors, whereas validation ensures that the model is sufficiently accurate within an acceptable range of accuracy for its intended purposes.

The verification process started by ensuring that the model is free of syntax errors. This was simply done by running the code and ensuring that syntax errors do not rise. The next step that followed was unit-testing, which ensures that individual functions that were used returned values that were to be expected. Unit-tests were only done on custom-made functions, not on the functions that were provided by the TUDAT and PyGMO libraries. The motivation behind this was that both TUDAT and PyGMO are well established libraries that have been used by professionals in academic fields. Furthermore, performing verification on the functions within these libraries would require a deep understanding on how the code of the functions work. This would be a very time consuming process, especially when considering that TUDAT utilises analytical/semi-analytical methods for simulating trajectory and that PyGMO incorporates complex algorithms for optimisation purposes. With this in mind, all of the custom-made functions were tested and no syntax nor calculation errors were detected during the verification process.

Furthermore, validation was also performed on the computer model. The chosen method for validation is called *face validity*, where an expert (Onur Çelik) in fundamental astrodynamics and interplanetary trajectory optimisation reviews the results of the model and makes an assessment on whether the model behaviour and input-output relationships were reasonable[63]. Furthermore, as the TUDAT library has aided in high amounts of research outputs, it is considered to be a library that consists of reliable and sufficiently accurate functionalities within the astrodynamics field.<sup>21</sup>

#### 4.5.7. Recommendations

While the current trajectory optimization meets the mission requirements and appears to be optimal, there are several recommendations to consider for further improvement. Firstly, exploring different algorithms provided by PyGMO could potentially lead to even more optimal trajectories. PyGMO offers a variety of optimization algorithms with different characteristics and strengths, such as evolutionary algorithms (e.g., NSGA-II, CMA-ES) and gradient-based methods (e.g., BFGS). Testing multiple algorithms can help find the best-suited one for the specific trajectory problem. Additionally, evaluating different transfer body orders could be beneficial. For instance, considering trajectories like Earth-Venus-Earth-Jupiter-Planet 9 could provide interesting insights and possibly more efficient paths. Each transfer body configuration can significantly affect the trajectory characteristics, such as flight time, delta-v requirements, and gravitational assists.

<sup>21</sup>URL [https://docs.tudat.space/en/latest/\\_src\\_about/research\\_output.html](https://docs.tudat.space/en/latest/_src_about/research_output.html) [cited 24 June 2024]

## 4.6 Propulsion

*Contributors: Flavio, Thijmen, Dhafin*

The propulsion system of a spacecraft provides the vast majority of its  $\Delta V$ . The main components are the propellant tanks and thrusters. The design of this subsystem is therefore closely linked to the mission trajectory. It is one of the critical subsystems as its design is decisive in determining whether several key missions requirements will be met.

In section 4.6.1, a preliminary estimate of the propulsion system cost is obtained. The propulsion system requirements and assumptions are listed in section 4.6.2 and in section 4.6.3 respectively. The propulsion type choice is explained in section 4.6.4, followed by the analysis of several bipropellant options in section 4.6.5. In section 4.6.6, the conceptual approach to sizing the tanks is covered. The motivation behind staging is disclosed in section 4.6.7, and subsequently some considerations about thrust are given in section 4.6.8. In section 4.6.9, the python program used to size the stages is covered, followed by the verification and validation procedures used to assess its authenticity in section 4.6.10. Finally, the final propulsion system design is described in section 4.6.11.

### 4.6.1. Market analysis

To determine a preliminary estimate of the total cost of the propulsion system, it is necessary to consider at the principal components of the latter. Most of the cost will come from the propellant required, a very rough estimate obtained using USA Department of Defense prices<sup>22</sup> gives a price close to €10 million FY2024. This includes oxidiser, fuel and pressurant gas, assuming nitrogen tetroxide ( $N_2O_4$ ), monomethylhydrazine (MMH) and helium (He) are used respectively. For what concerns thrusters, not enough data is available to the public, but an estimate based on some forum responses<sup>23</sup> indicates that the price per thruster unit lies in a range from €20k to €500k FY2024 for chemical propulsion. Taking the middle of this range and assuming 30 medium-small thrusters are used for each of two stages gives an approximate cost close to €15 million FY2024. Since it is not the plan to use off-the-shelf tanks for propellant (to size them exactly instead and save mass), it is hard to estimate a cost for manufacturing, but considering these tanks will most likely be made of a strong titanium alloy, total tank costs should not surpass €100k FY2024 [57]. Finally, the price of smaller components such as check valves, filters and pressure regulators are neglected as these are expected to be several orders of magnitude cheaper than the rest of the components discussed in this paragraph.

In conclusion, adding up all of the costs discussed above, a very preliminary estimate indicates that the total cost of the propulsion system should lay between €25 and €30 million FY2024.

### 4.6.2. Propulsion requirements

In order to design a system adequately, it is important to take note of the requirements that it must fulfill. These are shown in table 4.19.

Table 4.19: Propulsion Subsystem Requirements

| ID             | Requirement  |
|----------------|--|
| PL9-SUB-PRO-06 | The propulsion system shall be able to provide a total $\Delta V$ of 4.84 [km/s]   |
| PL9-SUB-PRO-07 | The propulsion system shall not exceed a mass of 97586 [kg]  |
| PL9-SUB-PRO-09 | The propulsion system shall not exceed a height of 18 [m]  |
| PL9-SUB-PRO-10 | The propulsion system shall not exceed a width of 7.6 [m]  |
| PL9-SUB-PRO-11 | Nitrogen tetroxide ( $N_2O_4$ ) in the oxidizer tank shall remain within the operational temperature range of 262 to 295 [K] |
| PL9-SUB-PRO-12 | Monomethylhydrazine (MMH) in the fuel tank shall remain within the operational temperature range of 221 to 360 [K]           |
| PL9-SUB-PRO-13 | Helium (He) in the pressurizer tank shall remain within the operational temperature range of 4.15 to 20.00 [K]               |

<sup>22</sup>URL [https://www.dla.mil/Portals/104/Documents/Energy/Standard%20Prices/Aerospace%20Prices/E\\_2019Oct1AerospaceStandardPrices\\_190920.pdf?ver=2019-09-26-081849-240](https://www.dla.mil/Portals/104/Documents/Energy/Standard%20Prices/Aerospace%20Prices/E_2019Oct1AerospaceStandardPrices_190920.pdf?ver=2019-09-26-081849-240) [cited 15 June 2024]

<sup>23</sup>URL <https://space.stackexchange.com/questions/26676/what-is-the-cost-of-the-propulsion-system-and-thrusters-as-a-of-the-total-sate> [cited 15 June 2024]

### 4.6.3. Assumptions

Several assumptions were made throughout the design process of the propulsion system. These are necessary to simplify the analysis and have been validated with industry experts at the TU Delft faculty of Aerospace Engineering or through research.

- **PRO-SZG-01:** The specific impulse is constant over time.
- **PRO-SZG-02:** The gravity losses experienced when performing flybys of celestial bodies are neglected.
- **PRO-SZG-03:** The optimal ullage volume fraction for propellant tanks is 10%.
- **PRO-SZG-04:** The mass flow of propellant is constant during the entire duration of the burn.
- **PRO-SZG-05:** The ratio of final to initial pressurant tank pressure is equal to the ratio of initial pressurant tank pressure to main tanks pressure.
- **PRO-SZG-06:** A clearance of 7.5 mm between the tanks is sufficient to avoid contact when vibrational loads are experienced during launch.
- **PRO-SZG-07:** The masses of smaller components such as check valves, filters and pressure regulators are neglected.

### 4.6.4. Propulsion type

Given the distance to be covered and the time constraint to reach Planet 9, the propulsion system of the spacecraft must be capable of providing a large  $\Delta V$ , on top of that provided by the launcher and by the gravity assists along the way. It was originally thought that a solution to this issue would be using low-thrust, continuous propulsion such as ion thrusters. NASA's Dawn mission, for example, only had little over 400 kg of Xenon at launch.<sup>24</sup> What makes ion propulsion unfeasible for NIBIRU is the power it requires to operate. In fact, such systems require a continuous supply of at least 0.5 kW.<sup>25</sup> Dawn has never gone farther than 3 AU away from the Sun, meaning that it is able to generate a large amount of power from its own solar arrays. This is not the case for NIBIRU, which will only have a BoL power of 290 W (see section 4.2.3), since solar arrays are not suitable for the mission profile.

Out of the options left available, chemical propulsion was deemed the safest choice. The latter has been around for a long time and has been widely used in spacecraft until now. From the available options within chemical propulsion, liquid propellants are preferred, as solid ones burn in their entirety once lit, making them less flexible. Liquid bipropellant systems offer the highest specific impulse [32], which is desirable to achieve the largest possible  $\Delta V$ . This comes at the cost of added complexity, as the oxidizer and fuel must be stored in separate tanks before they can react inside the engine. To force the propellants into the engine, the idea of using a pump-fed system was discarded as this would require a significant amount of power. The choice of using a pressure-fed system was made instead, which entails using a pressurant gas, typically helium [64], to feed the propellants into the engine. An additional high-pressure tank must therefore be carried on-board to guarantee the functionality of the pressure-fed system. It is important to note that such a system only requires power to open and close the valves that control the flow of propellants into the thrust chamber and the flow of pressurant gas into the oxidizer and fuel tanks. Furthermore, this power is only required when the system operates, which will be a negligible amount of time compared to the total mission duration.

To summarise the previous paragraphs, NIBIRU will have a pressure-fed liquid bipropellant propulsion system. More details on the oxidizer and fuel selection will be provided in the next subsections.

### 4.6.5. Bipropellant options

A wide variety of bipropellant combinations have been considered, based on literature and previous missions. The characteristics of interest for each are: specific impulse, optimal mixture ratio, and densities. The options that were deemed most suitable for this mission are shown in table 4.20, followed by some important considerations for each.

<sup>24</sup>URL <https://science.nasa.gov/mission/dawn/technology/ion-propulsion/> [cited 12 June 2024]

<sup>25</sup>URL <https://www1.grc.nasa.gov/space/sep/gridded-ion-thrusters-next-c/> [cited 13 June 2024]

Table 4.20: Bipropellant Combinations and Their Properties

| Oxidizer, Fuel     | $I_{sp}$ [s] | Mixture Ratio (O/F) | Density [kg/m <sup>3</sup> ] |
|--------------------|--------------|---------------------|------------------------------|
| $N_2O_4$ , MMH     | 321          | 1.65                | 1448.1005                    |
| $H_2O_2$ , Stock 2 | 306          | 5.48                | 1443.952                     |
| LOX, $LH_2$        | 465          | 5.88                | 1141.71                      |
| LOX, RP-1          | 348          | 2.36                | 1141.780                     |
| LOX, $CH_4$        | 380          | 3.8                 | 1141.439                     |

- Nitrogen tetroxide ( $N_2O_4$ ) and monomethylhydrazine (MMH): the main advantage of this hypergolic (oxidizer and fuel ignite spontaneously upon contact) bipropellant is the high density for both oxidizer and fuel, which is preferred as more propellant than other combinations can fit within the same volume, and therefore inside the spacecraft. It is important to note that this propellant is extremely toxic [65], but this is not deemed a major concern for deep space maneuvers.
- Hydrogen peroxide ( $H_2O_2$ ) and stock 2 fuel: this is a non-toxic hypergolic bipropellant, which has already been successfully tested [66]. The large mixture ratio indicates that much more oxidizer is required than fuel. This is favourable as  $H_2O_2$  has a larger density than stock 2 fuel, meaning that the larger the mixture ratio, the smaller the total volume of propellant required for a given  $\Delta V$ .
- Liquid Oxygen (LOX) and liquid hydrogen ( $LH_2$ ): the extremely low density of liquid hydrogen negatively affects the size of the propulsion systems, as even fitting low masses of fuel will require some relatively large dedicated tanks. Nonetheless, this propellant can provide the largest specific impulse out of all those mentioned in this list and operates in cryogenic conditions.<sup>26</sup>
- Liquid Oxygen (LOX) and rocket propellant-1 (RP-1): this bipropellant has been used for SpaceX's Falcon 9.<sup>27</sup> RP-1 offers a less toxic alternative to hypergolic fuels.<sup>28</sup> This comes with a mid-range specific impulse among the bipropellants listed here and it is important to note that RP-1 has a moderately lower density than MMH and stock 2 fuel.
- Liquid Oxygen (LOX) and methane ( $CH_4$ ): another alternative with LOX as oxidizer, of which the main advantage is that methane does not need to be stored at cryogenic temperatures like  $LH_2$ . This combination has been used for SpaceX's Super Heavy.<sup>29</sup> It provides a larger specific impulse than the RP-1 alternative, but the density of  $CH_4$  is lower, meaning that it might require larger fuel tanks.

The data gathered for each of these bipropellants has then been stored in a dictionary in order to have access to several options when sizing the propulsion system using the python program that will be discussed in section 4.6.9.

#### 4.6.6. Tank sizing

The starting point for sizing the tanks of the propulsion system is setting the  $\Delta V$  to be provided to the spacecraft. Other inputs include the spacecraft bus mass and the properties of the chosen bipropellant. Once all these values are known, given the rocket equation [32]:

$$\Delta V = g_0 I_{sp} \ln \left( \frac{m_0}{m_f} \right) = g_0 I_{sp} \ln \left( \frac{m_{dry} + m_{prop}}{m_{dry}} \right) \quad (4.54)$$

Where  $m_{dry}$  is the mass of the spacecraft at the end of the burn,  $m_{prop}$  is the propellant mass,  $g_0$  is the gravitational acceleration at sea level, and  $I_{sp}$  is the specific impulse. It is possible to re-arrange this for propellant mass:

$$m_{prop} = m_{dry} \left( e^{\frac{\Delta V}{g_0 I_{sp}}} - 1 \right) \quad (4.55)$$

<sup>26</sup>URL <http://www.astronautix.com/1/loxlh2.html> [cited 13 June 2024]

<sup>27</sup>URL <https://www.spacex.com/vehicles/falcon-9/> [cited 15 June 2024]

<sup>28</sup>URL <https://headedforspace.com/using-rp1-as-rocket-fuel/> [cited 15 June 2024]

<sup>29</sup>URL <https://www.spacex.com/vehicles/starship/#:~:text=Super%20Heavy%20is%20the%20first,back%20at%20the%20launch%20site.> [cited 15 June 2024]

Note that this relation makes use of assumptions PRO-SZG-01 and PRO-SZG-04. To determine the required  $\Delta V$ , PRO-SZG-02 was also taken into account.

Once the propellant mass is known, given the mixture ratio of the bipropellant it is possible to compute the masses of oxidizer and fuel.

$$m_{fuel} = \frac{m_{prop}}{(O/F)_{ratio} + 1} \quad (4.56)$$

$$m_{ox} = (O/F)_{ratio} \cdot m_{fuel} \quad (4.57)$$

Where  $(O/F)_{ratio}$  is the optimal mixture ratio.

Now that the individual masses are known, it is possible to determine the volume required to store each propellant using the respective density. For pressure-fed systems, it is necessary to include some ullage volume. This is additional space in the propellant tanks which guarantees the correct functioning of the system. An additional 10% volume was allocated to both the oxidizer and fuel tanks for this reason<sup>30</sup> (PRO-SZG-03).

$$V_{fuel} = \frac{m_{fuel}}{\rho_{fuel}} \cdot (1 + k_{ullage}) \quad V_{ox} = \frac{m_{ox}}{\rho_{ox}} \cdot (1 + k_{ullage}) \quad (4.58)$$

Where  $k_{ullage}$  is the aforementioned ullage volume fraction.

The total volume of propellant required can also be calculated by adding up the two volumes obtained above. This is required to determine the required pressurant gas mass. The following relation from literature was used [67]:

$$m_{pres} = \frac{P_u V_{prop}}{RT_0} \left( \frac{\gamma}{1 - P_{pres}/P_0} \right) \quad (4.59)$$

Where  $P_u$  is the pressure inside the propellant tanks,  $V_{prop}$  is the total volume of propellant,  $R$  is the universal gas constant of the pressurant gas,  $T_0$  is the initial temperature of the pressurant gas,  $\gamma$  is the ratio of specific heats of the pressurant gas, and  $P_{pres}/P_0$  indicates the ratio between the final and initial pressure inside the pressurant tank.

The initial pressures inside the main propellant tanks and inside the pressurant tank were extracted from literature as 1.72 MPa and 27.3 MPa respectively [32]. As for the  $P_{pres}/P_0$  ratio of final to initial pressurant tank pressure, it was assumed for simplicity to be equal to the ratio of pressurant tank pressure to main tanks pressure (PRO-SZG-05). In other words:

$$P_{pres}/P_0 = \frac{P_u}{P_0} = \frac{1.72}{27.3} = 0.063 \quad (4.60)$$

Similarly to what was done for the oxidizer and fuel, the required volume of pressurant gas can be found by simply dividing the mass by the density. It is important to note that no ullage volume is required for the pressurant tank.

Now that the volumes have been determined for both propellant types and for the pressurant gas, it is possible to compute the tank dimensions. The objective is to have either spherical tanks or cylindrical tanks with hemispherical ends, depending on the maximum width and height available for the propulsion system inside Starship's payload bay. Taking into account the space taken by the spacecraft bus, the payload bay allows for a maximum stage width of 8 m and a maximum total stage height of 18.44 m. Taking some margins, the maximum stage width is set to 7.6 m, and the maximum total height of the stages is set to 18 m. A clearance of 7.5 mm is included between the tanks (PRO-SZG-06). To obtain the tank dimensions, the procedure is the same for each of the volumes computed earlier; firstly, the radius of a spherical tank is computed from the required volume. If this radius exceeds half of the maximum

<sup>30</sup> <https://www.valispace.com/how-to-calculate-mission-specified-propulsion-system-parameters-part-iii/> [cited 13 June 2024]

allowed stage width of 7.6 m, then the radius is set to this value (3.8 m) and the additional volume required is obtained by making the tank cylindrical. Using this method, the dimensions can be determined for each tank and can then be used to determine the required thickness to withstand the pressure of the propellant inside. The thickness, including a safety margin of 5%, can be obtained as follows<sup>31</sup>:

$$t_{sphere} = \frac{pr}{2\sigma_{yield}} \cdot 1.05 \qquad t_{cylinder} = \frac{pr}{\sigma_{yield}} \cdot 1.05 \qquad (4.61)$$

Where  $p$  is the pressure inside the tank,  $r$  is the radius of the tank, and  $\sigma_{yield}$  is the yield strength of the material used.

The material chosen for the tanks is Ti-10V-2Fe-3Al (Ti 10-2-3) ST 760°C, a titanium alloy with a yield strength of 1200 MPa and density of 4650 kg/m<sup>3</sup>.<sup>32</sup> The high strength to density ratio of this material provides the ability to withstand the pressure inside the tanks without the need for an excessive amount of mass. A lower bound for tank thickness was also set to 0.5 mm for manufacturing reasons.

The approach discussed in this section has been used to create a python code dedicated to tank sizing, which will be covered in section 4.6.9

#### 4.6.7. Staging

While performing the preliminary sizing of tanks to assess the feasibility of achieving the required  $\Delta V$ , it became clear that fitting the propellant tanks inside the spacecraft bus would become a major issue for most other subsystems. A solution to most of these problems was found to be the implementation of kick stages attached to the spacecraft bus. With this approach, since the propulsion system will be placed inside the stages, the only propellant to be stored inside the spacecraft bus is the one needed for the ADCS subsystem. Furthermore, the stages can be detached after their propellant tanks are emptied, meaning that by the time the spacecraft will be on its final leg to Planet 9, it will have got rid of the entirety of its propulsion system. A summary of the major advantages of using stages for propulsion is provided below, split among the most affected subsystems.

- Propulsion: if optimised adequately, staging can guarantee a larger total  $\Delta V$  than a traditional on-board propulsion system. Since the structure of the stages will be dedicated exclusively to propulsion, it is possible exploit the entirety of the volume available to carry as much propellant as possible.
- ADCS: the moments of inertia and therefore the thrust magnitudes to be provided for attitude and trajectory adjustments will be reduced drastically once the last deep space maneuver will have been performed compared to having to carry the empty propellant tanks for the entire duration of the mission.
- Thermal Control: the reduced spacecraft bus size results in less heat required to maintain the components within the desired temperature ranges. This is particularly desired in later stages of the mission, when the spacecraft will receive very limited amounts of heat from the Sun.
- Structures & Mechanisms: similarly to for thermal control, a smaller and lighter spacecraft bus requires a lower structural complexity. Furthermore, designing for the cylindrical stage structure is not particularly time consuming as the required dimensions will be provided by the propulsion team, and they just need to be designed to carry launch loads.
- Payload: for a given required  $\Delta V$ , more mass is available, so that additional scientific instruments can be carried on-board.

<sup>31</sup>URL [https://pkel015.connect.amazon.auckland.ac.nz/SolidMechanicsBooks/Part\\_I/BookSM\\_Part\\_I/07\\_ElasticityApplications/07\\_Elasticity\\_Applications\\_03\\_Presure\\_Vessels.pdf](https://pkel015.connect.amazon.auckland.ac.nz/SolidMechanicsBooks/Part_I/BookSM_Part_I/07_ElasticityApplications/07_Elasticity_Applications_03_Presure_Vessels.pdf) [cited 13 June 2024]

<sup>32</sup>URL <https://www.matweb.com/search/DataSheet.aspx?MatGUID=ca1ec25e6ec3465bae22df7f35479041&ckck=1> [cited 13 June 2024]

The general approach to sizing the tanks for each stage does not deviate from what was discussed in the previous section. However, it is vital to correctly assess how the dry mass of each stage is to be defined. It is also important to define how the tanks will be placed within the stage structure, as this affects their maximum dimensions. It was decided that the tanks should all be stacked vertically, similarly to what is shown in figure 4.10 for a rocket, this way the fraction of the total available volume used to store propellant is maximised. Further details about the approach to sizing multiple stages will be covered in section 4.6.9.

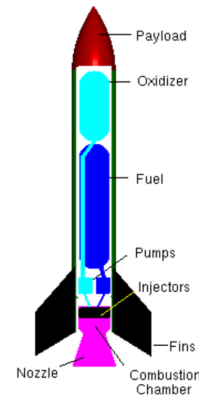


Figure 4.10: Vertical Tanks Stacking configuration<sup>33</sup>

#### 4.6.8. Thrust generation

For the spacecraft to physically accelerate and therefore generate a  $\Delta V$ , propellant needs to be expelled through thrusters at the bottom of each stage. It is assumed that all stage burns are impulsive maneuvers, meaning that ideally all of the propellant in that stage is burnt in a time span that is negligible compared to the duration of the journey to Planet 9.<sup>34</sup> The gravity loss of the spacecraft is inversely proportional to the propellant mass flow,<sup>35</sup> which means that a shorter burn time results in a smaller gravity loss. This is desirable as the latter results in less total  $\Delta V$  required. To minimise the burn time, the thrust must be maximised, which can be done by either using more powerful thrusters or mounting more of these for each stage. The latter option is preferred as the plan is to select an off-the-shelf thruster that is compatible with the chosen bi-propellant and then fit as many as possible at the bottom of each stage.

Given the mass flow of the thruster, once the maximum number of thrusters that can be fit at the bottom of the stage, the minimum burn time can simply be determined using:

$$t_{burn} = \frac{m_{ox} + m_{fuel}}{\dot{m} \cdot n_{thrusters}} \quad (4.62)$$

Where  $t_{burn}$  is the burn time,  $\dot{m}$  is the thruster mass flow and  $n_{thrusters}$  is the number of thrusters. The thruster mass flow is assumed to be constant (PRO-SZG-04)

#### 4.6.9. Sizing and optimisation in Python

To size the tanks and consequently the stages, a python program was created, which allows the user to select the number of stages and the desired  $\Delta V$  for each stage. The other inputs of the program are:

- Spacecraft bus mass
- Bi-propellant properties (type, specific impulse, mixture ratio, densities, tank pressure, thruster length and mass)
- Pressurant gas properties (type, temperature, tank pressure, temperature, specific heat ratio, gas constant)
- Structural properties (total maximum height and width of stages, structural mass per meter, properties of tank material)

Figure 4.11 shows how the user can input the  $\Delta V$  for each stage in a list, the length of which is equal to the number of stages of the spacecraft. It is important to note that the first value of the list always describes the first stage that burns, while the last always describes the upper-most kick stage, which is directly connected to the spacecraft bus. It can also be seen that the selected bipropellant can also be

<sup>33</sup>URL [https://www.grc.nasa.gov/www/k-12/rocket/TRCRocket/practical\\_rocketry.html](https://www.grc.nasa.gov/www/k-12/rocket/TRCRocket/practical_rocketry.html) [cited 15 June 2024]

<sup>34</sup>URL <https://orbital-mechanics.space/orbital-maneuvers/impulsive-maneuvers.html> [cited 14 June 2024]

<sup>35</sup>URL [https://web.stanford.edu/~cantwell/AA284A\\_Course\\_Material/Karabeyoglu%20AA%20284A%20Lectures/AA284a\\_Lecture7\\_Gravity\\_Loss.pdf](https://web.stanford.edu/~cantwell/AA284A_Course_Material/Karabeyoglu%20AA%20284A%20Lectures/AA284a_Lecture7_Gravity_Loss.pdf) [cited 14 June 2024]

inputted inside the `get_propellant_properties` function. This feature was not added for quick selection of pressurant fluid or tank material, as the best options for each of these were already selected in earlier stages of the design. The function `size_all_stages` performs the tank sizing for all stages, making use of a variety of other (sub-)functions, which will be discussed shortly.

```

delta_V = [1420.933 * 1.01, 3416.311 * 1.01]
m_sc_bus = 2395.167319

n_stages = len(delta_V)

print(size_all_stages(n_stages,
                    delta_V,
                    m_sc_bus,
                    get_propellant_properties('MMH_N2O4'),
                    get_pressurant_properties(),
                    get_structure_properties()))

```

Figure 4.11: User Interface of Propulsion Software

### size\_stage

This function sizes the tanks for an individual stage, making use of the mathematical relations covered in section 4.6.6.

The first input is a guess of the dry mass of the stage, as this is necessary to determine the mass of propellant needed, but cannot be known prior to sizing the tanks. The function `iterate_dry_mass` provides this guess and will be shortly discussed later. The second input is the spacecraft bus mass, it is important to keep in mind that this will only be equal to the actual bus mass for the last stage that fires. For every other stage, this value includes the actual spacecraft bus mass and the total mass of all stages above. The rest of the inputs are simply the  $\Delta V$  of the stage and the bi-propellant, pressurant and structural properties.

`size_stage` outputs a dictionary with all the dimensions and masses obtained from the sizing of all three tanks, as well as the calculated dry mass of the stage. The latter is useful for the `iterate_dry_mass` function.

### iterate\_dry\_mass

As mentioned earlier, to be able to determine the propellant mass required to achieve the desired  $\Delta V$ , it is necessary to know the dry mass of a stage before sizing it. This needs to be done for each stage. To perform this, `iterate_dry_mass` loops through a large range of dry masses and runs `size_stage` for each until the dry mass outputted by the stage sizing is the same as the guessed value. When this occurs, the guessed dry mass is set as the best guess.

When the desired  $\Delta V$  is low enough, it may happen that there is more than one dry mass guess that is close to the calculated dry mass. On the other hand, when the  $\Delta V$  is too large, there may be no solution at all. The helper functions `line_segment_intersection` and `find_intersection` are helpful in determining if and how many solutions there are. Furthermore, even if there are multiple solutions, the output of `iterate_dry_mass` is always the smallest dry mass.

### size\_all\_stages

This function is necessary to perform the propulsion system sizing when there is more than one stage. It makes use of `size_stage` for the individual stages, but as was hinted earlier, the spacecraft bus mass input is different for each stage. The easiest way to tackle this is to size the spacecraft from top to bottom, that is, sizing the top stage first and the bottom stage last. Using this approach, it is possible to initialise the spacecraft bus mass as the actual value and then adding to it the total stage mass before sizing the next stage.

Before moving onto the next stage, however, the function also checks that the total height of all stages sized until that moment as well as the width of the largest stage and the total spacecraft mass fit within the

limits set by the requirements in section 4.6.2. If that is not the case, the program informs the user about which requirement is not met. `size_all_stages` outputs a dictionary with the results of the propulsion system sizing for each individual stage.

### **optimize\_dV**

The user may desire to know, for a given spacecraft bus mass, for what number of stages and  $\Delta V$  split between them it is possible to achieve the maximum total  $\Delta V$ . This is exactly what the `optimize_dV` does by performing the propulsion system sizing for a range of inputs which can be chosen by the user.

#### **4.6.10. Verification & validation**

Considering the number of functions used in the program, it is bound to contain a wide range of errors. In order to minimise the inaccuracies in the outputs, verification and validation procedures have been performed on the code.

The first step in verifying the model consists of going through the code and looking for syntax errors, formula insertion mistakes and incorrectly initialised loops. Before the code was run for the first time, an extensive debugging session took place to solve all syntax and python logic errors until the program started running. Once the program runs, all syntax errors have been solved, however this does not guarantee that the outputs are the intended ones, as there might be undetected mistakes in the inputted formulae or in the for-, if- and while-loops used. To verify the model for a set of inputs, the variables were printed every few lines of code so that calculation verification could be performed by hand on the entire code. To ease the calculation verification process, many of the formulae section 4.6.6 were turned into functions and inserted in a separate python file. The model was also verified in its entirety by ensuring that it only gives an answer for the sizing if it fits within the dimensional constraints set by the requirements. For example, by ensuring that the outputted total stage height remained under the pre-established maximum.

To perform model validation, one must ensure that the model results are close to what one would expect in the real world. To validate the approach to the problem, a meeting took place with Dr. Cervone, expert in space propulsion at the faculty of aerospace engineering of TU Delft, during which the sizing method was shortly explained, and advice was provided on how to improve it further. To validate the results, the model was checked to not give an answer in the case that an extremely high  $\Delta V$  is provided as an input, and it was also checked to output very small tank dimensions in the case that the input  $\Delta V$  is set to a small value.

Validating the propulsion system sizing with other existing spacecraft is not an easy task, since all other spacecraft that went to the Kuiper belt and beyond, such as the Voyager missions and New Horizons, relied almost exclusively on pure gravity assists. This means that none of them were required to achieve  $\Delta V$  values with on-board propellant anywhere close to those that NIBIRU will have to provide by itself, and therefore none of them were equipped with kick stages this large. The necessity for amounts of propellants this large makes sense however, considering the amount of  $\Delta V$  that needs to be provided by the spacecraft itself on top of that to be achieved from the gravity maneuvers to travel such a large distance in less than 50 years.

#### **4.6.11. Final design**

Once all subsystems obtain a first set of design values, it is possible to iterate the design of the entire spacecraft until these all of these values converge. This iterative process is shortly explained below, followed by an overview of the design results for each stage. Additional details are then provided about the architecture of the propulsion system, followed by the total values for mass, power consumption and cost of the entire propulsion system. Lastly, the compliance of the final design with the subsystem requirements is checked.

### **Iteration**

For the propulsion subsystem, an iteration took place in collaboration with the structures and thermal control officers, before providing updated values for the moments of inertia of the stages to the ADCS department. Once the attitude control propellant tanks are sized for the updated values, the spacecraft

bus must be updated, which in turn affects the design of the propulsion system once more. The iteration can then be repeated for the new spacecraft bus mass, until the variation in design values becomes small enough. Once the iterative process has been completed, the sizing values obtained are final. These are presented in the next subsection.

### Design Results

After running the sizing python software for a variety of bipropellants,  $\Delta V$  and number of stages combinations, the best results by far were obtained when using  $N_2O_4$  and MMH. One of the advantages of this bipropellant is that the thruster it uses has a much shorter thruster length compared to others. Another advantage of this combination is its hypergolic nature, meaning that no power will be required to initiate combustion.

In the end, all tanks turned out to be spherical, as the propellant never required a volume larger than that of a sphere with the maximum allowed radius of 3.8 m. This limit follows from the maximum stage width being 7.6 m, and the fact that the tanks are stacked vertically as described in section 4.6.7.

For the Energetic NIBIRU Kick Interstage (ENKI) first kick stage, all of the tank sizing parameters are provided in table 4.21.

**Table 4.21:** Overview of Final Design Parameters for ENKI Kick Stage ( Total Stage Mass Includes Structure)

| ENKI                   |                           |                       |                             |
|------------------------|---------------------------|-----------------------|-----------------------------|
| Oxidizer               |                           |                       |                             |
| <i>Tank Radius [m]</i> | <i>Tank Thickness [m]</i> | <i>Tank Mass [kg]</i> | <i>Fluid Mass [kg]</i>      |
| 1.164                  | 0.005                     | 397.5                 | 8694                        |
| Fuel                   |                           |                       |                             |
| <i>Tank Radius [m]</i> | <i>Tank Thickness [m]</i> | <i>Tank Mass [kg]</i> | <i>Fluid Mass [kg]</i>      |
| 1.113                  | 0.005                     | 363.3                 | 5269                        |
| Pressurant             |                           |                       |                             |
| <i>Tank Radius [m]</i> | <i>Tank Thickness [m]</i> | <i>Tank Mass [kg]</i> | <i>Fluid Mass [kg]</i>      |
| 1.006                  | 0.012                     | 719.6                 | 908                         |
| Totals                 |                           |                       |                             |
| <i>Mass [kg]</i>       | <i>Height [m]</i>         | <i>Width [m]</i>      | <i>Propellant Mass [kg]</i> |
| 18575                  | 7.277                     | 2.338                 | 13963                       |

For the Efficient NIBIRU Long-range Interstage Launcher (ENLIL) second kick stage, all of the tank sizing parameters are provided in table 4.22.

**Table 4.22:** Overview of Final Design Parameters for ENLIL Kick Stage (Total Stage Mass Includes Structure)

| ENLIL                  |                           |                       |                             |
|------------------------|---------------------------|-----------------------|-----------------------------|
| Oxidizer               |                           |                       |                             |
| <i>Tank Radius [m]</i> | <i>Tank Thickness [m]</i> | <i>Tank Mass [kg]</i> | <i>Fluid Mass [kg]</i>      |
| 1.189                  | 0.005                     | 414.7                 | 9265                        |
| Fuel                   |                           |                       |                             |
| <i>Tank Radius [m]</i> | <i>Tank Thickness [m]</i> | <i>Tank Mass [kg]</i> | <i>Fluid Mass [kg]</i>      |
| 1.137                  | 0.005                     | 379.0                 | 5615                        |
| Pressurant             |                           |                       |                             |
| <i>Tank Radius [m]</i> | <i>Tank Thickness [m]</i> | <i>Tank Mass [kg]</i> | <i>Fluid Mass [kg]</i>      |
| 1.027                  | 0.012                     | 766.9                 | 967                         |
| Totals                 |                           |                       |                             |
| <i>Mass [kg]</i>       | <i>Height [m]</i>         | <i>Width [m]</i>      | <i>Propellant Mass [kg]</i> |
| 19673                  | 7.419                     | 2.388                 | 14880                       |

It is important to note that the total mass of each stage also includes an estimate for the structural mass. This is close to the actual value, but not exact, as making an approximation was necessary to reduce the duration of the iteration.

For what concerns thrust generation, the objective was to minimise the burn time, which required maximising the number of thrusters at the bottom of each stage. For this reason, thirty-four S400-15<sup>36</sup>

<sup>36</sup>URL <https://www.space-propulsion.com/spacecraft-propulsion/apogee-motors/> [cited 18 June 2024]

apogee motors by ArianeGroup,<sup>37</sup> each capable of providing 400 N of thrust, were implemented for each stage. The burn time was then computed for the worst-case scenario, which is the case for the stage with the most propellant mass, namely ENLIL. This gave a total burn time of just under 55 minutes, which is acceptable as it is significantly lower than the thrusters' qualified single burn life of 111 minutes.<sup>36</sup>

### Propulsion System Architecture

To complete the design of the propulsion system, it is important to establish how the tanks should be connected, as well as what valves, filters and other components are required to ensure proper operation. The typical architecture of such a system is shown in figure 4.12.

Please also note that it is assumed that all of the propellant flow control and filter components have a negligible mass compared to propellants and tanks (PRO-SZG-07). For this reason, these components are not counted towards the total mass of the propulsion system. The idea is also to use exclusively off-the-shelf components, as these are guaranteed to be available by the start of production due to their high TRL, and also because this implies that most of them have already been used in space. These components are discussed below.

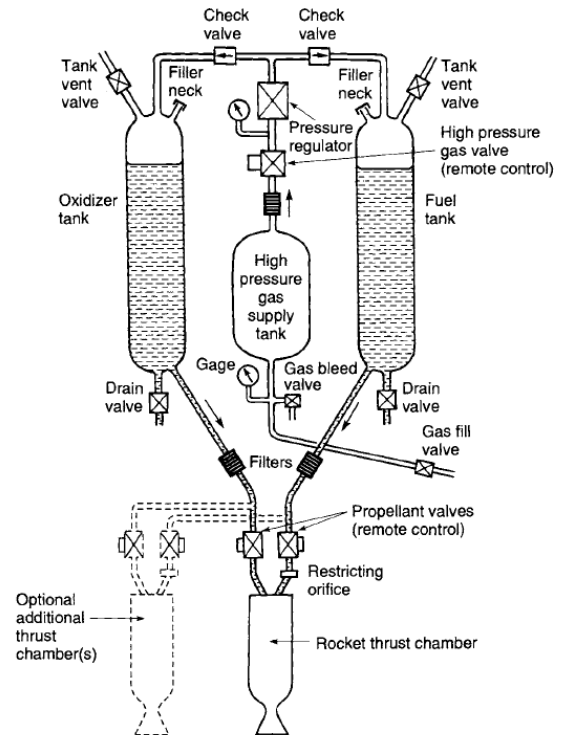


Figure 4.12: Typical Architecture of a Pressure-Fed Liquid Bipropellant Propulsion System<sup>38</sup>

- One pressure regulator from Marotta Controls<sup>39</sup> will be used per stage. These are labelled as space flight-qualified and highly reliable components, which makes them tremendously beneficial to the mission.
- One high pressure gas valve will be used per stage at the exit of the pressurant gas tank. The plan is to use a pyrotechnical valve by ArianeGroup<sup>40</sup> for this task
- The 250HFS check valves by The Lee Company<sup>41</sup> are suited for this propulsion system as they can withstand operating pressures up to 5000 psi or over 34 MPa, which is more than enough considering the helium in the pressurant tank is stored at just over 27 MPa. Two of these valves will be used for each stage.
- The large variant of the lightweight filters by Mott Corporation<sup>42</sup> will be used, as they are labelled for application sizes larger than 1000 kg, which is the case for the current system. These are suited both for the propellant and for the pressurant gas, meaning that three filters will be used per stage.
- The propellant valves are already included with the 400 N apogee thrusters. 68 of these valves will be present for each stage, since 34 thrusters are used.

<sup>37</sup>URL <https://www.ariane.group/en/equipment-and-services/satellites-and-spacecraft/400-n-bi/> [cited 18 June 2024]

<sup>38</sup>URL <https://aerospacenotes.com/liquid-propellant-feed-systems/> [cited 18 June 2024]

<sup>39</sup>URL <https://marotta.com/products/flow-controls/pressure-controls/pressure-regulators-reducers/> [cited 18 June 2024]

<sup>40</sup>URL <https://www.space-propulsion.com/brochures/valves/space-propulsion-valves.pdf> [cited 18 June 2024]

<sup>41</sup>URL <https://www.theleeco.com/product/250-hfs/> [cited 18 June 2024]

<sup>42</sup>URL <https://mottcorp.com/wp-content/uploads/2022/01/Mott-Propellant-Filters-Rev-0122.pdf> [cited 18 June 2024]

- Any of the fill and drain valves models by ArianeGroup<sup>40</sup> can be used for all three tanks for each stage.

### Final budgets

Before closing-off this section, it is useful to have a look at the total values for mass, power consumption and cost for the entire propulsion system across both stages. The mass is 38248 kg, cost is €25-30 million FY2024, and uses less than 10 W. Note that for a pressure-fed propulsion system, power is only required to actuate the high pressure valve, which only requires a small amount of electrical power for a short time<sup>43</sup>. The design has been made in compliance with the requirements presented in section 4.6.2.

## 4.7 Thermal Control System

*Contributors: Isha*

This section outlines the design process for the Thermal Control System (TCS) of the NIBIRU mission. It begins with a market analysis (section 4.7.1) to identify suitable off-the-shelf components and draws conclusions from comparable missions such as the Parker Solar Probe and New Horizons. Following this, the thermal control requirements are detailed in section 4.7.2, setting the constraints for the design process. The design steps are then discussed in section 4.7.3, including assumptions, defining the thermal environment, and iterative design for both EoL and BoL. Lastly, the implementation of thermal control for the kickstages and considerations for Sun proximity are addressed, concluding with verification and validation of the final design (section 4.7.4, section 4.7.5).

### 4.7.1. Market analysis

The TCS for the NIBIRU mission aims to use off-the-shelf components, drawing inspiration from comparable missions to ensure feasibility and reliability. By examining missions like the Parker Solar Probe and New Horizons, which represent the thermal extremes our mission will encounter, we can set the stage for the design.

First off, the New Horizons spacecraft is equipped with MLI. This insulation holds in heat from the operating electronics, maintaining the spacecraft's temperature between 10-30°C<sup>44</sup> throughout its journey. This demonstrates the efficacy of passive thermal control in similar temperature environments, suggesting that the NIBIRU spacecraft bus may also maintain the desired temperature passively. New Horizons utilises radiators close to significant heat sources such as the RTG to maximise radiator efficiency.<sup>45</sup> Additionally, as MLI absorbs radio waves, it is not placed on the antenna dish, which is something to keep in mind for our design as well. New Horizons uses Kapton for its MLI, with an outer layer of aluminised Kapton. This material choice offers a combination of transparency and reflectivity, creating the illusion of a gold surface. Although New Horizons employed heaters for active heating, it only had one RTG, unlike our mission, which will need to account for multiple RTGs in the design.

On the other side of the extremes, Parker Solar Probe employs a thermal protection system (TPS), a 2.3 m diameter shield<sup>46</sup> that protects the spacecraft from the Sun's intense heat and energy. The spacecraft reaches as close as 10 solar radii from the Sun's center,<sup>47</sup> similar to the NIBIRU mission, indicating that a similar thermal protection approach might be necessary.

The NIBIRU mission will include the kickstages ENKI and ENLIL, which will also require a thermal management system as the spacecraft gets closer to the Sun. SpaceX's Starship, the launcher of the NIBIRU mission, employs ceramic carbon tiles that, according to Elon Musk<sup>48</sup>, can withstand temperatures up to 2500°F, a comparable temperature to the Parker Solar Probe's sun-facing shield. If these tiles can maintain a stable equilibrium temperature for Starship, they could offer similar performance for our mission. However, reliable information on these tiles is limited, so their specifications must be carefully considered during this design process.

<sup>43</sup>URL <https://www.space-propulsion.com/spacecraft-propulsion/valves/pyrotechnic-valve.html> [cited 18 June 2024]

<sup>44</sup>URL <https://pluto.jhuapl.edu/Mission/Spacecraft/Systems-and-Components.php> [cited 17 June 2024]

<sup>45</sup>URL <https://mattcbergman.com/2015/08/02/new-horizons-thermal-control-system/> [cited 17 June 2024]

<sup>46</sup>URL <https://parkersolarprobe.jhuapl.edu/News-Center/Show-Article.php?articleID=30> [cited 17 June 2024]

<sup>47</sup>URL <https://science.nasa.gov/mission/parker-solar-probe/> [cited 17 June 2024]

<sup>48</sup>URL <https://www.space.com/spacex-starship-hexagon-heat-shield-tile-test.html> [cited 17 June 2024]

Finally, numerous companies offer coatings, radiator panels, thermal sensors, and MLI. This indicates that the TCS design for this mission can primarily rely on high TRL off-the-shelf components, ensuring a sustainable and reliable design.

#### 4.7.2. Thermal control requirements

The thermal control subsystem has a set of the following requirements, shown in table 4.23.

**Table 4.23:** TCS Requirements

| ID             | Requirement   |
|----------------|---|
| PL9-SUB-THE-01 | The TC subsystem shall continuously monitor the temperature of the spacecraft.  |
| PL9-SUB-THE-02 | The TC subsystem shall compare the measured subsystem temperatures against the predetermined subsystem operational temperatures |
| PL9-SUB-THE-03 | The TC subsystem shall remain in the operational temperature range of 270 and 290 [K]   |

Here, PL9-SUB-THE-03 will be the one analysed in greatest detail, such that PL9-SUB-THE-02 can be complied with. To get an overview again of the constraining thermal requirements of each component, these are summarised per subsystem in table 4.24.

**Table 4.24:** Summarised Temperature Constraints per Subsystem

| Subsystem  | Operational temperature range [K] |
|------------|-----------------------------------|
| Payload    | 238 - 308                         |
| EPS        | 250 - 305                         |
| TT&C       | 50 - 295                          |
| ADCS       | 263 - 323                         |
| Propulsion | 262 - 295                         |
| Structures | 243 - 303                         |
| OBDH       | 239 - 344                         |

It should be noted that these ranges exclude the helium tank of propulsion, assumes the spectrometer regulates its own temperature where required (see section 4.1).

#### 4.7.3. Design process

The design process for the TCS is structured in the following way. It begins with outlining assumptions to simplify the model, followed by defining the thermal environment for BoL and EoL. After this, the preliminary analysis establishes thermal requirements and identifies challenges for the design. The design then focuses on computing heat interactions at EoL and adapting the model for BoL conditions. Thermal control for the kickstages is addressed separately, ensuring they maintain thermal balance as well. Finally, considerations for thermal control during Sun proximity are discussed, recommending further detailed studies on this topic.

##### 0: Assumptions

Throughout the design process, several assumptions were made to simplify the model. These assumptions are listed below and are categorised in assumptions about the thermal environment (ENV), about the thermal design for the spacecraft bus (SC) and for the kickstages (KIC). Some of the assumptions are justified and validated immediately, and some will be verified and validated in a later subsection.

- **TC-ENV-A-1:** Albedo and IR radiation from Earth are negligible at BoL because the spacecraft is not in Earth orbit.
- **TC-ENV-A-2:** The antenna is assumed to receive sufficient heat from the spacecraft's temperature to operate, requiring no external heating.
- **TC-ENV-A-3:** Components with parts outside the spacecraft are connected from the inside, maintaining equilibrium temperature at necessary parts.

- **TC-SC-A-1:** Internal wiring heat contributions are not taken into account.
- **TC-SC-A-2:** When doing the calculations for heat transfer, only one RTG was taken into account with one radiator. It was assumed that for the other RTG on the opposite end of the spacecraft, the radiator would act in the same way due to symmetry.
- **TC-SC-A-3:** The internally generated heat from components is 20% of the total electrical power at BoL and EoL[32].
- **TC-KIC-A-1:** The kickstages are assumed to be thermally decoupled from the spacecraft bus.
- **TC-KIC-A-2:** The helium pressuriser tank, containing helium at 20 K, is assumed to be a perfect insulator with vacuum jackets, and thus is thermally decoupled from the rest of the structure [68].
- **TC-KIC-A-3:** The thrusters of each kickstage are assumed to be perfectly insulated from the tanks with a physical barrier, such that no heat is transferred from the thrusters to the tanks<sup>49</sup>

### 1: Defining the thermal environment

First, the thermal environment for extreme instances must be defined, specifically at the beginning and end of life (BoL and EoL). The spacecraft bus will be subjected to three types of heat (TC-ENV-A-1): radiation, conduction, and internally generated heat. At the BoL phase, radiation is primarily emitted by the Sun and the two RTGs. Moreover, conduction is considered for the struts that connect the RTG to the spacecraft for both phases. During the EoL phase, near Planet 9, the spacecraft will only receive heat from the RTGs via radiation and conduction, and internally generated heat from components. Equations (4.63) to (4.65)[33] explain the parameters that influence these sources in greater detail.

$$Q_{\text{solar}} = \alpha \cdot J_s \cdot A \quad (4.63)$$

Here,  $\alpha$  is the absorptivity of the surface receiving Solar radiation,  $J_s$  is the solar flux at BoL and  $A$  represents the area exposed to the Sun.

$$Q_{\text{conduction}} = k \cdot A \cdot \frac{\Delta T}{l} \quad (4.64)$$

In this formula,  $k$  is the thermal conductivity of the material,  $A$  is the cross-sectional area through which heat is conducted,  $\Delta T$  is the temperature difference across the material and  $l$  is the length of the material.

$$Q_{\text{radiation}} = \epsilon \cdot \sigma \cdot A \cdot (T^4 - T_{\text{env}}^4) \quad (4.65)$$

Here,  $\epsilon$  is the emissivity of the surface,  $\sigma$  is the Stefan-Boltzmann constant ( $5.67 \cdot 10^{-8} \text{ W/m}^2\text{K}^4$ ),  $A$  is the radiating area,  $T$  is the temperature of the radiating surface and  $T_{\text{env}}$  is the temperature of the environment.

### 2: Preliminary analysis

To establish a starting point for the design, a preliminary analysis was conducted. This analysis evaluated the thermal control requirements based on the mission's operational parameters and environmental conditions. The focus was on determining the desired temperature range and identifying potential challenges associated with maintaining these temperatures throughout the mission. It must be noted that the primary objective of this thermal control design process is not necessarily to achieve the optimised system, but rather to ensure that a functional system is developed. It is recommended that further studies be conducted to optimise these values and improve the system's efficiency and performance.

#### Desired temperature

Based on the mission requirements, it was determined that the TCS should maintain an equilibrium temperature range between 270 K and 290 [K]. This range ensures that all systems and instruments can operate efficiently and reliably. An important assumption made during this decision is that the

<sup>49</sup>URL <https://www.space-propulsion.com/spacecraft-propulsion/apogee-motors/> [cited 17 June 2024]

spectrometer will have its own dedicated radiator capable of maintaining the necessary cold temperatures for that instrument, as specified in section 4.1.

### Passive versus active TCS

By examining similar missions that have dealt with extreme thermal environments, such as the NASA New Horizons mission, it was revealed that maintaining the desired temperature range at EoL posed challenges.<sup>50</sup> These missions predominantly used passive thermal control systems, minimising the reliance on active heating or cooling. Given the mission's 50-year duration, a passive approach is also more essential to conserve power. Additionally, passive thermal control is preferred as it has a higher reliability. If something were to fail with an active system, the risk of mission failure would increase significantly. This way, the passive system avoids such risks and makes the overall design more robust and dependable.

### Design strategy

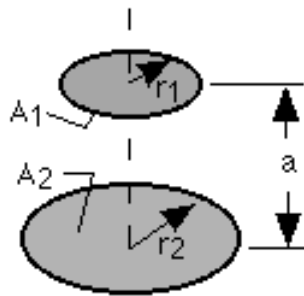
The primary issue identified from this analysis was that the spacecraft would be too cold at EoL. To address this, the design strategy focused on making sure that the temperature at EoL remains within the colder end of the acceptable range. This approach involves iterating the design to achieve an acceptable temperature at EoL first, and then evaluating the resulting (higher) temperature at BoL. If the temperature at BoL is found to be too hot, further iterations are conducted to adjust the EoL design within the allowable temperature range, until both BoL and EoL fall within the desired range of 270 K to 290 K.

## 3: Designing for EoL, adapting for BoL

### Designing for EoL

In designing the TCS for EoL (where 51 years have passed, see section 4.2), several steps were undertaken. The process involved computing the heat interactions between the RTG and a radiator, iterating with different parameters and making use of the aforementioned formulas and assumptions.

The first step involved implementing the view factor for the RTG and radiator. The RTG is assumed to be of cylindrical shape, and is mounted in such a way that the spacecraft bus only sees a circle, hence, a view factor computation was performed of a disk to a parallel coaxial disk of unequal radius. For this calculation, the radiator is taken to be circular as well, see figure 4.13. The view factor of a disk to parallel coaxial disk of unequal radius is shown in equation (4.67)[69, 70]:



$$R = \frac{r}{a}; \quad X = 1 + \left(1 + \frac{R_2^2}{R_1^2}\right) \quad (4.66)$$

$$F_{1-2} = \frac{1}{2} \left[ X - \left( X^2 - 4 \left( \frac{R_2}{R_1} \right)^2 \right)^{\frac{1}{2}} \right] \quad (4.67)$$

Figure 4.13: View Factor Disk to Parallel Coaxial Disk of Unequal Radius<sup>51</sup>

Next, the temperature of the RTG at EoL was determined. As specified in section 4.2, the RTG radiates 1854 W of heat at BoL, with a degradation rate of 0.6889%. This degradation affects the amount of heat generated over time. Using equation (4.68), the heat radiated from the RTG to the radiator was determined. This formula was taught by thermal engineering expert Martin Lemmen (9 June 2024), and was provided through private communication.

$$Q_{\text{rad},1-2} = \epsilon_1 A_1 F_{12} \cdot \epsilon_2 \cdot \sigma (T_1^4 - T_2^4) \quad (4.68)$$

$Q_{\text{rad},1-2}$  is the radiative heat transfer between the RTG and the radiator and  $\epsilon_1$  and  $\epsilon_2$  are the emissivities of the surfaces of the RTG and radiator, respectively. Furthermore,  $A_1$  is the circular area of the RTG, so that  $F_{12}$  is the view factor from the RTG to the radiator. Finally,  $\sigma$  is the Stefan-Boltzmann constant and  $T_1$  and  $T_2$  are the temperature of the RTG and desired temperature of the radiator, respectively. It is important to

<sup>50</sup>URL <https://spaceflight101.com/newhorizons/spacecraft-overview/> [cited 17 June 2024]

<sup>51</sup>URL <https://thermalradiation.net/sectionc/C-41.html> [cited 17 June 2024]

note that for the sake of simplicity, it is assumed that the RTG does not absorb the radiated heat from the spacecraft; the radiator radiates it directly into space. Furthermore, the view factors between components inside the spacecraft are not taken into account; it is assumed that the thermal environment inside the spacecraft is uniform. This assumption is accounted for by designing for the colder end of the acceptable range, so that any additional heat from the components that is neglected will not affect the feasibility of the thermal control design.

In addition to radiative heat transfer, the heat transferred through conduction was also considered. It is assumed that the RTG is mounted to the spacecraft using a number of struts, and the conductive coupling through these struts adds to the total heat absorbed by the radiator from the RTG.

On the other side of the equation, we calculated the heat radiated out to space from the radiator. Here, space was assumed to be at 3 K,<sup>52</sup> and the radiator would also be radiating out any internally generated heat. Equation (4.68) was used again, this time using the view factor from the disk to space ( $\epsilon_{space} = 1$ ), to determine the heat transfer from the radiator to space. The idea here is to ensure that the heat dissipated matches the heat absorbed, and iterating with radiator sizes, emissivity properties and the desired temperature until this is met. This ultimately means that the heat absorbed by the radiator from the RTG must also be expelled by the radiator to achieve thermal equilibrium. While it may seem counterintuitive to expel the heat generated by the RTG, it is the total amount of heat that determines the system's temperature. By balancing the heat absorbed and expelled, we ensure that the spacecraft maintains a stable temperature.

### Adapting for BoL

Having iterated for EoL, the model was adapted to verify that the system also functions adequately at BoL conditions. At BoL, the spacecraft is subjected to different thermal challenges due to the closer distance to the Sun. Again, the objective is to ensure that the spacecraft bus remains within 270 and 290 K without requiring active thermal management.

Naturally, at BoL the RTGs transfer more heat to the spacecraft than at EoL due to the reduced degradation and the closer proximity to the Sun of 1 AU. The spacecraft will eject from Starship at the edge of Earth's sphere of influence, approximately 1.01 AU<sup>53</sup> from the Sun. This distance will not significantly affect temperature calculations (maximum difference of 0.3 degrees). Therefore, it is assumed that BoL is at 1 AU to account for any margins and ensure the system can sustain itself at slightly higher temperatures. Furthermore, it is assumed that one year has passed since the production of RTGs, to comply with safety regulations (see section 4.2). The heat absorbed from the Sun is assumed to come from one face of the spacecraft and the exposed parts of the RTGs. In a worst-case scenario, both RTGs are oriented such that one side of each cylindrical RTG is fully exposed to the Sun, approximated as a rectangular area defined by the cylinder's diameter and length.

To ensure the spacecraft retains as much heat as possible, the entire spacecraft, except for the two radiators, will be wrapped in MLI. Kapton ITO (Indium Tin Oxide) was chosen for the MLI due to its common use in space mission applications.<sup>54</sup> The MLI will consist of 10 layers of Kapton ITO to balance effectiveness and redundancy. Kapton ITO has an absorption coefficient  $\alpha = 0.41$  at BoL and an emissivity of  $\epsilon = 0.76$ , M. Lemmen (private communication, 9 June 2024). Towards EoL, the absorption coefficient will increase to 0.59, further validating the decision to design EoL for the colder end of the acceptable range so this increase remains feasible. However, considering the number of layers and the differences in emissivities between the layers, for MLI of more than 1 m<sup>2</sup>, the effective properties are divided by 80, as taught by Martin Lemmen through private communication (9 June 2024). This results in effective properties of  $\alpha_{eff} = 0.005125$  and  $\epsilon_{eff} = 0.0095$ .

The total heat absorbed now includes contributions from both RTGs, the solar radiation absorbed by the exposed areas, internal heat and conduction. To calculate the equilibrium temperature, all emitting areas with their respective emissivities were taken into account. Again, this temperature was iterated to ensure that both BoL and EoL temperatures fell within the operational range of 270 K and 290 K. The

<sup>52</sup>URL <https://www.space.com/how-cold-is-space> [cited 17 June 2024]

<sup>53</sup>URL [https://en.wikipedia.org/wiki/Sphere\\_of\\_influence\\_\(astrodynamics\)](https://en.wikipedia.org/wiki/Sphere_of_influence_(astrodynamics)) [cited 15 June 2024]

<sup>54</sup> URL <https://www.dunmore.com/products/ito-aluminized-polyimide-film.html> [cited 17 June 2024]

equation used to calculate the thermal equilibrium temperature is given in equation (4.69). Furthermore, a visualisation the thermal model is shown in figure 4.14, note that only one of the radiators and RTGs is drawn.

$$T_{\text{eq,BoL}} = \left( \frac{Q_{\text{tot,abs}}}{\sigma(\epsilon_{\text{MLI}}A_{\text{MLI}} + 2\epsilon_{\text{rad}}A_{\text{rad}} + 2\epsilon_{\text{RTG}}A_{\text{RTG}})} \right)^{0.25} \quad (4.69)$$

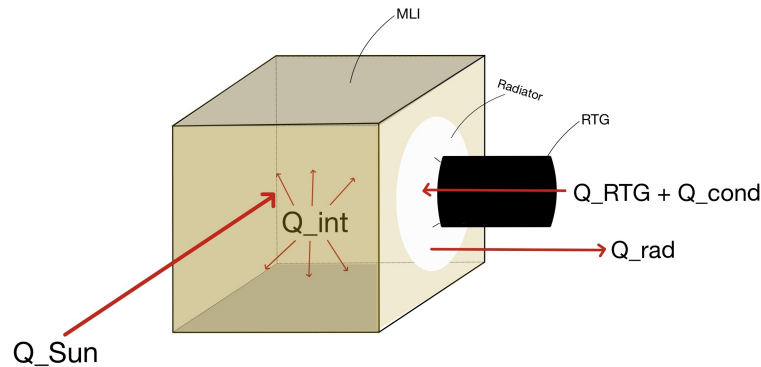


Figure 4.14: Thermal Model Sketch

#### 4: Implement thermal control for kickstages

Having assumed that the spacecraft bus is in thermal equilibrium for BoL and EoL, the next step is to ensure that the kickstages, ENKI and ENLIL, are also in a thermal balance. To simplify the situation, the kickstages are assumed to be decoupled from the main spacecraft thermal system, and so take as input the thermal equilibrium from the spacecraft. Based on the requirement of the propellant, the kickstages need to maintain a temperature between 270 K and 290 K. Using the aforementioned assumptions, iterations to balance the two heat transfers were performed until an equilibrium was met.

#### 5: Thermal control for Sun proximity

As this mission plans to approach as close as ten Solar radii from the Sun, we enter a new and challenging field of mission analysis. Due to time constraints and the scope of this project, the thermal control design for Sun proximity was not detailed extensively. Additionally, the NIBIRU team and direct external experts lack specific expertise on designing missions that venture this close to the Sun. Therefore, while rough estimations are provided, it is strongly recommended that further studies investigate this aspect in greater detail as it is beyond the scope of this project to fully design this aspect of the mission.

From the trajectory analysis, it is assumed that the NIBIRU spacecraft bus and ENLIL will be within 10 Solar radii and closer than one AU from the Sun for at least a year. The primary way to protect the spacecraft bus from this type of intense radiation is through a heat shield.

Based on the Parker Solar Probe's successful use of a heat shield at a similar proximity to the Sun, it is feasible to use similar technology for this mission. Although the specific design and sizing of this shield, the mass and size were estimated by scaling the specifications of Parker's shield. Assuming that the shield needs to be 1.5 m longer than the spacecraft bus dimensions (including the folded antenna), NIBIRU's shield would need to be at least 4 m in length. The Parker Solar Probe's shield weighs about 73 kg,<sup>55</sup> so by scaling, NIBIRU's shield should be about 127 kg. The material of the shield would also be similar to that of Parker, specifically carbon composite foam sandwiched between two carbon plates.<sup>55</sup> When the spacecraft has passed a distance of at least 0.5 AU from the Sun, the heat shield can be ejected as desired. Once again, this approximation requires more detailed analysis to refine it.

The thermal control design for the kickstages is more complex. It is assumed that the spacecraft will be flying parallel to the Sun during the kickstage firing, with only ENLIL remaining by the time we are

<sup>55</sup> URL <https://svs.gsfc.nasa.gov/cgi-bin/details.cgi?aid=12992&button=recent> [cited 17 June 2024]

near the Sun. The design for the kickstages is inspired by Starship, which uses state-of-the-art ceramic carbon tiles to protect against reentry thermal loads. Therefore, it is assumed that the tiles will be able to withstand intense solar radiation. Like on Starship, ENLIL and the adapter will have a "baking" side covered with the tiles and a "non-baking" side wrapped in MLI (see a sketch of this in figure 4.15). For simplicity at this stage of the design, it is assumed that the tiles act as perfect insulators, not transferring any heat to the underlying structure. Using the specifications on mass per tile, reaching weighing about 0.5 kg<sup>56 57</sup>, the iteration process began. This process involved iterating with the S&M subsystem and propulsion subsystem. The propulsion model provided the size of the kickstage, the thermal model calculated the required area covered by tiles and MLI, and this mass is then fed back into the S&M model to output a new mass for the cylindrical structure. This process was repeated until values for mass converged to an accuracy of three decimals.

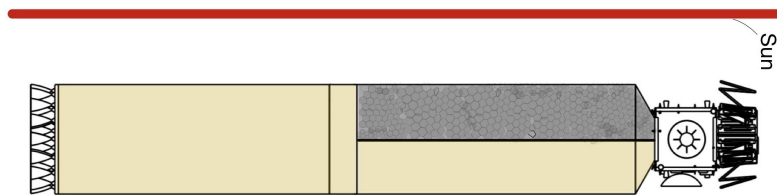


**Figure 4.15:** Sketch (Turned Sideways) of Kickstages and Adapter in Close Proximity to the Sun, Excludes Heat Shield for spacecraft bus

#### 4.7.4. Verification & validation

The design process of the TCS involved several computational steps, making it crucial to ensure that the model was both accurate and reliable. A comprehensive approach was adopted for verification and validation, involving multiple methods to achieve this objective.

First, verification ensured that the model was correctly implemented and solved the equations as intended. The main approach involved performing hand calculations and comparing them with the model outputs, where these calculations served as unit tests. This approach was applied to radiative and conductive heat transfer equations as well as thermal equilibrium temperatures. In all cases, the model successfully matched the manual computations, confirming its accuracy. Furthermore, a series of extreme-value system tests were performed to ensure the model's robustness under various (unrealistic) conditions. These tests also passed, further verifying the model's reliability.

Second, validation ensured that the model accurately represented the real-world system it was intended to simulate. The primary means of validation involved expert review and comparison with established missions and models. The model was reviewed by thermal engineer Martin Lemmen, who validated all assumptions made for the thermal environment and spacecraft bus, considering the early phase of the design. His suggestions to streamline the design process and improve the model, such as the process from designing for EoL and adapting for BoL, were incorporated as well. In addition, Ines Uriol Balbin, an expert in Aerospace Structures and professor of the "Spacecraft Thermal Design" course at TU Delft, reviewed the assumptions related to the thermal control design of the kickstages and heat shield, as well as the model outputs.

In terms of comparison with established models, a 25-node model of the NIBIRU spacecraft bus's thermal environment was created by Martin Lemmen using industry-level tools. The results from this model were compared with the outputs of our model, revealing only minor discrepancies. These discrepancies were within acceptable limits for this phase of the design, validating the model's use for this analysis. Furthermore, the values for absorptivity, emissivity, areas, and masses were compared against those from

<sup>56</sup> URL <https://space.stackexchange.com/questions/65703/how-many-heat-shield-tiles-are-installed-on-starship-and-what-is-their-total-vol> [cited 16 June 2024]

<sup>57</sup> URL <https://www.techbriefs.com/component/content/article/2292-arc-15201-1> [cited 16 June 2024]

comparable missions such as the Parker Solar Probe and New Horizons. These comparisons confirmed that the values used in the model were realistic and attainable. The equilibrium temperatures for NIBIRU were also compared to these missions and found to be within expected and achievable ranges. Additionally, the materials and insulation methods used in the model were consistent with those employed in these missions, validating the assumptions made.

#### 4.7.5. Final design

After iterating with these parameters and assumptions, the following design specifications were finalised for the spacecraft bus at BoL and EoL, shown in table 4.26. Furthermore, the kickstage specifications of the final iteration are summarised in table 4.27

**Table 4.25:** Thermal Design Specifications for the NIBIRU spacecraft bus and Kickstages

**Table 4.26:** NIBIRU spacecraft bus

| RTG specifications        | Value    |
|---------------------------|----------|
| $\epsilon_{RTG}$          | 0.89     |
| $\alpha_{RTG}$            | 0.96     |
| $T_{RTG,EoL}$             | 335 K    |
| $T_{RTG,BoL}$             | 365 K    |
| Structural specifications | Value    |
| Number of struts per RTG  | 6        |
| Material of struts        | Ti6Al4V  |
| Diameter per strut        | 0.01 m   |
| Length per strut          | 0.02 m   |
| Radiator                  | Value    |
| Material radiator         | AA6082   |
| Radius of radiator        | 0.45 m   |
| $\epsilon_{radiator}$     | 0.87     |
| Internal heat             | Value    |
| $Q_{int,BoL}$             | 56.55 W  |
| $Q_{int,EoL}$             | 15.94 W  |
| MLI                       | Value    |
| $\epsilon_{eff,RTG}$      | 0.005125 |
| $\alpha_{eff,RTG}$        | 0.0095   |

**Table 4.27:** The Kickstages

| Parameter                | Value              |
|--------------------------|--------------------|
| Height of total cylinder | 14.05 m            |
| Radius of adapter        | 1.312 m            |
| Surface area of adapter  | 5.5 m <sup>2</sup> |
| Material of adapter      | AA6082             |
| Height of ENLIL          | 7.42 m             |
| Height of heat shield    | 4 m                |
| Number of tiles required | 662                |
| $\epsilon_{tiles}$       | 0.9                |

The TCS will make use of 12 P0K1.202.6W.A.007<sup>58</sup> thermal sensors, two for each payload instruments (8 in total), two for the EPS and two for the OBDH. Each of these sensors use 0.1 mW of power. The sensors will redundantly ensure that the temperatures are being monitored at all times, so this data can be communicated with the OBDH. The iterated emissivities and absorptivities will be achieved using off-the-shelf organic coatings<sup>59,60</sup> and 10 layers of Kapton ITO MLI will be used for insulation.

The TCS component parameters are summarised in table 4.28. It must be noted that the material values (mass and cost per area) for the struts and radiators were taken from the library in 3DEXperience.

**Table 4.28:** Final Iteration Values for TCS

| Radiators        |                               | Ceramic tiles |             |
|------------------|-------------------------------|---------------|-------------|
| Mass             | 5.14 kg                       | Mass          | 296.32 kg   |
| Cost             | €16.45                        | Cost          | €400,034.06 |
| Coating radiator |                               | Heatshield    |             |
| Coating          | White AZ-400-LSW <sup>1</sup> | Mass          | 126.96 kg   |

<sup>58</sup>URL <https://www.ist-ag.com/en/products/pt100-class-f015-600-degc-optimized-esd-design> [cited 16 June 2024]

<sup>59</sup> URL <https://www.aztechnology.com/product/9/az-400-1sw> [cited 16 June 2024]

<sup>60</sup> URL <https://www.aztechnology.com/product/13/mls-85-sb> [cited 16 June 2024]

|                                 |                 |                |            |
|---------------------------------|-----------------|----------------|------------|
| Mass                            | 1.32 kg         | Cost           | €63,478.26 |
| Cost                            | €1,701.58       | <b>Sensors</b> |            |
| <b>Coating RTG</b>              |                 | Mass           | 0.01 kg    |
| Coating                         | Black MLS-85-SB | Cost           | €45.84     |
| Mass                            | 4.32 kg         | <b>MLI</b>     |            |
| Cost                            | €5,543.80       | MLI type       | Kapton ITO |
| <b>Struts RTG</b>               |                 | Mass_bus       | 0.88 kg    |
| Mass                            | 0.33 kg         | Cost_bus       | €9,086.00  |
| Cost                            | €7.58           | Mass_kickstage | 6.34 kg    |
| <b>Equilibrium temperatures</b> |                 | Cost_kickstage | €65,391.31 |
| T_BoL                           | 278.7 K         |                |            |
| T_kickstages                    | 273.6 K         |                |            |
| T_EoL                           | 273.4 K         |                |            |

Furthermore, all requirements proposed in section 4.7.2 have been complied with. This brings the Thermal Control subsystem to the total mass, cost and power for the complete subsystem, namely: 441.62 kg, €545,304.89 and 1.2 mW, respectively.

## 4.8 Structures and Materials

*Contributors: Iván*

The Structures and Materials subsystem is crucial in the design of spacecraft, as it ensures structural integrity and optimises performance. This section will present a market analysis and the subsystem requirements in sections 4.8.1 and 4.8.2, respectively. Secondly, a material trade-off will be conducted in section 4.8.3, which will conclude the final material choice for the structure of the spacecraft. Subsequently, the structural configuration and the sizing of the spacecraft will be determined in sections 4.8.4 and 4.8.5. Finally, the measures taken to protect the spacecraft from radiation are outlined in section 4.8.6.

### 4.8.1. Market analysis

Before delving into the design phase, a market analysis was conducted. This involved comparing past missions like New Horizons and JUICE, which provided valuable insights into their materials, configurations, and other structural implementations. These missions were also used as a source of inspiration, particularly in the design of the primary structural load carrier. For instance, New Horizons used a central cylinder design [71], which influenced the approach taken for NIBIRU. Additionally, the different launcher adapters available were researched. These adapters are crucial, as they connect the spacecraft or payload with the launch vehicle, ensuring they can withstand the loads experienced during launch. Particularly, the Starship launcher is compatible with 937, 1194, 1666 and 2624 [mm] clampband interface requirements.<sup>61</sup> These dimensions were taken into consideration when sizing the spacecraft and kickstages. Finally, regarding structural components, sandwich panels were researched for protection against micrometeoroids that cannot be detected. This led to the analysis of open-cell foam and honeycomb aluminum panels.

Regarding the material selection, a comprehensive material trade-off analysis was conducted using the Granta Edupack software [57] provided by TU Delft. This tool offered insights into the material market, providing useful data on aspects such as cost and environmental impact that might not be readily available on the Internet.

### 4.8.2. Requirements

Adding to the system requirements, the subsystem requirements for the Structures and Materials subsystem have been tabulated and are presented in table 4.29.

**Table 4.29:** Requirements for Structures and Materials Subsystem

| ID             | Requirement   |
|----------------|---|
| PL9-SUB-STR-01 | The lateral natural frequency of NIBIRU shall be greater than 10 [Hz] |
| PL9-SUB-STR-02 | The axial natural frequency of NIBIRU shall be greater than 25 [Hz]   |

Continued on next page

<sup>61</sup>URL [https://www.spacex.com/media/starship\\_users\\_guide\\_v1.pdf](https://www.spacex.com/media/starship_users_guide_v1.pdf) [cited 13 June 2024]

Table 4.29 – continued from previous page

| ID             | Requirement   |
|----------------|---|
| PL9-SUB-STR-03 | NIBIRU shall not buckle during launch   |
| PL9-SUB-STR-04 | NIBIRU shall withstand the tensile stresses exerted during launch   |
| PL9-SUB-STR-05 | The material used for NIBIRU shall not yield under the applied loads  |
| PL9-SUB-STR-06 | The S&M subsystem shall ensure impact from collisions is non-critical for mission operations                              |
| PL9-SUB-STR-07 | The material used for NIBIRU shall maintain its properties within the expected temperature range during the mission       |
| PL9-SUB-STR-08 | NIBIRU shall withstand shock loads encountered during separation events   |
| PL9-SUB-STR-09 | The structural design shall minimise mass while meeting all structural requirements                                       |
| PL9-SUB-STR-10 | The structural design shall accommodate and protect the payload during all mission phases                                 |
| PL9-SUB-STR-11 | The material used in the structure of the NIBIRU spacecraft shall stay in a temperature range between 243 [K] and 293 [K] |

### 4.8.3. Material trade-off

In this subsection, the different materials considered for the spacecraft bus and its structural components will be presented. Firstly, literature research on spacecraft materials aided in defining the materials that are most used for spacecraft missions. These materials are the following [33, 72]:

- Aluminum alloys
- Magnesium alloys
- Titanium alloys
- Beryllium alloys
- Steel
- Composites

Following this, a material analysis was carried out. For this, the software Granta EduPack [57] was used. This provides a database of materials and process information, as well as materials selection tools and a range of supporting resources.

Firstly, criteria and boundaries were selected in order to filter all the available materials, based on the mission requirements. These have been tabulated in table 4.30 and were considered based on the following reasoning [72]:

- A high Young's Modulus ensures sufficient stiffness to resist deformation under mechanical stresses and vibrations.
- A low density reduces overall mass, consequently reducing costs and improving payload efficiency.
- A high yield strength guarantees that the material can withstand mechanical loads without permanent deformation.
- A high fracture toughness provides resistance to crack propagation and catastrophic failure, ensuring robustness against potential debris collisions.
- A low cost balances performance and affordability, keeping the project within budget while ensuring the required mechanical properties.

Table 4.30: Material Criteria

| Property             | Filter                       |
|----------------------|------------------------------|
| Young's Modulus, $E$ | > 60 [GPa]                   |
| Density, $\rho$      | < 3000 [kg/m <sup>3</sup> ]  |
| $\sigma_{yield}$     | > 100 [MPa]                  |
| Fracture toughness   | > 10 [MPa M <sup>1/2</sup> ] |
| Cost                 | < 300 [EUR/kg]               |

Consequently, two charts were produced [57], showing the potential material options. The first one is Young's Modulus vs. Yield Strength. The second one is Density vs. Price. These have been depicted in figures 4.16 and 4.17, respectively.

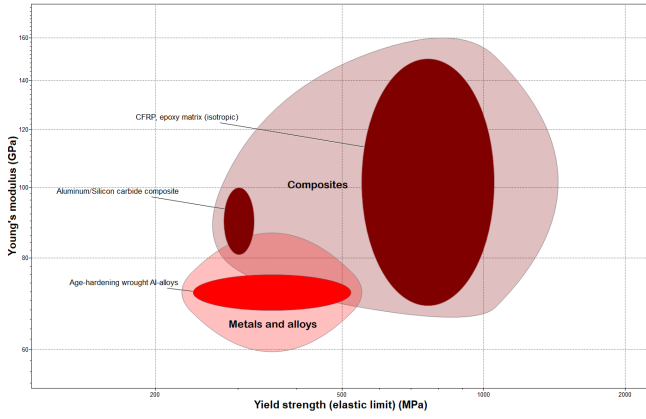


Figure 4.16: Young's Modulus vs. Yield Strength

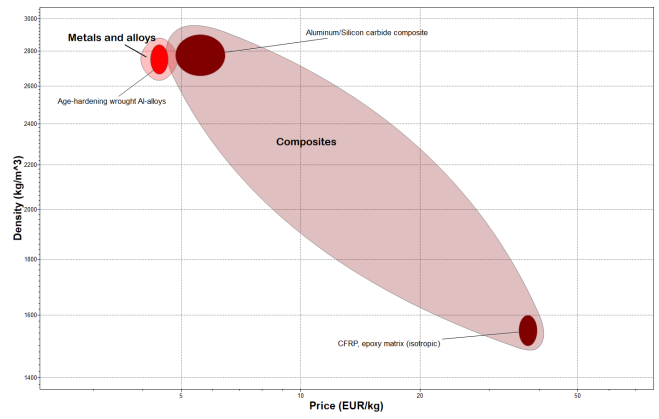


Figure 4.17: Density vs. Price Comparison Chart

As can be seen in the figures, the following materials were obtained as possible feasible options:

- CFRP-epoxy
- Aluminium/Silicon carbide
- Age hardening wrought aluminium alloys

The other materials mentioned beforehand that are commonly used for space applications were discarded as they do not meet the specified material properties [57]. Steel was excluded due to its high density, with an average density exceeding  $7800 \text{ kg/m}^3$ . Magnesium alloys were deemed unsuitable because they are not stiff enough, having a low Young's modulus of 45 GPa. Titanium alloys were also considered too dense, with an average density of  $4500 \text{ kg/m}^3$ . Lastly, beryllium alloys were discarded due to their high price of 371 EUR/kg.

Following this, specific materials options were gathered based on literature [72], and their properties were tabulated in table 4.31, using the data provided by Granta EduPack [57]. The materials considered were CFRP-epoxy, 7075-T6, 2014-T6, 2024-T36, Aluminium/Silicon carbide, and 6061-T6. It is important to note that these material properties are considered at 273 K. This is because, as the temperature increases, materials gradually lose their strength. However, this is not critical, as most of the loads that the spacecraft structure will have to withstand are those induced during launch, where the temperature remains in the range of 288 to 298 [K]. Additionally, for the rest of the mission, the thermal control subsystem will ensure that the temperature of the spacecraft remains within a specific range, where the material properties will be conserved.

To determine the most suitable material, a trade-off analysis was conducted using specific criteria: yield strength, young's modulus, toughness, density, and price, as shown in table 4.31. Each criterion was assigned an equal weight of 20% to reflect its importance in the overall evaluation.

Table 4.31: Material Options [57]

| Material                  | Yield Strength [MPa] | Tensile Strength [MPa] | Young's Modulus [GPa] | Toughness [ $\text{MPa M}^{1/2}\text{S}$ ] | Density [ $\text{kg/m}^3$ ] | Price [EUR/kg] |
|---------------------------|----------------------|------------------------|-----------------------|--|-----------------------------|----------------|
| CFRP-epoxy                | 945                  | 1040                   | 96.2                  | 13   | 1420                        | 37.5           |
| Aluminium/Silicon Carbide | 302                  | 327.5                  | 90.5                  | 19.5                                       | 2780                        | 5.6            |
| 2014-T6                   | 365                  | 415                    | 73                    | 30.5                                       | 2800                        | 3.5            |
| 2024-T36                  | 360                  | 475                    | 73.1                  | 39   | 2780                        | 3.5            |
| 6061-T6                   | 276                  | 310                    | 69                    | 33   | 2700                        | 3.25           |
| 7075-T6                   | 503                  | 572                    | 71.7                  | 26.7                                       | 2810                        | 6.5            |

Firstly, each material was ranked for each criterion. The rankings were converted into scores, with the highest-ranked material receiving a score of 6 and the lowest-ranked material receiving a score of 1,

ensuring that higher performance in a given criterion corresponded to a higher score. The scores for yield strength, Young's modulus, toughness, density, and price are as follows:

- **Yield Strength:** CFRP-epoxy (6), 7075-T6 (5), 2014-T6 (4), 2024-T36 (3), Aluminium/Silicon carbide (2), 6061-T6 (1).
- **Young's Modulus:** CFRP-epoxy (6), Aluminium/Silicon carbide (5), 2024-T36 (4), 2014-T6 (3), 7075-T6 (2), 6061-T6 (1).
- **Toughness:** 2024-T36 (6), 6061-T6 (5), 2014-T6 (4), 7075-T6 (3), Aluminium/Silicon carbide (2), CFRP-epoxy (1).
- **Density:** CFRP-epoxy (6), 6061-T6 (5), Aluminium/Silicon carbide (3.5), 2024-T36 (3.5), 2014-T6 (2), 7075-T6 (1).
- **Price:** 6061-T6 (6), 2024-T36 (4.5), 2014-T6 (4.5), Aluminium/Silicon carbide (3), 7075-T6 (2), CFRP-epoxy (1).

For the density and price criteria, where Aluminium/Silicon carbide and 2024-T36, and 2024-T36 and 2014-T6, respectively, had identical properties, they were assigned the average of their ranks as their scores. Subsequently, the weighted score for each material was calculated by multiplying each score by the weight of the criterion (20%). The results were tabulated in table 4.32.

Table 4.32: Material Scores

| Material                      | Yield Strength | Young's Modulus | Toughness | Density | Price | Total Score |
|-------------------------------|----------------|-----------------|-----------|---------|-------|-------------|
| CFRP-epoxy                    | 6              | 6               | 1         | 6       | 1     | 4           |
| Aluminium/<br>Silicon carbide | 2              | 5               | 2         | 3.5     | 3     | 3.1         |
| 2014-T6                       | 4              | 3               | 4         | 2       | 4.5   | 3.5         |
| 2024-T36                      | 3              | 4               | 6         | 3.5     | 4.5   | 4.2         |
| 6061-T6                       | 1              | 1               | 5         | 5       | 6     | 3.6         |
| 7075-T6                       | 5              | 2               | 3         | 1       | 2     | 2.6         |

As seen in the table, **2024-T36** achieved the highest total score, making it the most suitable material for the structural elements of the spacecraft. With this material selected, the next step is to proceed with the actual sizing of the spacecraft's structural elements.

#### 4.8.4. Structural configuration

The primary function of the structural system in a spacecraft is to maintain its overall integrity [73]. This involves preventing the spacecraft from deforming, ensuring connectivity with the launch vehicle and protection against debris and radiation, amongst others. These structural elements can be classified into three different types [33]. These are:

- **Primary** structure, responsible for transmitting loads to the base of the satellite and guaranteeing structural integrity. This structure also provides an interface between the satellite and the payload bay of the launcher through a launch vehicle adapter.
- **Secondary** structure, comprising all the required support structures to carry loads from the various components of the spacecraft equipment to the primary structure, including panels, beams and trusses. A secondary structure failure is not critical for success of the mission, as it does not affect structural integrity, but can impact the mission in terms of other subsystems, such as propellant leakage or thermal control fluctuations. comprises the brackets, panels and support
- **Tertiary** structures, encompassing the smallest structural elements, such as brackets, component housings, and electronic boxes.

Spacecraft are usually designed using simple geometric forms that reflect their underlying structural form and their attitude control strategy [73]. The different design options are: three-axis stabilised spacecraft,

which is box shaped, a spinner spacecraft, which consists of a cylinder, and no control, shaped as a sphere. NIBIRU will be a three-axis stabilised spacecraft, therefore, it will shaped as a box.

For the primary structure, i.e. the load-carrying structure, there are an infinite number of design options. However, the most common ones are [74]:

- Structure with central tube and cone. As shown in figure 4.18a, the equipment is supported by sandwich panels around a central cylinder, chosen for its efficient load transfer and global stiffness. The circular clamp band interface ensures continuity and high axial stiffness, beneficial for bending and torsion. This design is common in medium to large satellites.
- Structure with shear panels and without central cylinder. This design is suitable for small, short spacecraft where a central cylinder is impractical. As shown in figure 4.18b, discrete hard point interfaces are used instead of a clamp band, which makes the structure less stiff but acceptable for small spacecraft.
- Box design with solid aluminium walls. This design is simpler but less efficient, but eases construction and testing. As shown in figure 4.18c, it uses a circular clamp band interface, with the panel working in bending unless shear walls are added. This is most suitable for small satellites where natural frequencies remain tolerable. This configuration is typical in small to very small satellites.

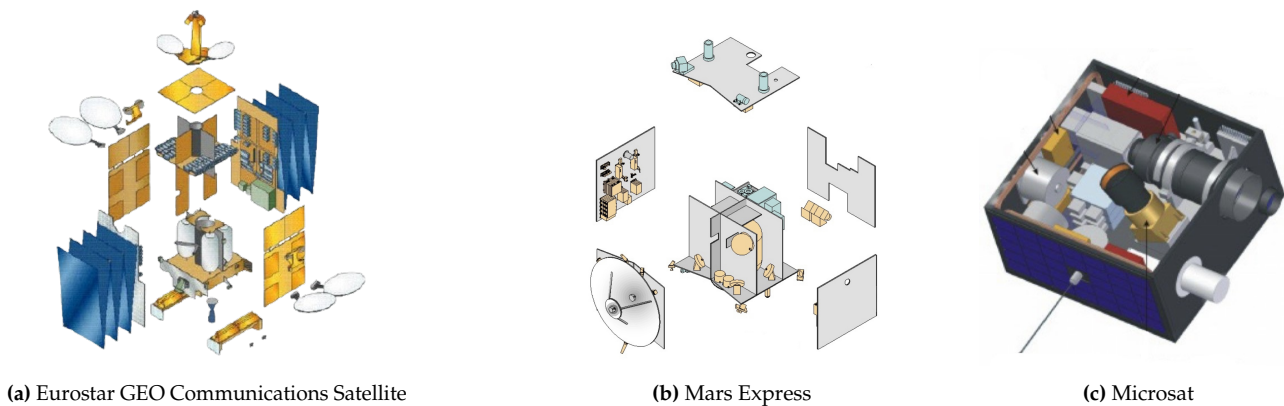


Figure 4.18: Structure Types [74]

Due to the aforementioned reasons, for a large spacecraft designed for an interplanetary mission, the central tube structure is the most suitable choice. The primary reason is the efficient load transfer provided by the circular clamp band, which is crucial for handling the heavy loads NIBIRU will be subjected to during launch. This design option aligns well with the loading demands, ensuring durability and reliability over the mission's lifetime. Additionally, the cylindrical structure will be surrounded by panels arranged in a cubic shape. This arrangement improves the spacecraft's strength and structural integrity while providing space for the necessary components to remain safe from outer Space.

#### 4.8.5. Sizing

During launch, the spacecraft will be subjected to various loads [75]. Therefore, the cylinder, which will act as the main load-carrying structure, will be sized to prevent structural failure considering the following load cases:

- Vibrations: This involves ensuring that the spacecraft's lowest natural frequency is sufficiently high to prevent resonance with the launch vehicle.
- Quasi-static loads: These include tensile forces induced by axial loads, bending moments, and compressive forces that may cause buckling, all induced from the acceleration of the mass during launch and ascent.

#### Factors of Safety

Before starting with the design, for the spacecraft structure to function safely and avoid failure, factors of safety must be introduced to reduce uncertainties in the design. The Factor of Safety describe the

structural capacity of a system beyond the applied loads or actual load. It is specifically used to increase the capability of the structure such that the risk of a failing structure is reduced to an acceptable level. These factors of safety were obtained from Zandbergen [33] and are standard values. The Yield load safety factor is 1.1 and the Ultimate load safety factor is 1.25

### Conceptualisation

For the design, the NIBIRU bus and its kickstages will be considered as two different cantilevered beams, which will be treated independently, as depicted in figure 4.19. Additionally, it will be assumed that the cylinders have uniform thickness and by definition no ring or long stiffeners. It will also be assumed that the attachments between the different stages transfer loads efficiently from the launcher to the structure. This is done as preliminary sizing and for simplicity, but should be further analysed in future phases of the design process.

This gives two beams, of height 1.5 m and 14.05 m, for the spacecraft bus and the kickstages, respectively. The cube enclosing the cylinder was assigned a length of 1.5 m, comparable to sizes used in other space missions, enabling it to house all components on both the inner and outer surfaces. The height of the kickstages has been determined in section 4.6.11, to accommodate the propellant tanks and ensure sufficient clearance between them. Regarding the diameters, the bus cylinder was given a diameter of 0.9 m, as this is the maximum size that allows all components to fit inside the spacecraft. The kickstage will have the same diameter as the Payload Adapter Fitting (PAF) of the launcher. This is designed for increased stiffness, as the closer the diameters match, the more rigid the structure becomes, resulting in more efficient load transfer. This relationship is illustrated in figure 4.20 [74]. Due to the size of the propellant tanks, as explained in section 4.6.11, the minimum cylinder width has been found to be 2.6 m. Therefore, to comply with the diameter of the PAF, the cylinder diameter was set to 2.624 m.

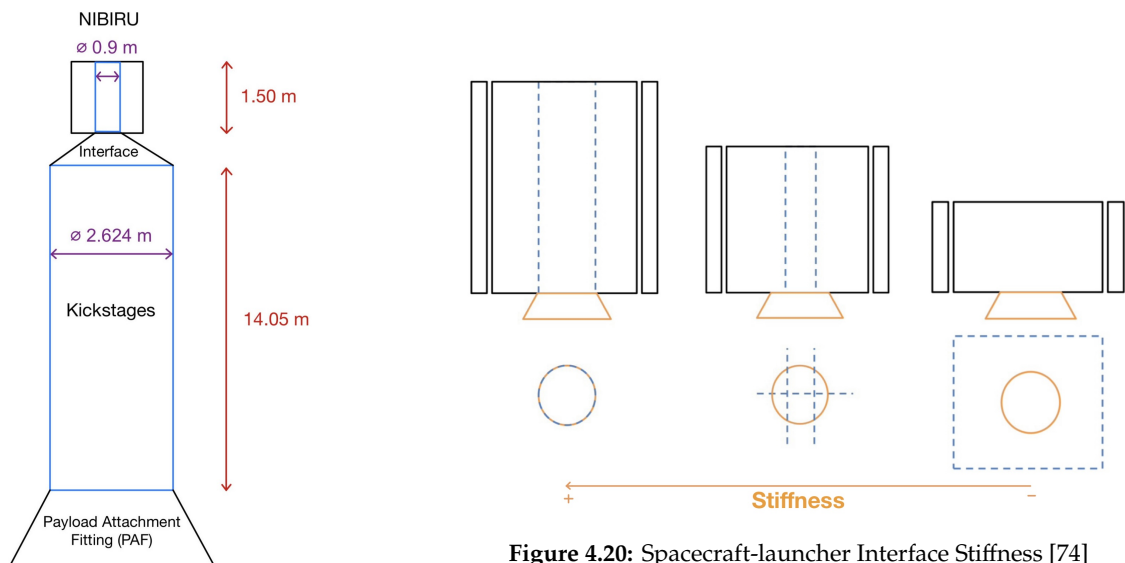


Figure 4.19: Diagram of NIBIRU and Cylinders

### Launcher-Spacecraft Interface

The payload fairing is a crucial component of the launch vehicle, shielding the payload from harsh conditions during launch and ascent, such as aerodynamic heating and pressure [33]. It is essential that the spacecraft and kick stages fit inside this bay. The payload bay for the Starship launcher has been depicted in figure 4.21.

Once fitted, the spacecraft and launcher are connected through the Payload Adapter (PLA) mount. This is crucial for transferring loads from the different stages of the launcher to the spacecraft. Instead of distributing the load over a wider area, the loads are concentrated into the primary structure of the spacecraft, in this case, within the central cylinder. The PLA consists of three components and have been illustrated in figure 4.22 [76]:

- The Payload Adapter Fitting (PAF), a critical component that provides an attachment point for the payload on the launcher. It serves as the primary interface between the launch vehicle and the payload, ensuring secure and stable integration. The PAF is designed to withstand the significant mechanical loads and stresses encountered during launch and ascent.
- The Payload Separation System (PSS), a structural separation interface that facilitates the safe and reliable separation of the payload from the launch vehicle once it reaches its designated orbit. The PSS can be mounted directly on a PAF or an optional Payload Interface Adapter (PIA), depending on the specific mission requirements. It is designed to provide a clean and controlled separation, minimising the risk of mechanical shocks and ensuring the payload is deployed accurately and without damage.
- The Payload Interface Adapter (PIA), an optional structural and service interface positioned between the Payload Adapter Fitting (PAF) and the Payload Separation System (PSS). It is specifically designed to maximise the available diameter and height, being able to accommodate for a wider range of spacecraft and payload configurations.

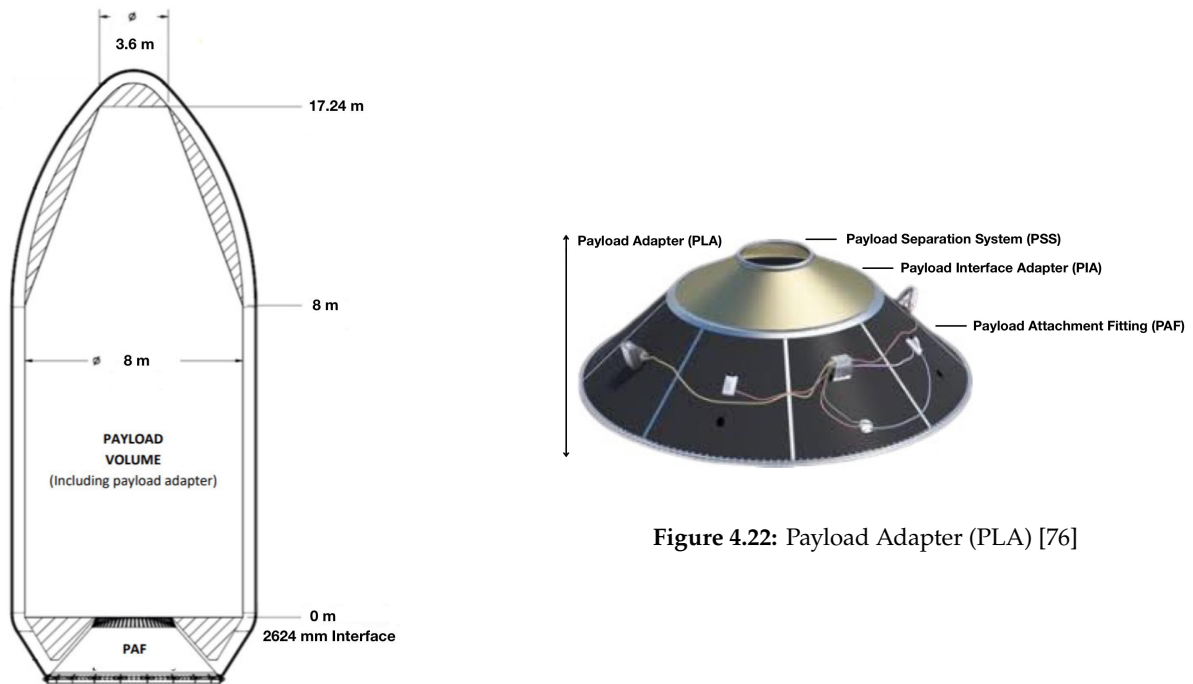


Figure 4.21: Payload Fairing Dimensions<sup>61</sup>

During launch, the spacecraft, along with its thrusters, is housed within the payload fairing. The kickstages are divided into two parts: ENLIL (top) and ENKI (bottom). Enki connects to the Payload Attachment Fitting (PAF) using a clampband, with the thruster configuration inside the PAF. This setup reduces the required length of the cylinder and protects the thrusters from atmospheric drag and acoustic vibrations.

ENLIL and ENKI are connected with an attachment of matching diameter and thickness, secured with a clampband at the top. Finally, Enlil attaches to NIBIRU using an adapter to accommodate the different cylinder sizes, secured with a final clampband at the top. These clampbands incorporate a low-shock separation system that minimises structural impact and allows a safe detachment from the base [77].

### Sizing for stiffness

Firstly, the cylinders will be sized for rigidity to meet the frequency requirements. In order to account for stiffness, the structure's dimensions and material choice should be chosen so that the excitation frequency is significantly smaller than the first natural frequency, or eigenfrequency [75]. The minimum frequencies to design for were taken from Falcon 9, as Starship is still in development and these values have not been made public yet. Therefore, for the Falcon Heavy launcher, payloads should consider maintaining the primary lateral frequency above 10 [Hz] and a primary axial frequency above 25 [Hz],<sup>62</sup> to avoid

<sup>62</sup>URL <https://www.spacex.com/media/falcon-users-guide-2021-09.pdf> [cited 13 June 2024]

interaction with launch vehicle dynamics and most importantly, resonance. These frequencies were used to size the kickstages' cylinder, and the obtained kickstage frequencies were then adjusted by a factor of 5 to size the bus' cylinder, ensuring a significant difference to avoid resonance.

As previously explained, the cylinders will be modelled as cantilever beams with a uniform mass  $m_B$ , and a length  $L$ , as illustrated in figure 4.23. Subsequently, equations (4.70) and (4.71) describe the natural lateral and axial frequencies, respectively [40]. The mass used for the calculations includes an approximation of the structure mass, which has been obtained after iterating together with the propulsion and thermal control subsystems.

**Table 4.33:** Required Parameters for Sizing of NIBIRU Bus and Kickstages

| Bus       |           | Kickstages |            |
|-----------|-----------|------------|------------|
| Parameter | Value     | Parameter  | Value      |
| Mass      | 2400 [kg] | Mass       | 38248 [kg] |
| Length    | 1.5 [m]   | Length     | 14.05      |
| Radius    | 1.312 [m] | Radius     | 0.45 [m]   |

**Table 4.34:** Properties of Aluminum 2024-T36 [57]

| Material Property | Value                     |
|-------------------|---------------------------|
| Yield Strength    | 360 [MPa]                 |
| Tensile Strength  | 475 [MPa]                 |
| Young's Modulus   | 73.1 [GPa]                |
| Density           | 2780 [kg/m <sup>3</sup> ] |
| Design FoS        | 1.25                      |

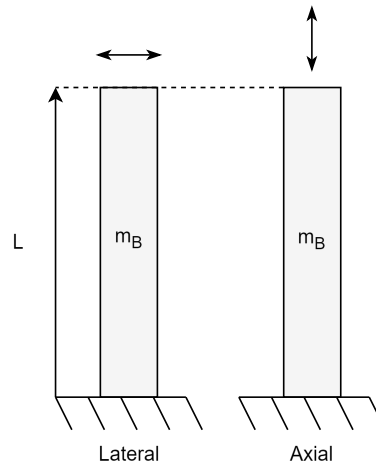


**Figure 4.23:** Natural Frequencies of a Beam with Uniform Mass

$$f_{\text{nat}_{\text{lateral}}} = 0.560 \sqrt{\frac{EI}{m_B L^3}} \quad (4.70)$$

$$f_{\text{nat}_{\text{axial}}} = 0.250 \sqrt{\frac{AE}{m_B L}} \quad (4.71)$$

Here,  $E$  represents the Young's modulus of the material, indicating its stiffness,  $I$  the area moment of inertia of the cross-section about the axis of bending and  $A$  the cross-sectional area of the beam. From these equations, the required cylinder area and moment of inertia can be solved for independently:

$$I = \frac{m_B L^3}{E} \left( \frac{f_{\text{nat}_{\text{lateral}}}}{0.560} \right)^2 \quad (4.72)$$

$$A = \frac{m_B L}{E} \left( \frac{f_{\text{nat}_{\text{axial}}}}{0.250} \right)^2 \quad (4.73)$$

Now, using the cross sectional area of a thin walled cylinder and the area moment of inertia, the minimum required thickness can be solved for in both cases:

$$A = 2\pi R t \quad (4.74)$$

$$I = \pi R^3 t \quad (4.75)$$

Here,  $R$  is the radius of the cylinder. From these, the required thicknesses can be obtained. These have been tabulated in table 4.35 using the following formulae:

$$t_{required} = \frac{A}{2\pi R} \quad (4.76)$$

$$t_{required} = \frac{I}{\pi R^3} \quad (4.77)$$

**Table 4.35:** Thicknesses Required to Meet Frequency Requirements

| Bus                      |            | Kickstages               |             |
|--------------------------|------------|--------------------------|-------------|
| Parameter                | Value      | Parameter                | Value       |
| $t_{required_{area}}$    | 5.913 [mm] | $t_{required_{area}}$    | 8.989 [mm]  |
| $t_{required_{inertia}}$ | 4.061 [mm] | $t_{required_{inertia}}$ | 65.741 [mm] |

**Sizing for tensile strength**

Secondly, the cylinder can be sized for tensile strength. The applied and equivalent loads can be calculated. This is done by multiplying the spacecraft weight by the load factors, giving the maximum expected loads. The load factors for the launcher can be found on the User Manual of Starship, provided by SpaceX.<sup>61</sup> These are presented in figure 4.24. Additionally, the bending moment can be determined by multiplying the lateral load with the moment arm, where the center of mass is taken to be at the center of the cylinder. The calculation of these limit loads has been tabulated in table 4.36 [40], where the distance is measured from the base to the center of mass of the cylinder, which has been assumed to be the center of the cylinder.

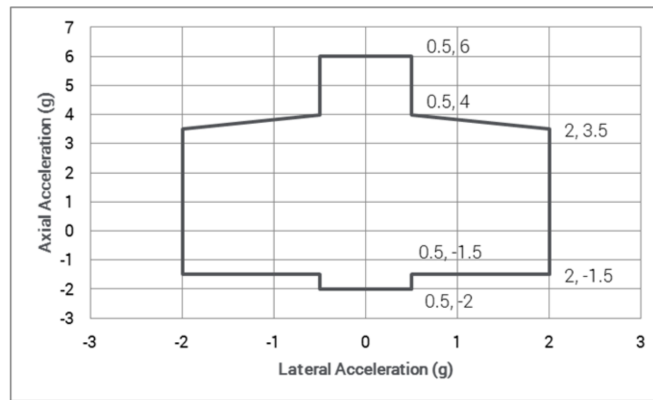


**Figure 4.24:** Payload Maximum Design Load Factors.<sup>63</sup>

**Table 4.36:** Cylinder Applied Loads

| Type of load   | Weight [N]  | Distance [m]  | Load Factor | Limit Load                                   |
|----------------|-------------|---------------|-------------|--|
| Axial          | $m \cdot g$ | -             | 6           | $6 \cdot m \cdot g$ [N]                      |
| Lateral        | $m \cdot g$ | -             | 3.5         | $3.5 \cdot m \cdot g$ [N]                    |
| Bending Moment | $m \cdot g$ | $\frac{L}{2}$ | 3.5         | $3.5 \cdot m \cdot g \cdot \frac{L}{2}$ [Nm] |

The equivalent axial load can be calculated using equation (4.78) [40]. Here,  $M$  represents the bending moment and  $R$  the radius of the cylinder.

$$P_{eq} = P_{axial} + \frac{2M}{R} \quad (4.78)$$

$$P_{eq} \cdot \text{Ultimate Factor of Safety} = \text{Ultimate Load} \quad (4.79)$$

The equation for axial stress is  $\sigma = P/A$ . Using the ultimate load  $P_{eq}$  and the material's allowable stress  $\sigma_{ult}$ , the area of the cross section,  $A = 2\pi R t$  can be used to solve for the required thickness, tabulated in

table 4.37 using the following formulae:

$$\sigma_{ult} = \frac{P_{eq}}{2\pi R t} \quad (4.80)$$

$$t_{required} = \frac{P_{eq}}{2\pi R \sigma_{ult}} \quad (4.81)$$

**Table 4.37:** Thicknesses Required for Tensile Strength

| Bus            |            | Kickstages     |            |
|----------------|------------|----------------|------------|
| Parameter      | Value      | Parameter      | Value      |
| $t_{required}$ | 0.408 [mm] | $t_{required}$ | 5.250 [mm] |

### Sizing for stability

Finally, the cylinder can be sized for stability by ensuring it meets the required compressive strength. The cylinder must withstand an ultimate equivalent load of  $P_{eq}$ , as calculated before. For this, the maximum thickness calculated previously will be used. The equation for cylinder buckling stress is [40]:

$$\sigma_{cr} = 0.6\gamma \frac{Et}{R} \quad (4.82)$$

Here,  $\gamma$  acts as a reduction factor, linking theoretical predictions to experimental results. This factor is governed by a cylinder-specific geometric parameter,  $\phi$ . These parameters are defined by equations (4.83) and (4.84) [40].

$$\phi = \frac{1}{16} \sqrt{\frac{R}{t}} \quad (4.83)$$

$$\gamma = 1.0 - 0.901 (1.0 - e^{-\phi}) \quad (4.84)$$

Where  $R$  is the radius,  $t$  is the thickness and  $L$  the length of the cylinder. Having calculated the buckling stress, the cylinder's cross-sectional area can be used to calculate the critical buckling load, as  $\sigma = P/A$ . This will have to be equal to or larger than the  $P_{eq}$ .

$$P_{cr} = A\sigma_{cr} \quad (4.85)$$

Finally, structural integrity can be assessed using the Margin of Safety (MS), which must be equal to or greater than 0. This calculation involves comparing the critical buckling load  $P_{cr}$  with the ultimate load  $P_{eq}$  [40].

$$MS = \frac{\text{Allowable Load or Stress}}{\text{Design Load or Stress}} - 1.0 = \frac{P_{cr}}{P_{eq}} - 1.0 \quad (4.86)$$

If MS is negative, the thickness of the cylinder has to be increased, and vice versa. A numerical model has been written to optimise for the MS, aiming for the positive that is closest to 0, giving the minimum required thickness and, consequently, giving the lowest cylinder mass. The iteration values, specifically for the initial and final iterations, have been tabulated in tables 4.38 and 4.39 for the bus and the kickstages, respectively.

**Table 4.38:** Iteration Data for Bus

| Iteration | Thickness [mm] | $\gamma$ | $\sigma_{cr}$ [MPa] | Area [m <sup>2</sup> ] | $P_{cr}$ [N] | MS    |
|-----------|----------------|----------|---------------------|------------------------|--------------|-------|
| Initial   | 5.913          | 0.621    | 358.1               | 0.0167                 | 5,987,350    | +9.92 |
| First     | 2.083          | 0.459    | 93.119              | 0.00589                | 548,523      | +0.00 |

Now that the cylinder thickness has been determined, the final mass can be calculated using equation (4.87)

Table 4.39: Iteration Data for Kickstages

| Iteration | Thickness [mm] | $\gamma$ | $\sigma_{cr}$ [MPa] | Area [m <sup>2</sup> ] | $P_{cr}$ [N] | MS     |
|-----------|----------------|----------|---------------------|------------------------|--------------|--------|
| Initial   | 65.74          | 0.780    | 1715.32             | 0.542                  | 929,601,000  | +44.22 |
| First     | 11.52          | 0.561    | 216.25              | 0.0950                 | 20,537,900   | +0.00  |

[40]. The final masses have been tabulated in table 4.40.

$$m = \rho 2\pi R t L \tag{4.87}$$

Table 4.40: Final Cylinder Mass Values

| Bus       |            | Kickstages |              |
|-----------|------------|------------|--------------|
| Parameter | Value      | Parameter  | Value        |
| Mass      | 27.02 [kg] | Mass       | 3709.64 [kg] |

**Micrometeoroid protection**

It is important to protect the spacecraft from micrometeoroid impacts that could compromise its functionality. These impacts can arise from various sources such as planetary debris, asteroids, and comets. Since most micrometeoroids are too small to be detected, passive protection must be implemented. Without adequate protection, potential failure scenarios include catastrophic rupture, leakage, erosion, and reduced structural strength.<sup>64</sup>

The MLI used to regulate the spacecraft’s internal temperature throughout the mission also serves the secondary purpose of shielding the vehicle from micrometeoroids.<sup>64</sup> As discussed in section 4.7.1, the MLI blankets used for NIBIRU consist of ten layers that act as an insulator, but also as a protective shield. When a micro meteoroid or other projectile hits the MLI, these layers intercept it, dispersing the fragments and reducing their velocity before they reach the interior walls.

However, MLI is not primarily designed for micrometeoroid protection. Given that NIBIRU must travel across the Kuiper Belt, where the risk of debris collisions increases, additional protection is necessary. For this, foam-core and honeycomb sandwich panels were considered, comprising a front and rear layer with a core in between, as illustrated in figures 4.25 and 4.26, respectively [78]. Here,  $t_f$  and  $t_r$  represent the face and rear panel thickness respectively, while  $S$  is the spacing between these faces, also referred to as core thickness.

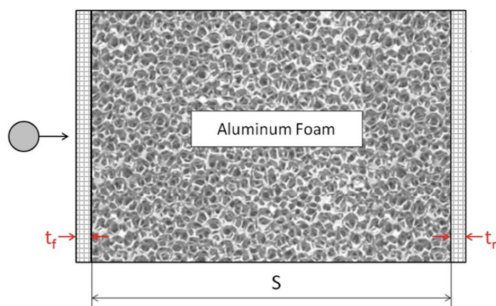


Figure 4.25: Open Foam Aluminum Panel [78]

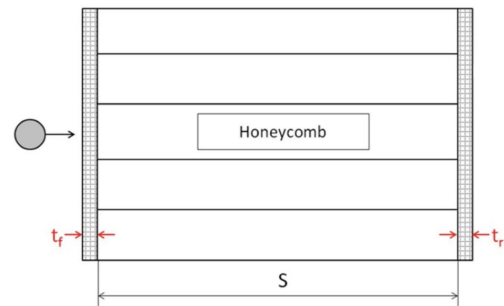


Figure 4.26: Honeycomb Aluminum Panel [78]

These two configurations have similar performance. However, a recent study on the hypervelocity impact performance of open cell foam core sandwich panels revealed that these foam panels demonstrate a higher shielding performance compared to lower PPI foams and traditional honeycomb panels under both normal and oblique impact conditions [79]. Moreover, they provide a level of protection comparable to Whipple shields. For these reasons, open cell foam core sandwich panels will be used as the inner casing of the spacecraft for this mission, surrounding the cylinder and forming a cube.

<sup>64</sup>URL <https://11is.nasa.gov/lesson/705> [cited 15 June 2024]

There are four parameters that need to be determined: the front and rear face thickness, the core thickness, the material, and the pores per inch (PPI). Studies indicate that shielding performance improves with increasing pore density [79]; therefore, a 40 PPI core will be used. Furthermore, studies show that a standard configuration with a core thickness of 25.4 [mm] and front and rear face thicknesses of 0.254 [mm] serves as effective preliminary sizing, capable of stopping debris traveling at speeds up to 7 [km/s] with a diameter of up to 3 [mm] [79]. The material selected will be the same as that used for the cylinder, Aluminium 2024-T36, as it has already been deemed optimal. In future design phases, these parameters can be further analysed to obtain more accurate debris protection. The front and rear faces will be adhered to the core using epoxy resin, providing an efficient transfer of loads [79].

Following this, the mass of each panel can be calculated. The density of the front and rear panels is 2780 [kg/m<sup>3</sup>], whereas the density of the core is 7% of that of the front and rear panels [78], resulting in a core density of 194.6 [kg/m<sup>3</sup>]. The size of the top and bottom panels will be 1.5 x 1.5 [m]. The front and back panels will have dimensions of 1.5 [m] x 1.4482 [m] and the right and left panels 1.4482 [m] x 1.4482 [m]. This can be observed in figure 4.27, where the thickness of each panel is also visible. It is important to note that the panels have been sized to ensure that the final length of each side is exactly 1.5 meters.

**Table 4.41:** Mass of Open Cell Foam Core Sandwich Panels

| Part       | Surface Area (m <sup>2</sup> ) | Volume of Rear and Front Faces (m <sup>3</sup> ) | Volume of Core (m <sup>3</sup> ) | Mass of Rear and Front Faces [kg] | Mass of Core (kg) | Sum (kg) | Number of Faces | Total Mass [kg] |
|------------|--------------------------------|--|----------------------------------|-----------------------------------|-------------------|----------|-----------------|-----------------|
| Top/Bottom | 2.25                           | 0.00114  | 0.0572                           | 3.178                             | 11.121            | 14.299   | 2               | 28.599          |
| Front/Back | 2.172                          | 0.00110  | 0.0552                           | 3.068                             | 10.737            | 13.805   | 2               | 27.610          |
| Right/Left | 2.097                          | 0.00107  | 0.0533                           | 2.962                             | 10.367            | 13.33    | 2               | 26.656          |
|            |                                |  |                                  |                                   |                   |          |                 | 82.865          |

Now that the dimensions and composition of the panels have been determined, the next step is their assembly. L-joints will therefore be used to secure the sandwich panels together [80]. Two sets of connectors have been used, one set to connect the vertical panels and another pair to connect the top and bottom panels with the vertical panels. These have been illustrated in figure 4.28. Each pair of connectors differs in length to ensure precise alignment both inside and outside the panels. Finally, bolts will be used to secure these connectors along their length.

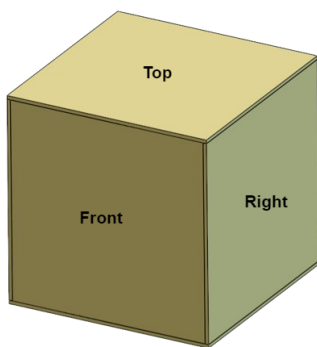


**Figure 4.27:** Sandwich Panels

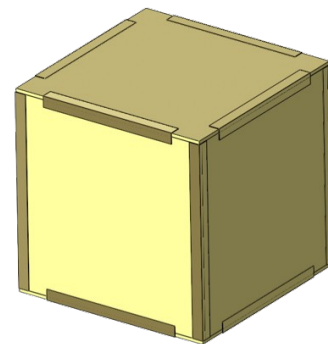


**Figure 4.28:** Sandwich Panels and Connectors

### 4.8.6. Radiation protection

It is crucial for NIBIRU to be protected against radiation to ensure the safety of the spacecraft and its components. In designing NIBIRU, four key factors have been taken into account for radiation protection: the choice of materials, the MLI, and the heatshield, as well as shielding tiles for ENLIL, the top kickstage.

Firstly, the use of Aluminium as the main material for the structure of the spacecraft is one of the primary strategies for shielding against radiation. This material is approximately 100 times more resistant to radiation damage compared to other common materials used in spacecraft structures<sup>65</sup> However, gamma

<sup>65</sup>URL <https://industrialmetalservice.com/metal-university/aluminum-radiation-shielding-in-3d-imaging/> [15 June 2024]

radiation is highly penetrating and not effectively shielded by aluminum. Therefore, further research will have to be conducted to analyse the levels of gamma radiation NIBIRU will be exposed to and to determine if additional shielding measures are necessary to ensure the proper functionality of the spacecraft and its components.

Moreover, the use of MLI serves as an additional protective barrier for the spacecraft against incoming solar and infrared (IR) flux.<sup>66</sup> The multiple layers of radiation shields in the MLI reflect a large percentage of the radiant heat flux back in the opposite direction of heat flow, preventing the radiation from penetrating the spacecraft [81].

Finally, the spacecraft's heatshield is designed to protect against the intense radiation emitted by the Sun. As NIBIRU will be at a mere distance of 10 solar radii from the Sun at one point of the trajectory, the specialised shield, inspired by the Solar Parker Probe,<sup>67</sup> will ensure that the spacecraft can endure prolonged exposure to this level of solar radiation without compromising its functionality. In addition, ENLIL, the top kickstage, also requires protection at such a close distance to the Sun. For this, the side of the kickstage facing the Sun will be covered in ceramic tiles, similar to those used on the Starship. These tiles are integrated into the launcher to shield against the high levels of ionizing radiation experienced during reentry into Earth's atmosphere.<sup>57</sup> Thus, this shielding will offer significant protection against incoming radiation. However, further investigation is required to confirm their efficacy for this mission. The tiles require thorough testing and validation to ensure they meet the mission's requirements.

#### 4.8.7. Verification & validation

For the material selection, GrantaEdupack software provided by TUDelft was used. This includes a comprehensive database of materials and process information, materials selection tools and a range of supporting resources. From this database, all necessary mechanical and thermal properties of the different considered materials, as well as cost and mass data, were obtained. The reliability of this data was verified and cross-checked with other sources, resulting in a negligible error margin.

For structural design, a computational model was developed, requiring both verification and validation, to ensure a correct approach. Verification involved ensuring that the model was correctly implemented according to the conceptual design and was error-free. This was achieved by performing manual calculations and comparing them with the model outputs. Variables were printed at various points in the code to facilitate hand verification of the calculations. Several sizing problems were also solved using the program, consistently producing the correct results.

Finally, validation was required to confirm that the model is an accurate representation of the real system. This was done by having the model conceptualisation reviewed by Inés Uriol Balbin, an expert in Aerospace Structures and a current professor at TU Delft.

#### 4.8.8. Final design

Now that the cylinders have been designed and the panels for the cubical configuration have been determined, we can calculate the final mass and cost budgets for the Structures and Materials subsystem. Firstly, an overview of the important parameters calculated in this section is tabulated in table 4.42. Subsequently, the final budgets can be found in table 4.43.

**Table 4.42:** Final Values for Structural Sizing of NIBIRU

| Parameter      | Bus Cylinder | Kickstages Cylinder | Panels         |
|----------------|--------------|---------------------|----------------|
| Mass [kg]      | 27.02        | 3709.6              | 82.865 (total) |
| Thickness [mm] | 2.083        | 11.52               | 25.9 / panel   |
| Length [m]     | 1.5          | 14.05               | -              |
| Diameter [m]   | 0.9          | 2.624               | -              |
| Material       | 2024-T36     | 2024-T36            | 2024-T36       |

**Table 4.43:** Budgets for S&M Subsystem

| Budgets   |          |
|-----------|----------|
| Mass [kg] | Cost [€] |
| 3816.34   | 13357.36 |

<sup>66</sup>URL <https://www.nasa.gov/smallsat-institute/sst-soa/thermal-control/#7.2.1> [cited 15 June 2024]

<sup>67</sup>URL [https://parkersolarprobe.jhuapl.edu/The-Mission/docs/SolarProbe\\_FS\\_WEB.pdf](https://parkersolarprobe.jhuapl.edu/The-Mission/docs/SolarProbe_FS_WEB.pdf) [cited 15 June 2024]

Finally, the design has been made in compliance with the requirements as shown in section 4.8.2.

## 4.9 On-Board Data Handling

*Contributors: Ruth*

The On-Board Data Handling (OBDH) subsystem is the brain of the spacecraft, and is responsible for the orchestration of all its operations and functionalities. It handles the data acquisition related to the scientific payload and subsystem telemetry, the commanding and health monitoring of subsystems, timekeeping, and more. This section begins by presenting an overview of the OBDH market and the systems used in past missions in Subsection 4.9.1, and the definition of OBDH subsystem requirements in Subsection 4.9.2. The OBDH houses electronics that are sensitive to the radiation environment, therefore the type of radiation and type of errors that may occur are presented in Subsection 4.9.3. This is followed by an analysis of the concept of dependability for the OBDH in Subsection 4.9.4, and Subsection 4.9.5 discussed how it can be increased with the use of redundancy. Then, the system architecture is traded off and defined in Subsection 4.9.6. This is followed by the identification of assumptions, and the sizing of the data and commands required for the OBDH and subsystem functionalities in Subsection 4.9.7. Once the required resources are defined, the hardware components are selected or designed, and mass, power, and volume budgets are computed in Subsection 4.9.8. Subsection 4.9.9 defines the software that will be used, and Subsection 4.9.10 estimates the amount and cost of software code that must be developed. Verification and validation of the design is done in Subsection 4.9.11, and the final design is summarised and presented in Subsection 4.9.12. Finally, recommendations for further stages of the design are presented in Subsection 4.9.13.

### 4.9.1. Market analysis

The OBDH system is integral to every spacecraft, and thus has a relatively large market. However, the OBDH is comprised of several individual components and functionalities that can be integrated in various different ways. Therefore, there are many different OBDH configurations, the choice of which is driven by a spacecraft mission's specific needs, constraints, and objectives. For deep space missions, the requirements for the OBDH are stringent due to the need for reliability, high level of autonomy, long lifetime, and extreme unknown external conditions. This significantly reduces the available size, requiring a decisions to be made between COTS products or mission-specific in-house components. Overall, the OBDH system is comprised of many different components, therefore the market can be segmented per component group: the on-board computer and data/command handling, the data recorder (memory), and the clock.

#### Existing market: computer system

Before designing the NIBIRU OBDH system, it is interesting to investigate the market of OBDH systems previously used for deep space missions. For deep-space missions, the on-board computer (along with data and command handling) must be failure resistant and the market options are limited. Therefore, existing systems with flight heritage are important baselines for the OBDH design.

Voyager 1 and 2 (launched in 1977) operate with computers based on three systems: the Computer Command System (CSS), Flight Data Subsystem (FDS), and Attitude and Articulation Control System (AACS). The CCS was an existing product, while the FDS and AACS were developed for these missions. The CCS is responsible for the command and memory management, and the overall health monitoring, and is programmable in-flight. All three systems had one redundant component to maintain the lifespan of the system. The CCS had a memory of approximately 70 kilo-Bytes, and the software was written using Fortran 5, but now is in Fortran 77 with some software in C. Operations of the two CSSs could be done in three modes: each CSS completes tasks independently, both CSS work on a task together, and each CSS works on the same task independently (used during payload operations near targets). The FDS is used to collect, format, and store data. It was sized based on the input and output data rates, and data was recorded on magnetic tapes. The AACS is responsible for determining the orientation of the spacecraft bus, and is a modified version of the CSS and a new technology (Hybrid Programmable Attitude Control Electronics).<sup>68</sup>

---

<sup>68</sup>URL <https://www.allaboutcircuits.com/news/voyager-mission-anniversary-computers-command-data-attitud-e-control/> [cited 15 June 2024]

The Rosetta probe (launched in 2004) has a Command and Data Management Subsystem (CDMS) with a modular structure and comprised of two Data Processor Units (DPUs), two Real Time Clocks (RTCs), two Central Interface Unit (CIU) boards, two Mass Memory boards, and a Power Distribution board. All these are connected via a common mother board. The CDMS is designed for high fault tolerance. Therefore, both DPUs run simultaneously, with the primary DPU completing the nominal tasks and the secondary DPU monitoring the functionality of the former. The DPU boards use Harris RTX2010 processors for low power consumption, radiation hardening, and space qualification.<sup>69</sup> The payload is stored in the Solid State Mass Memory (SSMM), with a total capacity of approximately 23 GigaBits and a peak data rate of approximately 1150 bps (bits per second) [82].

The New Horizons spacecraft (launched in 2006) has a Command and Data Handling (CDH) system centred around a Mongoose V processor. It processed data and commands, is responsible for the spacecraft's autonomy, health monitoring, and sequencing Earth communications. The spacecraft stores data on two Solid State Recorders (SSRs), one of which is for redundancy. Each SSR has a capacity of 8 GigaBytes. All the spacecraft electronics, including the CDH processor, data recorder, power converters, guidance and control processors, radio science and tracking electronics, are housed in an Integrated Electronics Module (IEMs). The spacecraft has a redundant IEM.<sup>70</sup>

For more recent deep space missions, the available information regarding Command and Data Handling systems reduces. This is already visible with the New Horizons mission, and poses a challenge for the design and preliminary sizing of OBDH systems.

#### **Existing market: clock**

The clock and timekeeping of a spacecraft is a very important process to ensure correct navigation and overall operations. There are several viable options for clocks. The most feasible options is determined to be the use of a deep space atomic clock, which provides high accuracy in location determination and is resistant to the radiation conditions of deep space. Crystal oscillators are widely used, but for smaller spacecraft, and are more susceptible to environmental conditions. However, there are still viable options for the NIBIRU mission. Optical clocks are a novel technology that can prove to be one of the most accurate methods of timekeeping, however the current technology readiness is not at the level that is desired.

#### **Market gaps, drivers, and trends**

As the number of deep space missions increase, so does the market need. The main requirements for OBDH systems that drive the market are long lifetimes, high levels of autonomy, low power consumption, reliability and redundancy.

Reliability and redundancy are required for all space missions, therefore the market already places a focus on the development of products that fulfill this need. On the contrary, lifetimes of 50+ years are not commonly designed for, and such missions also largely constrain the power requirements below the market standard for spacecraft sizes and complexity levels similar to that of NIBIRU.

Overall in the space industry, the trend for OBDH systems are towards miniaturization and development of easily integratable COTS products. Additionally, more focus is placed on the use of Artificial Intelligence and Machine Learning for on-board data classification and reduction, as well as error detection and prediction, and increase of autonomous operations.

It is also important to note that the OBDH systems are highly configurable. Therefore, a system that complies with the requirements of deep space missions can also be made feasible by combining COTS technologies and products that individually comply with the requirements. This reduces the development costs, but extensive testing and verification is required to ensure that the products can be integrated and form a coherent well-operating OBDH system.

#### **4.9.2. OBDH requirements**

The first step in the design of the OBDH system is the definition of requirements. These are at a subsystem level, and flow down from three different system requirements. The requirements set for the OBDH

---

<sup>69</sup>URL [http://www.sgf.hu/newsgfweb3\\_005.htm](http://www.sgf.hu/newsgfweb3_005.htm) [cited 15 June 2024]

<sup>70</sup>URL <https://www.eoportal.org/satellite-missions/new-horizons#new-horizons-mission> [cited 15 June 2024]

system are listed in Table 4.44. They are related to both the hardware and software of the subsystem. The design is driven by the capability to handle and store data, both from the payload and for the operation of the subsystems (subsystem telemetry and health monitoring data). The spacecraft must operate with a high level of autonomy, therefore requirements are also set for the handling and operating speed of the system. Finally, the OBDH has to comply with a power requirement.

**Table 4.44:** OBDH Requirements

| ID              | Requirement   |
|-----------------|---|
| PL9-SUB-OBDH-01 | The OBDH subsystem shall be able to read received commands from Earth-based stations.         |
| PL9-SUB-OBDH-02 | The OBDH subsystem shall command all subsystems by using Ada software language.               |
| PL9-SUB-OBDH-03 | The OBDH subsystem shall be able to store telemetry data of 371917 bits.                      |
| PL9-SUB-OBDH-04 | The OBDH subsystem shall handle the received data within the On-Board Computer (OBC).         |
| PL9-SUB-OBDH-05 | The OBDH subsystem shall remain in the operational temperature range of 239-344 K.            |
| PL9-SUB-OBDH-06 | The OBDH subsystem shall be able to store payload data of 1.6 GBytes.                         |
| PL9-SUB-OBDH-07 | The OBDH subsystem shall have 120 I/O channels for subsystem interactions.                    |
| PL9-SUB-OBDH-08 | The OBDH shall process and store science data from the payload with a data rate of 1306 kbps. |
| PL9-SUB-OBDH-10 | The OBDH shall operate with a handling speed of 670 KIPS.                                     |
| PL9-SUB-OBDH-13 | The OBDH shall send data to the ground station with a read out speed of 137.0 bps.            |

### 4.9.3. Effects of radiation environment

In space environments, radiation effects play a large role in the reducing the reliability and lifetime of electronic components. The information regarding the specific conditions of the environment in the outer solar system (past the Voyager missions), and their effects on electronic components, is limited. Additionally, degradation of electronic components due to radiation is aggregated by the long mission duration. Thus, it is critical to evaluate the risks related to radiation, to determine the mitigation strategies that must be taken into account during the design phase.

The three main sources of radiation in space are trapped particles in radiation belts, solar energetic particles, and cosmic rays. One type of cosmic rays present in our solar system are Galactic Cosmic Rays (GCRs). The prevalent types of radiation in the solar system can be seen in Table 4.45. During its lifetime, the NIBIRU spacecraft will cross the heliopause, after which the radiation conditions change with respect to the inner bounds of the solar system. Specifically, beyond the heliopause (approximately 123 AU from the Sun), there is an increase in Galactic Cosmic Ray (GCR) particles, and a decrease in solar wind particles. This difference was observed by the two Voyager missions, which are the only spacecraft to cross the heliopause (in 2012 and 2018).<sup>71</sup>

**Table 4.45:** Space Radiation in Orbits

| Orbit          | Radiation  |
|----------------|--|
| LEO (ISS)      | Inner radiation belt (protons) and solar particles   |
| LEO (polar)    | Inner radiation belt (protons), solar particles and GCR over the poles                     |
| MEO and GEO    | Outer radiation belt (electrons), solar particles and GCR                                  |
| Jupiter        | Jupiter radiation belts, solar particles and GCR   |
| Interplanetary | Solar particles and GCR. Trapped particles only during the passage through the belts [83]. |

<sup>71</sup>URL <https://www.britannica.com/science/heliosphere> [cited 15 June 2024]

There are two main categories of effects caused by space radiation: cumulative effects and Single Event Effects (SEEs). Cumulative effects are caused by long-term exposure to many radiation events. SEEs are caused by single energetic particles that disturb the atoms and molecules of a material. Specifically, as an energetic particle passes through a material, the phenomenon of ionization occurs when the atoms or molecules lose an electron and become positively charged. Charges caused by ionization during SEEs are diffused due to electric fields and temperatures in semiconductor materials, becoming dangerous for the functionality of electronics. The cumulative effect of ionization is measured with the Total Ionisation Dose (TID), which is the total amount of radiation energy absorbed and is measured in rad.

Disruptions of operations due to cumulative effects can be mitigated by designing with redundancy and safety factors, ensuring that the electronics components are radiation hardened, and providing structural protection against radiation. Radiation hardening can be achieved in three ways:

1. Physical radiation hardening techniques: use various insulating materials, integrated circuits, radiation tolerant components, etc.
2. Logical radiation hardening techniques: use error correcting memory and other software implementations, watchdog timers, etc.
3. Shielding: use a physical box or other structural component to protect the electronics from the environment.

Radiation hardened electronics can typically withstand TID of 100-1000 krad, while COTS can withstand only approximately 1-10 krad. Additionally, aluminium can be used as a protective shielding material.<sup>72</sup>

Mitigation strategies of SEEs can be determined by further analysing the different types of possible SEEs: soft SEEs cause errors that are recoverable, and hard SEEs cause errors that are non recoverable. More details regarding the risks, causes, mitigation and contingency strategies can be found in Table 7.1. There are two important design consideration that can be concluded from the risk analysis:

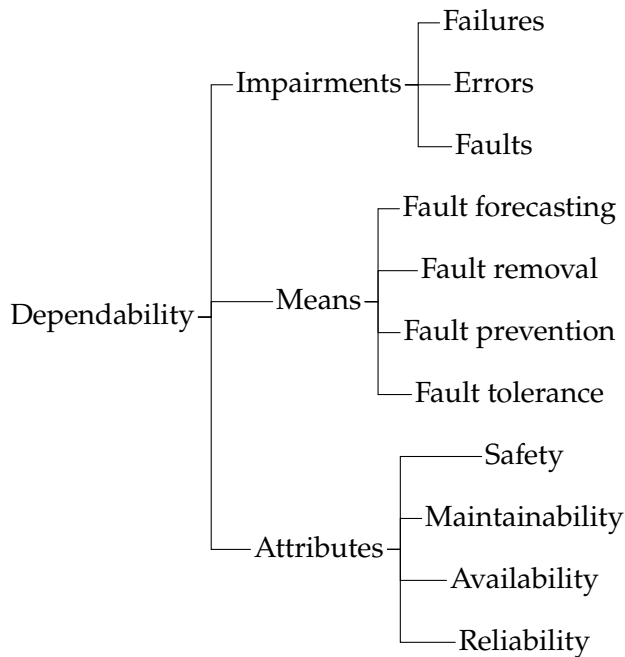
1. Recovery from soft SEEs can usually be done with a soft reboot, therefore the system must be able to recognise the SEEs and command a reboot.
2. Recovery from hard SEEs is not possible, however the catastrophic effects can be minimized by quickly removing power from the affected area/component.

#### 4.9.4. Dependability

The OBDH is one of the most risk prone subsystems, and possible malfunction can have effects on the functionality of the mission. In order to design a fail-safe OBDH, the dependability of the subsystem is analysed. According to the European Cooperation for Space Standardization, dependability is defined as the extent to which the fulfillment of a required function can be justifiably trusted. It can be dissected as

---

<sup>72</sup>URL <https://ocw.tudelft.nl/wp-content/uploads/1.0-Command-and-Data-Handling-Lecture-Notes.pdf> [cited 15 June 2024]



follows:

An analysis on the “attributes” has been conducted in the RAMS section Section 10.2. The types of “impairments” that may occur have been analysed as risks, for which mitigation strategies have been defined based on the “means”. One important point to note is the difference between reliability and fault tolerance: fault tolerance can improve the reliability of a system by keeping it functional when software or hardware faults occur, however that does not mean the system inherently has a high reliability. For example, if single errors can be tolerated but their likelihood of occurrence is high, then the reliability is still low. Therefore, in the design of the OBDH both reliability and fault tolerance must be treated as separate concepts.

#### 4.9.5. Redundancy

One of the ways in which impairments can be avoided is by designing with redundancy. Redundancy can be added in four ways:

1. Hardware redundancy: addition of extra components to detect or tolerate faults
2. Software redundancy: addition of extra software that what is required to perform a function, to detect (and possibly tolerate) faults
3. Information redundancy: addition of extra information than required to implement a function, to detect codes e.g. error detection codes
4. Time redundancy: addition of time to perform functions to allow for fault detection and fault tolerance

There are several techniques that can be used to add redundancy in these categories, which will be analysed further in the explanation of the design.

#### 4.9.6. System architecture

The OBDH subsystem is comprised of five main components, all housed within an Integrated Electronics Module (IEM). Specifically:

1. The **On-Board Computer (OBC)** is the brain of the spacecraft. It manages all the operation of the subsystems through the other OBDH components, supports Earth communications, and handles the Fault Detection Isolation and Recovery (FDIR). It is also responsible for the algorithms regarding location determination and timekeeping using the spacecraft clock. The OBC includes several sub-components:
  - The **encoder** is responsible for compiling and coding the packages of information or data that will be downlinked to Earth through the telecommunications subsystem.
  - The **decoder** is responsible for decoding and de-compiling the messages received by uplink via the telecommunications subsystem.

- The **EEPROM** (Electrically Erasable Programmable Read Only Memory) is the OBC's non-volatile memory, used to store telemetry data, computer operational data, and other.
  - The **SRAM** (Static Random Access Memory) is the OBC's volatile memory, used to temporarily store data that will be downlinked to Earth and other operational temporary data.
  - The **FPGA** (Field Programmable Gate Array) is used for the acceleration of machine learning and artificial intelligence algorithms for payload operations (e.g. dynamic targeting) and FDIR.
2. The **Data Handling and Acquisition Unit (DHAU)** is responsible for the handling of subsystem telemetry data. This includes subsystem housekeeping and health monitoring data, and managing the acquisition of payload data. This data is processed and handled in the OBC.
  3. The **Command Handling Unit (CHU)** is responsible for the commanding of the subsystems. This includes ensuring that the subsystems are operating in the correct modes, and that they provide the DHAU and OBC with regular housekeeping and health monitoring data.
  4. The **Solid State Recorder (SSR)** is where the data which will be transmitted to Earth is stored. The majority of this data is the scientific payload data, but it also includes housekeeping and health monitoring subsystem telemetry data.
  5. The **clock** is responsible for the timekeeping onboard the spacecraft. This is crucial for determination of location and attitude. The clock communicates with the OBC, and the information is then used for the respective functions.

The interaction of the subsystems with the OBDH components is defined as the architecture of the system. A centralised architecture is immediately discarded due to the complexity of the spacecraft and required amount of input and output channels. A bus architecture is commonly used in spacecraft and is scalable, and determined feasible for the NIBIRU mission. Similarly, a network architecture is the optimal option when large transmission rates are required due to complexity and increased number of subsystems and components. The positive and negative aspects of the bus and network architecture are explained further in order to perform a qualitative trade-off.

#### Bus architecture: Pros

Modular and scalable  
Standardized interface for all units and sub-systems  
Easy to integrate and test  
Easy to monitor all traffic

#### Bus architecture: Cons

Difficult to isolate faulty components that disrupt the bus communication  
Limited data rates

#### Network architecture: Pros

Modular and scalable  
Standardized interface for all units and sub-systems  
High data rates possible  
Distributed fault tolerance

#### Network architecture: Cons

Difficult to monitor all traffic  
Difficult to isolate faulty components that disrupt other communications

For this design, the factors that are most important are high fault tolerance, the desire for high data rates due to the complexity of the spacecraft and its high-level of autonomy, scalability, and ease of testing and integration. The network architecture performs better for the first two factors, and is considered to be the most optimal option for the NIBIRU spacecraft. The implementation of this architecture for the spacecraft can be seen in Figure 4.29. The router is responsible for relaying information from the subsystems to the other components of the OBDH and vice versa.

#### 4.9.7. Data and command sizing

The requirements set for the OBDH components are consequences of the resource needs of the spacecraft. These can be distinguished into needs for application software (closely related to the other subsystem designs) and the needs for operating system functions. The needs are evaluated in terms of code size, data size required, and throughput. The estimates are based on 16-bit words and a 1750A-class Instruction Set Architecture [32]. It is assumed that the data rates and sizes of housekeeping and health monitoring

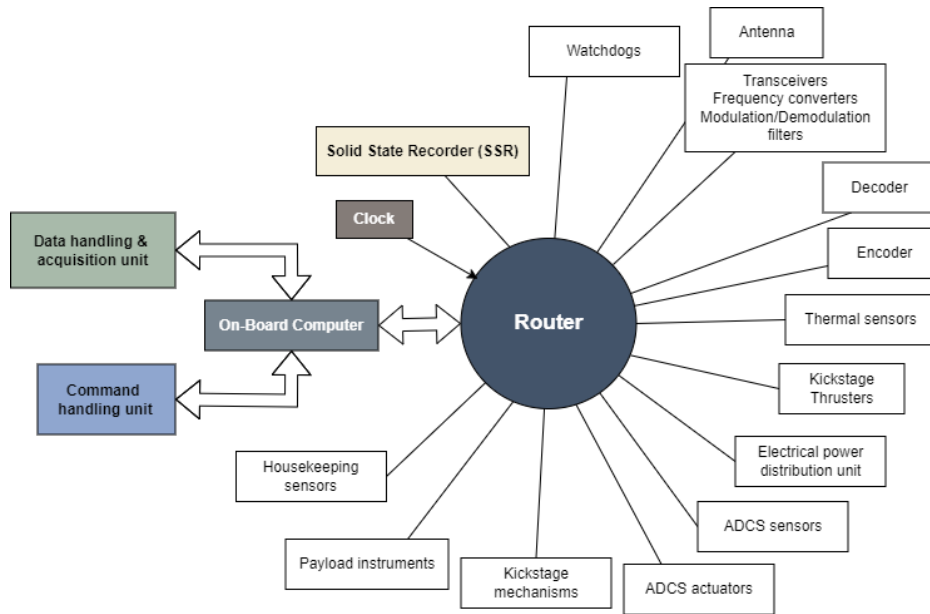


Figure 4.29: OBDH Network Architecture.

sensors are included in the estimations of application software of subsystems. Figure 4.30 and Figure 4.31 depict the percentage distribution of required resources among the different subsystems (excluding the OBDH). It can be observed that for both the code and data size the most needy subsystem is the ADCS, followed by the payload. This result is realistic and verifies the estimation methods, since very accurate pointing is required by the ADCS for telecommunications and payload operations, and the payload acquisitions will be conducted autonomously from multiple different instruments, adding complexity to the system.

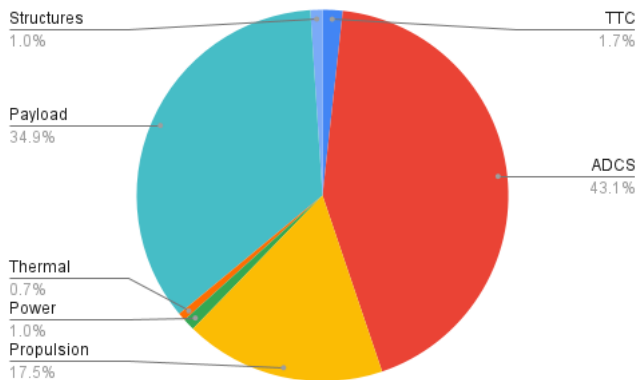


Figure 4.30: OBDH Code Distribution

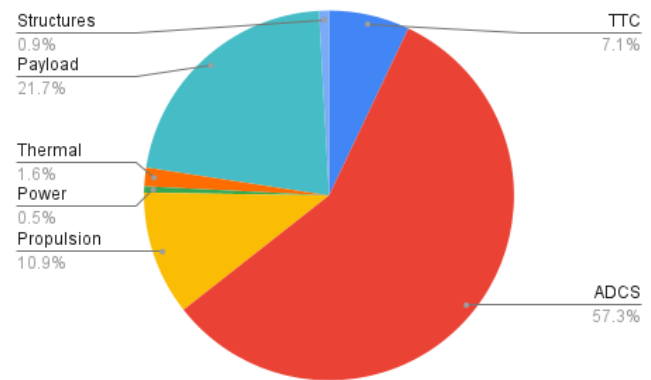


Figure 4.31: OBDH Data Distribution

Figure 4.32 shows the resources required by each subsystem and the flow of commands and data between the subsystems and OBDH system. The specific functions taken into account in the analysis, and the internal interrelations of the OBDH components in the IEM are explained further.

**Within the IEM**

The OBC requires resources for the operating system software and other additional global functionalities. These include:

- **operating system software:**

- executive
- run-time kernel
- I/O device handlers
- built-in test and diagnostics
- math utilities

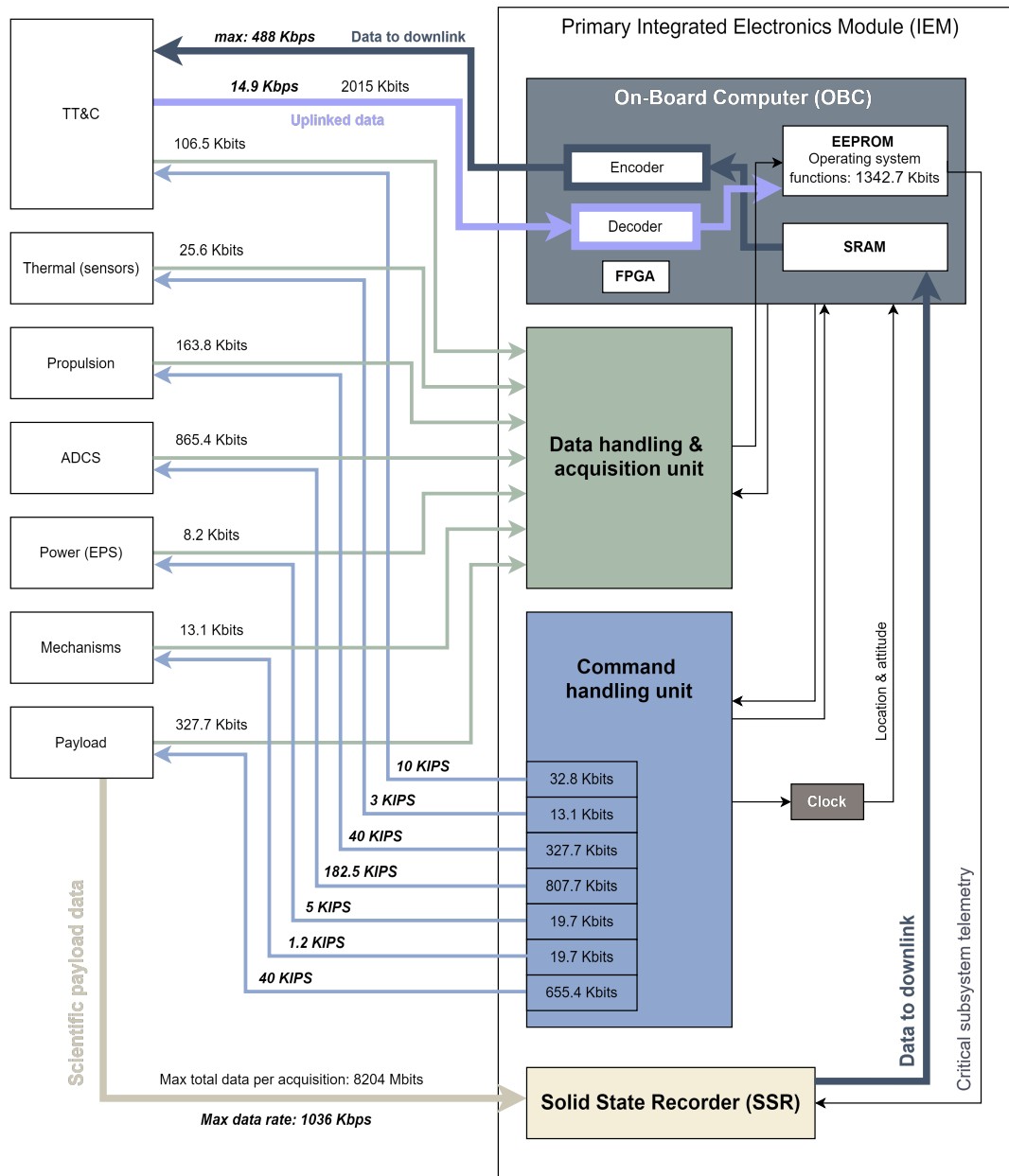


Figure 4.32: Subsystem Data Flow Diagram (DFD)

- **complex autonomy** (25% factor for autonomous payload and kickstage operation)
- **fault detection:**
  - fault monitoring
  - fault correction
- **kalman filter:** estimating the state of the spacecraft system based on past and present sensor measurements using a dynamic model
- **watchdog operation**

The resources for the above are stored in the EEPROM. The EEPROM allows for individual bytes of data to be erased and reprogrammed, which is crucial for error correction and the implementation of software updates.

The OBC is responsible for the alignment of operations between the DHAU, CHU, SSR, clock, and TT&C subsystem. Data that is received from the TT&C is directed to the decoder, after which it is processed in the EEPROM. This is so that there is no risk of losing uplinked data if the OBC loses power during its operations. The EEPROM also receives the subsystem data from the DHAU. Critical telemetry is directed to the SSR, where it can be stored for future downlink. The SRAM is used to transmit the data to be downlinked from the SSR to the encoder, which in turn directs it to the TT&C subsystem. The OBC also

directs commands to the CHU and retrieves relevant command responses. Finally, it is also assumed that the router and its operations are handled by the OBC, therefore it is not treated as an individual component.

The DHAU has to be capable of receiving the telemetry data of the subsystems (excluding scientific payload data). The data required by each subsystem is annotated on the green arrows in Figure 4.32. Similarly, the CHU must be capable of storing the code required to command the subsystems. This is noted in the blue sections of the CHU in Figure 4.32. The CHU must also be capable of operating with the processing speed required by the subsystems. This is estimated using KIPS (Kilo Instruction Per Second), and KIPS required by each subsystem are noted on the blue arrows.

Finally, the SSR receives payload scientific data from the payload and critical telemetry data from the EEPROM. It is stored until a downlink opportunity is present, when it is directed via the SRAM to the encoder.

For TT&C, the data rate of information to be downlinked to Earth is determined to be no more than 140 Kbps in the phase of primary scientific objective operations. The amount of data to downlink is not relevant since it is acquired continuously from the SSR and differs during the lifetime and operational modes of the spacecraft. The data rate of information uplinked is defined by the telecommunications subsystem. The size of data received via uplink is the maximum size of a software update. This is estimated to be equal to the total size of code and data resources for the OBC operating system software. The value is multiplied by a factor of 1.5 to account for potential data size increases and redundant code for error detection and handling. For the operation of the TT&C subsystem itself, the functions taken into account are the command processing (external commands) and telemetry processing (internal data).

In the case of thermal management, the spacecraft has 12 thermal sensors responsible for housekeeping by monitoring the temperatures near critical subsystems. The telemetry data is sampled and processed by the OBC to ensure that the temperatures are as expected, and if not, to command the power distribution unit to act accordingly.

Next, the propulsion subsystem is comprised of two kickstages, each using its own set of thrusters. The thrusters on each kickstage are controlled centrally, to reduce the amount of input and output channels required, as well as the amount of items commanded. The code and data required for each kickstage is sized by similarity, with a margin applied. Specifically, the operation of a thrusters on a kickstage can be considered to be similar to the operation of an ADCS thruster. All the thrusters on the kickstage are identical, therefore it is assumed that commanding them in a centralized manner reduces the code required per thruster by two thirds, as well as the data acquired from their operation. However, some additional complexity exists due to the need of determining when the separation and thrust occurs, therefore a margin of 30% is applied to the code required. The throughput required is estimated similarly to the code required.

Moving on to ADCS, the ADCS functionalities that require resources are related to attitude sensor processing and attitude determination and control. Specifically:

- **attitude sensor processing:**
  - 1 IMU operation: each IMU consists of 3 gyros and 3 accelerometers. The IMU is sized based on similarity with the operation of 6 gyros.
  - 2 star tracker operation
- **attitude determination and control:**
  - kinematic integration: estimation of spacecraft attitude by integrating sensed body rates
  - error determination: determination of difference between current and desired spacecraft orientation
  - precession control: maintenance of attitude control
  - ephemeris propagation: calculation of future positions and velocities of the spacecraft
  - complex ephemeris: more detailed prediction on positions and velocities of spacecraft
  - orbit propagation: predicting future position and velocity of spacecraft and its trajectory based on gravitational forces and perturbation effects
  - 18 thruster control

It is important to note that the IMUs, star trackers, and thrusters have limited operational lifetime, therefore the components used will be changed during the mission. The additional functionalities required to complete this transition are taken into account by applying a 25% margin to the amount of code required, and a 10% margin to the amount of data generated.

Power management includes monitoring the charge and discharge of batteries, the operational modes, and the control of the power distribution unit.

The mechanisms that must function are the release of two kickstages and the antenna deployment. These are simple operations, and are sized by similarity to the operation of a thruster (a single straightforward command).

There are four payload instruments in total. They are sized by similarity to kickstage operation, due to the fact that the instruments operate with the help of their own internal processors. For the code and data needs, all four instruments are taken into account. For the throughput estimate, however, only two are, since at any instance in time a maximum of two instruments are operating simultaneously.

For the payload operations the flow of scientific data is also taken into account in the sizing. The scientific data is recorded directly into the SSR. The exact amount of data and the data rate depend on the phase during the operations, thus the design is sized for the maximum values (during the primary objective operations at Planet 9).

#### 4.9.8. Hardware selection and design (incl. budgets)

Once the required resources have been defined, the components must be designed or selected from available COTS products. As mentioned previously, the availability of components that comply with the requirements of deep space missions are limited. Therefore, as a baseline, the OBDH system of the New Horizons mission is used, and it is assumed that by the time of spacecraft development and manufacturing, the OBDH system components will be able to operate for a lifetime of no less than 51 years (within the conditions of the deep space mission). This assumption is made to define that this mission is feasible with respect to the OBDH functionality. An overview of the components selected for the IEM is shown in Figure 4.33. Further details are given in this section, and the total power, mass, and volume budgets are presented.

Additionally, it is determined that a redundant IEM will be carried on-board the spacecraft. It will be non-operational, and only used in case of failure of components in the primary IEM. The IEM will be made out of aluminium, to provide shielding from radiation.

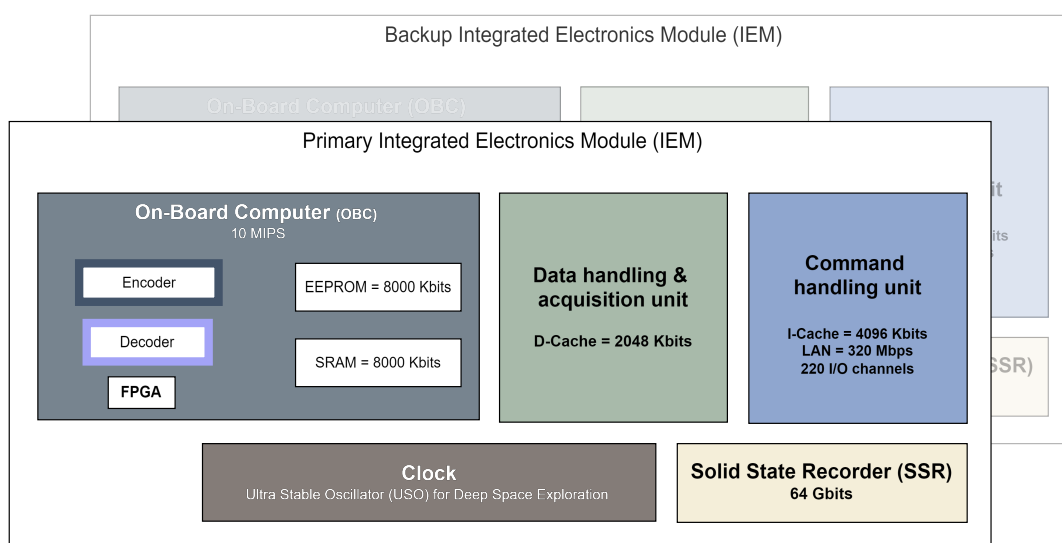


Figure 4.33: OBDH Hardware Specifications

#### OBC, DHAU, and CHU

The New Horizons mission uses an OBC, DHAU, and CHU system centered around the use of the 12 MHz Mongoose V processor. The computer used in NIBIRU is selected to be the Sandia Satellite

Computer (SSC), which uses the NASA Goddard R3000 (Mongoose 1) CPU. The SSC is radiation hardened, high-reliability, low-power component. Its integration and use in the NIBIRU OBDH system can be seen in Figure 4.33, along with the relevant specifications.<sup>73</sup>

The power usage of the component is defined using available literature, for both the payload operations and the non-payload operations. The mass and volume of the component are sized using statistical sizing equations [33]. For the sizing of the mass and volume of the DHAU the metric used is the amount of I/O channels (220), while for the CHU it is the number of items to be commanded (42). For the OBC, the metric used is the processing capacity in MIPS. It is important to note that when using the respective estimations for power consumption estimation, the resulting values were significantly larger than the known values. Thus, it is likely that the mass and volume are over-estimated. This is considered acceptable for the current design phase, but it is recommended that further investigation into the exact values is conducted.

### SSR

As mentioned in the market analysis, there is very limited information regarding available SSR components for deep space and long lifetime missions. Therefore, this component will have to be commissioned for production for the NIBIRU mission. This increases its cost, but ensures that it fulfills the requirements. A storage capacity of 8 GBytes is selected to ensure that data can be stored for all the different scientific operational phases, and to account for the event that a telecommunications opportunity is not possible for a longer time than anticipated. The mass of the SSR is sized using statistical sizing estimations using the storage capacity as a metric, while the volume and power are defined using averages of data of existing SSRs in similar missions.

### Clock

As explained in Subsection 4.9.1, there are two feasible options for clocks: the NASA Deep Space Atomic Clock (DSAC) and a crystal oscillator. The most optimal option is the DSAC, due to its precision and advanced technology. However, during the iterative process of the spacecraft design, it was determined that it is not possible to include due to its high power requirement (approximately 40 W). Therefore, a crystal oscillator clock is selected, which is designed for deep space exploration and was used by ESA's JUICE mission. Mass, volume, and power values can be determined from the product specification sheet.<sup>74</sup>

### OBDH required and available performance

With the selection of OBDH components, it is necessary to compare their specification with the required resources defined in the previous section. This comparison, and verification that the OBDH meets the required standards, is performed with respect to various criteria:

1. The total size of memory required for code of subsystems is no more than available in the I-Cache.
2. The total size of memory required for telemetry data of subsystems is no more than available in the D-Cache.
3. The total size of data required for code and telemetry of OBDH operations within the IEM is no more than available in the EEPROM.
4. The payload data rate is less than the available PDN (payload data network rate) and less than the SSR handling data rate
5. The maximum payload size is less than the SSR memory size
6. The Earth downlink and uplink rates are less than the computer handling speed (LAN)
7. The total throughput estimates are less than the available KIPS

By comparing the values of the computer specifications with the required resources, it can be seen that the design is compliant for all of these criteria. Additionally, the performance of the OBDH system is determined to be compliant with the OBDH requirements listed in Subsection 4.9.2. Therefore, this OBDH system design is feasible for the mission.

### Hardware budgets

The budgets for mass, volume, and power for the OBDH are summarized in Table 4.46. It is assumed that the weight, volume, and cost of the wiring for data and command transition is taken into account in

<sup>73</sup>URL <https://klabs.org/DEI/Processor/Mongoose/jigaona.pdf> [cited 15 June 2024]

<sup>74</sup>URL [https://www.accubeat.com/\\_files/ugd/debaa7\\_e6c1a4d0c57a45b0b27e311ff214d86a.pdf](https://www.accubeat.com/_files/ugd/debaa7_e6c1a4d0c57a45b0b27e311ff214d86a.pdf) [cited 15 June 2024]

the estimations of the wire harness in the power subsystem. Additionally, it is assumed that the FPGA does not add significant idle power and mass to the OBDH subsystem. Its power consumption during computing does not overlap with the payload operation mode of the OBDH, and does not surpass the maximum value of OBDH power consumption during payload operations.

Table 4.46: Budgets of Primary and Backup OBDH Components

| Component                                    | Mass [kg]    | Volume [m <sup>3</sup> ] | Specific Power [W] | Power for Payload Off [W] |
|--|--------------|--------------------------|--------------------|---------------------------|
| <b>Primary IEM</b>                           |              |                          |                    |                           |
| Data handling/acquisition unit: TM channels  | 11.000       | 0.0110                   | 15.80              | 1.22                      |
| Command handling unit: items to be commanded | 2.100        | 0.0021                   | incl. in above     | -                         |
| OBC + encoder + decoder: MIPS                | 7.000        | 0.0050                   | incl. in above     | -                         |
| SSR: capacity                                | 12.484       | 0.0205                   | 10.00              | 10.00                     |
| Clock  | 2.000        | 0.0017                   | 8.00               | 8.00                      |
| <b>Backup IEM</b>                            |              |                          |                    |                           |
| Data handling/acquisition unit: TM channels  | 11.000       | 0.0110                   | -                  | -                         |
| Command handling unit: items to be commanded | 2.100        | 0.0021                   | -                  | -                         |
| OBC + encoder + decoder: MIPS                | 7.000        | 0.0050                   | -                  | -                         |
| SSR: capacity                                | 12.484       | 0.0205                   | -                  | -                         |
| Clock  | 2.000        | 0.0017                   | -                  | -                         |
| <b>Total</b>                                 | <b>69.17</b> | <b>0.08</b>              | <b>33.80</b>       | <b>19.22</b>              |

The final values computed are in the same order of magnitude with values computed in the Space Mission Analysis and Design book for OBDH components [32]. The values for NIBIRU are larger, which is logical due to the lifetime requirements and size of the spacecraft.

#### 4.9.9. Software selection and design

The software language used by the selected computer is Ada. Ada is a state-of-the-art programming language for real-time and large-scale embedded software applications. Ada also allows for easy integration with C and C++, which are commonly used for space missions due to their increased speed, space heritage, and compatibility with operating systems such as Linux.<sup>75</sup>

Another important consideration related to the software operations is the selection between a synchronous or asynchronous communications framework. Synchronous communications is when the time and sequence that communications are made are defined and sequential, while asynchronous communications is when the process of sending and receiving a message are independent, and messages or commands can be processed continuously and as soon as they are received. For Earth communications, a synchronous communications framework is the best, since the latency of communications is very large, the transfer of information must be efficient and resistant to radiation. On the other hand, for internal communications in the spacecraft an asynchronous communication is chosen to allow for automation and real-time communication of the spacecraft elements.

#### 4.9.10. Source lines of code (SLOC)

For any space mission or spacecraft, code must be developed. This is an expensive activity, therefore it is valuable to perform a high-level estimate of the cost. The cost is determined by estimating the amount of code required for each functionality of the spacecraft. Additional SLOC is considered to account for the payload operations and the increased level of autonomy of the spacecraft (including the kickstages). An overview of the estimate can be seen in Figure 4.34. The total amount of SLOC is 126,600.

<sup>75</sup>URL <https://www.adacore.com/about-ada> [cited 15 June 2024]

For a cost of 150 dollars per SLOC, the total cost of the software development is 19 Million Dollars. When comparing this result to past missions, it is concluded that it is realistic and comparable. An overview of past missions and their SLOC can be seen in Figure 4.35. It can be noted that for the New Horizons mission (which is considered comparable) the total SLOC is slightly less than 115,000. The NIBIRU mission has more complexity in terms of operation and design, therefore it is logical that the SLOC is increased.

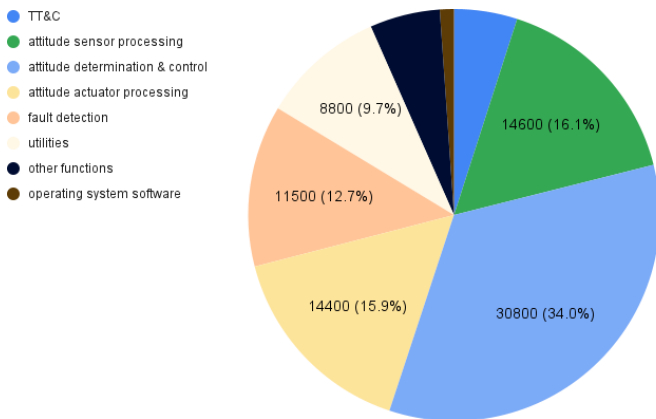


Figure 4.34: Estimates of Source Line of Code

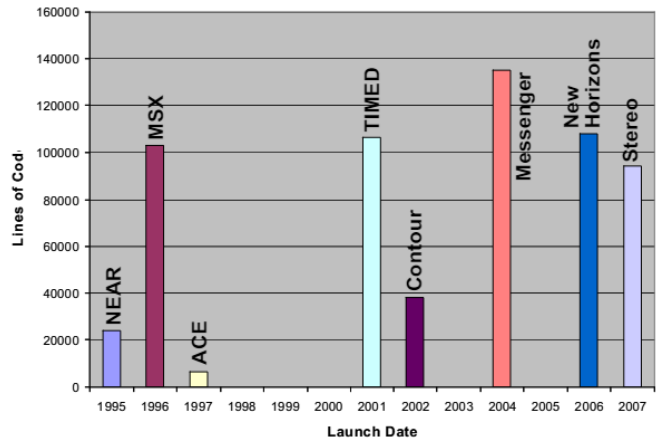


Figure 4.35: SLOC for Past Missions [84]

#### 4.9.11. Verification and validation

The sizing and design of the OBDH system is completed by determining the requirements and resources that the spacecraft requires, and selecting components (radiation hardened) that are able to fulfil those needs. This is a logic based design process, however it is still necessary to verify and validate the design with respect to the logic and methods used, as well as the outcomes.

First off, verification of the calculation and methods used was conducted by carefully examining the interrelations of the values and the calculations performed. Most equations used are simple and don't require complicated models, therefore the verification was also simple.

It is important to note that the sizing estimations (for both data and mass/power) are based on general statistical equations that are derived from missions that are quite different from what our spacecraft aims to achieve. To account for discrepancies that may have occurred because of this, the estimations conducted always used the worst case values, in addition to several margins that were applied to the data requirements. However, there is a risk that this may also lead to overestimation of the needs for the OBDH system. It is observed that for the majority of criteria for which the chosen computer and required resources were compared, the difference between required and available values was not significant. During the iterative process, specifically, when adding components and increasing the complexity of the spacecraft, the amount of memory required by the DHAU was a critical parameter and is on the verge of rendering the OBDH system unfeasible. This computer was used aboard the New Horizons mission, therefore is considered to be of representative specifications, and this serves as a validation of the estimation methods.

For additional validation of the design, the relation of the mass and power, with the processing speed (KIPS) and memory of the final OBDH was compared with those of existing OBDH's in past missions. It was observed that the OBDH of NIBIRU was within similar orders of magnitude with past missions, however its performance is higher than most of the other missions. This is logical, since this mission is pushing the limits of what spacecraft technology can achieve.

#### 4.9.12. Final design

The final design of the OBDH is presented in terms of hardware, software, and data. The OBDH controls the spacecraft with a network architecture, using a router to gather all information on the OBC.

The hardware components of the OBDH can be seen in Figure 4.33. The OBC has a Mongoose radiation hardened CPU with flight heritage and high reliability. The encoder and decoder are responsible for

communication with the telecommunication subsystem. The EEPROM is responsible for storing the functionalities of the OBDH system itself, and the SRAM is used for temporary storage of telemetry and scientific data. An FPGA is integrated into the OBC to provide accelerated processing of AI and machine learning operations. The DHAU and CHU are responsible for the subsystem interactions. The clock is a deep space, radiation hardened clock with heritage on the JUICE mission. The scientific data and telemetry data is stored on the SSR, which has a significant amount of extra space for storage of telemetry in case a telecommunications opportunity is delayed. All the electrical components are housed in an IEM made out of aluminium for radiation protection, and a redundant IEM is taken on the spacecraft (idle) for redundancy.

The computer system (OBC, DHAU, and CHU) and the clock are COTS products and account for most of the hardware cost of the subsystem. Specifically, the computer system amounts to a cost of 35,600 euros,<sup>76</sup> and the clock to 200,000 euros.<sup>77</sup> Each of these components is purchased twice, for redundancy.

The software language used is Ada, which is integratable with C and C++. Commanding of the subsystems is done through the CHU, which also houses the code required for the operations. The required amount of software can be estimated using Source Lines of Code (SLOC) estimations. The total amount of SLOC required is 126,600. For a cost of 150 Dollars per SLOC, this amounts to a total cost of 19 Million Dollars.

The data acquired from the payload differs per operational phase. The maximum amount of data acquired is during the primary scientific operations. All the data will be acquired and stored in the SSR before it can be downlinked to Earth. Subsystem telemetry data is acquired through the DHAU. Critical data is stored in the SSR via the EEPROM.

The final design of the OBDH is as follows. The mass is 69.2 kg, cost is €17,329,600, and the power is either 19.2 W or 33.8 W for payload off or on respectively.

### General considerations

Some general considerations are taken into account in the design of the OBDH related to the radiation environment and the dependability of the spacecraft. Radiation hardened components are selected, and logical radiation hardening is applied to software and data (addition of error correcting codes). The risks of the OBDH due to radiation are considered in the respective chapter. The dependability of the OBDH must be evaluated in terms of impairments that may occur, the means of prevention, and relevant attributes. These are specifically taken into account in the risk analysis of the OBDH. The design is in compliance with the requirements as they are set out in section 4.9.2.

#### 4.9.13. Recommendations

The OBDH is critical for the operation of the spacecraft, and this design is pushing the boundaries of what is feasible in terms of lifetime and radiation degradation. Therefore, it is valuable to present recommendations of analysis that can help improve the confidence in the operation of the OBDH system, and aid in providing more precise and accurate estimations of mass, power, and data requirements.

1. An initial estimation of the space environment in the areas the spacecraft with traverse is conducted, however it lacks detail and accuracy for the outer regions of the solar system. There are available tools developed for modeling of the radiation environment and the calculation of the Total Ionizing Dose that the spacecraft will have to resist, but the integration of a 9th Planet and NIBIRU's exact trajectory was not possible within the timeframe of this design phase. However, it can provide valuable insights into the type of hardware and software that is optimal for the design, and any further risk mitigation strategies that are required.
2. Currently the baseline for the designing of the OBDH was the computer system used for New Horizons. However, it is valuable to compare and trade-off more OBDH configurations, OBCs, or CPUs. This requires an advance market analysis to determine what components are available for long deep space missions, and whether their TRL is high.

<sup>76</sup>URL <https://cpushack.com/space-craft-cpu.html> [cited 15 June 2024]

<sup>77</sup>URL [https://www.accubeat.com/\\_files/ugd/debaa7\\_e6c1a4d0c57a45b0b27e311ff214d86a.pdf](https://www.accubeat.com/_files/ugd/debaa7_e6c1a4d0c57a45b0b27e311ff214d86a.pdf) [cited 15 June 2024]

3. Apart from the inclusion of redundant hardware components, more hardware redundancy techniques can be applied. Passive techniques use fault masking and rely on voting mechanisms, while active techniques achieve fault tolerance by detecting/locating the fault and performing a contingency action. At this level in the design it is assumed that such techniques will be implemented, but detailed analysis has not yet been completed.
4. Additional redundancy techniques can also be defined for information redundancy and time redundancy, such as the definition of error detection codes for the software and data of the spacecraft.
5. The compression method and communication protocol used for the spacecraft operations has not been defined at this stage in the design. However, determining what will be used can help make the estimations of data and code size, as well as throughput and communications data flow, more accurate.

## 5 System Integration

By system integration, the coming together of the system as a whole is described. In this chapter, the integration of all subsystems is addressed. This starts with a CAD model of the whole spacecraft in section 5.1. Then, the compliance with the requirements stated in chapter 3 is given in a matrix in section 5.2. Next, the relevant technical diagrams are given in section 5.3. Finally the total mass and power budget of NIBIRU is given in section 5.4.

### 5.1 Final CAD Model

*Contributors: Iván*

In this section, the final CAD model will be presented. The different parts for every subsystem have been designed and assembled on 3DEXPERIENCE, a CAD software tool that integrates multiple applications and tools for design, simulation, manufacturing, data management, collaboration and innovation.<sup>1</sup>

A render of the NIBIRU spacecraft bus and the Kickstages, as well as of only the NIBIRU spacecraft bus is presented in figures 5.1 and 5.2. Additionally, the technical drawings for the spacecraft bus and the kickstages can be found in section 10.3.6 at the end of the document.



Figure 5.1: NIBIRU Spacecraft Bus and Kickstages

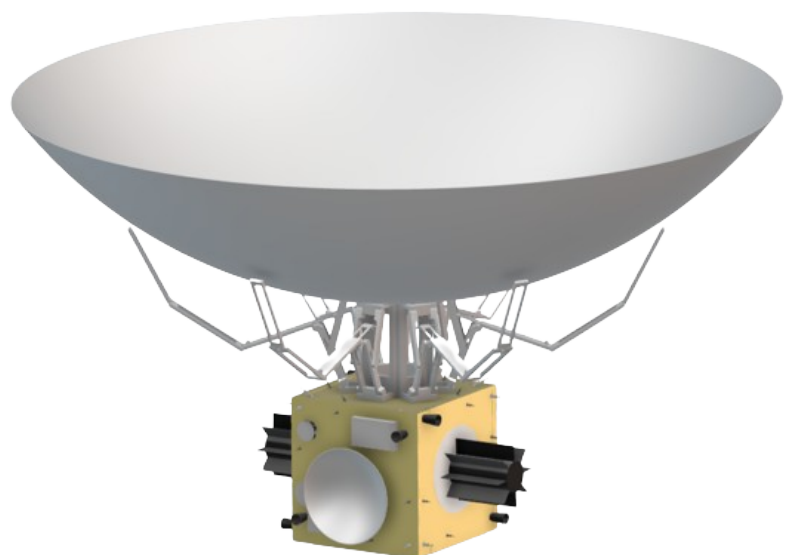


Figure 5.2: NIBIRU Spacecraft Bus

<sup>1</sup>URL <https://www.3ds.com/3dexperience/design?wockw=design> [cited 15 June 2024]

## 5.2 Compliance Matrix

*Contributors: Thijmen, Anton, Pepijn*

To ensure all requirements set up for NIBIRU and the mission, like stated in chapter 3 are complied with, a compliance matrix can be build. This is a matrix that includes all requirements and the compliance of it. Requirements can:

- Compliant: The requirement is met by the final design of NIBIRU.
- Not compliant: The requirement is not met by the final design of NIBIRU.
- Uncertain: If it is not certain that the requirement is met by the design.
- Not applicable: If the requirement is not applicable to the final design.

Next to this, there is also a column with the verification method in it, there are 4 verification methods for verifying a requirement:

- Analysis: Computational or analytical proof.
- Test: Empirical testing or experimental validation.
- Inspection: Visual or physical examination.
- Review: Functional demonstration or simulation.

For the requirements, a program called Valispace was used. This is a model-based system engineering program, which helped centralise values and requirements, as talked about in section 3.3. The compliance matrix for mission requirements can be viewed in table 5.1.

**Table 5.1:** Mission Requirement Compliance Matrix

| ID             | Requirement  | Verification Method     | Component               | Compliance |
|----------------|--|-------------------------|-------------------------|------------|
| PL9-MIS-TP-1.1 | NIBIRU shall incorporate an imaging system   | Inspection              | Imager                  | Compliant  |
| PL9-MIS-TP-1.2 | The payload subsystem camera shall have a per pixel angular resolution better than 9.25 [microrad] | Analysis/<br>Test       | Imager                  | Compliant  |
| PL9-MIS-TP-1.3 | NIBIRU shall be able to point its imaging system towards Planet 9                                  | Analysis                | ADCS                    | Compliant  |
| PL9-MIS-TP-1.5 | NIBIRU shall be able to establish a stable communication link with Earth at a distance of 550 AU   | Analysis                | Antenna                 | Compliant  |
| PL9-MIS-TP-2.1 | NIBIRU shall carry instruments capable of determining the mass of Planet 9 with 5% accuracy        | Inspection/<br>Analysis | Payload                 | Compliant  |
| PL9-MIS-TP-2.2 | NIBIRU shall carry instruments capable of determining the radius of Planet 9 with 5% accuracy      | Inspection/<br>Analysis | Payload                 | Compliant  |
| PL9-MIS-TP-3.1 | All subsystems on NIBIRU shall have a lifetime of at least 50 years                                | Analysis                | Spacecraft              | Compliant  |
| PL9-MIS-TP-3.2 | The subsystems of NIBIRU shall withstand the radiation environment during the entire trajectory    | Analysis                | Structures & Mechanisms | Compliant  |
| PL9-MIS-TP-3.4 | NIBIRU shall be in range to take a picture of Planet 9   | Analysis                | Trajectory              | Compliant  |
| PL9-MIS-TP-4.3 | NIBIRU shall withstand the critical vibrational loads experienced during launch                    | Analysis/<br>Test       | Structures & Mechanisms | Compliant  |
| PL9-MIS-TP-4.4 | NIBIRU shall be able to withstand impacts from space debris  | Analysis                | Structures & Mechanisms | Compliant  |
| PL9-MIS-TP-4.5 | NIBIRU shall not fly closer than 0.04 AU from the Sun  | Analysis                | Trajectory              | Compliant  |
| PL9-MIS-TP-5.1 | NIBIRU shall have a communication system   | Inspection              | TT&C                    | Compliant  |
| PL9-MIS-TP-5.2 | NIBIRU shall be capable of orienting its antenna towards Earth                                     | Analysis                | ADCS                    | Compliant  |
| PL9-MIS-SC-1.1 | NIBIRU shall carry instruments capable of estimating the mass of Planet 9                          | Inspection/<br>Analysis | Payload                 | Compliant  |

Continued on next page

Table 5.1 continued from previous page

| ID             | Requirement  | Verification Method | Component               | Compliance    |
|----------------|--|---------------------|-------------------------|---------------|
| PL9-MIS-SC-1.2 | NIBIRU shall carry instruments capable of estimating the radius of Planet 9  | Inspection/Analysis | Payload                 | Compliant     |
| PL9-MIS-SC-2.1 | NIBIRU shall carry instruments capable of imaging Planet 9   | Inspection/Analysis | Imager                  | Compliant     |
| PL9-MIS-SC-3.1 | NIBURU shall carry instruments capable of analysing the surface features of Planet 9   | Inspection/Analysis | Spectrometer            | Compliant     |
| PL9-MIS-SC-3.2 | NIBURU shall carry instruments capable of analysing the atmospheric features of Planet 9   | Inspection/Analysis | Spectrometer            | Compliant     |
| PL9-MIS-SC-4.1 | NIBIRU shall carry instruments capable of analysing the presence of moons around Planet 9  | Inspection/Analysis | Imager                  | Compliant     |
| PL9-MIS-SC-4.2 | NIBIRU shall carry instruments to investigate the presence of rings around Planet 9  | Inspection/Analysis | Imager                  | Compliant     |
| PL9-MIS-SC-5.1 | NIBIRU should carry instruments to analyse the atmospheric composition of Planet 9   | Inspection/Analysis | Spectrometer            | Compliant     |
| PL9-MIS-SC-6.1 | NIBIRU should carry instruments to determine the oxygen isotope ratios of Planet 9   | Inspection/Analysis | Spectrometer            | Compliant     |
| PL9-MIS-SC-7.1 | NIBIRU should carry instruments to investigate potential biosignatures of Planet 9   | Inspection/Analysis | Payload                 | Compliant     |
| PL9-MIS-CN-1.1 | The total mission cost shall not exceed €M1500 (FY2024), excluding launch cost   | Inspection          | Total sc                | Non-compliant |
| PL9-MIS-CN-2.1 | A launcher that is completely operational by 2034 shall be used  | Inspection          | Launcher                | Compliant     |
| PL9-MIS-CN-2.2 | The development, testing, and integration phases of NIBIRU shall be completed by 2034  | Inspection          | Total sc                | Non-compliant |
| PL9-MIS-CN-2.3 | The mission shall make use of existing ground element(s)   | Inspection          | TT&C                    | Compliant     |
| PL9-MIS-CN-4.2 | NIBIRU shall not damage the launcher under the loads specified in the launch vehicle catalogue                                   | Analysis            | Structures & Mechanisms | Compliant     |
| PL9-MIS-CN-4.3 | NIBIRU shall fit within the launcher used  | Analysis/Test       | Total sc                | Compliant     |
| PL9-MIS-CN-5.1 | The production plan shall be distributed to each manufacturing company that will work on NIBIRU                                  | Inspection          | Total sc                | Compliant     |
| PL9-MIS-CN-5.2 | The mission shall adhere to quality assurance protocols during production and assembly   | Inspection          | Total sc                | Compliant     |
| PL9-MIS-CN-5.3 | The mission shall make use of existing production processes  | Inspection          | Total sc                | Compliant     |
| PL9-MIS-CN-5.4 | The mission shall make use of existing assembly processes  | Inspection          | Total sc                | Compliant     |
| PL9-MIS-CN-5.5 | Lean Manufacturing principles shall be implemented throughout the manufacturing process  | Inspection          | Total sc                | Compliant     |
| PL9-MIS-CN-6.2 | The mission shall include a compliance verification process for all materials used   | Inspection          | Total sc                | Compliant     |
| PL9-MIS-CN-6.3 | The mission shall have a monitoring system in place capable of detecting and managing any inadvertent use of toxic materials     | Inspection/Analysis | Total sc                | Compliant     |
| PL9-MIS-CN-6.4 | The mission shall implement a sustainable End-of-Life disposal strategy, aligning with regulations and feasibility               | Analysis            | Total sc                | Compliant     |
| PL9-MIS-CN-6.5 | The mission shall develop an emergency response strategy for radioactive material mishaps during the production phase and launch | Inspection          | Total sc                | Compliant     |

NIBIRU does not comply with the requirements PL9-MIS-CN-1.1 and PL9-MIS-CN-2.2. The former is about the cost of 1500 million euros, as will be explained in section 8.2 the cost of the mission will be over budget. However, this is due to the addition of the secondary objectives as the mission will be within budget if only the primary objective is performed. After a discussion with the client, it was determined

that having a more costly mission in exchange for all the valuable data from the secondary objectives is worthwhile. The latter refers to being done with the development, testing and integration before 2034. Section 10.1 shows that it will take 12 years for the final development, manufacturing and testing and 1 year for integration and performing the final checks. This means that the mission will be ready before the launch in 2038 with 1 year in to spare. The difference between 2034 in the requirement and the launch in 2038 comes from the fact that the trajectory does not line up well for a launch in 2034. Again in collaboration with the client, it has been decided that it is more important to get there quicker even though the launch is 4 years later, compared to launching 4 years earlier and arriving at Planet 9 later.

### 5.3 Technical Diagrams

*Contributors: Ruth, Pepijn*

To have a good overview of all of the components from the subsystem and how they are connected a number of diagrams have been created. The electrical diagram shows how all of the components receive their power from the EPS and can be seen in figure 5.3. The power lines are indicated with the arrows and they include the voltage level of the connections as well. The power generation and storage is done on 33 V, after which the PCDU distributes the power on either a 5, 25, or 28 V power line. The PCDU will be able to do this with the different voltage levels with ease.

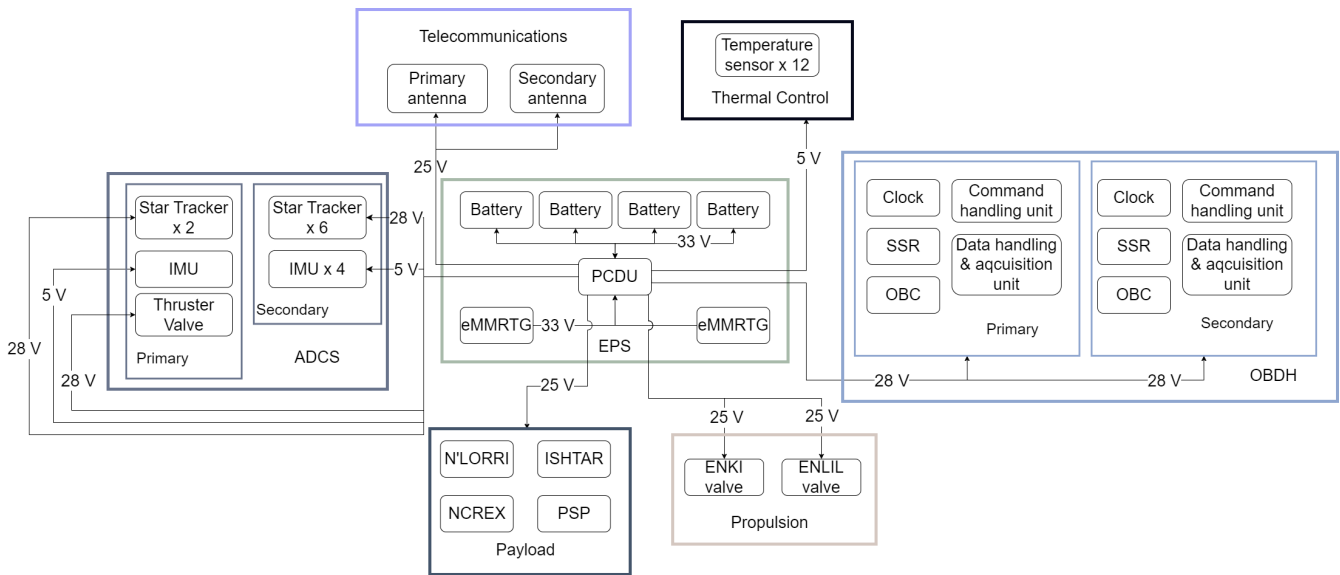


Figure 5.3: Electrical Diagram

It is also valuable to define the software sequences of unique or critical operations of the spacecraft. One such operation is the dynamic targeting of the payload during the primary scientific objectives. This operation is complex and determines the amount and quality of data acquired, therefore it is critical that it is correctly defined. The software sequence can be seen in the diagram in Figure 10.3.6. The data inputted and outputted from the various operations is depicted in the ovals. The functionalities of the OBDH and FPGA are also defined at each step, and decisions made are indicated in the triangles. The sequence of operations is defined from the initiation of a single dynamic targeting acquisition until its termination with the acquisition of a fault-free spectral acquisition.

Additionally, the operation of the watchdog is critical for the housekeeping and health monitoring of the spacecraft. An example of its operation has been defined in the software diagram in figure 10.3.6 at the end of the document.

### 5.4 Budget Breakdowns

*Contributors: Anton, Iván*

The total mass and power of NIBIRU have been calculated to finalise the system integration. The spacecraft NIBIRU itself has a mass of 2400.142 kg. The kickstage ENKI (bottom) has a mass of 18 575.029 kg, and the kickstage ENLIL (top), including the radiation shielding tiles, has a mass of 19 673.079 kg. This results in a total mass of 40 648.250 kg, including the spacecraft bus mass. Considering the requirement of staying under 100 tons for the launcher, the total mass of this mission is feasible.

The generated power is distributed to all subsystems, each requiring a constant amount of power except for the TT&C subsystem. All excess power is allocated to the TT&C to ensure stable communications while maintaining the functionality of other subsystems, this can be seen in table 4.6. This power allocation is feasible as the strategy of using batteries to achieve peak power when RTGs are used is normal. Furthermore, safety margins have been included which would make it theoretically possible to operate the satellite with only the available power. However, without using the batteries not all 170 images can be transmitted within a year. But having these types of MOO is normal in spacecraft. Finally, the total cost of the components per subsystem equals to 367.3 million Euros, however, this still excludes the cost of the rest of the mission, and this will be explained further in section 8.2.

## 6 Sensitivity Analysis

Given the high complexity and various intricacies and uncertainties of the NIBIRU mission, conducting a sensitivity analysis on several critical mission parameters is essential to determine how sensitive the design is to variations in these parameters. This section will focus on the sensitivity analysis of four key design parameters: spacecraft mass, required  $\Delta V$ , spacecraft power, and mission cost. The consequences of Planet 9 being in a different location than that assumed are also discussed in the final section of this chapter.

### 6.1 Spacecraft Mass

*Contributors: Dhafin*

The total spacecraft mass is dependent on various parameters, such as the masses of individual subsystems. However, performing sensitivity analysis on each of these parameters is impractical. Rather, it is best to first identify where the majority of the spacecraft mass originates from. After assessing the mass budgets of each subsystem, it is clear that the propulsion subsystem makes up a large portion of the spacecraft mass. Therefore, the parameters that will be assessed are the ones that influence the propulsion subsystem mass. In the method of the sizing of the propulsion subsystem, four parameters are taken as input: the spacecraft dry bus mass, the required  $\Delta V$  of each stage, the number of stages and finally the propellant and pressuriser properties. It is within reason that the parameter that will inhibit the most uncertainty is the required  $\Delta V$  of each stage. This is because the  $\Delta V$  was obtained from the trajectory simulation which in itself is a very complex model. Executing the exact trajectory as the one presented by the simulation will be a near impossible task. Presented with such uncertainties, it is likely that the actual required  $\Delta V$  will vary to the one calculated by the simulation. In contrast, the remaining parameters are simply design choices; for example, the number of stages is decided by the number of planetary flybys that the spacecraft will perform and the propellant and pressuriser properties have been selected from further analysis regarding suitable propellant types for this mission. Therefore, the sensitivity analysis of the spacecraft mass will be performed by varying the required  $\Delta V$  for each stage. The goal of this analysis is to assess the degree to which the spacecraft mass changes due to increasing  $\Delta V$ . Additionally, the analysis will dive deeper into the specific components of the spacecraft mass that drive significant changes in the total spacecraft mass.

The sensitivity analysis begins by progressively increasing the  $\Delta V$  values from their initial estimates. The resulting graph is shown below.

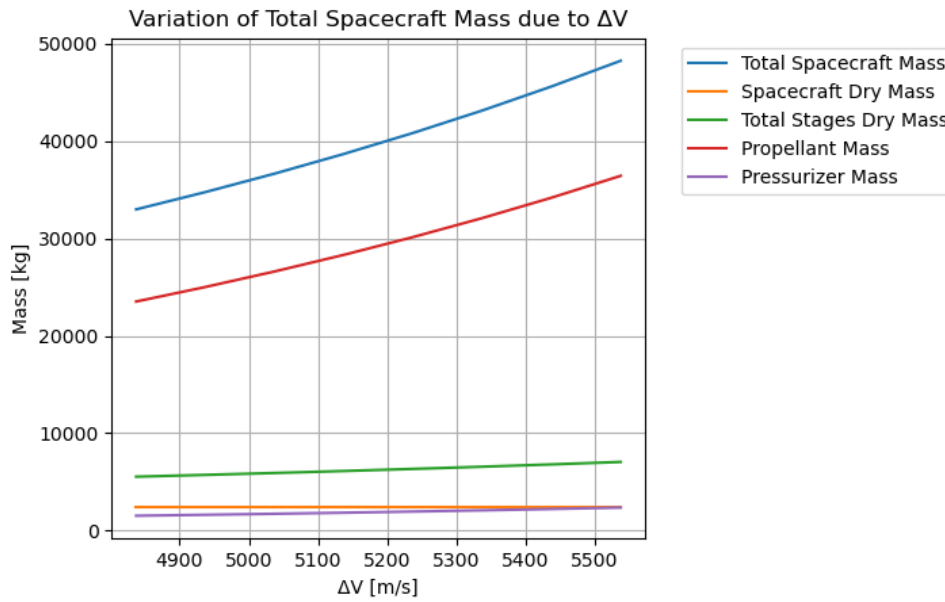


Figure 6.1: Variation of Total Spacecraft Mass due to Increasing  $\Delta V$

As can be seen in Figure 6.1, an increasing  $\Delta V$  substantially increases the total spacecraft mass. To further identify what component of the total spacecraft mass is driven significantly by the required  $\Delta V$ , Figure 6.1 can be further analysed with regards to the total spacecraft mass breakdown. Figure 6.1 suggests that while propellant mass constitutes the largest portion of the total spacecraft mass, it is also the component most sensitive to changes in  $\Delta V$ . In contrast, the total stages dry mass and pressurizer mass do not increase nearly as significantly. It is clear that the relationship between the  $\Delta V$  and total spacecraft mass is non-linear. This is due to the fact that the spacecraft mass ratio (between its initial wet mass and the dry mass after which the  $\Delta V$  is performed) exponentially grows with  $\Delta V$ , as implied by the rocket equation in Equation (4.54). This sensitivity analysis indicates that the total spacecraft mass is highly sensitive to even slight changes in  $\Delta V$ , primarily due to the significant impact on propellant mass.

## 6.2 $\Delta V$

*Contributors: Dhafin*

As mentioned in the previous section, the spacecraft mass is sensitive to the required  $\Delta V$ , therefore it is crucial to perform a sensitivity analysis on the required  $\Delta V$ . Upon performing the trajectory optimisation, it was clear that the required  $\Delta V$  was quite sensitive to the distance of the closest approach to the Sun. This can be explained by the explanation of the Oberth maneuver in Section 4.5, where a higher incoming velocity will be more effective in gaining kinetic energy after the burn.

In reality, it is very unlikely that the trajectory that the spacecraft will follow is going to be the same as the one executed by the trajectory simulation. Therefore, it is useful to analyse how much the required  $\Delta V$  changes as the spacecraft varies its distance of the closest approach to the Sun, while keeping every other simulation parameter constant. Note that only distances larger than 10 SR is considered, this is because the heat shield is designed for this distance. The results are visualised in Figure 6.2:

As displayed in Figure 6.2, it is clear that the required total  $\Delta V$  substantially increases with increasing Solar Oberth Maneuver distances. Upon performing the analysis, the spacecraft can have an offset of  $1.496 \times 10^6$  km, with the extra  $\Delta V$  that the propulsion system is capable of providing. This might seem large in an absolute sense, however in the massive scale of outer space, this distance is relatively small. To assess whether the degree of accuracy to which the spacecraft will be able to follow, with respect to the planned trajectory designed by the simulation, further analysis should be conducted.

## 6.3 Spacecraft Power

*Contributors: Ruth*

The power available for the operation of subsystems is one of the most driving parameters for the design. Additionally, it influences the latency and capacity of communication with ground, including the amount

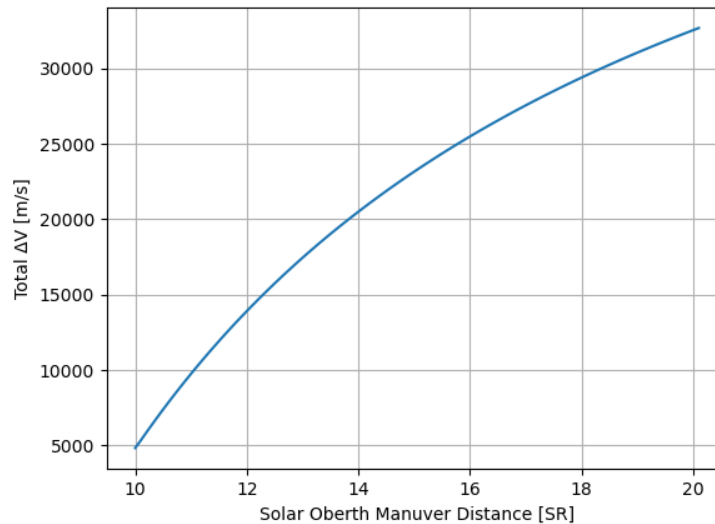


**Figure 6.2:** The Variation of Required Total  $\Delta V$  with Increasing Distances for the Sun Oberth Maneuver

of time needed to transmit scientific data. For the majority of operation modes of the spacecraft, the power that is not used by the subsystems is allocated to Earth communications, therefore small increases in power consumption of components do not render the design unfeasible, but only less efficient. However, for the SAFE mode this is not the case, making it the critical operational mode with respect to power.

When analysing the power budget, it can be seen that the subsystems that consume the most power are the OBDH and ADCS. These subsystems are also the ones that operate most constantly, therefore it is useful to analyse the sensitivity of the power budget with respect to their power consumption.

### 6.3.1. OBDH

The power draw of the OBDH is distributed among three groups of components: the computer (including the DHAU, CHU, and OBC), the SSR and the clock. The power consumption of the computer and clock are defined by the specifications of the components, and are not expected to change significantly. This is due to the fact that even if the complexity of the spacecraft or its mass increase, or if parameters such as the trajectory change, the same computer and clock can be used. Very significant changes would have to occur to lead to different selections. On the other hand, the SSR is sized based on statistical estimations, and it is susceptible to change. It is important to note that the power consumption of the three groups are in the same order of magnitude.

The percentage of change in the total OBDH power consumption relative to a percentage change in the SSR power consumption is plotted in Figure 6.3. It is seen that the design is more sensitive for the phase when the payload is off, however for both cases a change of SSR power consumption of 10% (which is significant) leads to a change of OBDH power of approximately 5%, which is not an extreme value.

In Figure 6.4 and Figure 6.5 the change in SSR power consumption and the change in OBDH power consumption respectively are plotted against the total available power to determine when the mission would become unfeasible. The available power at end of life assumes a lifetime of 51 years, for the SAFE mode. It can be seen that the design becomes unfeasible at 51 years for a change of SSR power consumption of more than 5%. Similarly, for a change in total OBDH power unfeasibility is reached when this change is more than only approximately 2%. Therefore, the mission feasibility in terms of power is sensitive to the power change of the OBDH components, which is a logical conclusion based on the fact that power is one of the most driving constraints of the design.

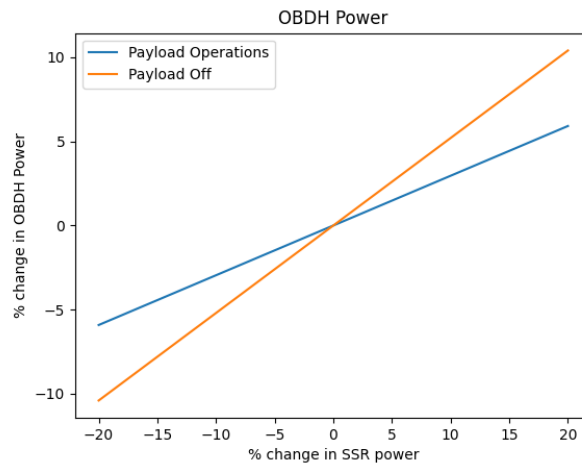


Figure 6.3: Change in OBDH Power vs. Change in SSR Power

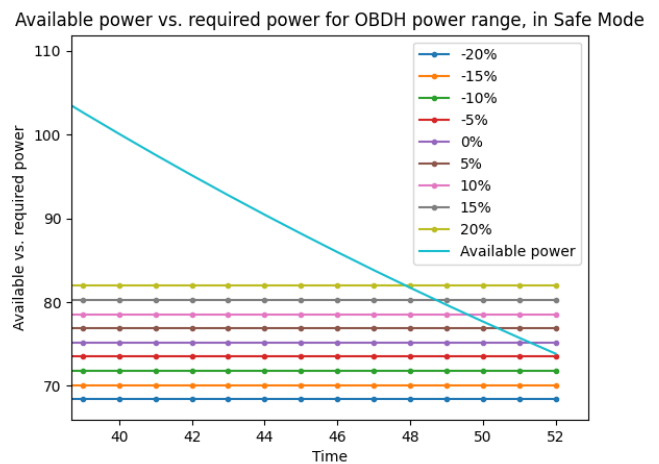
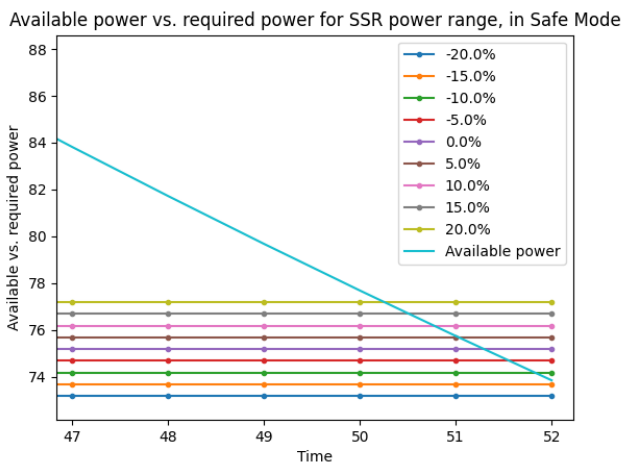


Figure 6.4: Available Power vs. Required Power for SSR, in Safe Mode

Figure 6.5: Available power vs. required power for OBDH, in Safe Mode

### 6.3.2. ADCS

The ADCS uses the largest partition of power of any subsystem. Within the ADCS, the most power is consumed by the sensors (more than three times as much as the actuators). The power of the thrusters is based on the assumption that the power needed to open a valve is independent of the number of thrusters, however even if this assumption is not completely correct the difference between the power consumption of sensors and actuators is still significant. Therefore, possible increase of ADCS power due to the thrusters is taken into account when evaluating the change of the total ADCS power with respect to the available power. Another important consideration is that the ADCS consumes different power in its nominal operations and its peak operations.

For the change of ADCS power with respect to change in sensor power, both the peak and nominal performance is evaluated. The percentage of change in the total ADCS power consumption relative to a percentage change in the sensor power consumption is plotted in Figure 6.6. It is seen that the design is very slightly more sensitive in the case of the peak performance, and that an increase of 10% sensor power consumption leads to an increase of approximately 7.5% of total ADCS power. This is more than the case for OBDH, due to the larger difference between sensor and actuator power consumption. Since the difference between the peak and nominal performance is minimal, the further analysis is conducted only for the peak performance (worst case scenario).

In Figure 6.7 and Figure 6.8 the change in sensor power consumption and the change in ADCS power consumption respectively are plotted against the total available power to determine when the mission

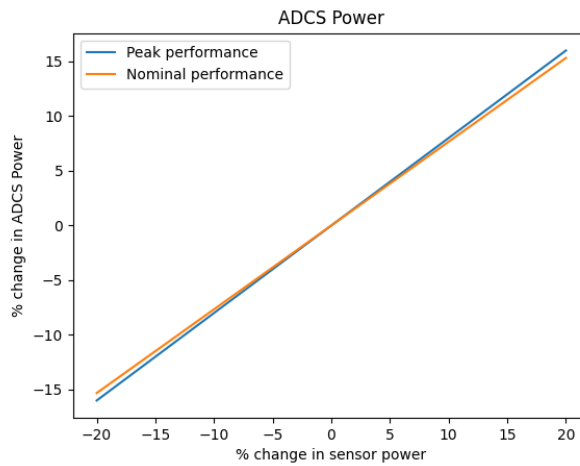


Figure 6.6: Change in ADCS Power vs. Change in Sensor Power

would become unfeasible. Similarly to the OBDH analysis, the lifetime is set to 51 years. It can be seen that the design becomes unfeasible at 51 years for a change of sensor power consumption of more than 1-2%. Similarly, a change of total ADCS power consumption of 1-2% also renders the design unfeasible. Therefore, the design can be concluded to be very sensitive to change in ADCS power consumption. This is a logical conclusion since the ADCS is the most power heavy subsystem.

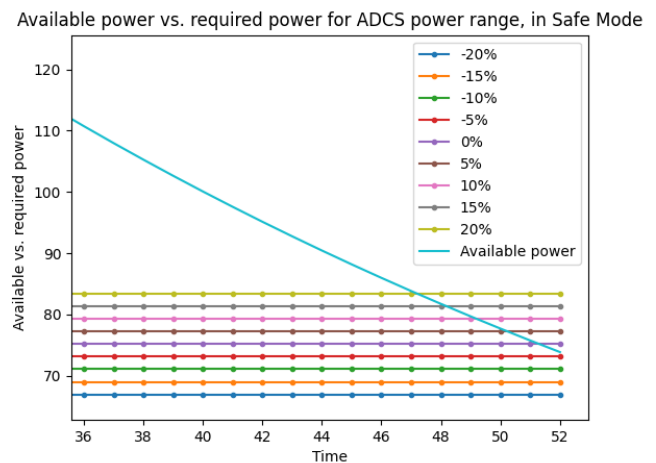
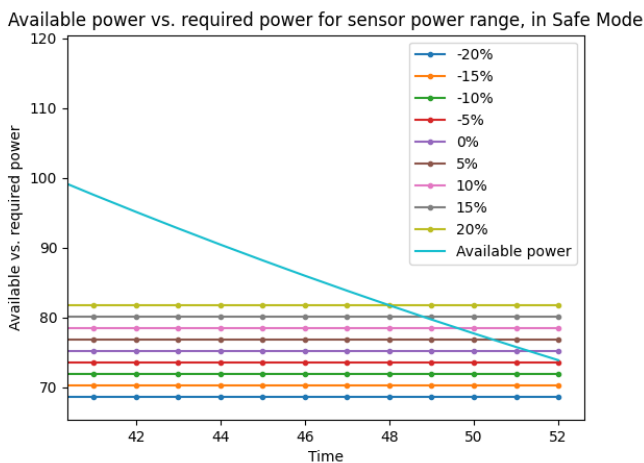


Figure 6.7: Available Power vs. Required Power for Sensors, in Safe Mode

Figure 6.8: Available power vs. required power for ADCS, in Safe Mode

## 6.4 Cost

*Contributors: Thijmen*

An important mission parameter in space missions is the cost. For example, the design, development and production of the James Webb Telescope had an initial budget of \$1B. Due to unforeseen problems during these phases, this eventually increased to \$10B.<sup>1</sup> Going over the budget is undesirable and should be avoided by making good and conservative estimations of the mission cost in early phases of the project. In the case that a large error in the cost estimation is made late in the project, when already a lot of resources have been put in to the development, stopping the project might be too expensive and continuing will require a lot more funding. This situation is very undesirable. Therefore it is important to see how sensitive the cost of the mission is to a changes in other mission parameters.

From Table 8.2 it can be seen that there are 4 mission elements that make up the total mission budget. This is excluding the launch cost and the risk mitigation cost, as the stakeholder has specified that the launch cost are not included in the budget and the risk mitigation cost is simply a 25 % margin which is

<sup>1</sup>URL <https://usafacts.org/articles/how-much-did-nasas-james-webb-space-telescope-cost/> [cited 18 June 2024]

added to the total budget calculated. The 4 components that do influence the total cost are: Component Production, Design and Development, Ground Segment and Mission Operations. The influence of these parameters on the total budget will be discussed in this section.

### **Design and development**

The design and development phase of a mission can have a lot of unexpected extra cost, as was the case for the James Webb Telescope mentioned above. Therefore, a sensitivity analysis on this cost component is important to be able to predict and prevent an unwanted cost increase.

The approach for this was looking at regular yearly costs for comparable missions and the average duration of the phase. The average yearly design and development cost of the New Horizons mission of €50M was taken into account in the cost breakdown. However, the yearly cost of the phase fluctuated between €25M and €200M a year, so a cost calculation needs to be run with these best and worst case values.

Then the development time that was taken into account in the cost breakdown was 10 years, however, this is also an unknown parameter, so the total cost needs to be analysed over a range of development times. The lower bound was set to 8 years, as a development duration shorter than this is unlikely. The upper bound was set to 13 years, as we are then in the year 2037, which is a year before the launch date, so the design and development has a deadline in that year.

Combining these two, the cost estimation lines can be drawn in Figure 6.9. It can be seen that higher yearly costs for design and development have a big influence on the total mission cost. If the phase has a duration of 13 years, the difference between having €50M or €200M yearly cost will result in a change of almost 200% in total mission cost. So it is critical to keep the design and development cost per year as low as possible.

### **Component production**

The component production estimate from the cost breakdown is at €337M for the current design. As a lot of the chosen components are off the shelf components, this value is not expected to change by a lot. However, if it does change, this change will have a simple linear relation with the total mission cost. The component production cost is simply a single value that is added to the total mission cost, so an increase in this cost category will directly change the total mission cost by the same amount.

As this value is not expected to change a lot, the total mission cost is not very sensitive for this cost category.

### **Ground segment**

The cost that are involved with the ground station segment of the mission are given by the operational cost of the NASA's Deep Space Network. From Section 8.2, the hourly contact price of the system is €4650,-. This value will not change, so the only thing that the total cost is influenced by in this category is the amount of contact hours. The lower limit of the amount of contact hours is the amount of hours that is needed to send all primary science data from Planet 9 back to earth. From Subsection 4.3.7, this results in 780 contact hours. The upper limit is the amount of contact hours to send back all secondary science data back to earth. From Subsection 4.3.7, this results in 118260 contact hours.

This means the cost of the ground segments depends on how much of the secondary science data is sent back to earth. From Figure 6.10, it can be seen that the total mission cost will scale linearly between €2700M and €3400M depending on how much secondary science data is sent back to earth. Therefore it is desirable for the cost to send as less data back as possible. This is done, for example, by compressing the data and improving the data quality with on board AI, which is discussed in Section 4.1.

### **Mission operations**

The mission operations cost, from Section 8.2, was estimated from the average yearly operational cost of the New Horizons mission. This is estimated at €26.56M per year. However, this value fluctuates between €10M and €30M per year. So graphs were made for the best and worst case estimations for the yearly operational cost as well. Next to this, the number of years that ground operations are needed can change as well, depending on the level of autonomy of the spacecraft. The best case for this is where the spacecraft

will fully autonomously head to Planet 9 and will then only need ground operations for 2 years to retrieve and analyse the data. The worst case is that the mission will need the full 50 years of ground operations to keep track of telemetry and retrieve secondary science data.

So depending on the level of autonomy, the cost in this category will increase. As can be seen from Figure 6.11, the total mission cost is very sensitive to the yearly operational cost. If the yearly operational cost are €30M, the total mission cost can double when increasing the operational time. Therefore it is very desirable to have a high level of spacecraft autonomy.

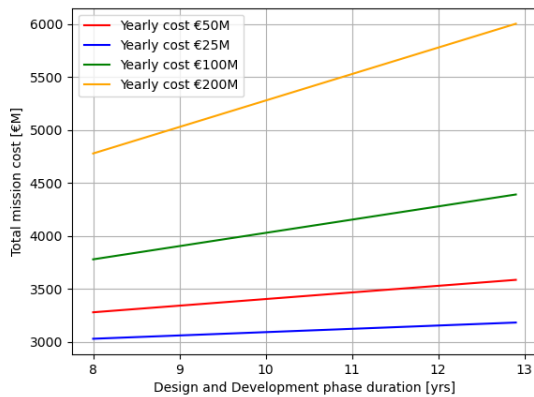


**Figure 6.9:** Variation of the Total Cost with Changes in the Design and Development Cost

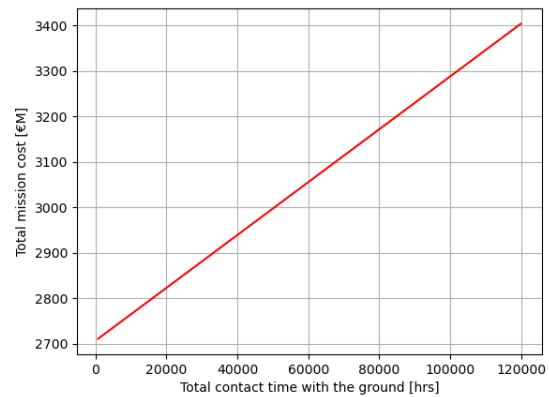


**Figure 6.10:** Variation of the Total Cost with Changes in the Ground Station Cost

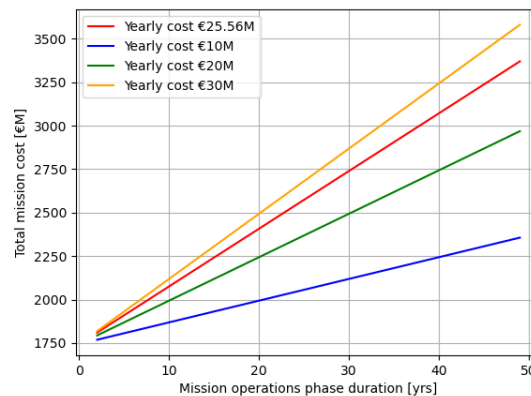


**Figure 6.11:** Variation of the Total Cost with Changes in the Operational Cost

## 6.5 Planet 9 Location

*Contributors: Flavio*

There is a high chance that the orbit of Planet 9 will be different from the one assumed for this design. This implies that the planet will not be located where it was originally hypothesised. A high-level analysis was performed to determine to what extent a different destination location would impact the design of NIBIRU. To do this, the orbit parameters of Planet 9 discussed in section 4.5.3 (except for the semi-major axis) were altered, placing the latter in several locations with respect to Earth. This analysis also took into account Planet 9 locations outside those with high probability, described in literature [60]. The results of the trajectory software showed that for the vast majority of the orbit parameters covered, the required  $\Delta V$  to reach destination within 50 years did not increase substantially. A possible reason for this is the fact that the last maneuver before the final leg to Planet 9 is a solar oberth maneuver, which does not need the spacecraft to arrive and leave at a specific angle to fully benefit from it, considering that the Sun has a negligible velocity compared to the other solar system bodies. In other words, if the last celestial body before the final leg had been Jupiter, this would be more sensitive to the location of Planet 9 as it must be

approached at a specific angle to get the most  $\Delta V$  out of the gravity assist, which would in turn make only make it a suitable trajectory for a restricted range of Planet 9 locations. It is important to keep in mind however, that the departure date should still be optimised in the trajectory program, as the most favorable launch time might still change to some extent, even with the solar oberth maneuver.

In conclusion, the design of the spacecraft will only vary marginally if Planet 9 were to be located in a different place compared to what was assumed for the current iteration. This does not apply to larger Planet 9 distances from the Sun however, as trivially these would negatively affect the design, which is why a conservative value for this is assumed in the first place. Moreover, the N'LORRI imager on board the spacecraft is capable of detecting Planet 9 from about 20 AU away. At such distances, the ADCS thrusters allow to correct NIBIRU's trajectory substantially, meaning that any smaller inaccuracies in the determination of Planet 9's location do not have an impact on the design either.

## 7 Technical Risk Assessment

In this chapter, the risks are first identified and assessed using a set of likelihood and severity categories in section 7.1. Using these metrics, all risks are plotted within a risk map in section 7.4, which accounts for their scores in both likelihood and severity. In section 7.2, mitigation actions are devised to reduce the likelihood of risks when possible. The results of these actions are then visualised in an updated version of the aforementioned risk map. Lastly, in section 7.3, a contingency plan is included to provide guidance on actions to take if one or more risks materialise.

### 7.1 Risk Identification & Assessment

*Contributors: Flavio, Isha, Dhafin, Ruth*

In this section, the risks are first identified, then assessed by allocating them in the severity and likelihood categories, which will be discussed shortly.

Risks relevant to the mission can be split into three different categories that are linked to each other [85]:

- Technical Performance Risks (RSK-SYS-XX)
- Schedule/Time Risks (RSK-SCH-XX)
- Cost/Resources Risks (RSK-CST-XX)

The technical performance risks that will be faced can be split by space department, all of these subcategories and their identifier formats are listed below:

- Structures & Materials: RSK-STR-XX
- Telecommunications: RSK-COM-XX
- Electrical Power System: RSK-EPS-XX
- Payload: RSK-PLD-XX
- Thermal Control System: RSK-TCS-XX
- Attitude Determination & Control System: RSK-ADC-XX
- Propulsion System: RSK-PRO-XX
- Astrodynamics: RSK-AST-XX
- On-Board Data Handling: RSK-OBDAH-XX

In order to assess individual risks, it is necessary to define severity and likelihood categories. This allows to allocate risks within these categories, which provides a more quantitative insight on how each risk impacts the mission. The categories are delineated in table 7.1 and table 7.2.

**Table 7.1:** Technical Risk Severity Categories [85]

| Category | Description  | Criteria   |
|----------|--------------|--|
| I        | Catastrophic | Could result failure of the mission, discontinuation of development or severe reputation damage.   |
| II       | Critical     | Could cause major deviations from the mission goal, significant reduction in technical performance or severely disrupt development. Significant reputation damage. |
| III      | Marginal     | Could lead to degradation of secondary mission or small reduction in technical performance. Limited reputation damage.   |
| IV       | Negligible   | Could be the cause of an inconvenience or have a non-operational impact<br>No reputation damage.   |

**Table 7.2:** Technical Risk Likelihood Categories [85]

| Category   | Likelihood (PR)       | Description   |
|------------|-----------------------|---|
| Frequent   | $PR \geq 0.70$        | Likely to occur often throughout the mission.                         |
| Probable   | $0.50 \leq PR < 0.70$ | Will occur several times throughout the mission.                      |
| Occasional | $0.30 \leq PR < 0.50$ | Likely to occur at some point during the mission.                     |
| Remote     | $0.01 \leq PR < 0.30$ | Unlikely but can occur at some point during the mission.              |
| Improbable | $PR < 0.01$           | So unlikely, it can be assumed its occurrence may not be experienced. |

The identified technical performance risks can be found in the subsections below, including a short description and assessment of each.

### Structures & materials

**RSK-STR-01: Launcher Failure:** The launcher vehicle fails during the launch phase, resulting in failure of the mission. This clearly fits into the catastrophic severity category. It also cannot be considered unlikely and can only occur once during a mission, meaning that it must be placed in the remote likelihood category.

**RSK-STR-02: Stress Failure:** If the spacecraft bus structure cannot withstand all critical loads, mission failure will follow, which puts this risk in the catastrophic category. If verification and validation is not performed properly, this can even happen occasionally.

**RSK-STR-03: Fatigue Failure:** If the spacecraft bus experiences oscillatory loading, material fatigue could occur in which small cracks will propagate throughout the material. The consequence of this could be critical, with an improbable probability.

**RSK-STR-04: Material Degradation:** The spacecraft materials will deteriorate over time [86], given the length of the mission, this is of marginal importance in selecting an adequate set of materials. Since degradation will always occur, it is placed in the frequent category.

**RSK-STR-05: Mechanical Failure:** Given the length of the mission, mechanical failures are bound to occur at some point. Depending on the subsystem, these can be critical. This type of failure constitutes 32% of all on-orbit spacecraft failures [87] which indicates that, assuming a failure will occur at some point during the mission, the likelihood can be expected to be somewhere in the occasional category.

**RSK-STR-06: Advanced Extraterrestrial Life:** Living creatures on planet 9 disrupt the mission by attacking the spacecraft. This is extremely unlikely but would have catastrophic consequences as it would most likely result in the complete destruction of the spacecraft bus.

**RSK-STR-07: Resonance:** Alignment of natural frequencies with external vibrations can amplify oscillations, causing excessive stress, fatigue, or failure of structural components. This is very unlikely but would result in complete spacecraft failure.

**RSK-STR-08: Buckling:** Compressive stresses exceeding critical load capacity can cause deformation or collapse of structural components, leading to significant structural failure and compromising the mission. This can happen, however not likely, and would also be catastrophic for the structure of the spacecraft.

**RSK-STR-09: Space Debris Impact:** High-velocity impacts from space debris can damage structural components, leading to breaches in the thermal protection system and compromising structural integrity and mission-critical systems. Since the spacecraft will be crossing the Kuiper belt, the likelihood against any other mission is quite high, depending on what components get damaged this could also result in mission failure.

**RSK-STR-10: Ejection Failure Kickstages:** An ejection failure could result from mechanical malfunction, misalignment, or insufficient separation force. Such a failure would prevent the spacecraft from reaching its designated path, potentially leading to mission failure or loss of the spacecraft.

**RSK-STR-11: Misalignment or Warping:** Structural components can become misaligned or warp due to thermal stresses, impacts, or manufacturing defects, affecting the spacecraft's overall performance and functionality. This is mostly accounted for using safety factors, and if this happens then some parts of the spacecraft may degrade in function.

**RSK-STR-12: Ejection Failure Heat shield:** Failure in the ejection mechanism, due to mechanical issues, misalignment, or software errors, could prevent the heat shield from deploying or separating properly. This would expose the spacecraft to extreme temperatures, risking damage to critical systems and instruments. This would be catastrophic for the mission.

**RSK-STR-13: Launcher Unavailability:** If for some reason the Starship launcher is discontinued by the

time of launch, in which case a launch contract cannot be finalised, this would be catastrophic for the mission. Based on specifications such as the refuelling option and the size which are essential to the mission, any other launcher would not suffice. However, since the Starship has been in a successful curve of increasing TRL, the likelihood of this is very low.

### Telecommunications

**RSK-COM-01: Signal Loss:** If the telecommunications experience signal loss with regards to transmitting data back to Earth or receiving commands from Earth, there is no means of communication between ground control and the spacecraft. This is a catastrophic risk, and its likelihood is remote.

**RSK-COM-02: Low Bit Rate:** If data cannot be transferred at a viable bit rate between the spacecraft and Earth, none of the scientific goals of the missions can be finalised as the data is not transmitted. This risk can be considered to have critical consequences and an occasional likelihood.

**RSK-COM-03: Signal Interference:** Interference of transmitted signals due to environmental phenomena or relative motion of the spacecraft with respect to Earth. This is something that happens throughout the mission, but it only has negligible consequences as data can still be transmitted and read for the most part.

**RSK-COM-04: Communication Hardware Failure:** Failure of hardware related to the telecommunications subsystem, such as the antenna, making reception and transmission from/to Earth impossible. This can result in catastrophic mission failure in the case where there is no way of restoring the link with Earth, but an event with remote probability considering previous deep space missions have not experienced permanent hardware failure.

**RSK-COM-05: Bit Flips:** The values of memory data stored in the spacecraft can be switched from 0s to 1s and vice versa due to high-energy charged particles striking the memory hardware.<sup>1</sup> This is something that rarely happens and has marginal consequences on communication.<sup>2</sup>

**RSK-COM-06: Antenna Deployment Failure:** If it is partially deployed, then the mission is not lost but its performance is decreased, and the latency is increased. If it fails completely, then the mission is lost since no communication is possible with Earth, and any discrepancies would be ignored.

**RSK-COM-07: Pointing Inaccuracy:** The pointing of the antenna is not precise or accurate enough. This will compromise the communication capabilities with Earth. As the spacecraft is travelling quite far, pointing accuracy is a strong requirement.

**RSK-COM-08: Modulation Failure:** The modulation of the signal is not correct. This will compromise the communication capabilities and the efficiency and performance of communications. This is very unlikely, but would impact the mission to quite a considerable extent.

### Electrical power system

**RSK-EPS-01: Complete Power Loss:** If the EPS suddenly loses its capability to provide power, all of the remaining subsystems will not be able to operate. Therefore, this risk is considered to have catastrophic consequences, however the likelihood is remote.

**RSK-EPS-02: Insufficient Power Production:** In the case that insufficient power production occurs, several subsystems might not receive sufficient power to operate. Therefore, this risk is considered to have critical consequences with a remote likelihood.

**RSK-EPS-03: Inefficient Cable Management:** Poor cable management leads to tangled cables, unnecessary weight due to excess cables, as well as power and signal loss. This risk is not inherently too severe, therefore it could be considered to be a negligible risk with a remote likelihood.

**RSK-EPS-04: Excessive Power Degradation:** The decline in power output from the EPS is exceeding initial expectations, primarily due to degradation factors such as component aging and radiation exposure. This has a critical impact on the mission, but it is not catastrophic as the spacecraft will still be capable of operating to some extent after significant degradation. This has occasional likelihood.

**RSK-EPS-05: Overheating Battery:** Batteries can overheat due to excessive charging rates, thermal runaway, or short circuits. Overheating can lead to chemical reactions within the battery, in extreme cases causing a fire. This can damage the EPS and other critical spacecraft components. It is quite unlikely that this would have as extreme consequences as leading to mission failure.

---

<sup>1</sup>URL <https://www.scienceabc.com/innovation/what-are-bit-flips-and-how-are-spacecraft-protected-from-them.html> [cited 15 May 2024]

<sup>2</sup>URL <https://www.scientificamerican.com/article/solar-storms-fast-facts/> [cited 15 May 2024]

**RSK-EPS-06: PCDU failure:** The PCDU is essential for managing and distributing power to various subsystems. A failure in the PCDU can result in the loss of power to critical components, leading to the malfunction or shutdown of essential systems. This could jeopardise the mission and the spacecraft's operational capabilities.

**RSK-EPS-07: Nuclear Fallout:** As the spacecraft relies on RTGs, any failure or damage to these units can result in the release of radioactive materials. This fallout can contaminate the spacecraft and surrounding space, posing severe health and safety risks to any future missions or nearby satellites. While this is extremely unlikely, this would severely impact the mission's success.

### **Payload**

**RSK-PLD-01: Planet 9 Non-existence:** If planet 9 turns out to not exist, the mission can be considered a partial failure. It is given that there is evidence at hand [4] but it can be considered a remote possibility. However, since the mission also has other objectives which can be carried out regardless, the consequence of this event is marginal.

**RSK-PLD-02: Instrumentation Failure:** The journey to destination might take a long time, therefore it is probable that some of the on-board instrumentation of the spacecraft will stop working. The consequence of this is critical towards the mission.

**RSK-PLD-03: Insufficient Payload Resolution:** The payload resolution determines the quality of data that will be obtained by the spacecraft and transmitted back to Earth. Therefore, insufficient payload resolution will reduce the quality of data, which could render them less useful for data analysis. As the mission objective is to collect data on Planet 9, this risk is considered to be of critical consequence with remote probability.

**RSK-PLD-04: Insufficient Payload Spatial Coverage:** The payload coverage determines the size of captured area per unit of time. If the payload coverage is low, then the spacecraft will capture less geographical area although with higher resolution, and vice versa. Therefore, insufficient payload coverage indirectly affects the data resolution. This risk is considered to be critical with remote probability.

**RSK-PLD-05: Incorrect Instrument Calibration:** Here the risk is that the imagers are not calibrated to the correct settings to capture quality images. This is likely due to the lack of experience with in-situ measurements in that part of the Solar System. Calibration tends to be required often, so it is likely that this can happen. In the case that these are not calibrated correctly, then the objectives would not be able to be carried out correctly, influencing the mission's success.

### **Thermal control system**

**RSK-TCS-01: Inaccurate Thermal Load Estimation:** Both under- and overestimating the thermal loads the spacecraft will be subjected to, can be harmful for the mission. In the former case, components might malfunction or, in more critical cases, the spacecraft might succumb to thermal loads; in the latter case, excessive thermal instrumentation will be carried on board, leaving less mass available for scientific instrumentation. This is a critical consequence of the mission, but remote probability.

**RSK-TCS-02: Inadequate Heat Flow:** In the case that inadequate heat flow from the TCS occurs, the subsystem components and instrumentation could experience temperatures beyond its operational temperature range which will effect their performance or even rendering them nonoperational. Therefore, this risk is considered to have catastrophic consequences, with remote likelihood.

**RSK-TCS-03: Thermal Sensor Failure:** If a thermal sensor fails, it cannot report overheating to the OBDH. This means the system cannot shut down or adjust affected components, risking overheating. This disruption can impact the spacecraft's thermal equilibrium, potentially causing damage and compromising operations. Sensor failure happens all the time, and this would compromise the components to an extent.

**RSK-TCS-04: Radiator Failure:** Surface degradation over time can reduce the radiator's emissive properties, impairing its ability to dissipate heat. Physical damage or contamination can further compromise its function. It is unlikely that large parts of the radiator are impaired, but if they are then this would heavily impact the operation capabilities of the instruments.

**RSK-TCS-05: Micro meteoroid Impact:** Micro meteoroids and space debris can impact the spacecraft, causing physical damage to radiators, ceramic tiles, or the heat shield. Such impacts can puncture surfaces, reduce thermal insulation, and impair heat dissipation. This is likely to happen, and if not accounted for could be critical.

**RSK-TCS-06: Ceramic Tile Cracking:** Ceramic tiles can crack due to thermal cycling, mechanical stresses during launch, or impacts from micro meteoroids. Cracked tiles can compromise thermal protection and allow heat to penetrate the underlying structure. This is likely to happen as these tiles are quite brittle, however, depending on the number of compromised tiles this will affect the impact more negatively.

**RSK-TCS-07 Adhesive Failure:** The adhesive that bonds ceramic tiles to the kickstage cylinder can degrade over time due to thermal stresses or space radiation. If the adhesive fails, tiles could detach, exposing the underlying structure to extreme temperatures. This is not likely to happen, however, depending on the number of compromised tiles this will affect the impact more negatively.

**RSK-TCS-08: Ablation Material Erosion Heat shield:** The carbon heat shield might include ablative materials designed to erode during intense heat exposure. Excessive or uneven erosion can reduce the heat shield's effectiveness and alter the spacecraft's thermal profile. While it is unlikely to happen, severe effects will result in heat shield failure, which in return becomes mission failure.

**RSK-TCS-09: Thermal Fatigue Heat Shield and Tiles:** Repeated exposure to extreme temperature variations can cause thermal fatigue in both ceramic tiles and carbon materials. This can lead to micro-cracks and material degradation over time. As the spacecraft is exposed to extreme temperatures both hot and cold, this is likely to occur and could be critical.

**RSK-TCS-10: Delamination of Composite Layers:** The carbon heat shield is made of layered composites. Delamination can occur due to thermal cycling, mechanical stresses, or manufacturing defects, reducing the structural integrity and thermal protection capability. This happens in industry as well, in case gone unnoticed, this could be catastrophic for the mission.

**RSK-TCS-11: Insulation Degradation (MLI):** Degradation of MLI due to space environment exposure could reduce its effectiveness in thermal regulation. Over the mission duration, this is unlikely to have more than a marginal impact.

## ADCS

**RSK-ADC-01: Sensor Hardware Malfunction:** Components of the sensors can malfunction due to manufacturing defects and wear/tear. This could result in the sensors inability to obtain attitude measurements of the spacecraft. Such risk has critical consequences with a remote probability.

**RSK-ADC-02: Sensor Calibration Errors:** Improper calibration of the sensors could lead to inaccurate measurements which detrimentally affects the performance of the sensors. Due to this, measurements of the orientation and attitude of the spacecraft is deemed less reliable. This risk has an occasional likelihood and a critical consequence.

**RSK-ADC-03: Sensor Communication Errors:** If the sensors are unable to communicate with other components and subsystems, the spacecraft attitude measurements cannot be transmitted to them thus rendering the sensors ineffective. This risk is considered to have remote likelihood and critical consequences.

**RSK-ADC-04: Actuator Mechanical Malfunction:** The actuators could become jammed or stuck which limits their movement. This results in the inability to effectively orient the spacecraft as desired. Such risk is considered to have an occasional likelihood with critical consequences.

**RSK-ADC-05: Actuator Structural Failure:** The actuators could experience excessive loads which could permanently damage the actuator system, thus hindering its functionality. This risk is considered to have remote likelihood with critical consequences.

**RSK-ADC-06: Actuator Control System Errors:** The algorithms contained in the control system software can cause errors which result in inaccuracies in the determination of actuator displacements. This risk is considered to have remote likelihood with marginal consequences.

**RSK-ADC-07: Thruster Collision with Debris:** An external thruster collides with space debris. This will cause the thruster to be inoperable, and result in a temporary loss of control. This is very unlikely and will only have marginal impact on mission success.

**RSK-ADC-08: Star Sensor Collision with Debris:** The star sensor, which is external of the spacecraft, collides with space debris. This will cause incorrect determination of attitude and in turn incorrect pointing of the spacecraft. This can lead to inability to communicate with Earth or inability to take quality images of the objects of interest. This is extremely unlikely but could be catastrophic for the mission.

**RSK-ADC-09: Incorrect Location and Attitude Determination and Commanding by OBDH:** The attitude and location determination algorithms in the OBDH fail to produce correct results. This will cause

incorrect orientation or scheduling of the spacecraft, and may cause inability of Earth communications and image acquisitions due to incorrect pointing. This is extremely unlikely but could be catastrophic for the mission.

**RSK-ADC-10: Sensor Startup Failure:** The ADCS subsystem includes multiple components of the same sensors due to lifetime limitations, and the subsequent ones fail to start up. This will cause incorrect operations of the ADCS subsystem, and may cause inability of Earth communications and image acquisitions due to incorrect pointing. This is extremely unlikely but could be catastrophic for the mission.

**RSK-ADC-11: Actuator Startup Failure:** The ADCS subsystem includes multiple components of the same actuators due to lifetime limitations, and the subsequent ones fail to start up. This will cause incorrect operations of the ADCS subsystem, and may cause inability of Earth communications and image acquisitions due to incorrect pointing. This is extremely unlikely but could be catastrophic for the mission.

### Propulsion system

**RSK-PRO-01: Insufficient Thrust Levels:** If the required thrust levels are not able to be performed by the propulsion system, the spacecraft could deviate from its planned trajectory and prolong the mission duration. In the worst scenario, this is critical but not catastrophic, since the spacecraft could still manage to reach the destination. Considering the length of the mission, this fits into the occasional likelihood category.

**RSK-PRO-02: Propellant Depletion:** If the propulsion system exhibits excessive propellant consumption, the spacecraft could run out of propellant. This will prevent the spacecraft from following its planned trajectory and terminating the mission completely. This is catastrophic for the mission, but it has a remote probability.

**RSK-PRO-03: Propulsion Failure:** If the main thrust interface malfunctions, the spacecraft will not be able to perform the required maneuvers. This is obviously catastrophic, but a remote occurrence.

**RSK-PRO-04: Propellant Leak:** If the propellant leaks from the fuel tank, the propulsion system will be deprived of propellant much more quickly which could lead to the spacecraft not being able to perform all the intended maneuvers. This is critical but improbable.

**RSK-PRO-05: Propellant Degradation and Contamination:** Propellant could lead to reduced thrust efficiency and damage to the propulsion system. This can alter the mission profile and is therefore critical. Propellant can also contaminate other spacecraft components [86]. Nonetheless, these can be considered remote events.

**RSK-PRO-06: Gravity Losses due to High Burn Time:** A larger burn time results in a larger gravity loss, which results in a loss of  $\Delta V$  for a given amount of propellant. As we require a significant amount of  $\Delta V$  from the kickstages and the number of thrusters are limited, it is very likely that the burn time is large to result in this gravity loss. As the  $\Delta V$  margin is limited, this could have a critical impact on whether the spacecraft can reach Planet 9 in time.

### Astrodynamics

**RSK-AST-01: Non-optimal Trajectory Selection:** The selected trajectory for the mission proves to not be suitable or not optimum to reach the destination within the intended time or to reach it at all. This has critical consequences in the former case, but catastrophic in the latter. Given the enormous range of possible trajectories, this is a probable event.

**RSK-AST-02: Inaccurate Trajectory Calculations:** Errors are made in computing the trajectory parameters. Consequently, the spacecraft does not follow the intended trajectory. The consequence of this is critical due to its impact on the mission and also probable due to the complexity of the calculations involved.

**RSK-AST-03: Collision with Space Objects:** The spacecraft collides with space debris, asteroids or other objects on its way to destination. This is improbable as collisions with space debris are extremely unlikely, but catastrophic if it were to happen.

**RSK-AST-04: Gravity Perturbations:** The spacecraft will cover a large distance, including areas that have not been reached by any human-made object before. The gravity of known or unknown celestial bodies in proximity of the spacecraft might alter its trajectory.

**RSK-AST-05: Incorrect Planet 9 Location:** The predicted location of Planet 9 is incorrect, meaning that the spacecraft cannot reach the planet. This is considered probable and it would have a catastrophic impact on the mission if it was the only objective. However, since secondary objectives are present, this is only

has a marginal impact.

**RSK-AST-06:** Crashing Into Another Spacecraft: NIBIRU crashes into another spacecraft. This is something that is much more likely at the beginning of the mission, when leaving Earth, but that becomes increasingly unlikely in later stages. For this reason, it is considered a remote risk, and trivially its consequence would be catastrophic.

**RSK-AST-07:** Incorrect Orbital Parameters Planet 9: Misestimation of gravitational parameters or orbital characteristics can cause trajectory deviations, leading to a potential collision with Planet 9. By the time the mission launches, the orbital parameters of the planet should be well known to a certain accuracy, however, it is still likely that these will deviate from reality to an extent. Since even a small deviation could affect the mission, the impact was set to be critical.

## **OBDH**

**RSK-OBDH-01:** On-board Computer Shut Down: The OBC unexpectedly shuts down, all subsystems stop operating as their data cannot be processed and transmitted between them anymore. This is something that can cause mission failure in the case that it is permanent, which puts it into the catastrophic impact category. However, permanent shut downs are improbable.

**RSK-OBDH-02:** Mode Transition Error: The OBC fails to set the spacecraft to the desired operation mode, resulting in subsystems not performing expected tasks. It is of critical importance that the spacecraft subsystems do not waste power by performing undesired tasks. The complexity of the OBC program makes the probability of errors in the code and therefore mistakes in the operational mode selection something occasional.

**RSK-OBDH-03:** Data Handling Software Error: The OBC software performs data handling tasks incorrectly, resulting in improper operation of the individual subsystems. Once again, this is something critical towards the mission objectives. The complexity of the code behind the OBC software makes such errors hard to spot, thus the estimated probability is occasional.

**RSK-OBDH-04:** DHAU Shut Down: The DHAU unexpectedly shuts down, and the OBDH is not able to gather data to be used for interpretation by the OBC. Data includes payload scientific data, and sensor data, therefore if there is a malfunction with a subsystem, it will not be handled through the sensors. Furthermore, the data will not be able to be downlinked, and the uplinked data will not be able to be transmitted and processed by the OBC. While this is very unlikely, the impact would be catastrophic for the mission.

**RSK-OBDH-05:** Encoder Failure: The encoder fails or shuts down, resulting in the lack of encoding on data that will be downlinked to Earth. Therefore, there is a higher chance of data corruption, both scientific and other subsystem data (e.g. positioning, location, etc.). However, communications are not hindered completely. Hence, the likelihood is very low, and the impact would be critical, but not catastrophic.

**RSK-OBDH-06:** Decoder Failure: The decoder fails or shuts down, therefore the uplinked data and telecommands cannot be processed by the OBDH subsystem. This means that positioning correction commands, failure handling commands, and software updates cannot be processed, and the spacecraft has to operate fully autonomously. While this is very unlikely, the impact would be catastrophic for the mission.

**RSK-OBDH-07:** CHU Error: The CHU does not command subsystems correctly, leading to incorrect spacecraft operations. The effects depend on the subsystem that is commanded wrongly, and can range from taking images at the wrong time to complete trajectory failure due to wrong thruster orientation. This could happen, and the impact would at most be critical.

**RSK-OBDH-08:** CHU Shut Down: The CHU unexpectedly shuts down, leading to no commanding of subsystems. The spacecraft is then inoperable. While this is very unlikely, the impact would be catastrophic for the mission.

**RSK-OBDH-09:** SSR Scientific Data Storage Failure: The SSR does not operate correctly, leading to partial loss or incorrect storage of scientific data. The spacecraft is still operable, but the objectives are not fulfilled in the best way.

**RSK-OBDH-10:** SSR Shut Down: The SSR unexpectedly shuts down, leading to no storage of telemetry data or scientific payload data. The spacecraft is still mostly operable, but the mission has minimal scientific value.

**RSK-OBDH-11:** Clock Operation Error: The clock operates incorrectly, leading to wrong timekeeping of

the spacecraft and incorrect location determination. This results in incorrect use of ADCS and propulsion systems, and can affect operations of payload, spacecraft modes, and telecommunications.

**RSK-OBDH-12: Clock Shut Down:** The clock unexpectedly shuts down, resulting in no timekeeping and inability to determine location of spacecraft. This results in inability of ADCS to point spacecraft, therefore also inability for telecommunications, and loss of mission.

**RSK-OBDH-13: Software Update Failure:** The software updates from Earth are incorrectly received or incorrectly handled. This results in loss of capability to correct potential operational system failures, or make the spacecraft operations more efficient. However, the initial software is not affected, therefore the spacecraft can operate at its initial capacity. However, potential corrections to trajectory or payload acquisition modes may also not be possible, and can have serious effects due to the long timeline of the mission.

**RSK-OBDH-14: Data and Command Cable Failure:** The cables connecting subsystems with each other or with the OBDH fail. The spacecraft is complex, therefore the probability that this happens is not minimal. It will result in inability to command subsystems or inability to store data.

**RSK-OBDH-15: IO Channel Failure:** The input and output channels of the OBDH subsystem fail. The spacecraft is complex, therefore the probability that this happens is not minimal. It will result in inability to command subsystems or inability to store data.

**RSK-OBDH-16: Watchdog Timer Failure:** The watchdog timer fails, therefore the health monitoring and housekeeping of the spacecraft is compromised. This could mean that if a subsystem has a failure, it will not be detected or handled timely. This is unlikely, but would have a critical impact.

**RSK-OBDH-17: Integrated Electronics Module (IEM) Failure:** The primary IEM as a whole is inoperable. While this is unlikely, this results in loss of the mission.

**RSK-OBDH-18: Backup Integrated Electronics Module (IEM) Inoperable:** The backup IEM as a whole is inoperable. If there is no error with the primary IEM, there are no effects. If the primary IEM fails, the mission is lost.

**RSK-OBDH-19: Single Event Soft Error (SESE) - Single Event Upset (SEU):** SEU occurs in digital circuit due to a solar particle strike causing change in data state in a storage element. Solar particles will likely strike the spacecraft, however, the impact to the mission success is minimal.

**RSK-OBDH-20: SESE - Single Event Functional Interrupt (SEFI):** SEFI occurs due to a particle strike, leading to temporary non-functionality of a OBDH component. This is likely to happen, however, the impact to the mission success is minimal.

**RSK-OBDH-21: SESE - Single Event Transient (SET):** SET occurs due to a single ion, causing malfunction of a logic, clock, or control line. This is unlikely, but could be critical for the mission.

**RSK-OBDH-22: Single Event Hard Error (SEVE) - Single Event Latchup (SEL)** SEL occurs due to the passing of an energy particle through a sensitive region, resulting in an abnormal high-current spike in a device and loss of device functionality due to excessive overheating or bond wire failure.

**RSK-OBDH-23: SEVE: Single Event Gate Rupture (SEGR):** SEGR occurs due to a single energy particle strike resulting in the breakdown and creation of a conducting path through the gate oxide of a transistor. This leads to degradation or complete failure of the device. This is very unlikely, but would at most be critical for the mission.

**RSK-OBDH-24: SEVE: Single Event Burnout (SEB):** SEB occurs due to a single energy particle strike resulting in a induced localised high-current state in a device, leading to thermal runaway and destructive failure. While this is very unlikely, the impact would be catastrophic for the mission.

**RSK-OBDH-25: OBDH System Overheat:** The OBDH system overheats, causing partial or whole failure of the components. This leads to partial or whole loss of the operational capacity of the spacecraft. This is not unlikely, and if not mitigated could be critical for the mission.

**RSK-OBDH-26: Cumulative Radiation Effects:** The OBDH system components' operation is affected by cumulative radiation effects (i.e. total ionising dose, displacement damage). This leads to partial or whole loss of the operational capacity of the spacecraft. The likelihood of this happening is increased due to long mission time and travel into unexplored areas of the solar system, past the heliopause, with increased gamma rays.

**RSK-OBDH-27: Incorrect Autonomous Operations:** Incorrect operation of the autonomous functions of the spacecraft will lead to critical issues with the trajectory, image acquisition, and operation of other subsystems. The communication latency with Earth is very large, therefore the impact will be significant.

**RSK-OBDH-28: Invaluable Data Gathered:** Data produced by the instruments is not valuable and does not add to scientific insights. This is likely to happen, and since the quality of the mission is affected it is set to have a critical impact to the mission.

### Scheduling risks

The recognised schedule/time risks are described below. These did not require any subcategories.

**RSK-SCH-01: Improper Design Planning:** Not having the final design ready by the designed time to start production can result in significant delays in the mission and is therefore critical. This is something probable to occur.

**RSK-SCH-02: Improper Production Planning:** Not having the assembled product ready by the designed launch time will result in failure to meet some key mission requirements. This is therefore critical for the mission and a probable occurrence.

**RSK-SCH-03: Short Launch Window:** If the mission profile only allows for a short launch window, it is more likely that any unforeseen circumstances result in missing the window. This is critical as it can result in a significant amount of time wasted. For such a mission it is probable to occur.

**RSK-SCH-04: Adverse Weather:** The launch can be postponed due to adverse weather conditions. In extreme cases, this can lead to missing the launch window. Considering the potential consequences of such delays, it fits into the critical category. Since adverse weather events occur often, it is placed in the occasional likelihood category.

**RSK-SCH-05: Inadequate Ground Operations:** If there is an issue on board the spacecraft and there is no ground team assigned to monitor the spacecraft when the ground station is notified, the problem might get worse as no immediate actions are taken. This is of critical importance and is probable to occur.

**RSK-SCH-06: Insufficient Technology Readiness Level:** Some of the technologies used on board the spacecraft are not ready by the start of production, resulting in delays. This is something probable considering the scale of the mission, but it has a marginal consequence as the delay would be justified.

**RSK-SCH-07: Not Reaching Planet 9 In Time:** It is a hard task to make proper subsystem-level choices in early stages of design, meaning that there is a chance it is impossible to reach Planet 9 within the time constraint with current technology. If that is the case, there can be some delays due to the team having to look for alternative design solutions and having to start over. This has critical consequences on the mission and is considered an occasional event.

**RSK-SCH-08: Insufficient Quantification:** In early design stages, it is hard to quantify the performance of each independent subsystem in order to perform an entirely consistent trade-off for the concepts. This could result in having to review the design concept selection and having to start over when in more advanced design stages. This has critical consequences on the mission and is considered to have an occasional likelihood.

**RSK-SCH-09: International Relations:** International conflicts might break out during the design or production phase of the spacecraft. These conflicts could limit the amount of collaboration between space companies globally and push back the launch. This is considered a probable event, but with only marginal consequence as it would affect all missions equally and therefore would not disadvantage NIBIRU with respect to those.

**RSK-SCH-10: Manufacturing Human Error:** During the production of a spacecraft of this type, it is probable that errors are made by workers. The consequence of this can vary, but is considered critical in the end as the likelihood of catastrophic errors is much lower in comparison.

**RSK-SCH-11: War:** War occurs for countries that play a significant role in the ground operations of the mission, leading to scheduling delays and potential mission cancellation. A lot of stakeholders are involved in the development, production, and operations of the mission, so the likelihood is increased.

### Cost risks

The identified cost risks are described below. Once again, these are not split into subcategories.

**RSK-CST-01: Exceeding Cost Budget:** The final cost budget surpasses the initial limit set for the mission. This results in some reputation damage and puts this risk into the marginal severity category. Exceeding the cost budget is frequent with missions of this scale [88].

**RSK-CST-02: Extra Maintenance:** The need for unplanned maintenance due to unforeseen events during the spacecraft's journey results in additional unplanned costs. Reasoning similarly as was done for the

last risk, this goes into the marginal severity category and has occasional likelihood.

**RSK-CST-03: Loss of Reputation:** A loss of reputation due to unforeseen events harmful to the mission can make it more difficult to finance the mission. Trivially, this is of critical severity. Considering the complexity of the mission, there is a large variety of ways in which reputation can be damaged, which makes it a frequent occurrence.

**RSK-CST-04: Improper Resource Allocation:** If excessive resources (e.g. engineers) are allocated to segment A of the mission leaving a subsequent segment B without enough resources, the costs will increase as extra resources will be necessary to be able to perform the duties of segment B. This is of marginal importance and will probably happen.

**RSK-CST-05: Inflation:** The cost of materials and services can fluctuate due to inflation or changes in market prices. This can result in higher-than-anticipated expenses for essential components and services. This is quite likely to happen, however, it would at most have marginal impact on the mission success.

**RSK-CST-06: Currency Exchange Rate Volatility:** For international projects, fluctuations in currency exchange rates can impact the overall budget, especially if significant transactions occur in foreign currencies. Similarly as for inflation, this is likely to happen, however, it would at most have marginal impact on the mission success.

**RSK-CST-07: Bankruptcy:** The financial instability of a key contractor or supplier can lead to bankruptcy, disrupting the supply chain and causing delays. This can result in additional costs to find and qualify new suppliers, as well as potential project rework. The impact of such a disruption can be critical, affecting the project's timeline and budget.

## 7.2 Risk Mitigation

*Contributors: Dhafin, Isha, Flavio, Ruth*

Actions can be taken to reduce the likelihood and impact of risks. There are four different approaches to mitigating risks [35]:

- **Remove** the risk: by changing the design to exclude it.
- **Reduce** the risk: by performing actions to reduce its likelihood and potential consequence.
- **Accept** the risk: by not performing any action to mitigate it, and just monitoring it instead. This is a common practice for risks that are highly unlikely to materialise.
- **Transfer** the risk: assign the responsibility to a third party to optimise the mitigation.

These mitigation strategies have different effects on the likelihood and consequence of each risk. The effect of removing a risk for instance, is shown by moving the risk to the bottom left part of the risk map (negligible impact, improbable likelihood). Reducing a risk will usually reduce its likelihood, but also its impact in some specific cases. On the other hand, accepting a risk will not affect its position in the risk map. For this reason, usually only non-frequent risks that are not critical are accepted. More dangerous risks are rarely accepted, when no suitable mitigation action is possible and removing them is not possible due to the mission requirements. Finally, transferring a risk will have a similar effect to reducing it, sometimes marginally better in terms of overall mitigation as the responsibility is transferred to a team of experts on the specific matter. For each of the risks described in the previous section, the mitigation strategy and action, as well as the responsible team member are specified in table 7.3. Not all risks are mentioned in this table below, the identifiers that are missing are risks that are accepted and do not have a mitigation action.

**Table 7.3:** Mitigation Strategies, Actions and Responsible Managers for Technical Risks

| ID         | Mitigation Strategy | Mitigation Action  | Responsible Officer         |
|------------|---------------------|--|-----------------------------|
| MIT-STR-01 | TRANSFER            | Transfer responsibility to launcher company to provide a working launcher for the loads provided in the launch vehicle catalogue.                        | External Relations (Pepijn) |
| MIT-STR-02 | REDUCE              | Perform extensive verification and validation as part of the structural design of the spacecraft. Account for critical loads and include safety margins. | Structures Officer (Iván)   |
| MIT-STR-04 | REDUCE              | Ensure that the spacecraft surfaces are coated with materials that diminish the effects of degradation and test it under similar conditions.             | Structures Officer (Iván)   |
| MIT-STR-05 | REDUCE              | Avoid complex mechanisms where possible, especially for most critical subsystems.  | Structures Officer (Iván)   |

Table 7.3: (continued)

| ID         | Mitigation Strategy | Mitigation Action   | Responsible Officer                |
|------------|---------------------|---|------------------------------------|
| MIT-STR-07 | REDUCE              | Conduct thorough vibration testing and analysis during the design phase to identify potential resonant frequencies.   | Structures Officer (Iván)          |
| MIT-STR-08 | REDUCE              | Use materials with higher buckling resistance and incorporate safety factors into the design  | Structures Officer (Iván)          |
| MIT-STR-09 | REDUCE              | Design the spacecraft with a sandwich structure to protect against micrometeoroid and space debris impacts.   | Structures Officer (Iván)          |
| MIT-STR-10 | REDUCE              | Conduct rigorous pre-launch testing of ejection mechanisms under simulated space conditions.  | Structures Officer (Iván)          |
| MIT-STR-11 | REDUCE              | Use materials with low thermal expansion coefficients and design the structure to accommodate thermal stresses  | Structures Officer (Iván)          |
| MIT-STR-12 | REDUCE              | Conduct rigorous pre-launch testing of ejection mechanisms under simulated space conditions.  | Structures Officer (Iván)          |
| MIT-COM-04 | REDUCE              | Perform extensive verification of communication hardware prior to launch.   | Telecommunications Officer (Anton) |
| MIT-COM-08 | REDUCE              | Perform extensive verification and validation. Monitor subsystem operation and reaction to commands with watchdog. Implement fault masking techniques (error correcting memories and majority voting), and reconfiguration techniques (fault detection, location, containment, recovery). | Telecommunications Officer (Anton) |
| MIT-EPS-02 | REDUCE              | At any given time during the mission, only keep interfaces that are in use switched on.   | EPS Officer (Pepijn)               |
| MIT-EPS-04 | REDUCE              | Frequent monitoring and inspection of power production.   | EPS Officer (Pepijn)               |
| MIT-EPS-05 | REDUCE              | Include onboard thermal sensors to detect overheating   | OBDR Officer (Ruth)                |
| MIT-PLD-01 | TRANSFER            | Transfer responsibility to scientific community to prove the existence of planet 9 by the start of production of the spacecraft.  | External Relations (Pepijn)        |
| MIT-PLD-02 | REDUCE              | Verify and validate the performance of on-board instrumentation before launch.  | Payload Officer (Jim)              |
| MIT-PLD-04 | REDUCE              | Perform extensive research with regards to the necessary instrumentation as well as the required spacecraft altitude to achieve the required spatial coverage.  | Payload Officer (Jim)              |
| MIT-PLD-05 | REDUCE              | Perform extensive research with regards to the necessary instrumentation settings and test the instruments in a simulated environment. Implement on-board payload verification and validation procedures to check quality.  | Payload Officer (Jim)              |
| MIT-TCS-02 | REDUCE              | Perform extensive verification of the heat flow analysis by the thermal control design team.  | Thermal Control Officer (Isha)     |
| MIT-TCS-04 | REDUCE              | Design radiators with robust materials to withstand space environment and potential impacts.  | Thermal Control Officer (Isha)     |
| MIT-TCS-05 | REDUCE              | Design the spacecraft with a sandwich structure to protect against micrometeoroid and space debris impacts.   | Structures Officer (Iván)          |
| MIT-TCS-06 | REDUCE              | Conduct rigorous testing to ensure durability under expected conditions.  | Structures Officer (Iván)          |
| MIT-TCS-07 | REDUCE              | Select adhesives with high thermal and mechanical stability. Perform extensive qualification tests under simulated space conditions.  | Structures Officer (Iván)          |
| MIT-TCS-08 | REDUCE              | Use advanced ablation materials with high resistance to erosion. Conduct detailed modeling and testing to predict ablation rates accurately.  | Structures Officer (Iván)          |
| MIT-TCS-09 | REDUCE              | Use materials specifically designed for high thermal fatigue resistance   | Thermal Control Officer (Isha)     |
| MIT-TCS-10 | REDUCE              | Conduct rigorous testing to detect and address potential delamination issues.   | Thermal Control Officer (Isha)     |
| MIT-TCS-11 | REDUCE              | Use high-durability MLI materials with resistance to space environmental factors. Conduct thorough testing to ensure long-term performance.   | Thermal Control Officer (Isha)     |
| MIT-ADC-01 | REDUCE              | Ensure that sensors are tested under critical space conditions, and that they remain functional.  | ADCS Officer (Milan)               |
| MIT-ADC-02 | REDUCE              | Perform regular recalibration by implementing high quality calibration standards.   | ADCS Officer (Milan)               |

Table 7.3: (continued)

| ID          | Mitigation Strategy | Mitigation Action   | Responsible Officer            |
|-------------|---------------------|---|--------------------------------|
| MIT-ADC-03  | REDUCE              | Ensure that the integration between the sensors and other subsystem components result in seamless communication flow.   | ADCS Officer (Milan)           |
| MIT-ADC-04  | REDUCE              | Ensure that the mechanical functions of the actuators work fine under test conditions, in addition to regular maintenance and inspection of actuators.  | ADCS Officer (Milan)           |
| MIT-ADC-05  | REDUCE              | Test actuator structures for expected critical loads under space conditions prior to launch.  | ADCS Officer (Milan)           |
| MIT-ADC-06  | REDUCE              | Perform verification and validation on the control algorithms.  | ADCS Officer (Milan)           |
| MIT-ADC-09  | REDUCE              | Perform extensive verification and validation of ADC software. Include redundant pieces of software to detect errors. Implement fault masking techniques (error correcting memories and majority voting), and reconfiguration techniques (fault detection, location, containment, recovery) to mitigate effects.  | OBDH Officer (Ruth)            |
| MIT-PRO-01  | REDUCE              | Test the propulsion subsystem in an appropriate testing facility to evaluate whether the thrust levels are as expected.   | Propulsion Officer (Flavio)    |
| MIT-PRO-02  | REDUCE              | Ensure that propellant usage is optimized such that mission operations are performed without unnecessary and excessive fuel consumption.  | Propulsion Officer (Flavio)    |
| MIT-PRO-03  | REDUCE              | Identify several failure modes that the propulsion subsystem may experience and test whether said failure modes are likely to occur under simulated conditions.   | Propulsion Officer (Flavio)    |
| MIT-PRO-06  | REDUCE              | Add more thrusters to reduce the burn time  | Propulsion Officer (Flavio)    |
| MIT-AST-01  | REDUCE              | Perform a trade-off between possible trajectories.  | Astrodynamics Officer (Dhafin) |
| MIT-AST-02  | REDUCE              | Perform verification and validation on the numerical calculations of trajectory.  | Astrodynamics Officer (Dhafin) |
| MIT-AST-04  | REDUCE              | Unless part of the mission objectives, avoid close fly-bys of already known celestial bodies.   | Astrodynamics Officer (Dhafin) |
| MIT-AST-07  | REDUCE              | Conduct detailed observational campaigns, use advanced modeling tools, and collaborate internationally for accurate data.   | Astrodynamics Officer (Dhafin) |
| MIT-OBDH-02 | REDUCE              | Perform extensive verification and validation on the code that selects the operation mode of the spacecraft. Monitor subsystem operation and reaction to commands with watchdog.  | OBDH Officer (Ruth)            |
| MIT-OBDH-03 | REDUCE              | Perform extensive verification and validation on the data handling software code. Implement fault masking techniques (error correcting memories and majority voting), and reconfiguration techniques (fault detection, location, containment, recovery).  | OBDH Officer (Ruth)            |
| MIT-OBDH-07 | REDUCE              | Perform extensive verification and validation on the code that selects the operation mode of the spacecraft. Monitor subsystem operation and reaction to commands with watchdog. Implement fault masking techniques (error correcting memories and majority voting), and reconfiguration techniques (fault detection, location, containment, recovery). | OBDH Officer (Ruth)            |
| MIT-OBDH-09 | REDUCE              | Perform extensive testing of SSR operation, select radiation hardened component with high reliability and long operational lifetime. Include code segments in data for error detection.   | OBDH Officer (Ruth)            |
| MIT-OBDH-11 | REDUCE              | Perform extensive testing of clock operation, select radiation hardened component with high reliability and long operational lifetime. Include code segments in data for error detection. Conduct regular sanity checks on clock operations.  | OBDH Officer (Ruth)            |

Table 7.3: (continued)

| ID           | Mitigation Strategy | Mitigation Action  | Responsible Officer          |
|--------------|---------------------|--|------------------------------|
| MIT-OBDDH-13 | REDUCE              | Perform extensive verification and validation of operating software and software update functionality. Include redundant pieces of software to detect errors. Implement fault masking techniques (error correcting memories and majority voting), and reconfiguration techniques (fault detection, location, containment, recovery) to mitigate effects. | OBDDH Officer (Ruth)         |
| MIT-OBDDH-14 | REDUCE              | Implement fault masking techniques (error correcting memories and majority voting).  | OBDDH Officer (Ruth)         |
| MIT-OBDDH-15 | REDUCE              | Implement fault masking techniques (error correcting memories and majority voting).  | OBDDH Officer (Ruth)         |
| MIT-OBDDH-16 | REDUCE              | Implement fault masking techniques. Create architecture that allows for fault containment.   | OBDDH Officer (Ruth)         |
| MIT-OBDDH-26 | REDUCE              | Select radiation hardened components and perform extensive testing. Include redundant code to monitor health and radiation effects.  | OBDDH Officer (Ruth)         |
| MIT-OBDDH-27 | REDUCE              | Perform extensive verification and validation of operating software and autonomous functionalities. Include redundant pieces of software to detect errors. Implement fault masking techniques (error correcting memories and majority voting), and reconfiguration techniques (fault detection, location, containment, recovery) to mitigate effects.    | OBDDH Officer (Ruth)         |
| MIT-OBDDH-28 | REDUCE              | Implement AI for dynamic pointing to improve the quality of the data. Furthermore, AI will be used to detect quality of data and decide whether more measurements need to be taken   | OBDDH Officer (Ruth)         |
| MIT-SCH-01   | REDUCE              | Ensure that organisational and scheduling tools such as the Gantt chart and work flow diagram are adhered to, and constantly updated to adapt to the team's progress.  | Systems Engineer (Thijmen)   |
| MIT-SCH-02   | REDUCE              | Include a margin when planning the work hours for each production phase  | Systems Engineer (Thijmen)   |
| MIT-SCH-03   | REDUCE              | Avoid trajectory designs that rely on rare planet alignments.  | Systems Engineer (Thijmen)   |
| MIT-SCH-04   | REDUCE              | Ensure that weather forecasts are taken into consideration when selecting a launch date.   | Systems Engineer (Thijmen)   |
| MIT-SCH-05   | TRANSFER            | Transfer responsibility to the space agency in charge of the mission.  | External Relations (Pepijn)  |
| MIT-SCH-06   | REDUCE              | Try to minimize the use of technology that is not available today.   | Systems Engineer (Thijmen)   |
| MIT-SCH-08   | REDUCE              | Perform design concept trade-off by performing an extensive qualitative analysis.  | Systems Engineer (Thijmen)   |
| MIT-SCH-09   | REDUCE              | Avoid excessive collaboration with companies outside the country in terms of design, production, and operations.   | Systems Engineer (Thijmen)   |
| MIT-SCH-10   | REDUCE              | Perform extensive verification and validation of the spacecraft bus at the end of production.  | Sustainability Officer (Jim) |
| MIT-CST-01   | REDUCE              | Perform analysis related to technical resource management such as a cost breakdown and cost estimation, while also considering appropriate cost contingencies.   | Business Manager (Milan)     |
| MIT-CST-02   | REDUCE              | Ensure that ground operations are readily available in the case that the spacecraft needs unexpected maintenance.  | Business Manager (Milan)     |
| MIT-CST-03   | REDUCE              | Work with stakeholders who are familiar with the field and understand the uncertainties involved.  | Business Manager (Milan)     |
| MIT-CST-04   | REDUCE              | Perform various resource allocation methods to provide insights as to how resources can effectively be utilized.   | Business Manager (Milan)     |
| MIT-CST-05   | TRANSFER            | Use fixed-price contracts with suppliers and vendors to lock in costs and reduce the impact of inflation on the project budget.  | Business Manager (Milan)     |
| MIT-CST-06   | TRANSFER            | Work with financial experts to manage currency risks and reduce exposure to exchange rate fluctuations.  | Business Manager (Milan)     |

Table 7.3: (continued)

| ID         | Mitigation Strategy | Mitigation Action   | Responsible Officer      |
|------------|---------------------|---|--------------------------|
| MIT-CST-07 | REDUCE              | Conduct thorough financial assessments of contractors and suppliers before engagement. Include clauses in contracts for immediate notification and action plans in case of financial instability. Diversify the supplier base to avoid dependence on a single contractor or supplier. | Business Manager (Milan) |

### 7.3 Contingency Plan

*Contributors: Dhafin, Isha, Flavio, Ruth*

In the case that any of the risks covered earlier in this section materialise, actions can be taken to reduce the damage as much as possible. These contingency measures are provided in table 7.4 for each risk. Risks that are not mentioned in the table are risks that do not have an contingency plan.

Table 7.4: Contingency Actions for Technical Risks. The Responsible Officer for Each Risk Does not Change from Earlier

| ID         | Contingency Action   |
|------------|--|
| CON-STR-01 | Design emergency system to save the spacecraft bus in case of catastrophic launcher failure.   |
| CON-STR-02 | Isolate the affected area of the spacecraft to prevent further propagation of the damage.  |
| CON-STR-03 | Isolate the affected area of the spacecraft to prevent further propagation of the damage.  |
| CON-STR-04 | Plan emergency actions to take in case material degradation starts occurring.  |
| CON-STR-05 | Include redundant mechanisms for most critical subsystems.   |
| CON-STR-06 | Attempt approaching aliens in a friendly manner.   |
| CON-STR-07 | Monitor vibration levels during the mission using onboard sensors. If resonance is detected, adjust operational procedures or use active damping systems to mitigate the effects.  |
| CON-STR-11 | Use onboard sensors to detect and correct any warping or misalignment dynamically.   |
| CON-STR-13 | The mission would be on hold until a launcher of similar specifications becomes available.   |
| CON-COM-01 | Ensure the spacecraft has an operational safe mode, to be turned on when there is a complete loss of signal.   |
| CON-COM-02 | When transmitting data back to Earth, give priority to information that is key to the mission objectives.  |
| CON-COM-03 | Re-transmit clean version of noisy data back to Earth.   |
| CON-COM-04 | Implement backup communication hardware.   |
| CON-COM-05 | If a bit flip is detected, reboot OBC.   |
| CON-COM-06 | Use redundant antenna. Continue trying to deploy antenna. If error persists, compile message with component telemetry for error detection on OBC or on Earth, and re-evaluate power strategy to allow for efficient communications.                                      |
| CON-COM-07 | Try to regain accuracy with ADCS. Pause Earth communications to reduce unnecessary power consumption.  |
| CON-COM-08 | Reboot component. If error persists, switch on redundant component, and compile message with component telemetry for error detection on OBC or on Earth. Avoid transmitting payload scientific data (will be corrupt), and focus on transmission of subsystem telemetry. |
| CON-EPS-01 | Implement a backup power supply.   |
| CON-EPS-02 | Shut down non-fundamental systems.   |
| CON-EPS-03 | Shut down non-fundamental systems.   |
| CON-EPS-04 | Shut down non-fundamental systems.   |
| CON-EPS-05 | Have OBDH turn system off  |
| CON-EPS-07 | In the event of a nuclear fallout, implement emergency procedures to isolate and contain the affected area.  |
| CON-PLD-01 | Fulfill secondary mission objectives.  |
| CON-PLD-02 | Implement redundant instrumentation.   |
| CON-PLD-03 | Adjust distance from Planet 9 to perform the measurement at a higher resolution.   |
| CON-PLD-04 | Adjust the spacecraft's altitude such that the desired spatial coverage is obtained.   |
| CON-PLD-05 | Adjust settings of instruments. If error persists, request an instrument software update.  |
| CON-TCS-01 | Adjust the heat inflow and outflow setting of the thermal interfaces to bring the thermal load back within the desired range.  |
| CON-TCS-02 | In the case the overheating occurs in a concentrated part of the spacecraft, implement a mechanism that redistributes heat uniformly such that components are less prone to damage.  |
| CON-TCS-03 | Use redundant thermal sensors in critical areas to ensure backup measurements are available if a primary sensor fails.   |

Table 7.4: (continued)

| ID           | Contingency Action  |
|--------------|---|
| CON-TCS-07   | Implement redundant adhesive bonding where possible.  |
| CON-TCS-08   | Adjust spacecraft trajectory or orientation to reduce heat load if erosion exceeds expectations.  |
| CON-TCS-10   | Monitor for signs of delamination using non-destructive testing methods.  |
| CON-ADC-01   | Implement sensor redundancies.  |
| CON-ADC-02   | Implement automated calibration systems.  |
| CON-ADC-03   | Reboot ADCS components.   |
| CON-ADC-04   | Implement actuator redundancies.  |
| CON-ADC-05   | Implement actuator redundancies.  |
| CON-ADC-06   | Reboot ADCS components.   |
| CON-ADC-07   | Implement thruster redundancies.  |
| CON-ADC-08   | Implement star sensor redundancies.   |
| CON-ADC-09   | Update software. Use redundant OBC. Pause trajectory travel until issue is fixed to avoid traveling far off track.  |
| CON-ADC-10   | Include redundant component. Reboot component. If error persists, switch on redundant component, and compile message with component telemetry for error detection on OBC or on Earth.   |
| CON-ADC-11   | Include redundant component. Reboot component. If error persists, switch on redundant component, and compile message with component telemetry for error detection on OBC or on Earth.   |
| CON-PRO-01   | Activate redundant thrusters.   |
| CON-PRO-02   | If it leads to mission failure, adjust mission objectives that are feasible with the remaining propellant. Otherwise, select a trajectory that minimizes propellant consumption.  |
| CON-PRO-03   | Implement redundant spacecraft thrusters.   |
| CON-PRO-04   | If the propellant tank is divided into multiple sections, first use all the propellant in the section that has a leak.  |
| CON-PRO-05   | Implement a smaller backup propellant tank that is separate from the main one.  |
| CON-PRO-06   | Readjust trajectory where required  |
| CON-AST-01   | Re-adjust trajectory mid-flight to a more optimal one.  |
| CON-AST-02   | Re-adjust trajectory mid-flight to aim for the correct destination.   |
| CON-AST-03   | Identify which subsystems are still functional, if any, and proceed with fulfilling as many mission objectives as possible. In addition to this, a safe mode in the case of collision can also be activated until the ground team gives orders.   |
| CON-AST-04   | Carry extra propellant on board to adjust the trajectory in case of gravity perturbations.  |
| CON-AST-05   | If the planet is not too far from the predicted location, the spacecraft trajectory can be adjusted accordingly. If that is not possible, the spacecraft primary mission becomes characterizing the Oort cloud.   |
| CON-AST-06   | No contingency action can be taken.   |
| CON-AST-07   | Implement trajectory correction protocols, continuous monitoring, and prepare for manual or autonomous adjustments in-flight.   |
| CON-OBDAH-01 | Implement a simpler, backup data handling system to take over in case the main OBC shuts down.  |
| CON-OBDAH-02 | If spacecraft is set to incorrect operation mode, reboot OBC.   |
| CON-OBDAH-03 | Reboot DHAU. If error persists, switch on redundant DHAU, and implement a software update to be transmitted from Earth to resolve the issue.  |
| CON-OBDAH-04 | Include redundant component. Reboot DHAU. If error persists, switch on redundant DHAU, and compile message with component telemetry for error detection on OBC and on Earth.  |
| CON-OBDAH-05 | Include redundant component. Reboot component. If error persists, switch on redundant component, and compile message with component telemetry for error detection on OBC or on Earth. Avoid transmitting payload scientific data (will be corrupt), and focus on transmission of subsystem telemetry. |
| CON-OBDAH-06 | Include redundant component. Reboot component. If error persists, switch on redundant component, and compile message with component telemetry for error detection on OBC or on Earth.   |
| CON-OBDAH-07 | Include redundant component. Reboot component. If error persists, switch on redundant component, and compile message with component telemetry for error detection on OBC or on Earth.   |
| CON-OBDAH-08 | Include redundant component. Reboot component. If error persists, switch on redundant component, and compile message with component telemetry for error detection on OBC or on Earth.   |
| CON-OBDAH-09 | Include redundant component. Reboot component. If error persists, switch on redundant component, and compile message with component telemetry for error detection on OBC or on Earth. Until the error is fixed, pause imaging.  |
| CON-OBDAH-10 | Include redundant component. Reboot component. If error persists, switch on redundant component, and compile message with component telemetry for error detection on OBC or on Earth. Until the error is fixed, pause imaging.  |
| CON-OBDAH-11 | Include redundant component. Reboot component. If error persists, switch on redundant component, and compile message with component telemetry for error detection on OBC or on Earth.   |
| CON-OBDAH-12 | Include redundant component. Reboot component. If error persists, switch on redundant component, and compile message with component telemetry for error detection on OBC or on Earth.   |

Table 7.4: (continued)

| ID          | Contingency Action   |
|-------------|--|
| CON-OBDH-13 | Return to most correct past version of software, and transmit error message to Earth.  |
| CON-OBDH-14 | Include redundant cabling.   |
| CON-OBDH-15 | Include redundant channels.  |
| CON-OBDH-16 | Include redundant watchdogs. Monitor telemetry of components that cannot be monitored with watchdog.   |
| CON-OBDH-17 | Include redundant component. Reboot component. If error persists, switch on redundant component, and compile message with component telemetry for error detection on OBC or on Earth.  |
| CON-OBDH-18 | Include redundant component. Reboot component. If error persists, switch on redundant component, and compile message with component telemetry for error detection on OBC or on Earth.  |
| CON-OBDH-19 | Soft reboot affected component. If error persists, hard reboot affected component.   |
| CON-OBDH-20 | Soft reboot affected component. If error persists, hard reboot affected component.   |
| CON-OBDH-21 | Soft reboot affected component. If error persists, hard reboot affected component.   |
| CON-OBDH-22 | Remove power from component quickly and use the redundant ones if possible.  |
| CON-OBDH-23 | Remove power from component and use the redundant ones if possible.  |
| CON-OBDH-24 | Remove power from component quickly and use the redundant ones if possible. Check for thermal effects on spacecraft.   |
| CON-OBDH-25 | Remove power from component quickly and use the redundant ones if possible. Check for thermal effects on spacecraft.   |
| CON-OBDH-26 | Use redundant components and monitor health of components.   |
| CON-OBDH-27 | Stop payload operations and use power to establish good Earth communications. Go into safe mode.   |
| CON-SCH-01  | Hold a meeting with stakeholder representatives to present the issues and indicate the action points that will be taken to resolve the situation.  |
| CON-SCH-02  | Update the production plan to minimize the extra time required to complete production.   |
| CON-SCH-03  | Implement measures that would allow the launch window to be more flexible such as lessen the number of planetary fly-bys.  |
| CON-SCH-04  | Make use of a launch vehicle that can land back on the ground in case of mid-flight appearance of adverse weather conditions.  |
| CON-SCH-05  | Ensure the spacecraft has an operational safe mode, to be turned on when no indications are received from the ground station for a given period of time following an incident.   |
| CON-SCH-06  | If the predicted delay is too long, replace the technology with one that is already available.   |
| CON-SCH-07  | Request extension on the time requirement.   |
| CON-SCH-08  | If it is impossible to fulfill the science objectives, select alternative design concept from the trade-off.   |
| CON-SCH-09  | Reallocate internally the technical tasks that were allocated to parties that are no longer collaborating.   |
| CON-SCH-10  | If the spacecraft is still on the ground, replace the faulty parts using a lean manufacturing approach to minimize the delay   |
| CON-SCH-11  | Reschedule launch and operations, ensure that technical expertise is not lost.   |
| CON-CST-01  | Request more financial support from stakeholders.  |
| CON-CST-02  | For any recurring malfunction, allocate a team to be in charge of periodically fixing the issue. This can save costs compared to only soliciting technicians once the flaw appears.  |
| CON-CST-03  | Hold a meeting with stakeholder representatives to present the issues and indicate the action points that will be taken to resolve the situation.  |
| CON-CST-04  | Re-evaluate resource allocations and develop a new protocol to reallocate the resources appropriately.   |
| CON-CST-05  | Regularly review and adjust the project budget to reflect current economic conditions and maintain financial flexibility.  |
| CON-CST-06  | Monitor exchange rates closely and adjust financial plans as needed to mitigate adverse effects.   |
| CON-CST-07  | Develop a list of alternative suppliers and contractors that can be quickly engaged if a key partner goes bankrupt. Maintain critical supplies and materials in reserve to ensure project continuity while transitioning to new suppliers. |

## 7.4 Risk Maps

*Contributors: Dhafin, Isha, Flavio, Ruth*

Individual risks can be plotted on a risk map based on their likelihood and impact levels. This allows for a visual representation of the risks and aids in identifying risks that need to be mitigated. Two risk

maps have been created in this risk analysis: a pre-mitigation risk map and a post- mitigation risk map which captures the effect of mitigation actions on individual risks. The pre-mitigation plan is displayed in table 7.5. The risk maps are color-coded such that the severity of the risks is visualised. The objective is to construct mitigation plans for high level risks, which can be identified in the red and orange cells. However, mitigation plans for several risks in the yellow and green cells were also constructed despite their lower risk level. The mitigation plan and actions mentioned in section 7.2 and its effects on the risk levels can now be visualised in the post-mitigation risk map, as displayed in table 7.6.

**Table 7.5: Pre-Mitigation Risk Map.**

|                   |              |   |  |   |  |                                    |
|-------------------|--------------|---|--|---|--|------------------------------------|
| <b>Impact</b>     | Catastrophic | RSK-STR-06, RSK-STR-07, RSK-STR-13, RSK-COM-01, RSK-COM-06, RSK-EPS-07, RSK-ADC-09, RSK-AST-03, RSK-OBDH-01, RSK-OBDH-04, RSK-OBDH-06, RSK-OBDH-08, RSK-OBDH-12, RSK-OBDH-17, RSK-OBDH-24 | RSK-STR-01, RSK-STR-08, RSK-STR-10, RSK-STR-12, RSK-COM-04, RSK-EPS-01, RSK-EPS-06, RSK-TCS-02, RSK-TCS-04, RSK-TCS-08, RSK-TCS-10, RSK-ADC-10, RSK-ADC-11, RSK-PRO-02, RSK-PRO-03, RSK-AST-06, RSK-OBDH-22                              | RSK-STR-02, RSK-STR-09  | RSK-AST-01   |                                    |
|                   | Critical     | RSK-COM-08, RSK-ADC-08, RSK-PRO-04, RSK-OBDH-05, RSK-OBDH-10, RSK-OBDH-13, RSK-OBDH-16, RSK-OBDH-18, RSK-OBDH-23  | RSK-STR-03, RSK-STR-11, RSK-COM-07, RSK-EPS-02, RSK-PLD-03, RSK-PLD-04, RSK-TCS-01, RSK-TCS-05, RSK-ADC-01, RSK-ADC-03, RSK-ADC-05, RSK-PRO-05, RSK-OBDH-07, RSK-OBDH-11, RSK-OBDH-15, RSK-OBDH-21, RSK-OBDH-25, RSK-OBDH-27, RSK-SCH-11 | RSK-STR-05, RSK-COM-02, RSK-EPS-04, RSK-PLD-05, RSK-TCS-03, RSK-TCS-06, RSK-TCS-09, RSK-ADC-02, RSK-ADC-04, RSK-PRO-01, RSK-AST-04, RSK-AST-07, RSK-OBDH-02, RSK-OBDH-03, RSK-OBDH-14, RSK-OBDH-26, RSK-OBDH-28, RSK-SCH-04, RSK-SCH-07, RSK-SCH-08 | RSK-PLD-02, RSK-AST-02, RSK-SCH-01, RSK-SCH-02, RSK-SCH-03, RSK-SCH-05, RSK-SCH-10 | RSK-CST-03                         |
|                   | Marginal     | RSK-COM-05, RSK-ADC-07  | RSK-EPS-05, RSK-PLD-01, RSK-TCS-07, RSK-ADC-06, RSK-OBDH-09  | RSK-TCS-11, RSK-CST-02  | RSK-AST-05, RSK-SCH-06, RSK-SCH-09, RSK-CST-04                                     | RSK-STR-04, RSK-PRO-06, RSK-CST-01 |
|                   | Negligible   |   | RSK-EPS-03   | RSK-OBDH-19, RSK-OBDH-20  |  | RSK-COM-03                         |
|                   |              | Improbable  | Remote   | Occasional  | Probable   | Frequent                           |
| <b>Likelihood</b> |              |   |  |   |  |                                    |

**Table 7.6:** Post-Mitigation Risk Map.

|        |              |   |  |   |                                    |            |  |
|--------|--------------|---|--|---|------------------------------------|------------|--|
| Impact | Catastrophic | RSK-STR-06, RSK-STR-13, RSK-COM-01, RSK-EPS-07, RSK-AST-03, RSK-OBDH-01   | RSK-STR-02, RSK-STR-10, RSK-STR-12, RSK-COM-04, RSK-EPS-01, RSK-EPS-06, RSK-TCS-02, RSK-TCS-08, RSK-TCS-10, RSK-PRO-02, RSK-PRO-03, RSK-AST-06   |   |                                    |            |  |
|        | Critical     | RSK-STR-07, RSK-COM-06, RSK-COM-08, RSK-ADC-09, RSK-PRO-04, RSK-OBDH-06, RSK-OBDH-08, RSK-OBDH-10, RSK-OBDH-12, RSK-OBDH-16, RSK-OBDH-17, RSK-OBDH-18 | RSK-STR-01, RSK-STR-03, RSK-STR-05, RSK-STR-08, RSK-STR-09, RSK-STR-11, RSK-COM-07, RSK-EPS-02, RSK-EPS-04, RSK-PLD-03, RSK-PLD-04, RSK-TCS-01, RSK-TCS-04, RSK-TCS-05, RSK-TCS-06, RSK-TCS-09, RSK-ADC-01, RSK-ADC-02, RSK-ADC-03, RSK-ADC-04, RSK-ADC-05, RSK-PRO-01, RSK-PRO-05, RSK-AST-04, RSK-AST-07, RSK-OBDH-03, RSK-OBDH-07, RSK-OBDH-27, RSK-OBDH-28, RSK-SCH-04, RSK-SCH-08, RSK-SCH-11 | RSK-COM-02, RSK-PLD-02, RSK-AST-02, RSK-OBDH-02, RSK-SCH-01, RSK-SCH-02, RSK-SCH-03, RSK-SCH-07, RSK-SCH-10, RSK-CST-03 |                                    |            |  |
|        | Marginal     | RSK-COM-05, RSK-ADC-08, RSK-OBDH-04, RSK-OBDH-09, RSK-OBDH-13, RSK-OBDH-15, RSK-OBDH-23, RSK-OBDH-24  | RSK-EPS-05, RSK-PLD-01, RSK-PLD-05, RSK-TCS-03, RSK-TCS-07, RSK-TCS-11, RSK-ADC-06, RSK-ADC-10, RSK-ADC-11, RSK-OBDH-11, RSK-OBDH-14, RSK-OBDH-21, RSK-OBDH-22, RSK-OBDH-25, RSK-OBDH-26, RSK-CST-02   | RSK-PRO-06, RSK-AST-01, RSK-SCH-05, RSK-SCH-06, RSK-SCH-09, RSK-CST-04  | RSK-STR-04, RSK-AST-05, RSK-CST-01 |            |  |
|        | Negligible   | RSK-ADC-07, RSK-OBDH-05   | RSK-EPS-03   | RSK-OBDH-19, RSK-OBDH-20  |                                    | RSK-COM-03 |  |
|        |              | Improbable  | Remote   | Occasional  | Probable                           | Frequent   |  |
|        |              |   |  | Likelihood  |                                    |            |  |

## 8 Market Analysis

A market analysis is an essential part of the design process of a spacecraft. It will give insight on what opportunities there are, and how to make use of those opportunities. The market analysis per subsystem has already been presented in chapter 4. This chapter, the cost breakdown will be given, the return on investment is discussed, and finally the impact that NIBIRU may have on society will be addressed.

### 8.1 Cost Breakdown

*Contributors: Anton*

To get a good view on the cost of NIBIRU, several parameters must be investigated. In chapter 4, the cost per subsystem can be viewed. This is summarized in table 8.1. Note that the cost for payload are now estimated at 0 euros. This is because it is assumed, just like stated in section 4.1, that the instruments are going to be paid for by the companies and countries producing them.

**Table 8.1:** Cost per Subsystem on NIBIRU

| Subsystem                    | Cost in M€    |
|------------------------------|---------------|
| Payload                      | 0             |
| EPS                          | 278.6         |
| Telecommunications           | 38.7          |
| ADCS                         | 2.09          |
| Propulsion                   | 30            |
| Thermal Control              | 0.55          |
| Structures and Mechanisms    | 0.0134        |
| On Board Data Handling       | 17.3          |
| <b>Total subsystem costs</b> | <b>367.25</b> |

A total cost for the spacecraft components would then be 367.25 million euros. This is however not the

only cost component, since this spacecraft has to be produced and tested as well. For this, New Horizons was used as a reference. This spacecraft cost €340M in total to develop.<sup>1</sup> Since NIBIRU is a little bit more complicated, with its kickstages, and inflation has happened over the period of 2006-2024, a development cost of €500M will be taken as first estimation.

Next, the ground operations and Deep Space Network usage is evaluated. For the ground operation, New Horizons can again be used, since it is known that in 12 years, New Horizons cost €215.6M in total, making it cost almost €M18 per year. This is again accounted for inflation, and a cost of €M26.56 per year is a good estimated cost for NIBIRU in operations. NIBIRU has to operate for 50 years, making the total operational costs over these 50 years €1328M. The ground station Deep Space Network also is expensive to get communication time to, about €4650,- per hour. As for now, a planning of 120000 total contact hours has been scheduled for NIBIRU, making the total ground station costs €558M.

Finally, a risk mitigation budget is set up, as safety factor, of 25% of the total budget, so €M688.3[40]. The launch is not included in the budget given, however it is useful to state that Starship is planning to cost €1M per launch.<sup>2</sup> Since the mission will need 2 launches, 1 for the payload and one refuelling mission, this adds up to €2M. This makes a total budget that can be seen in table 8.2, with a final total mission cost of €M3441.6.

**Table 8.2:** Total Costs NIBIRU

| Segment              | Cost in M€    |
|----------------------|---------------|
| Components           | 367.25        |
| Design & Development | 500           |
| Ground Segment       | 558           |
| Operations           | 1328          |
| Safety Budget        | 688.3         |
| <b>Total costs</b>   | <b>3441.6</b> |

This does not comply with the requirement PL9-STK-ESA-10: The mission cost shall not exceed €B1.5 (FY 2024), excluding launch cost. This can however be negotiated with the stakeholder. This was done in an extensive session and the idea of including other space agencies came up. It is because of this that NIBIRU will also contact NASA in the following steps to try to collaborate and find a way to fund the whole mission. Note that for now, if it is decided to only do the measurements at Planet 9, only 5 hours of work needs to be done, making the operational costs a lot lower. This can result in a mission that meets the requirement of €B1.5 (FY 2024), however has way lower value in return, this will be further elaborated on in the next section.

## 8.2 Return on Investment

*Contributors: Anton*

It is important that the Return of Investment (RoI) is evaluated for NIBIRU such that a good estimate for the cost and market share can be made.

### 8.2.1. Market volume & share

The spacecraft market is one of the fastest growing markets in the world, with an expected value in 2032 of 10.4 billion US dollars, and double the amount of unmanned spacecraft being launched.<sup>3</sup> A budget of 3.5 billion euros was assigned for NIBIRU, however this does include ground operations as well, so this is not all contributing to the 10.4 billion US dollars. Simultaneously, the amount space exploration missions is also growing. More deep space spacecraft are being developed, like New Horizons, LUCY, and JUICE, creating momentum for this market and thus expanding it. At the moment, there is no mission prepared to go to Planet 9, so this mission will be a first in its kind. There have been missions to the Kuiper Belt, however not as much further as NIBIRU is designed for. This can give various new insights on the forming of the solar system.

<sup>1</sup>URL: <https://www.planetary.org/space-policy/cost-of-new-horizons> [cited 13 June 2024]

<sup>2</sup>URL: <https://payloadspace.com/payload-research-detailing-artemis-vehicle-rd-costs/> [cited 17 June 2024]

<sup>3</sup>URL: <https://www.alliedmarketresearch.com/spacecraft-market-A10721> [cited 13 June 2024]

### 8.2.2. Value of acquired data

The data NIBIRU will bring back from Planet 9 will be extremely valuable, but with the amount of risk involved with this mission it cannot be the only science return. With the mission being primarily funded by ESA/NASA the public essentially pays for the mission and will thus demand return on their investment. If the mission's (risky) payoff is only at some point 50 years in the future it will be hard to get the public motivated and involved with the mission. Through the use of additional instruments that can be used en-route a steady stream of data for the scientists and interesting facts for the public are guaranteed. The more tangible returns of the mission are discussed in section 8.4.

## 8.3 Societal Impact

*Contributors: Anton*

The societal impact of a deep space mission to hypothetical Planet 9 could be profound, influencing various aspects of science, education, technology, and culture. NIBIRU, designed to research the mass, radius, and atmospheric composition of Planet 9, and with secondary objectives including investigations of Jupiter, the Kuiper Belt, and the Heliopause, would have far-reaching implications.

### 8.3.1. Scientific advancement and knowledge

The discovery and exploration of Planet 9 would represent a monumental leap in our understanding of the solar system. Determining its mass, radius, and atmospheric composition would help scientists refine models of planetary formation and evolution. The data collected could provide insights into the conditions required for planet formation and the potential for life in the outer reaches of our solar system.

Additionally, studying Jupiter during the mission's slingshot maneuver would yield valuable data on its atmosphere, magnetic field, and potentially its moons. This information could enhance our understanding of gas giants, which are common in other star systems. The Kuiper Belt and Heliopause investigations would shed light on the boundary regions of our solar system, contributing to our knowledge of the interstellar medium and the forces shaping our cosmic neighborhood.

### 8.3.2. Educational and inspirational value

A mission to Planet 9 would captivate the public's imagination, inspiring future generations of scientists, engineers, and explorers. Educational programs and outreach initiatives could leverage the excitement surrounding the mission to promote STEM (Science, Technology, Engineering, and Mathematics) education. Schools and universities could develop curricula based on the mission's findings, fostering a deeper interest in space science and technology.

The mission could also stimulate international collaboration and competition in space exploration. Countries worldwide might increase investment in their own space programs, leading to a global surge in space-related research and development. This could ultimately result in more rapid technological advancements and a greater collective knowledge base.

### 8.3.3. Technological innovation

Deep space missions drive technological innovation as they require advanced solutions to challenges in propulsion, communication, power generation, and materials science. Developing the necessary technology for the Planet 9 mission would likely result in spinoffs that benefit other industries. For example, advancements in propulsion systems could improve transportation technologies on Earth, and innovations in remote sensing and autonomous systems could enhance applications in environmental monitoring, disaster response, and more.

### 8.3.4. Economic impact

The mission would likely stimulate economic activity, creating jobs in aerospace engineering, manufacturing, and related fields. Companies contracted to develop the mission's components would benefit from the investment, and the technological advancements could lead to the creation of new markets and industries. Furthermore, the global interest in such a mission could boost the space tourism industry and related sectors.

### 8.3.5. Cultural and philosophical implications

Exploring Planet 9 would prompt reflections on our place in the universe, much like past space missions. Discovering new planetary environments and potentially habitable conditions far from Earth could influence our philosophical and existential understanding of life and the cosmos. The mission might also encourage a renewed sense of unity and cooperation among humanity as we pursue shared goals in space exploration.

### 8.3.6. Environmental considerations

While space missions have a relatively small direct impact on Earth's environment, the technologies developed could have environmental applications. For instance, advancements in solar power and energy-efficient systems could contribute to sustainable practices on Earth. Additionally, the mission could raise awareness of the importance of protecting our planet by highlighting the fragility and uniqueness of Earth in the vastness of space.

## 8.4 Market Gap

*Contributors: Anton*

A market gap means looking at the specific market you are trying to target and seeing the opportunities that have not been capitalised on. In this section, these gaps will be explained, and the opportunities will be highlighted.

### 8.4.1. Deep space missions

Since NIBIRU is classified as a deep space mission, it is important to know the competitors in this field. Throughout this report, there have been a few examples already, like New Horizons, Voyager and Cassini. The main objectives will be summarized below:

- New Horizons: investigate Pluto system and the Kuiper Belt.<sup>4</sup>
- Voyager 1 & 2: to extend the NASA exploration of the solar system beyond the neighborhood of the outer planets to the outer limits of the Sun's sphere of influence, and possibly beyond.<sup>5</sup>
- Cassini: characterize Saturn as planet, its rings, its magnetosphere, and icy moons.<sup>6</sup>
- JUICE: to characterise Jupiter's moons as both celestial bodies and possible habitats for life (either past or present).<sup>7</sup>

These missions show that there has never been a mission planned further than the Kuiper Belt. NIBIRU will however characterize the Heliopause and then move on to Planet 9 as well. It is therefore the first in its kind. Voyager did reach the Heliopause in 2012 already, however it was not designed to do measurements here.<sup>8</sup> Voyager was originally only scheduled to last 5 years,<sup>9</sup> however it is already lasting 47 years, with possibly extension until 2036.<sup>10</sup>

### 8.4.2. Durability

No space mission has ever been designed for to last over 50 years, with one of the longest before this being New Horizons with 'only' 10 years original lifetime. This means that an incredible amount of data can be gathered. NIBIRU is also intending to make a flyby at the Sun, and this is also quite an unique opportunity to do measurements here. No spacecraft has ever performed a solar slingshot, so NIBIRU will be a first in this here as well.

All this means that NIBIRU has to be extremely reliable, for example to keep power to distribute to all components. Normally, spacecraft instruments are not made to survive 50 years in space. Due to radiation and all sorts of other influences, this is normally not done. However, NIBIRU shall make sure this is

<sup>4</sup>URL <https://astrobiology.nasa.gov/missions/new-horizons/> [cited 14 June 2024]

<sup>5</sup>URL <https://voyager.jpl.nasa.gov/mission/interstellar-mission/> [cited 14 June 2024]

<sup>6</sup>URL <https://sci.esa.int/web/cassini-huygens/2085-objectives/> [cited 14 June 2024]

<sup>7</sup>URL [https://www.esa.int/Science\\_Exploration/Space\\_Science/Juice/The\\_science\\_Juice\\_s\\_key\\_objectives\\_a\\_t\\_Jupiter](https://www.esa.int/Science_Exploration/Space_Science/Juice/The_science_Juice_s_key_objectives_a_t_Jupiter) [cited 14 June 2024]

<sup>8</sup>URL <https://voyager.jpl.nasa.gov/mission/interstellar-mission/> [cited 14 June 2024]

<sup>9</sup>URL <https://voyager.jpl.nasa.gov/frequently-asked-questions/fact-sheet/> [cited 14 June 2024]

<sup>10</sup>URL <https://voyager.jpl.nasa.gov/frequently-asked-questions/> [cited 14 June 2024]

feasible for the planned mission.

### 8.4.3. Communication

NIBIRU will travel further than any spacecraft has ever done before. This means that it will also have to communicate further than any spacecraft ever. This provides an opportunity to have a new look at traditional communication methods for spacecraft. Foldable antennae is an upcoming technology which can be tested in the implementation for NIBIRU.

In conclusion, the market gap that NIBIRU will fill is exploring in detail the outer Kuiper Belt, the Heliopause, interstellar space, and Planet 9. It can provide a platform for new extremes in reliability, duration, and communication.

## 9 Sustainable Development Strategy

Sustainability can be defined as “The ability to meet the needs of the present at a global scale without compromising the ability of future generations to meet their own needs” [2]. In other words, sustainability is about maintaining or improving environmental, social, and economic health over time without depleting resources or harming ecosystems. In section 9.1, the sustainability options considered for the design of NIBIRU are addressed. Subsequently, in section 9.2, the contribution that NIBIRU can have to sustainability is explained.

### 9.1 Sustainability in Design

*Contributors: Anton, Iván, Isha*

This section explores various aspects of the mission and assesses how sustainability principles can be integrated into each of the mission’s phases. For this, the launcher, propulsion, power generation, material selection, trajectory and subsystem components were considered to ensure a sustainable mission.

#### 9.1.1. Launcher

The launch is a critical part of the mission, and the chosen launcher significantly influences the design. Environmental impacts vary based on the launcher; for instance, reusable launchers like the Falcon Heavy or Starship are more sustainable compared to expendable rockets like the Ariane 6. In the end, the team selected Starship as the final launcher due to its full reusability and higher payload capacity. This choice also allows for a potential shared ride if NIBIRU does not use all the space in the payload bay, improving sustainability by reducing the number of launches.

#### 9.1.2. Propellant and power generation

The propellant for Starship, determined by SpaceX, is methane.<sup>1</sup> Although methane is environmentally harmful, it cannot be changed in the design. However, the fuel for the kickstage can be chosen to be more consciously. Currently, the team has chosen chemical propulsion, namely nitrogen tetroxide (N<sub>2</sub>O<sub>4</sub>) and monomethylhydrazine (MMH), as detailed in section 4.6.5. While this propellant is toxic, it will be burned far from Earth, ensuring no toxic gases reach our atmosphere. In the future, if more sustainable fuels achieve the required densities and DeltaV to reach Planet 9 within the 50-year timeframe, they should be implemented in the project plan immediately.

Regarding power generation, two enhanced Multi-Mission RTG (eMMRTG) developed by NASA will be employed, as explained in section 4.2.1. For these, Plutonium-238 will be used to generate power. This radioactive isotope produces mainly alpha-particle radiation, which is easy to shield from, and little gamma radiation, making it safer to handle and deal with compared to other isotopes. In terms of safety, this material can be used safely in a ceramic form that is not easily absorbed by humans or animals in the event of material release.<sup>2</sup>

---

<sup>1</sup>URL <https://www.space.com/spacex-starship-rocket-launches-environmental-impact> [cited 14 June 2024]

<sup>2</sup>URL <https://science.nasa.gov/planetary-science/programs/radioisotope-power-systems/faq/> [cited 18 June 2024]

### 9.1.3. Material and manufacturing

Material selection was primarily based on strength, stiffness, as well as cost and density. These were the key criteria for the trade-off. However, sustainability has also been taken into account. Factors related to material selection and manufacturing, such as emissions, toxicity, mining of raw materials, and lean manufacturing (the continuous elimination of waste to create value) in section 10.1.2 are considered. For both the kick stages and the bus of NIBIRU itself, Aluminium 2024-T36 will be used.

Aluminium is one of the most plentiful resources on this planet. It is also highly sustainable, as it is almost endlessly recyclable.<sup>3</sup> However, it is a significant source of CO<sub>2</sub> emissions, contributing to almost 3% of the world's direct industrial CO<sub>2</sub> emissions.<sup>4</sup> Nonetheless, over the last decade, the global average direct emissions intensity of aluminium production has decreased moderately, at a rate of around 2% per year. However, under the Net Zero Emissions by 2050 Scenario, this drop must accelerate significantly, reaching approximately 4% per year by 2030. This will increase the sustainability of the mission during manufacturing and production of NIBIRU.

### 9.1.4. Mission operations

During NIBIRU's journey to Planet 9, a control center must be active to maintain a communication link between Earth and the spacecraft. This is one of the factors that significantly influences the sustainability of the project. All the computers and hardware used need to be powered. As of 2024, this is still primarily done by fossil fuels, which are very harmful to the environment, especially given the mission's duration of 50 years. As a team, we can advocate for the NASA Deep Space Network to switch to or increase the use of green fuels, ensuring that ground operations are more sustainable.

### 9.1.5. Trajectory and end-of-life

Choosing a mission trajectory impacts the amount of propellant needed and thus the environmental footprint. There is a significant difference in propellant usage between a direct flight and the use of a flyby or gravity assist. Additionally, the mission duration will also have an effect on propellant usage. EoL strategies are a primary part of the sustainability strategy. Preventing contamination of Planet 9 by safely stowing the spacecraft in a "graveyard" orbit or flinging it off into deep space is preferred over deorbiting the spacecraft and crashing into the planet.

The weighting of sustainability in trajectory planning is quite low; the mission duration and objectives will prioritise quicker routes despite higher propellant use. In contrast, sustainability is heavily weighed when choosing the EoL strategy, as it could have a significant impact on Planet 9 depending on the mission's findings. Hence, a fly-by has been chosen as the preferred option for reaching Planet 9. If an orbit were chosen, the fuel needed in the kickstages would increase by a significant amount, raising the total DeltaV required, and thus increasing the fuel needed from Starship. By choosing a flyby, NIBIRU can travel even further than Planet 9 and perform additional measurements, adding to the value of the mission.

### 9.1.6. Off-the-shelf components

Finally, it is important to emphasize that the use of selected off-the-shelf components is more viably sustainable than the development of new technologies, which require a high amount of resources to be invested. For the NIBIRU mission, multiple off-the-shelf components have been considered for the different subsystems, leveraging on reusability and fomenting sustainability. Additionally, the main advantages of off-the-shelf components are their immediacy and cost-effectiveness. They can be deployed quickly and are generally less expensive upfront than custom, new technological components.

## 9.2 Product Contribution to Sustainability

*Contributors: Anton, Iván*

The contribution of a spacecraft mission to sustainability might not be as obvious and straightforward as applications in aircraft design that lead to increased sustainability, like research and use of alternative fuels. However, the mission to Planet 9 can contribute to sustainability. There are a number of potential pathways through which such missions could support broader sustainability goals. These are outlined below.

<sup>3</sup>URL <https://www.duration.co.uk/AluminiumSustainability.asp> [cited 18 June 2024]

<sup>4</sup>URL <https://www.iea.org/energy-system/industry/aluminium> [cited 18 June 2024]

### 9.2.1. Technology development

Technological advancements developed for the mission to Planet 9 could have applications back on Earth for promoting sustainability. For instance, innovations in RTG usage or energy efficiency can be adapted for terrestrial use. NIBIRU’s payload instruments have been leveraged by increasing their usability to take different types of measurements and last the whole mission’s lifetime. This could have an impact on instrument efficiency and how to make those used on Earth more sustainable.

### 9.2.2. Scientific research & data

The mission to Planet 9 could gather critical data about its climate, which scientists in Earth can use to help improve climate models. Understanding Planet 9’s atmosphere and geological history can provide insight into Earth’s future and lead to mitigation strategies to alleviate environmental issues.

### 9.2.3. Inspiring policy & international cooperation

A successful mission to Planet 9 could foster global cooperation and inspire policies that prioritise sustainable development. As space exploration inherently has a collaborative nature, it requires international partnerships that could potentially lead to an improved management of global resources.

## 10 Project Design & Development

This chapter covers the aspects of the project that are relevant to the post-DSE activities and logistics. In section 10.1 the post-DSE activities such as more detailed design, manufacturing, testing and integration are covered in detail. Additionally a post-DSE project Gantt chart was constructed, shown in figure 10.5. In section 10.2 the project’s approach to reliability, availability, maintainability and safety (RAMS) are outlined. In section 10.3 the different mission phases from launch to EoL are covered in detail.

### 10.1 Activities after DSE

*Contributors: Jim, Anton*

After the DSE has been completed a massive effort will start, involving thousands of people working for 10 years to ensure the spacecraft is ready for launch in 2038. First the design has to be worked out into greater detail, after which the manufacturing, testing and integration phases can begin. A project design & development logic diagram can be seen in figure 10.1. For a better view of the project timeline the post-DSE gantt chart was made, using JUICE’s project plan as a reference, seen in figure 10.5 at the end of the document [89].

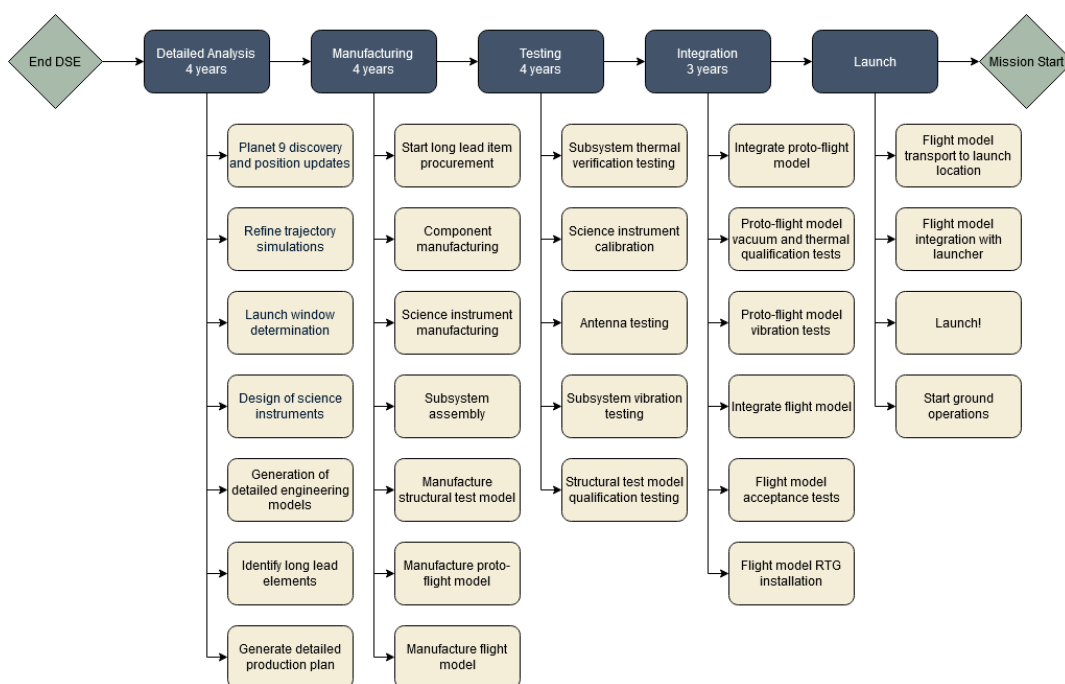


Figure 10.1: Project Design & Development Logic

### 10.1.1. Detailed analysis

More detailed design work is needed to finalise the mission. For this post-DSE phase roughly 4 years are needed based on the JUICE mission planning [89]. Updates on Planet 9's probable location during this time or even its potential discovery will greatly influence the design. Updated trajectory simulations have a large impact on the trajectory and launch window, as well as thermal, ADCS, propulsion and communication subsystems. During this phase a tender will be brought out, inviting research institutions to design the science instruments. More resources will allow for detailed engineering models and analysis methods to be used, aiding in the design. Components with a long lead time such as RTGs and components needing specialised manufacturing tools have to be identified to limit delays in the manufacturing process. Finally a detailed production plan must be generated such that the multitude of components can be manufactured, assembled and integrated.

### 10.1.2. Manufacturing

The manufacturing process of NIBIRU will be quite extensive, since there are a lot of separate parts, including the kick-stages. The manufacturing process will be divided into the bottom kickstage, ENKI, the upper kickstage, ENLIL, and NIBIRU itself. For all manufacturing plans the concept of lean manufacturing will be used. 4 Years are again assigned for the manufacturing phase, similar to the JUICE schedule. Manufacturing of long lead items can already begin during the previous phase, as seen in figure 10.5.

#### Production techniques

For manufacturing NIBIRU and its kickstages, multiple production techniques can be applied. They are listed below, along with an explanation and why they could be used in the production process.

- **Computer Numerical Control (CNC) machining:** This is a way of machining that uses computer models, like a CAD model, to specifically construct a product. This can be used very well in the case of NIBIRU, since all subsystems have design their system in CAD.
- **Drilling:** This can be used to drill holes in a sheet of material, for example aluminium. These holes can then be used for rivets or bolts, to connect the plates.
- **Turning or milling:** This can be used to give indents or other shapes in sheets or plates. This is done to give a desired shape to the outside of the plates.
- **Tungsten Inert Gas (TIG) welding:** This type of welding is often used for welding aluminium.<sup>1</sup> It works by using a non-consumable tungsten electrode to create an arc that melts the base metal, and argon gas shields and cools the electrode and weld puddle to produce clean, strong welds.

#### NIBIRU

The NIBIRU spacecraft is the most complex element of the mission. A plethora of highly specialised components are needed to make the mission work. Thus, companies with the technical know-how and equipment are needed. Thales Alenia Space and Airbus are logical partners to lead the manufacturing process, as most recent ESA missions have been primarily designed and manufactured by them [90]. Many more companies/institutes are of course involved, but this analysis aims to be high-level.

To allow for sufficient testing of the hardware, without subjecting flight hardware to potentially damaging tests, several models of the spacecraft are manufactured. First a breadboard model (BBM) is constructed to test the layout during development. Next an engineering model (EM) and structural and thermal model (STM) are made. These are made early and subjected to rigorous tests to validate the design work. Because of this they are less detailed and cheaper than the actual flight hardware. Next the proto-flight model (PFM), flight model (FM) and spare flight model (FMS) are constructed [90]. These are identical and include all components necessary to complete the mission, apart from the RTGs.

Components for these different models will be manufactured by the different companies led by the prime contractor. Assembly of the subsystems into the different models is done at dedicated facilities of the prime contractor, such as AIRBUS' Toulouse plant. Here they are integrated and tested before moving to different testing locations.

---

<sup>1</sup>URL <https://www.millerwelds.com/resources/article-library/tig-it-how-a-tig-welder-works-and-when-to-tig-weld> [cited 14 June 2024]

### **Energetic NIBIRU kick interstage**

The lower kickstage that will be ignited first during the Jupiter slingshot is called ENKI: the Energetic NIBIRU Kick Interstage. This kickstage will be made out of an aluminium cylinder, covered by MLI, with a diameter of 2.32 meters, and 7.23 meters high. Next to this, it will feature 34 thrusters, which will be off-the-shelf, so they will just have to be assembled in the total structure. The outer structure of ENKI will be assembled and produced in the same facility as where NIBIRU itself will be assembled to a final product.

Within the cylinder, above the thrusters, the fuel tanks will be present of course. This has to be manufactured as well. The fuel tanks will be pressure vessels, one for the hydrazine, one for the oxidizer, and one for the pressure gas. These will be produced in the same facility as the outer structure of ENKI.

### **Efficient NIBIRU long-range interstage launcher**

The upper kickstage that will be used is ENLIL, the Efficient NIBIRU Long-range Interstage Launcher. It will be used at the slingshot around the Sun, to give direct trajectory to Planet 9. It also will consist of a cylinder outer structure, made out of aluminium, covered with MLI. For manufacturing, the same set up as for the other kickstage will be used, since this stage also used 34 thrusters to propel NIBIRU. ENLIL will be 7.38 meters tall, and it has a diameter of 2.37 meter. This requires a minor adjustments in the dimensions, however all other details will remain the same.

### **10.1.3. Testing**

The testing phase begins as soon as the first major components are assembled. Again 4 years are dedicated to this, but testing and verification does not stop even during the integration phase. Testing on the different models that are constructed often happens concurrently, with smaller sub-assemblies being subjected to a large variety of tests. To avoid going into too much detail, only the main tests performed on the models mentioned in section 10.1.2 will be discussed.

The engineering model (EM) is subjected to rigorous structural tests. These include shock, sine- and random vibration tests. The EM is relatively expendable, as it is much quicker and cheaper to produce than (near-)flight hardware. The structural and thermal model (STM) is subjected to qualification tests related to the mechanical and thermal design. In general, qualification tests are designed to stress the hardware, meaning there is a risk of damage. The STM will verify that the thermal and mechanical design is sound. Next the proto-flight model (PFM) undergoes similar qualification tests to the STM, as well as acceptance tests. These tests are designed to test the functionality of the hardware without stressing it too much, reducing the risk of damage. The flight model (FM) and spare (FMS) are both only subjected to acceptance testing [90].

Performing certain types of testing requires dedicated facilities. ESA's ESTEC facility in Noordwijk has many of the needed facilities. The testing facilities at ESTEC can accommodate the NIBIRU spacecraft but not the fully integrated stack, including the kick stages. The facilities include shaker tables to do vibration testing, an acoustic test chamber to simulate the acoustic loads experienced during launch, shock test bench to simulate shocks (from e.g. stage separation), the Large Space Simulator for thermal vacuum testing, electromagnetic compatibility testing chamber and an antenna test range.<sup>2</sup>

### **10.1.4. Integration and launch**

The PFM, FM and FMS are all fully integrated and will undergo acceptance testing of all the subsystems. Once fully integrated and qualified, the FM and spare will be ready for launch. Starship is expected to launch from Kennedy Space Center so the different models and their kick stages have to be transported there. This can be done either by ship or by air. At most a year before launch the RTG must be installed on the FM, as otherwise too little power will remain for the Planet 9 operations. After the final checks are completed, the spacecraft and kick stages are fueled and integrated with each other. Due to the unusual nature and size of this stack, a specialised facility will be necessary for this. It is currently unknown what facilities will be present at SpaceX's expanded KSC site, but it is expected that facilities capable of installing a payload of Starship's maximum size will be made available.

---

<sup>2</sup>URL <https://technology.esa.int/lab/test-centre> [cited 14 June 2024]

## 10.2 RAMS Analysis

*Contributors: Pepijn*

To ensure that the design has been made to the correct standards a Reliability Availability, Maintainability and Safety (RAMS) analysis will have to be performed. This is done to ensure that the final design is reliable enough to survive the entire mission lifetime. Furthermore, it helps the manufacturing and assembly phases to guarantee enough components are available so that possible faults can be maintained as soon as possible. Lastly, safety ensures that the operators who manufacture and assemble the spacecraft are not exposed to unnecessary risks.

### 10.2.1. Reliability

The ECSS describes reliability to be the: “ability of an item to perform a required function under given conditions” [91]. As NIBIRU will make use of mostly COTS components, the determination of the exact reliability of the spacecraft is difficult<sup>3</sup>. Companies typically do not share all of their data regarding reliability in publically available materials.

The datasheets of the payloads do not show the reliability [16, 18, 21, 22]. However, all the payloads have been used on previous missions. They have been used successfully so the assumption will be made that they will also work for the NIBIRU mission. The payloads will also undergo an extensive testing campaign to further show that they will be reliable in the NIBIRU mission profile.

NASA is very secretive about the exact design of the eMMRTGs as they do not want design specifics to get released in fear of people building their own nuclear reactors, which means that reliability data is limited [20, 29]. As there are a limited number of available eMMRTGs it will not be possible to give them the same testing campaigns as will be used for other components. It will be assumed that the degradation rate of 2.5% per year will remain stable over the entire mission duration [20, 29]. Given that the Voyager missions are also using an RTG which is still operational although its designed lifetime has passed a long time ago, it can be assumed the same will hold for NIBIRU. Furthermore, the eMMRTG uses Pu-238 which has a half-life time of 87.7 years and the eMMRTG does not make use of any dynamic moving parts to convert the thermal energy to electrical energy, it is thought that this is a valid assumption. The PCDU will have to be extensively tested to determine the reliability as it currently does not have any information on that. It will not only undergo the vibrational and TVAC testing but also charge-discharge cycles simulating the different modes the spacecraft will be in. The batteries’ reliability depends on the number of power cycles they have to endure. As will be explained in section 10.3 the batteries are only used once the satellite arrives at Planet 9 limiting the number of cycles to around 750 per battery, which ensures a good lifetime of the battery.

The communications components also do not have any documentation regarding their reliability. These will be tested for vibrations, TVAC again. Now also use will be made of the ESTEC Antenna Test Facility to determine the quality and reliability of the two antenna dishes.

The ADCS makes use of four different components, two types of thrusters, one IMU and a star sensor. The star sensor has a failure in time (FIT) of 172 per billion hours [55]. This can be converted to mean time between failures (MTBF) in hours with the following formula [33].

$$MTBF = 1000000000 \cdot \frac{1}{FIT} \quad (10.1)$$

This leads to an MTBF of 5813953 hours, which is approximately 13 times longer than the mission duration. However, just to be safe 3 redundant pairs which ensure enough reliability and allows the attitude to be determined from multiple sides. The two thrusters can be fired for multiple hours, but they will only be used for impulse shots which means that they are used for a couple of seconds [92, 93]<sup>4</sup>. So the thrusters are also safe to use for the mission duration. The final component used are the IMUs which are commercially of the shelf from Honeywell [56]. Unfortunately, they do not share the exact reliability of the IMU, so before the IMU is used in the spacecraft it will go through an extensive testing campaign to

<sup>3</sup>According to an ESA RAMS specialist in a private conversation it sometimes is even excluded in the reliability analysis and only covered in the extensive testing campaigns.

<sup>4</sup>URL <https://www.space-propulsion.com/spacecraft-propulsion/apogee-motors/> [cited 14 June 2024]

determine the reliability of the component. Tests that will be performed are vibrational, TVAC testing and an accelerated lifetime test to quickly get the reliability of the IMUs. Additionally, for redundancy purposes, 5 IMUs will be taken on board, which will be used consecutively to allow the entire spacecraft to keep an IMU in operation for the entire mission.

The kickstages will make use of the 400N model No S400-15 apogee motor of the ArianeGroup [94]. It is qualified to survive a single burn of up to 1.85 hours and a total burn time of 8.5 hours with a maximum of 135 burn cycles [94]. As the thruster will only be used for a short while it will be assumed that this thruster is reliable as well, similar to the thrusters used for the ADCS.

The thermal system components also do not provide reliability [95]. So the thermal system will also have to show its reliability in an extensive TVAC testing campaign.

The structure of the satellite is self-made by the NIBIRU team so it will have to undergo extensive testing to qualify and to be able to determine numbers like reliability. This will be done by placing the entire structure in a vibrational test facility where the structure will endure extreme loads to ensure that the structure is safe to use.

The OBDH has reliability in their datasheet of 0.9707 for one year [96]. This would be problematic as this would then mean a reliability of only 0.226 after a 50 year mission. However, the OBDH has been used on the New Horizons mission<sup>5</sup> and NASA is currently planning on extending operations until 2028<sup>6</sup> which is when New Horizons will leave the Kuiper Belt. Additionally, newer estimates put the maximum lifetime of the New Horizons mission up until 2050<sup>6</sup>, as it launched in 2006<sup>7</sup> this means the lifetime of the New Horizon mission and also its OBDH is estimated to be 44 years. As the NIBIRU mission will be longer and to decrease the risk of something happening to the OBDH one additional OBDH will be taken on board of the spacecraft to ensure reliable operations from the OBDH.

### 10.2.2. Availability

The availability is defined as the “ability of an item to be in a state to perform a required function under given conditions” [91]. This means that the components used on board of the spacecraft should be available and well-maintained. As most of the components are COTS they will all be bought in at least threefold to be able to make an engineering model, a qualification model and a flight model. The first will be used to run tests on while the flight model is in space before for example a software update is sent. The second is used to perform all qualification tests that the spacecraft will have to do. The last one will be the actual satellite that will be sent to space. The maintainability will be discussed in the following section.

### 10.2.3. Maintainability

The ECSS describes maintainability as the “ease of performing maintenance on a product” [91]. Companies that will provide the components generally also provide documentation which have more details than are publically available before buying the components. This normally includes information on how to maintain the components, otherwise the responsible companies can be contacted to ask them for help in maintaining it. The last possible option would be sending the component back to the manufacturer who will then perform the necessary repairs. Cheaper components, like connectors, will be bought in bulk to ensure quick maintenance work, however, the bigger components like the payloads, or bigger components of the spacecraft are too expensive to buy more for then the 3 that are used on the different models.

### 10.2.4. Safety

The last part of the RAMS analysis is the safety which is described as the “state where an acceptable risk is not exceeded” by the ECSS” [91]. The safety of the people working on manufacturing and assembling the spacecraft will be ensured by making use of the following Hazard Analysis and Safety standards [97, 98]. The production plan will be analysed in detail to determine all of the potential problems that may

---

<sup>5</sup>URL <https://www.eoportal.org/satellite-missions/new-horizons#spacecraft-systems-and-components> [cited 14 June 2024]

<sup>6</sup>URL <https://www.scientificamerican.com/article/beyond-pluto-new-horizons-gets-a-reprieve-from-nasa/> [cited 14 June 2024]

<sup>7</sup>URL <https://science.nasa.gov/mission/new-horizons/> [cited 14 June 2024]

arise. Furthermore, all steps will be described in detail to ensure that the operators cannot make mistakes. However, even with a high level of detail it is not possible to get rid of all the possible hazards so with the help of the standard these will be identified [97]. After this has been identified it will be required to come up with a strategy to limit risks and ensure the safety of the operators. Every hazard has a different approach to improving safety, the mitigation strategy will be decided with the help of the safety standard [98].

### 10.3 Operations and Logistics

*Contributors: Pepijn*

The spacecraft will have to operate at a number of stages. These are defined as the operations and logistics of the spacecraft which will be the topic of this section. Figure 10.2 shows the operational concept that will be used for the NIBIRU mission. Each phase will be explained in more detail below. The timeline can be seen in figure 10.5.

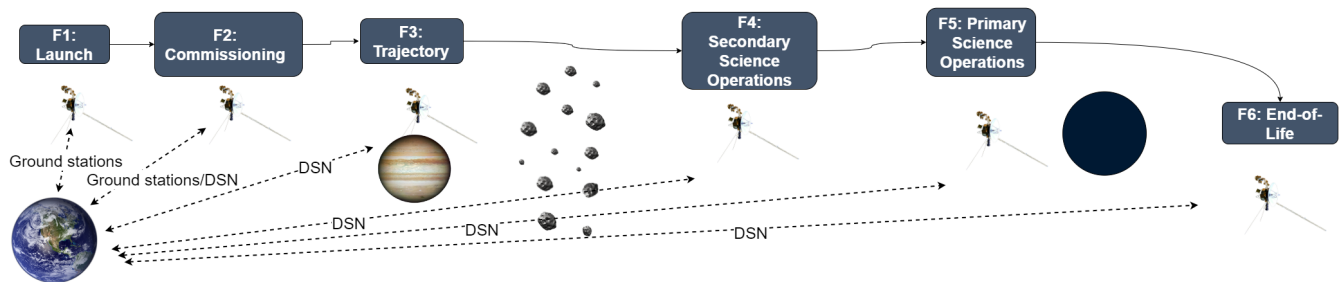


Figure 10.2: Operations Performed by the NIBIRU Spacecraft, Image is not to Scale.

#### 10.3.1. Launch

The spacecraft will be launched with a SpaceX Starship. Starship will go to a LEO of 300 km where it will then be refuelled by another Starship launcher to ensure that the rocket with the NIBIRU spacecraft can provide as much  $\Delta V$  as possible which is an option that SpaceX provides.<sup>8</sup> After the Starship has been refuelled it will start the journey to Jupiter, once all of the propellant has been used the NIBIRU spacecraft will separate from the launcher.

#### 10.3.2. Trajectory

After launching the satellite the complicated trajectory to reach Planet 9 within 50 years will start. This will be done with the help of two kick-stages which separate after they are used. The ENKI will fire at Jupiter launching the spacecraft back to the Sun, ENKI will separate once all propellant has been used. Once the spacecraft reaches the Sun the ENLIL kick-stage will be used, after all propellant is used both the kick-stage and the heat shield will separate. Then the spacecraft will be on its way towards Planet 9 which it will reach in 49.5 years, after launch from Earth. On the way the spacecraft will be performing safety checks, and study objects it will pass. This will be explained further in the following subsections.

#### 10.3.3. Commissioning

While NIBIRU is on its way to Jupiter, the spacecraft will commission itself to be able to start its operational life. The spacecraft will power cycle all of the components and the OBDH will log all of the housekeeping data which will include the health status of the components. This will then be communicated back to Earth, with the secondary antenna where the operators in the ground station will compare the telemetry with the data that was achieved by the tests performed on Earth on the engineering model. When the data is similar it will be assumed the systems are operating correctly, if not the ground station crew will perform additional tests and troubleshoot from the ground while the spacecraft is on its way to Jupiter. To finally officially validate the functioning of the payloads they will take images of Jupiter which will then be compared to known images to see if the payloads are set up correctly. Once all of this is comparable the first stage of commissioning will be successfully completed.

<sup>8</sup>URL <https://www.spacex.com/vehicles/starship/> [cited 12 June 2024]

As was mentioned earlier the primary antenna will remain in the folded position to decrease the size of the heat shield when slingshotting around the Sun. Additionally, it will decrease the risk of having micrometeorites impact the primary antenna while passing through the Kuiper Belt. Hence the primary antenna will only be deployed after the spacecraft has passed the Kuiper Belt. The secondary antenna still functions at that distance so the ground station operators will send the command that the spacecraft can unfold the primary antenna. Once this has been done the primary antenna will be commissioned by trying to communicate through that antenna instead of the secondary one. The procedure for this will be that the ADCS will orient the spacecraft with the primary antenna towards Earth, after 30 minutes the ADCS will reorient the spacecraft so the secondary antenna points to Earth again in case something goes wrong. If the operators receive data they will know that the primary antenna is operating nominally and that will conclude the commissioning the spacecraft will have to do, so from that point onward the primary antenna will be used.

#### 10.3.4. Secondary objectives

As specified in section 1.2 the NIBIRU mission has multiple secondary objectives which will add value to the mission by performing more scientific operations. Jupiter will not only be used to validate the functionality of the payloads as mentioned in section 10.3.3. NIBIRU will also use Jupiter as the first planet to perform operations and image both the planet and its moons. The Oberth manoeuvre around the Sun will not be studied. As the spacecraft will pass the Sun at only 10 Solar radii, so all effort must be made to reduce the heat coming to the spacecraft by the heat shield and it will not be possible to then image the Sun.

Now that the manoeuvres are done the spacecraft is on its way to Planet 9. However, not all of the secondary objectives have been completed yet. The spacecraft will go into sleep mode where only the OBDH is active to monitor the health of the components. Once the Kuiper Belt is reached, which the OBDH will know due to its internal clock, the spacecraft will awaken from sleep mode and it will start to use its payloads in the Kuiper Belt to characterise targets of opportunity that the spacecraft will pass. After the Kuiper Belt has been passed the spacecraft will continue the mission with characterising the Heliosphere. This data can be sent back to Earth via the primary antenna which significantly boosts the amount of bits that can be sent simultaneously.

The in-situ environmental experiments will start after having passed the Kuiper Belt at 50 AU and will continue until Planet 9 is reached at 550 AU. This will take approximately 36 years in which the Heliosphere, Heliopause and the interstellar medium will be investigated. It has been decided that measurements will be spread out over 7 days to be able to have the data more spread out over the region. Then there are 33 days to communicate all the data back to Earth. The two environmental payloads get 5.2 Mbit data packs per measurement of which 3 will be done spread out over the 7 days. This data along with 4.4 Mbit of telemetry data will be sent down. The limiting case for the communications is when power is minimal which will be just before Planet 9 is reached at 550 AU. As the batteries will only be used for the primary objectives, only the power allocated to the communications in the safe mode in table 4.6, which is 15.278 W can be used. Placing this in the link budget tool of section 4.3 leads to a bitrate of 7 bit/s which can be maintained indefinitely. With having to transmit the 20 Mbit it will take 33 days for the final measurement just before Planet 9 to be transmitted. To ease the coding for the OBDH it has been chosen to maintain this constant interval with 7 days for measurements and 33 days for communications even though the frequency of measurements could be higher at the Kuiper Belt and then decrease gradually. In total, this will lead to 328 measurements which span 1.521 AU of which 0.266 AU is covered when measurements are taken.

A milestone in this secondary objectives phase is when the 100 AU mark has been passed because then the spacecraft is officially in the interstellar medium and it will then continue the mission to characterise interstellar space [8]. At 550 AU Planet 9 will be reached which will be further discussed in section 10.3.5.

#### 10.3.5. Primary objectives

After 49.5 years NIBIRU will finally encounter its final destination, Planet 9. Here the most important part of the mission lies ahead of the spacecraft. It will take at least a hundred and seventy images with both the imager and the spectrometer payload. This number has been chosen as this can be sent back down to

Earth in a reasonable amount of time. Here use will be made of the modes as described in section 4.2.6. The spacecraft will first be in the operational mode. Here all of the images of Planet 9 are taken and stored on the OBDH. NIBIRU will only be in the range of Planet 9 for 12 to 16 days so these days are only used for operations and not for communications. These days 6000 images of both the imager and spectrometer payload are taken, as this is the limit on what can be stored on the OBDH.

Once the spacecraft is out of reach of Planet 9 the communications mode will start. At first, the 170 images which are determined to be the best by the OBDH will be send down to Earth. This will be done by giving the telecommunications subsystem a boost in power by finally making use of the batteries. As shown in table 4.6 there is 568.2383 W available for the communication system which leads to a bit rate of 264 bits/s. The imager payload takes images of 1.2 Mbit and the spectrometer image has a data size of 2.9 Mbit per image. Furthermore, 2000 kbit of telemetry will be sent in total with the 170 images. As the transmission rate can only be maintained for an hour before the satellite will have to transition to the charging mode for 10.87 hours, it will take a year before all images and telemetry are transmitted. The ground station operators are working to receive all of the data but they will not be operating the pointing of the spacecraft due to the sheer distance and time delay it would encounter so the spacecraft is operating autonomously. After this year of transmitting all of the data, the formal part of the mission will be over and the satellite will go into the end of life phase.

### 10.3.6. End of life

The spacecraft aims to remain operational well beyond its primary science objectives, being the farthest spacecraft ever made. As long as power and functionality persist, it will transmit stored images of Planet 9 and perform occasional in-situ measurements of the interstellar medium beyond 550 AU. However, as the spacecraft travels farther, power availability and communication become increasingly challenging. Battery efficiency will degrade over time, reducing power output, while eMMRTGs decrease by 2.5% annually [20, 29]. Eventually, all subsystems will fail, and the spacecraft will drift in deep space. Although it will no longer send data, it carries a golden disk with information about human life for potential alien encounters.

## Conclusion & Recommendations

*Contributors: Flavio, Isha*

The intent of this report was to provide the finalised design of a mission capable of characterising Planet 9 under several scientific aspects. In earlier phases of this mission design, the decision was made to detail the design of a single spacecraft that travels to Planet 9. NIBIRU will launch using SpaceX's Starship in 2038.

The spacecraft's payload will include a variety of scientific instruments. Research was performed on many of these devices, to determine which ones are the most useful to fulfill the mission objectives. Having performed numerous iterations, the final instruments selected to fly on the NIBIRU mission were: the N'LORRI camera, the ISHTAR imaging spectrometer, the NCREX cosmic ray telescope, and the JUICE's PSP to perform low- to high energy particle science experiments. Thanks to these instruments, NIBIRU will be able to perform both science operations at Planet 9 and experiments during its journey to destination, adding significant value to the mission. As it is set to become the farthest human-made object, similarly to the Voyager missions, NIBIRU will carry a golden record on board, which will serve as a snapshot of humanity.

Power generation is a critical concern for the NIBIRU mission, as the only viable option at such large distances from the Sun is the use of RTGs. For the spacecraft, two eMMRTGs will be utilised. These are the latest generation of RTGs, currently under development and expected to be ready by the mission's start. The limited power generated does not allow all subsystems to operate simultaneously. To address this, four VES16 8s4p batteries are included on board, allowing power to be stored for use during more power-intensive modes. The eMMRTGs guarantee an end-of-life power of just under 80 W, sufficient to support all systems in SAFE and CHARGE modes. During OPERATIONS and COMMUNICATIONS modes, the batteries are discharged to provide the additional required power. The on-board PCDU

ensures that power is distributed as intended for each operational mode.

At such distances, a large antenna is required to communicate with Earth. To fit such a large surface inside Starship's payload bay, the plan is to use a folding antenna which is only unfolded to a diameter of 7.81 meters after the Kuiper belt. This is paired with a smaller 1 meter antenna that is used prior to that moment. Other telecommunication hardware includes cables, transceivers, frequency converters, and filters. The final values of the link budget for communication indicate a gain of 54 dB, beamwidth of 0.33 degrees, power output of 568 W, and a bit rate of 264 bps at Planet 9. It will take a total of 1 full year to transmit all data generated at Planet 9.

To manage attitude disturbances and to ensure that the antenna can be directed towards Earth for communication, a set of sensors and actuators are required on board. These include eight HORUS star trackers, five HG 9900 inertial measurement units, as well several thrusters, in two different sizes. To be able to operate the thrusters, sizing a hydrazine tank as well as a helium pressurizer tank was required. These two tanks will be positioned inside the spacecraft bus.

A suitable trajectory is required to reach Planet 9 within the time constraint of 50 years and without the need for an unachievable  $\Delta V$ . NIBIRU will perform a powered flyby of Jupiter, applying a  $\Delta V$  of 1.42 km/s, followed by a solar oberth maneuver with a  $\Delta V$  of 3.42 km/s. The spacecraft will reach its destination 49.5 years after launch.

To be able to perform the aforementioned flyby and Oberth maneuver, the required  $\Delta V$  will be provided by the two kick stages placed under the spacecraft bus. The first kick stage, ENKI, will fire at Jupiter, providing the required 1.42 km/s. The second kick stage, ENLIL, will fire at a distance of 9 solar radii from the Sun, providing the remaining 3.42 km/s. In total, the propulsion system has to provide 4.84 km/s across the two stages, which both consist of a pressure-fed bipropellant system that uses nitrogen tetroxide and monomethylhydrazine as oxidizer and fuel respectively, and helium as pressurant gas.

Thermal control is required to maintain the spacecraft within the equilibrium temperature range of 270 and 290 K. This range is the same for the bus and the kickstages. The TCS uses components such as radiators, thermal sensors, and MLI to ensure that all thermal requirements are met. The total mass of the TCS is over 440 kg, which includes the heat shield and ceramic tiles used to protect the spacecraft during the Solar Oberth maneuver.

The spacecraft structure must be designed to withstand launch loads, as well as the harsh space conditions it will be subjected to during the long journey to Planet 9. The structure needs to support the spacecraft bus as well as the two kick stages. The material used will be Aluminium 2024-T36. The spacecraft bus will be an almost perfect cube, with dimensions of 1.5x1.5x1.4482 m, and its walls will have a thickness of 2.083 mm. The cylindrical structure of the stages will have a thickness of 11.52 mm and a total height of 14.05 m.

The On-Board Data Handling subsystem is responsible for the correct operation of the spacecraft as a whole. It will consist of five main components: the OBS, the DHAU, the CHU, the SSR and the clock. The software language used will be Ada. All of the data acquired will be stored in the SSR awaiting its transmission to Earth. The total mass of the OBDH subsystem will not surpass 70 kg and it will be one of the most power demanding subsystems, with over 30 W required during payload operations.

Several recommendations are made to further improve the design presented in this report. Firstly, further research should be conducted to develop a more detailed thermal control solution to protect the spacecraft during the solar Oberth maneuver at 10 solar radii. Additionally, a close Sun maneuver would not be necessary if more RTGs could be used. Since RTGs degrade over time, having additional units would ensure that the required power for NIBIRU at end-of-life could be maintained for over 50 years. This would allow for a longer journey to Planet 9 with less reliance on flyby bodies for  $\Delta V$  assistance. Finally, the N'LORRI camera on NIBIRU can resolve Planet 9 from about 21 AU. If Planet 9 is not exactly at the hypothesised location but somewhere in the vicinity, a trajectory adjustment would require only a minimal amount of thrust, which could be managed using the on-board ADCS propellant.

This concludes the design of NIBIRU, the vision, innovation and versatility of which will serve as a good starting point for a future mission to Planet 9 and beyond.

# Bibliography

- [1] Tom Ruen. Planet Nine Artistic, 2016.
- [2] J. Sinke. Production of Aerospace Materials; 12\_Sustainability and aircraft production\_AE3211II. <https://brightspace.tudelft.nl/d21/1e/content/615479/viewContent/3634856/View>, 2024.
- [3] S Alan Stern and Joshua E. Colwell. Collisional Erosion in the Primordial Edgeworth-Kuiper Belt and the Generation of the 30-50 AU Kuiper Gap. *The Astrophysical Journal*, 490(2):879–882, 1997.
- [4] Konstantin Batygin and Michael E Brown. Evidence for a Distant Giant Planet in the Solar System. *The Astronomical Journal*, 151(2):22, 2 2016.
- [5] Adam Hibberd, Manasvi Lingam, and Andreas M Hein. Can We Fly to Planet 9?, 2022.
- [6] Rebecca G. Martin and Mario Livio. the Solar System As an Exoplanetary System. *Astrophysical Journal*, 810(2):1–8, 2015.
- [7] Michael E. Brown, Matthew J. Holman, and Konstantin Batygin. A Pan-STARRS1 Search for Planet Nine. <https://arxiv.org/pdf/2401.17977>, 2024.
- [8] J.R. Jokipii. The Heliospheric Termination Shock. *Space Science Reviews*, 176(1-4):115–124, 2013.
- [9] Sijme-Jan Paardekooper. Project Guide Design Synthesis Exercise: A First Look at Planet 9, 4 2024.
- [10] Jafar Rezaei. Best-worst multi-criteria decision-making method. *Omega*, 53:49–57, 2014.
- [11] Asif A Siddiqi. *Beyond Earth: A Chronicle of Deep Space Exploration, 1958-2016*. NASA, 2018.
- [12] F. Poulet et al. Moons and Jupiter Imaging Spectrometer (MAJIS) on Jupiter Icy Moons Explorer (JUICE). *Space Science Reviews*, 220(3), 2024.
- [13] Harry Y Mcsween and Jeffrey E Moersch. *Planetary Geoscience*. Cambridge University Press, Cambridge, England, UK, 2019.
- [14] S. T. Dye. Geoneutrinos and the radioactive power of the Earth. *Reviews of Geophysics*, 50(3):1–19, 2012.
- [15] F. M. Flasar et al. Exploring the Saturn system in the thermal infrared: The composite infrared spectrometer. *Space Science Reviews*, 115(1-4):169–297, 2005.
- [16] T H E Nims Science. MAPPING EXPERIMENT ON GALILEO Table of Contents. pages 457–502, 1992.
- [17] Dennis C. Reuter, S. Alan Stern, John Scherrer, Donald E. Jennings, James W. Baer, John Hanley, Lisa Hardaway, Allen Lunsford, Stuart McMuldroy, Jeffrey Moore, Cathy Olkin, Robert Parizek, Harold Reitsma, Derek Sabatke, John Spencer, John Stone, Henry Throop, Jeffrey Van Cleve, Gerald E. Weigle, and Leslie A. Young. Ralph: A visible/infrared imager for the new horizons pluto/kuiper belt mission. *New Horizons: Reconnaissance of the Pluto-Charon System and the Kuiper Belt*, (Mvic):129–154, 2009.
- [18] A. F. Cheng et al. Long-range reconnaissance imager on New Horizons. *Space Science Reviews*, 140(1-4):189–215, 2008.
- [19] Carolyn C. Porco et al. Cassini imaging science: Instrument characteristics and anticipated scientific investigations at Saturn. *Space Science Reviews*, 115(1-4):363–497, 2005.
- [20] ESA. CDF Study Report Ice Giants - A mission to the Ice Giants - Neptune and Uranus. Technical report, 2019.
- [21] H. E. Spence et al. CRaTER: The cosmic ray telescope for the effects of radiation experiment on the lunar reconnaissance orbiter mission. *Space Science Reviews*, 150(1-4):243–284, 2010.
- [22] A. Galli et al. Callisto’s Atmosphere and Its Space Environment: Prospects for the Particle Environment Package on Board JUICE. *Earth and Space Science*, 9(5), 2022.
- [23] P. C. Thomas. Radii, shapes, and topography of the satellites of Uranus from limb coordinates. *Icarus*, 73(3):427–441, 1988.
- [24] S. J. Conard et al. Design and fabrication of the New Horizons Long-Range Reconnaissance Imager. *Astrobiological and Planetary Missions*, 5906:59061D, 2005.
- [25] E.C. Stone. Cosmic Ray Investigation for the Voyager Missions; Energetic Particle Studies in the Outer Heliosphere-and Beyond. *Space Science Reviews*, 21(1):355–376, 1977.
- [26] Stas Barabash and Pontus Brandt. Unique Heliospheric Measurement Opportunities with the ESA JUICE mission: Science Case for Particle Environment Package (PEP). In *EGU General Assembly 2024*, 2024.
- [27] Romain Peyrou-Lauga and Pauline Gautier. JUICE (Jupiter Icy Moon Explorer) Spacecraft Thermal Control. 3(July):12–15, 2021.
- [28] M E Summers. ( REX ) [ Submitted Draft 8jan07 ]. pages 1–94, 2007.
- [29] Young Lee and Brian Bairstow. Radioisotope power systems reference book for mission designers and planners. JPL Publication 15-6, 2015. Accessed on 4-6-2024.

- [30] Bhavya Lal et al. Current Status and Future of Space Nuclear Power. 2018.
- [31] Christopher S.R. Matthes et al. A Status Update on the eMMRTG project. *Journal of Electronic Materials*, 45, 2015.
- [32] Wiley J. Larson and James R. Wertz. *Space Mission Analysis And Design*. Microcosm Inc, 2 edition, 1992.
- [33] B Zandbergen. *AE1222-II: Aerospace Design & Systems Engineering Elements I - Spacecraft (bus/platform) design and sizing*. 2021.
- [34] Saft. *Saft Solution for LEO and Small GEO Applications*. Saft Space & Defense Division Rue Georges Leclanché- BP 1039 86060, POITIERS Cedex 9- France, 2020. Accessed on 10-6-2024.
- [35] Eberhard Gill. Lecture #4 - Verification and Validation for the Attitude and Orbit Control System. <https://brightspace.tudelft.nl/d21/le/content/615478/viewContent/3384127/View>, 2024.
- [36] The Planetary Society. Cost of New Horizons. <https://www.planetary.org/space-policy/cost-of-new-horizons>.
- [37] V. M. Arsent'ev and V. I. Berzhatyj. KRT-10 space telescope. *Akademiia Nauk SSSR Doklady*, 264:588, 1982.
- [38] Vahid Hasanzade, Seyed Hassan Sedighy, and Majid Shahravi. Compact Deployable Umbrella Antenna Design with Optimum Communication Properties. *JSR*, 2017.
- [39] Stavros V. Georgakopoulos et al. Origami Antennas. *IEEE Open Journal of Antennas and Propagation*, 2:1020–1043, 2021.
- [40] J.R. Wertz and W.J. Larson. *Space Mission Analysis and Design*. Springer Dordrecht, 3 edition, 1999.
- [41] Hamid Fartookzadeh and Mahdi Fartookzadeh. Value Engineering and Function Analysis: Frameworks for Innovation in Antenna Systems. *Challenges*, 9(1):20, 4 2018.
- [42] NASA. What is the Deep Space Network?, 2020.
- [43] Dong K. Shin. Frequency and Channel Assignments. Technical report, California Institute of Technology, 2014.
- [44] Stefano Speretta. AE3524 Lecture\_15\_Telecommunications, 2023.
- [45] Stephen D. Slobin. Antenna Positioning. Technical report, 2014.
- [46] L. J. Crawford, T. B. Coughlin, and W. L. Ebert. COST ESTIMATION AND MODELING FOR SPACE MISSIONS AT APL/JHU. *Acta Astronautica*, 39, 1996.
- [47] Scott R. Starin and John Eterno. *GSFC 19.1 Attitude Determination and Control Systems*. Greenbelt, MD, 2011.
- [48] John A. Christian. A Tutorial on Horizon-Based Optical Navigation and Attitude Determination With Space Imaging Systems. *IEEE Access*, 9:19819–19853, 2021.
- [49] David Y. Kusnierkiewicz et al. A description of the Pluto-bound New Horizons spacecraft. *Acta Astronautica*, 57, 2005.
- [50] NASA. Cassini. <https://science.nasa.gov/mission/cassini/quick-facts/>.
- [51] NASA. Voyager 2 - First to Visit All Four Giant Planets. <https://science.nasa.gov/mission/voyager/voyager-2/>, 2024.
- [52] NASA. Voyager\_1\_data. <https://science.nasa.gov/mission/voyager/voyager-1/>, 2024.
- [53] Marcel J. Sidi. *Spacecraft Dynamics and Control*. Cambridge University Press, 1997.
- [54] Aerojet RocketDyne. In-Space Propulsion Data Sheet.
- [55] ArianeGroup. HORUS - Single Box Standalone Star Tracker, 2022.
- [56] Honeywell. HG9900 Inertial Measurement Unit.
- [57] Ansys. Granta Edupack, 2023. Accessed on 16-6-2024.
- [58] NASA. Voyager 1 The most distant human-made object. <https://science.nasa.gov/mission/voyager/voyager-1/>.
- [59] K.F Wakker. *Fundamentals of Astrodynamics*. Institutional Repository Library, 2015.
- [60] Michael E Brown, Matthew J Holman, and Konstantin Batygin. A Pan-STARRS1 Search for Planet Nine. *The Astronomical Journal*, 167(4):146, 3 2024.
- [61] Konstantin Batygin et al. Generation of Low-inclination, Neptune-crossing Trans-Neptunian Objects by Planet Nine. *The Astrophysical Journal Letters*, 966(1):L8, 4 2024.
- [62] Konstantin Batygin and Michael E Brown. EVIDENCE FOR A DISTANT GIANT PLANET IN THE SOLAR SYSTEM. *The Astronomical Journal*, 151(2):22, 1 2016.
- [63] Robert G Sargent. Verification and validation of simulation models. In *Proceedings of the 2010 Winter Simulation Conference*, pages 166–183, 2010.
- [64] James L. Cannon. Liquid Propulsion: Propellant Feed System Design. *Encyclopedia of Aerospace Engineering*, 2, 2010.
- [65] B. Nufer. HYPERGOLIC PROPELLANTS: THE HANDLING HAZARDS AND LESSONS LEARNED FROM USE. 2010.

- [66] Hongjae Kang, Dongwook Jang, and Sejin Kwon. Demonstration of 500 N scale bipropellant thruster using non-toxic hypergolic fuel and hydrogen peroxide. *Aerospace Science and Technology*, 49:209–214, 2 2016.
- [67] Rob Hermsen and Barry Zandbergen. Pressurization system for a cryogenic propellant tank in a pressure-fed high-altitude rocket. 2017.
- [68] James Fesmire. Cold Vacuum Pressure and Cryopumping in Thermal Insulation Systems for Vacuum-Jacketed Tanks. 2022.
- [69] H. B. Keene. A determination of the radiation constant. *Proceedings of the Royal Society of London. Series A, Containing Papers of a Mathematical and Physical Character*, 88(600):49–60, 1 1913.
- [70] A. Feingold. A New Look at Radiation Configuration Factors between Disks. *Journal of Heat Transfer*, 100(4):742–744, 11 1978.
- [71] LASP. New horizons model, January 11 2006. Accessed: 17/06/2024.
- [72] J.J. Wijker. *Spacecraft Structures*. 2008.
- [73] University of Surrey. Mechanical design course slides, 2012. Accessed on 16-6-2024.
- [74] TU Delft. Vibrations part 1 slides, 2024. Accessed on 16-6-2024.
- [75] René Alderliesten. Introduction to aerospace structures and materials. *Publisher's Name*, 2018.
- [76] J. B. Holladay, T. Sanders, and D. A. Smith. Enhanced feasibility assessment of payload adapters for NASA's space launch system. In *2019 IEEE Aerospace Conference*, 2019.
- [77] Alberto Sanchez Cebrian, Boris-Ulrich Halter, and Tobias Gerngross. RUAG's approach to develop a modular low shock separation and jettison system. 2019.
- [78] Riley Carriere and Aleksandr Cherniaev. Hypervelocity Impacts on Satellite Sandwich Structures—A Review of Experimental Findings and Predictive Models. *Applied Mechanics*, 2(1):25–45, 2 2021.
- [79] Shannon Ryan. Hypervelocity Impact Testing of Aluminum Foam Core Sandwich Panels. 2015.
- [80] Xiaolei Zhu et al. Mechanical Behavior of CFRP Lattice Core Sandwich Bolted Corner Joints. *Applied Composite Materials*, 24(6):1373–1386, 12 2017.
- [81] Che-Shing Kang. Multilayer Insulation for Spacecraft Applications. pages 175–179. 1999.
- [82] Miguel Pérez-Ayúcar et al. Science Data Volume management for the Rosetta spacecraft. In *SpaceOps 2016 Conference*, page 12, Reston, Virginia, 5 2016. American Institute of Aeronautics and Astronautics.
- [83] Alessandra Menicucci. On-board command and data handling: Part 2. 2023.
- [84] Adam West. NASA Study on Flight Software Complexity. Technical report, 2009.
- [85] Eberhard Gill. AE3211-I Systems Engineering & Aerospace Design; Lecture 3 - Risk Management & Concurrent Engineering. <https://brightspace.tudel1ft.nl/d21/1e/content/615478/viewContent/3384133/View>, 2024.
- [86] Joyce Dever et al. Handbook of Environmental Degradation of Materials. chapter Degradatio. 2005.
- [87] Mak Tafazoli. A study of on-orbit spacecraft failures. *Acta Astronautica*, 64(2-3):195–205, 2009.
- [88] Jay Wynn, Tina Laforteza, and Alex Denissov. Cost Overruns, Schedule Delays & Performance Failures in Civil Space Programs: Lessons Learned & Recommendations for the Vision for Space Exploration. Orlando, Florida, 2005.
- [89] H Hussmann et al. JUICE JUPiter ICy moons Explorer: Exploring the emergence of habitable worlds around gas giants. *Esa*, ESA/SRE(September), 2014.
- [90] Vicki Cripps. Phases of an ESA hardware Project explained. Technical report, Institutet för Rymdfysik, 2018.
- [91] European Cooperation for Space Standardization. ECSS system - ECSS-S-ST-00-01C Rev. 1, 2023.
- [92] Vincent C. Yarnot and Gerald T. Brewster. Life Test Results for a New 4N (1 lbf) Thrust Class Hydrazine Monopropellant Engine. In *48th AIAA/ASME/SAE/ASEE Joint Propulsion Conference & Exhibit*, Atlanta, Georgia, 2012.
- [93] Aerojet Rocketdyne. In-Space Propulsion Data Sheets, 2020.
- [94] ArianeGroup. 10N, 200N, 400N - Chemical Bipropellant Thruster Family, 2021.
- [95] Innovative Sensor Technology. P0K1.202.6W.A.007.
- [96] AccuBeat. Ultra Stable Oscillator (USO) for Deep Space Exploration, 2023.
- [97] European Cooperation for Space Standardization. Space Product Assurance, Hazard Analysis - ECSS-Q-ST-40-02C, 2008.
- [98] European Cooperation for Space Standardization. Space product assurance, Safety - ECSS-Q-ST-40C Rev.1, 2017.

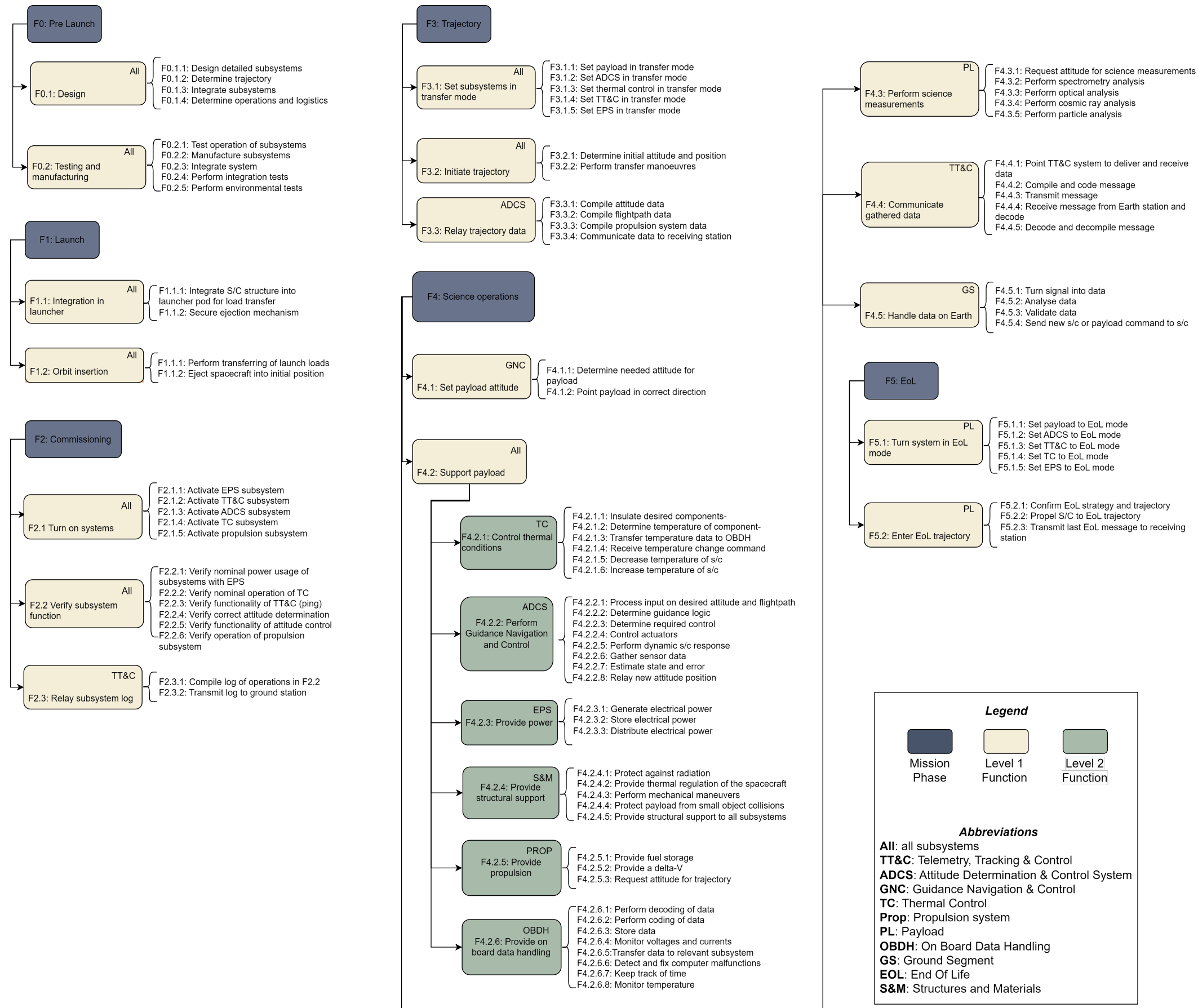


Figure 10.3: Functional Breakdown Structure

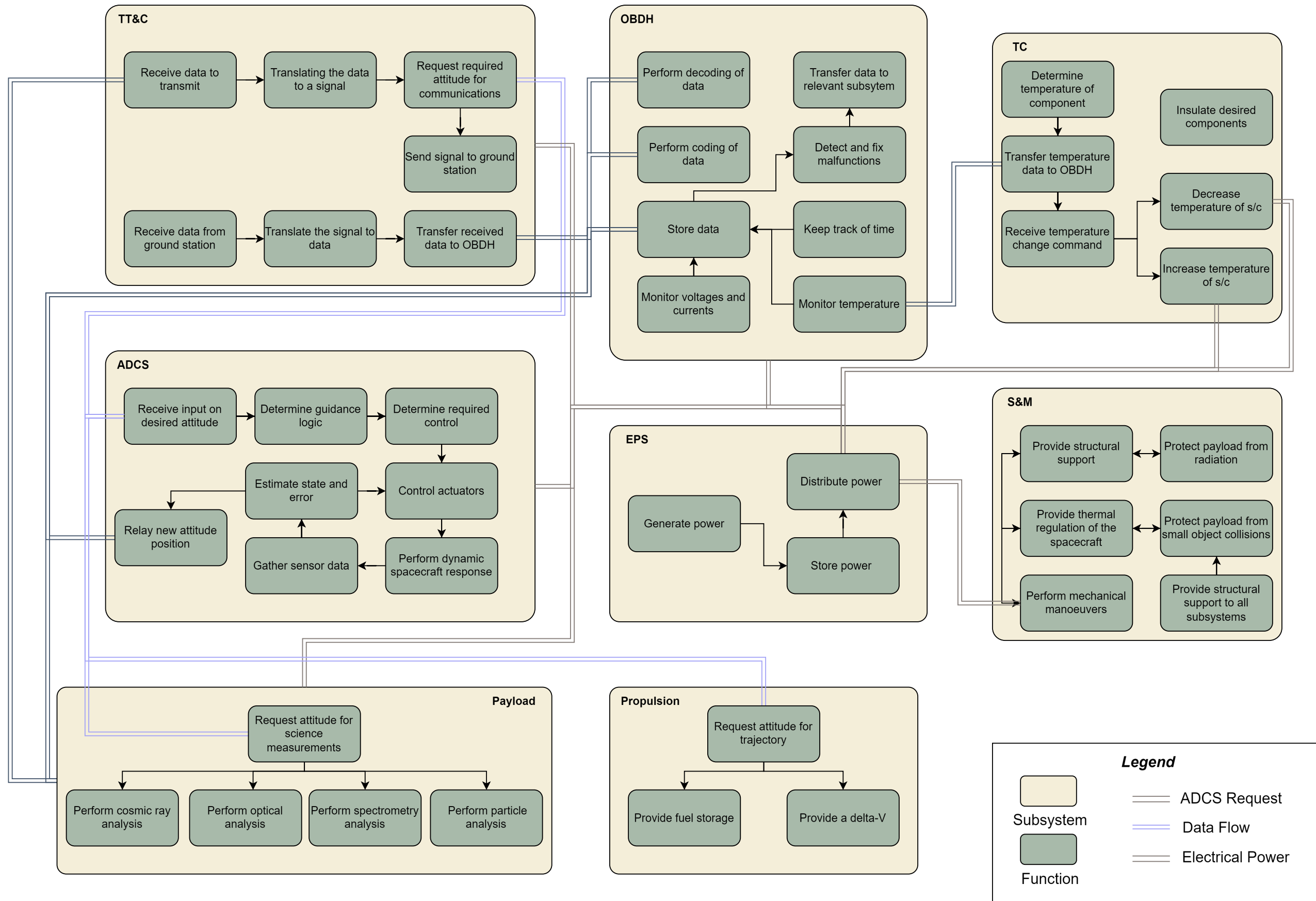
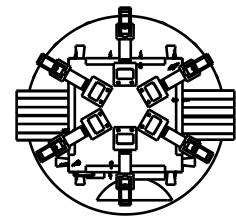


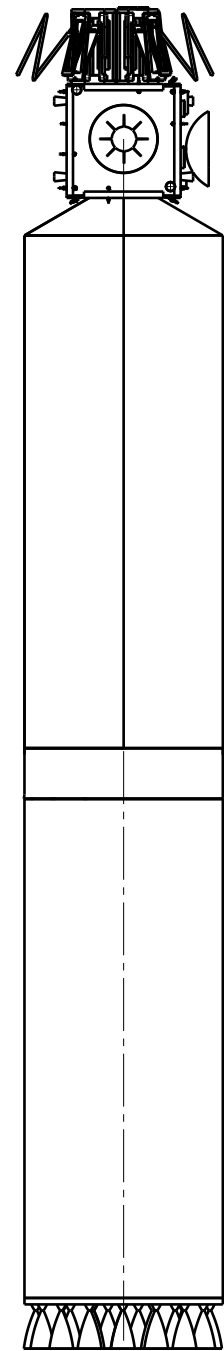
Figure 10.4: Functional Flow Diagram

H G F E D C B A

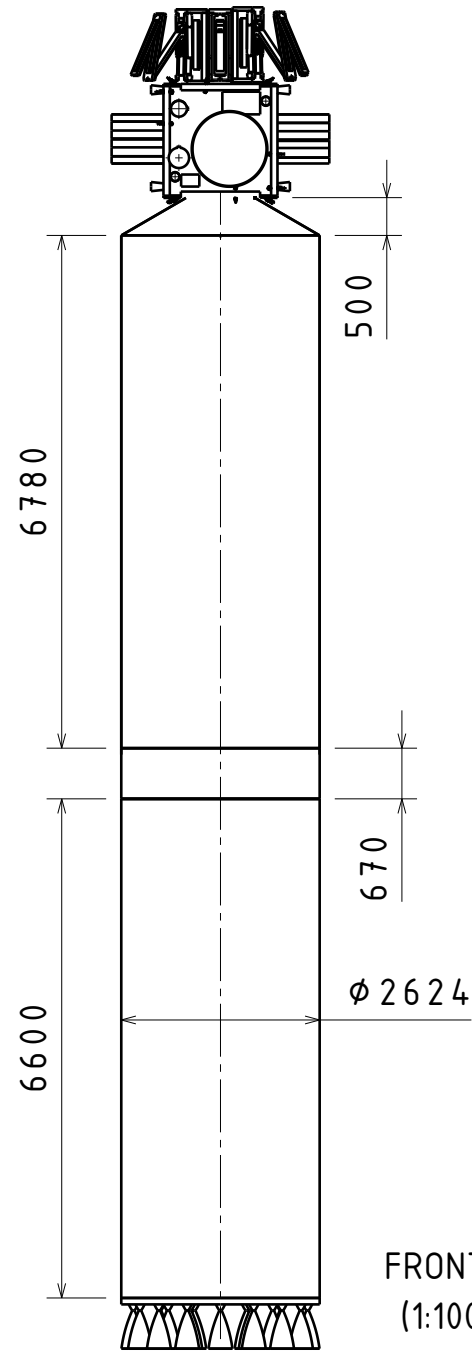
4  
3  
2  
1



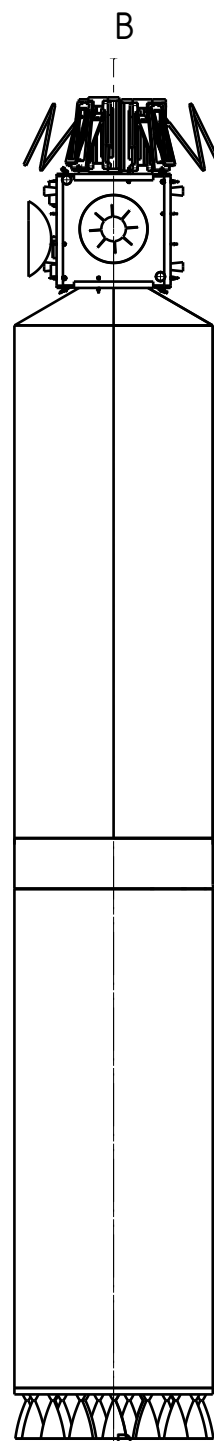
TOP  
(1:100)



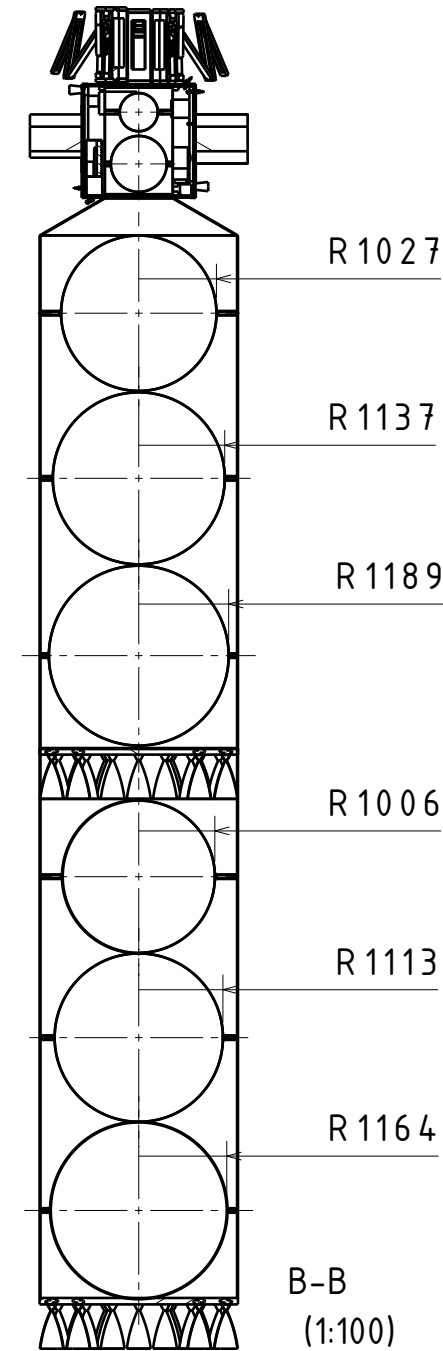
LEFT  
(1:100)



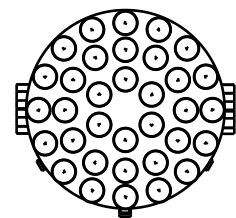
FRONT  
(1:100)



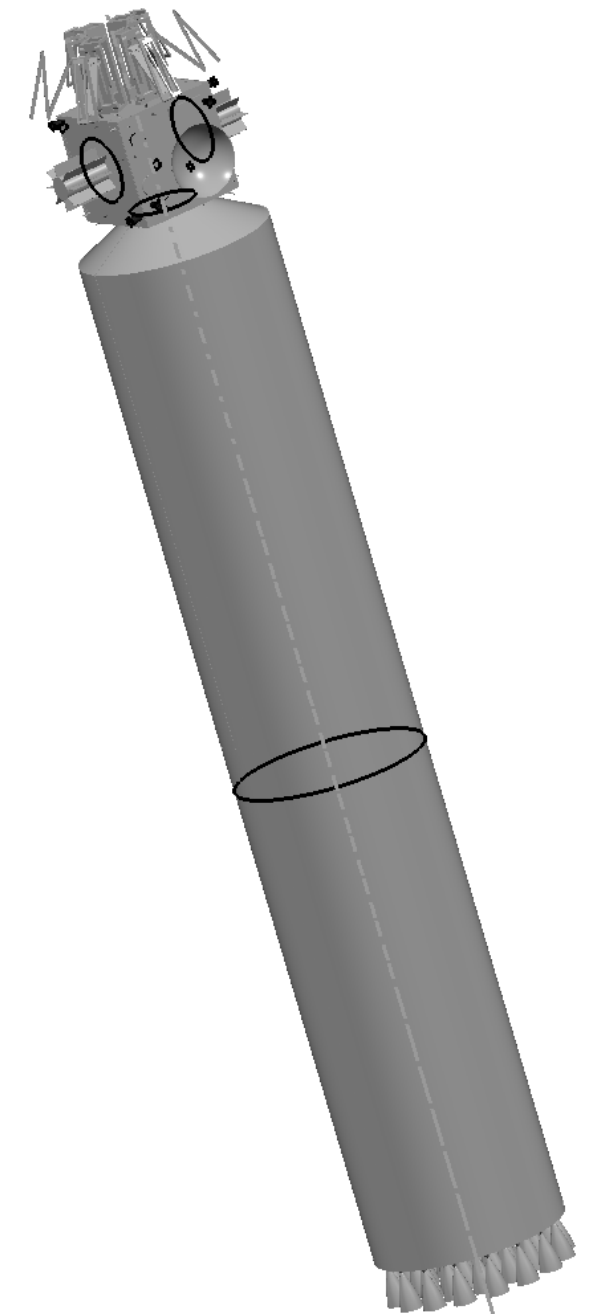
RIGHT  
(1:100)



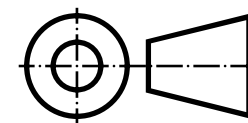
B-B  
(1:100)



BOTTOM  
(1:100)



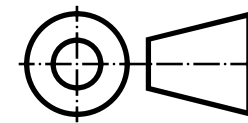
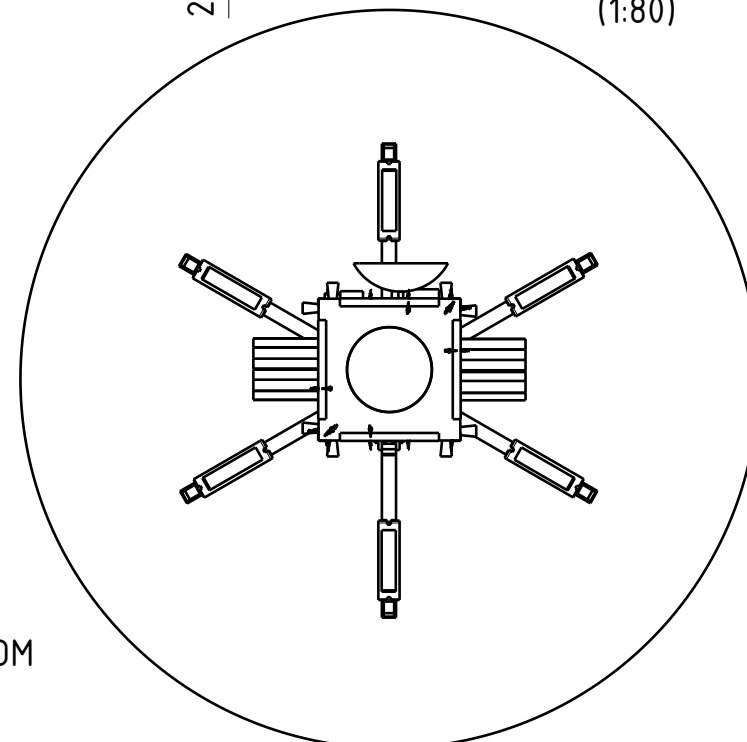
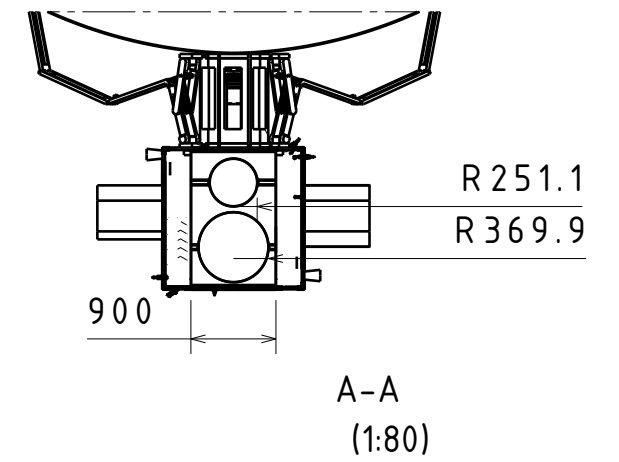
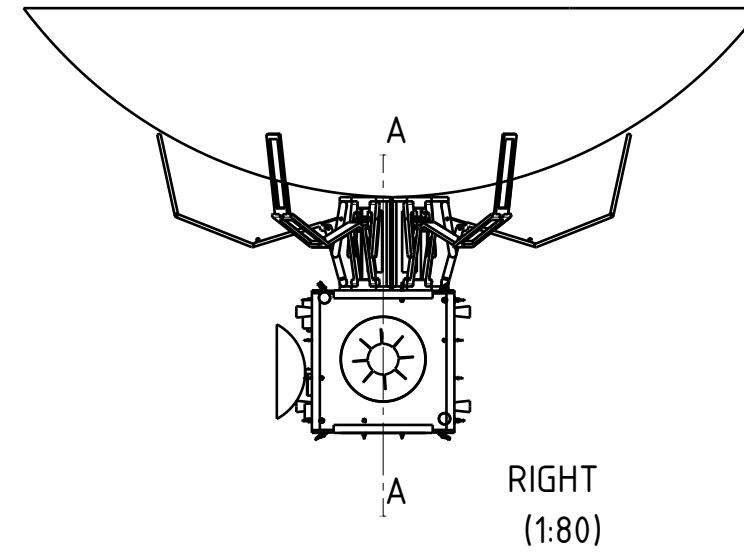
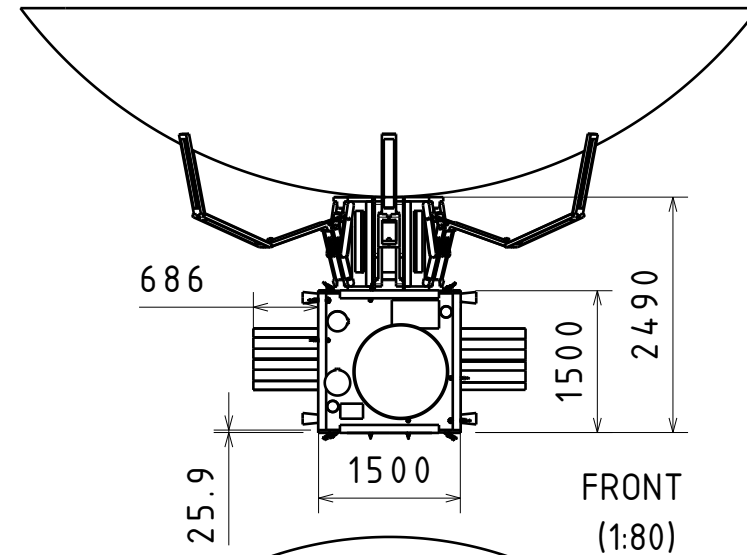
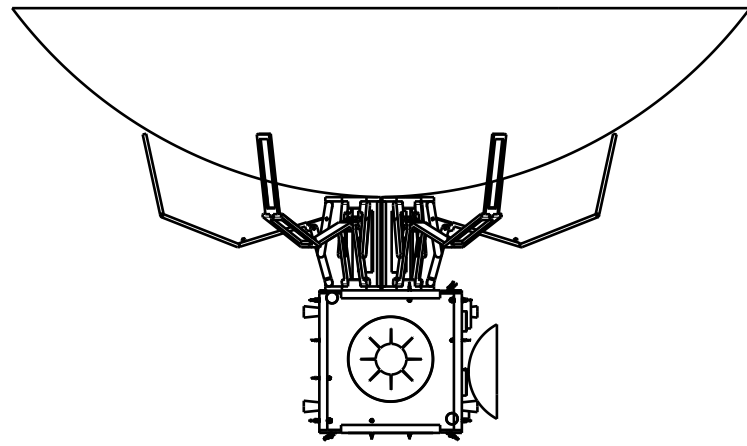
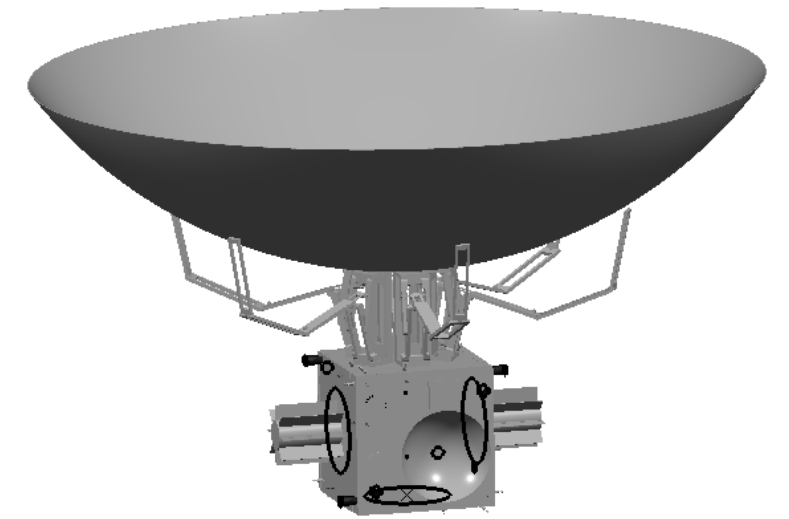
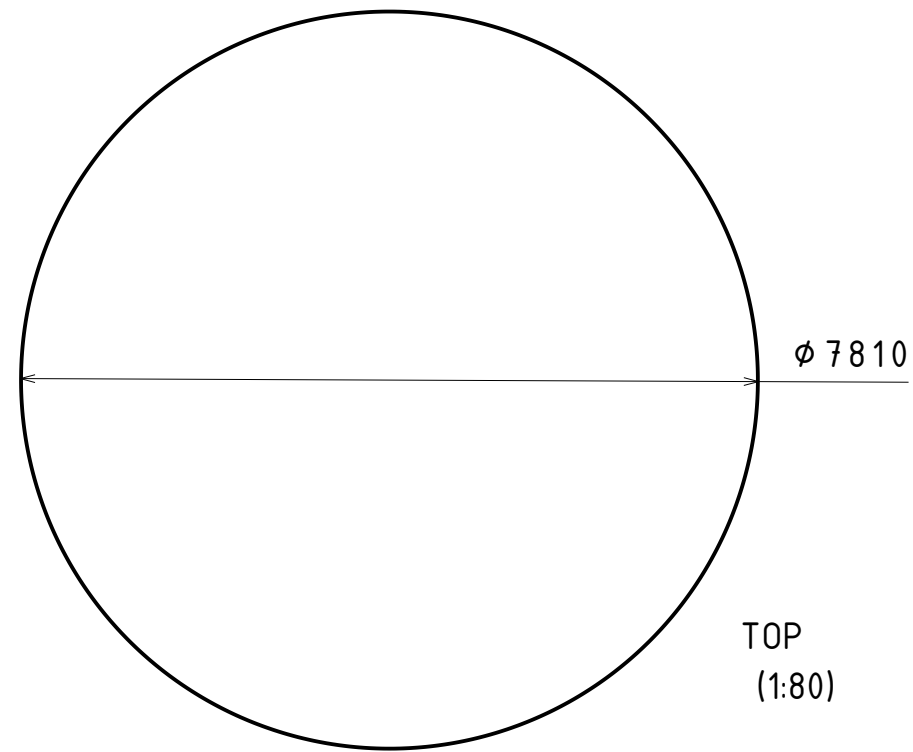
ISOMETRIC  
(1:100)



|                             |                    |
|-----------------------------|--------------------|
| DRAWN BY<br>Iván Pedrero    | DATE<br>18/06/2024 |
| CHECKED BY<br>Thijmen Duran | DATE<br>18/06/2024 |
| DESIGNED BY<br>DSE Group 25 | DATE<br>18/06/2024 |

|                             |                         |              |  |
|-----------------------------|-------------------------|--------------|--|
| Description                 |                         |              |  |
| NIBIRU Probe and Kickstages |                         |              |  |
| SIZE<br>A3                  | Title<br>NIBIRU         | REV<br>B.1   |  |
| SCALE<br>1:100              | WEIGHT(kg)<br>40648.250 | SHEET<br>1/1 |  |

H G B A

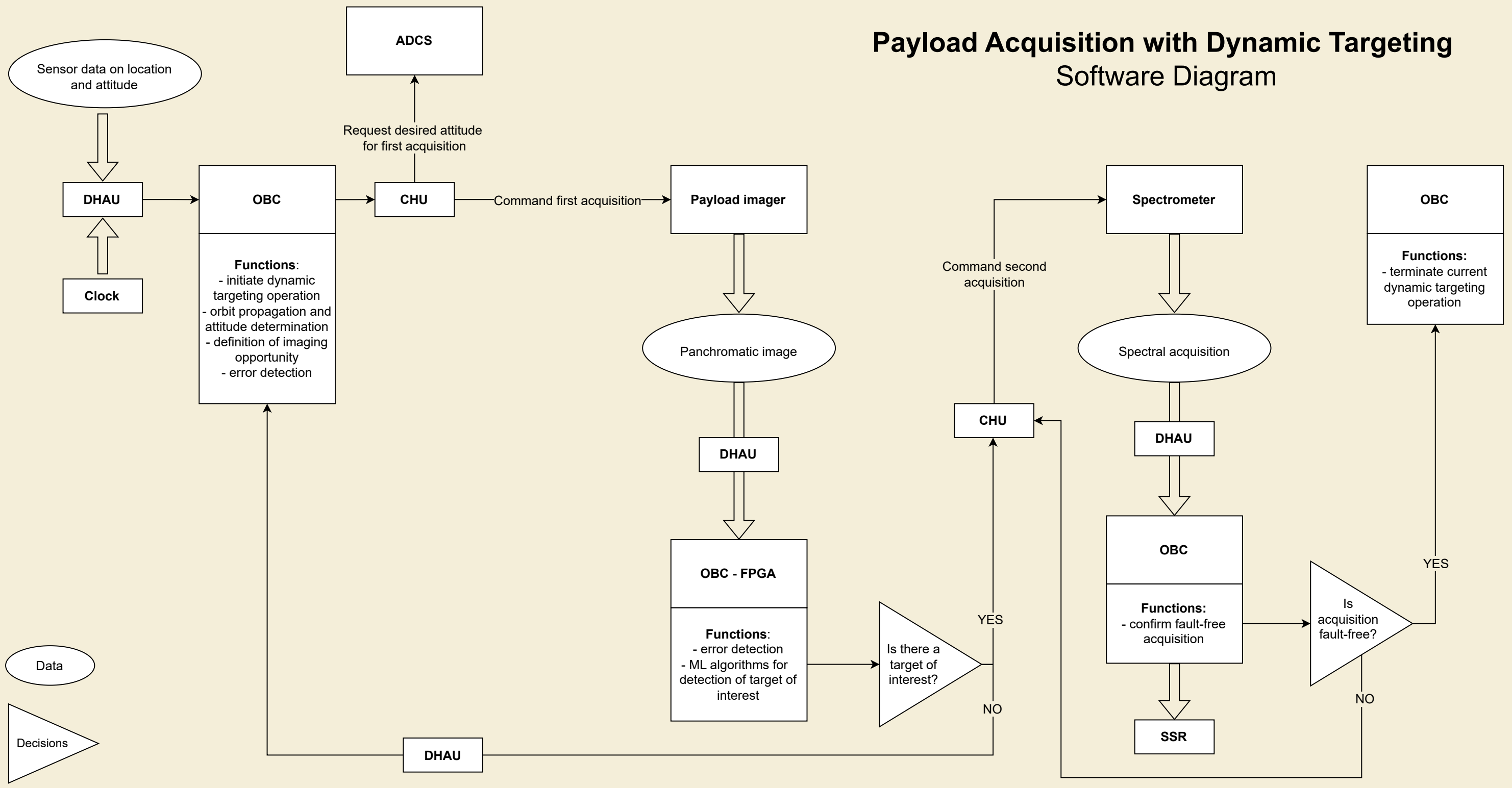


**TU Delft**

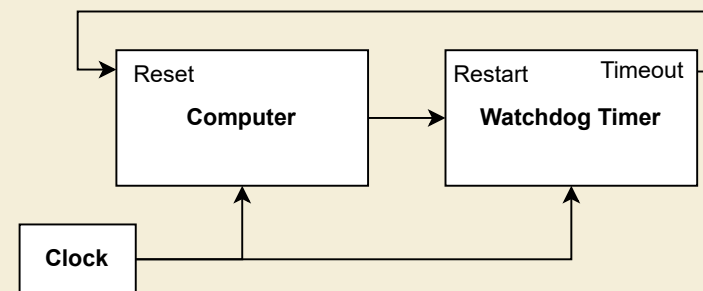
|                             |                    |
|-----------------------------|--------------------|
| DRAWN BY<br>Iván Pedrero    | DATE<br>18/06/2024 |
| CHECKED BY<br>Thijmen Duran | DATE<br>18/06/2024 |
| DESIGNED BY<br>DSE Group 25 | DATE<br>18/06/2024 |

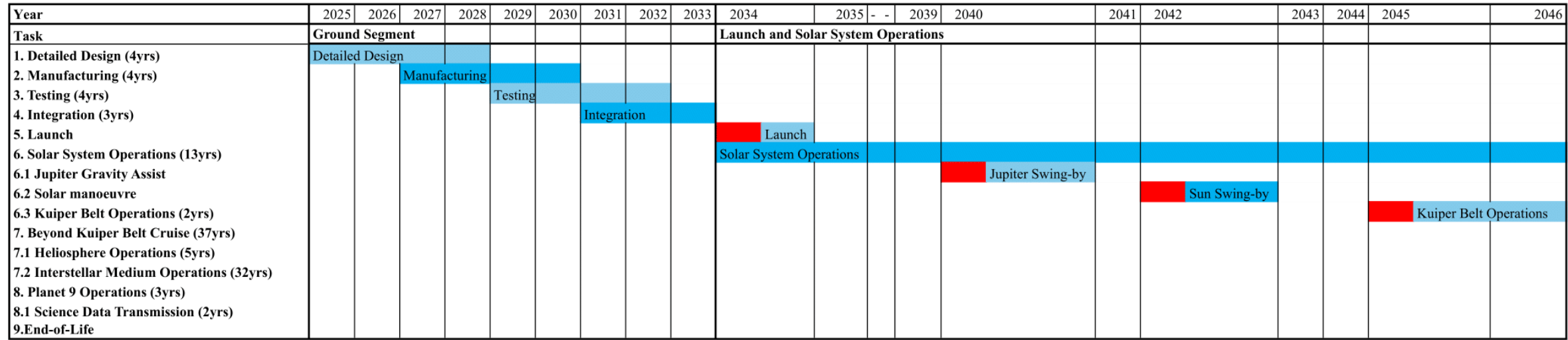
|               |                        |              |  |
|---------------|------------------------|--------------|--|
| Description   |                        |              |  |
| NIBIRU Probe  |                        |              |  |
| SIZE<br>A3    | Title<br>NIBIRU        | REV<br>B.1   |  |
| SCALE<br>1:80 | WEIGHT(kg)<br>2400.142 | SHEET<br>1/1 |  |

# Payload Acquisition with Dynamic Targeting Software Diagram

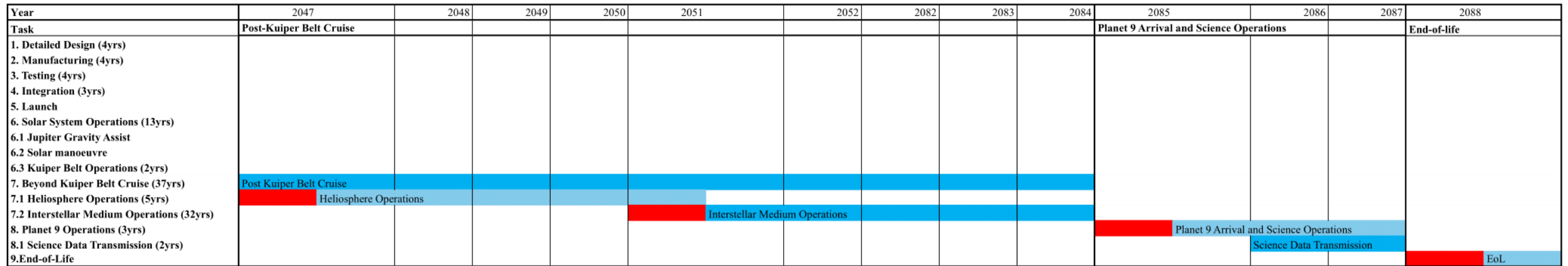


## Watchdog Operations Example with computer





(a) First Part of the Post-DSE activities of NIBIRU.



(b) Second Part of the Post-DSE Activities of NIBIRU.

Figure 10.5: Graphs Showing the Post-DSE Activities of NIBIRU.